

UNCLASSIFIED

AD 267 701

*Reproduced
by the*

**ARMED SERVICES TECHNICAL INFORMATION AGENCY
ARLINGTON HALL STATION
ARLINGTON 12, VIRGINIA**



UNCLASSIFIED

NOTICE: When government or other drawings, specifications or other data are used for any purpose other than in connection with a definitely related government procurement operation, the U. S. Government thereby incurs no responsibility, nor any obligation whatsoever; and the fact that the Government may have formulated, furnished, or in any way supplied the said drawings, specifications, or other data is not to be regarded by implication or otherwise as in any manner licensing the holder or any other person or corporation, or conveying any rights or permission to manufacture, use or sell any patented invention that may in any way be related thereto.

**Best
Available
Copy**

267701

1-68-1-4

MCL - 905/1+2

TECHNICAL DOCUMENTS LIAISON OFFICE
UNEDITED ROUGH DRAFT TRANSLATION

STEROMETRIC METALLURGY

BY: S. A. Saltykov

PAGES 310 - 604, PART II OF II PARTS

THIS TRANSLATION HAS BEEN PREPARED IN THIS MANNER
TO PROVIDE THE REQUESTER/USER WITH INFORMATION IN
THE SHORTEST POSSIBLE TIME. FURTHER EDITING WILL
NOT BE ACCOMPLISHED BY THE PREPARING AGENCY UN-
LESS FULLY JUSTIFIED IN WRITING TO THE CHIEF, TECH-
NICAL DOCUMENTS LIAISON OFFICE, MCLTD, WP-AFB, OHIO

PREPARED BY:

TECHNICAL DOCUMENTS LIAISON OFFICE
MCLTD
WP-AFB, OHIO

MCL - 905/1+2

Date 6 Oct. 1961

Chapter IV DETERMINING THE QUANTITY OF MICROPARTICLES PER UNIT VOLUME OF METAL OR ALLOY

Section 31. The Relationship Between Spatial and Planar Structures

Methods of stereometric metallography, presented in previous sections, are intended for the determination of structural composition of alloys and for the measurement of the specific extent of two-dimensional or one-dimensional elements of space structures. They are quite simple but at the same time assure the obtaining of comprehensive data. The problem, which is to be considered in this chapter, is much more complex. Until now there has been no method which would make it possible to determine experimentally, on the basis of planar microstructure, the number of microparticles of an arbitrary shape and size per unit volume of metal or alloy. Methods for determining the number of microparticles, developed for certain specific cases in which microparticles are of definite shape or size, in general are much more laborious than previously considered methods. The more comprehensive and accurate is the picture of a special microstructure that we want to obtain, the more complex are these methods. At the same time, the ability to determine the number of microparticles per unit volume of alloy is absolutely essential for the study of such an important process as crystallization, during which the basic structure of the alloy is being formed and, consequently, its properties are being predetermined.

In pure metals or in single phase alloys, microparticles of one and the same composition and internal structure, having their faces in direct contact with each other, completely fill the volume of metal in question. If the number of structural constituents is two or more, the microparticles of one of them are more or less uniformly distributed through the volume of the alloy, being completely separated or having a partial contact (in this case common

faces are formed).

Shapes of microparticles are quite diversified: they may be quite simple and geometrically regular (spheres, cubes, cylindrical rods, etc.), but at the same time, microparticles may be encountered that have extremely complex spatial configurations (for example, clusters of graphite lamella in gray cast iron). Sizes of microparticles of a given structural constituent may be more or less uniform within the limits of the volume of specimen subject to analysis. However, they may also fluctuate over a quite wide range. The distribution of microparticles in a volume of an alloy may be statistically uniform and their orientation random; however, a certain regularity of their distribution may also occur (for example, lineal arrangement of carbides or brittle nonmetallic inclusions in steel, lineal arrangement of microparticles during the crystallization in a constant magnetic field (149), etc.), as well as certain regularity of their orientation during plastic deformation and developed transfiguration. The number of microparticles per 1 mm³ of alloy may vary between a fraction of 1 microparticle to tens of millions of microparticles.

This diversity of shapes, sizes, number, disposition and orientation of microparticles is reflected quantitatively and qualitatively on the planar microstructure which may be regarded as a sectional drawing of spatial structure. At times, in order to conceive correctly a spatial structure, it is necessary to examine not one but several planar sections with different spatial orientation. In isolated instances the true spatial shape of microparticles of a given type may be revealed only by the construction profiles of miles of microparticles by means of repeated etching and taking photographs (or making drawings).

Due to the great diversity of factors which affect the picture of a planar section of spatial structures, there is no general singular relationship between the number of microparticles per volume

of the alloy or any parameter of a planar structure, for example the number of intersections of these microparticles per unit area of the plane of polish. Moreover, it is possible to demonstrate that this relationship cannot be established even when using not one but several parameters of a planar structure, if an attempt is made to avoid certain assumptions and approximations with regard to shape of microparticles.

Any microparticle, which is a microscopic geometrical body, may be bound by two parallel planes tangent to it on opposite sides in such a fashion that the particle is entirely confined between these two planes. Planes which bound a geometrical body are called reference planes. The distance between these two planes we shall designate as H and call it the height of a body or microparticle. It is quite obvious that with exception of certain specific shapes of bodies, for example a sphere, the height of one and the same body is dependent upon the disposition of reference planes with respect to the body (and vice versa) and may vary within definite limits for any concrete body. For example, the minimum distance between the reference planes in a cube is equal to the edge of the cube and the maximum distance is equal to the body diagonal. At any disposition of the axis of the cube with respect to reference planes, its height may vary between a and $a\sqrt{3}$ where a is the length of the cube's edge.

Hence we arrive at a notion of the mean height of a cube or of a body of any shape in general: if a body assumes uniformly any position in space at all times being tangent to one of the reference planes, then the mean distance between the fixed reference plane and the second reference plane, which is displaced parallel to itself when the body changes its positions and which is tangent to the body and limits it on the opposite side, is the mean height of the body which we shall designate as \bar{H} .

Now let us consider a group of microparticles which are convex

microbodies of any shape, statistically uniformly distributed with a random orientation, in a cube the edge of which is 1 mm⁽¹⁾. Having bound each microparticle by reference planes parallel to the basal plane of the cube, and having determined the corresponding heights of microparticles, let us replace all microparticles by intercepts which represent these heights with respect to length, direction and disposition. It is obvious that any plane parallel to the basal plane of a cube will intersect the number of intercepts precisely equal to the number of microparticles, if this plane were to intersect microparticles.

By substituting the heights of microparticles for microparticles themselves, we derive a system of mutually parallel intercepts, which we have reviewed in Section 30. We know that the total length of such intercepts per 1 mm³ is equal to the number of their intersections with a plane, perpendicular to them, per 1 mm² of the area of this plane, as defined by the formula (30.4). Therefore, if the heights of individual microparticles are designated as H_1, H_2, H_3, \dots , the mean height of these particles in the direction perpendicular to the basal plane of the cube is designated as \bar{H} , the number of microparticles per 1 mm³ is designated as N , and the number of sections of microparticles per 1 mm² of the area is designated as n , it is possible to write:

$$H_1 + H_2 + H_3 + \dots + H_N = n \quad (31.1)$$

Having divided both halves of Equation (31.1) by the number of microparticles per unit volume, N , we have:

$$\bar{H} = \frac{H_1 + H_2 + H_3 + \dots + H_N}{N} = \frac{n}{N} \quad (31.2)$$

⁽¹⁾ By a convex body we mean a body which contains the full length of any intercept, connecting any points of the volume.

The fact that here the quantity \bar{H} is not the mean height of an individual microparticle but a mean height of a group of microparticles of a given structural constituent, having different sizes and shapes (within the limits of a shape of microparticles typical for this constituent) should be taken into account. Inasmuch as we have assumed that microparticles are randomly oriented in space, we have grounds to believe that the mean height \bar{H} is valid not only for the direction perpendicular to the basal plane of the cube in question but for any other direction.

The relationship derived between N , n and \bar{H} is quite important, although it does not afford the possibility of calculating the number of microparticles per 1 mm³ of metal, N , inasmuch as from the plane of polish we can determine only the mean number of sections of microparticles per 1 mm² of its area, n , and we do not know the mean height of microparticles, \bar{H} . Formula (31.2) shows that a singular dependence cannot exist between quantities N and n even in the case when microparticles are convex bodies, inasmuch as the formula contains \bar{H} . Despite that, numerous attempts were made at establishing a dependence of precisely this type. For example, G Tamman [38] believed that it was possible to determine the number of crystallites per unit volume of metal from the formula:

$$N = n^{3/2} \quad (31.3)$$

In essence, this formula provides only a correct relationship between the dimensions of the terms found in it: nothing more than that!

If we are to assume that all microparticles of the alloy subject to investigation are absolutely identical bodies with respect to shape and size, even then some coefficient, not equal to unity, and reflecting the influence of the shape of microparticles on the relationship between planar and spatial parameters, must be present in Formula (31.3). When studying the problem

of determining the amount of graphite precipitates in annealed malleable cast iron, G. Schwarz noted with respect to relationship (31.3) that it could only be valid under the condition that all centers of spheroidal microparticles are on sites of a cubic lattice and the plane of polish passes through the centers of 1 layer of microparticles [65, 115]. It is clear that this assumption is too arbitrary and far removed from the real picture of distribution of microparticles in a volume of real metal.

Eliminating term n , by simultaneous solution of Equation (31.2) and Equation (31.3), proposed by G. Tammann, we derive:

$$\bar{H} = \frac{1}{\sqrt[3]{N}} = \frac{3V}{\sqrt{V}} \quad (31.4)$$

where V is the volume of 1 microparticle, if the structure is single phase.

The relationship (31.4) clearly shows that Equation (31.3) of G. Tammann is erroneous, inasmuch as the Formula (31.2) is indisputable. Even if it is postulated that all microparticles are bodies of equivalent size and shape, for example cubes, even then the relationship (31.4) is not satisfied: according to (31.4) we have that the mean height of the cube is equal to the length of its edge, whereas we have seen that the height of the cube varies between a and $1.732a$ and, consequently, its mean height in any case is greater than the length of the edge a . From the derived relationship (31.4) it would follow that the mean height of a body is singularly determined by its volume, which absolutely does not conform to reality, inasmuch as it is the shape of the body that plays the essential role. Mean heights of bodies of identical volume but of different shapes may differ considerably. On the basis of the aforesaid we arrive at the conclusion that the number of microparticles per unit volume cannot be determined on the basis of a parameter of the planar

structure alone, (that is, on the basis of the number of sections of microparticles per unit area of the plane of polish) even if microparticles are convex bodies. Later we shall demonstrate that the relationship of (31.3) type is valid in the case of bodies of equal size and identical shapes under the condition that a coefficient is introduced in it, the value of which is dependent upon the specific volume of microparticles of a given structural constituent and upon their shape. Therefore, in some instances formulas of this type may be used in practice but only as approximations. The exact solution requires, however, a determination of many parameters of a planar structure and is possible only when microparticles are of an identical shape and may be considered as convex bodies.

The precise solution of the problem becomes impossible if microparticles consists in that if a microparticle is not a convex body, it may be intersected by the plane of polish more than once, and several sections of one and the same microparticle, isolated and connected with each other, will be visible in the plane of polish. We have already cited such examples (see Section 5, Figures 5 and 6). It is possible to assert that in the case of convex microparticles the number of sections of particles per unit area is minimum with the number of microparticles per unit volume being the same.

In the light of the aforesaid, in passing it is possible to state that the long and widely practical metallographic evaluation of the "grain size", based on the mean size of the planar grain or on the number of planar grains per unit area of the plane of polish (standard E19 ASTM; GOST 565-51), cannot provide a correct notion of either the true size of spatial grain or the number of such grains per unit volume of metal. Although the technique of estimating the "grain size" from standard charts appeared for the first time in the U. S. A., American metal scientists also regard it as invalid [43, 18].

We have demonstrated that the most correct (from the viewpoint of the influence on the properties and behavior of metals), effective,

and at the same time, extremely simple quantitative characteristic of a polycrystalline structure is the magnitude of the specific surface area of crystallites (151). However, it happens that the determination of the number of microparticles per volume of alloy is absolutely necessary for the quantitative experimental study of the mechanism and kinetics of the crystallization process, during its various stages.

At the present time, there is available a number of methods of microanalysis, which permit determination of not only the total number of microparticles per unit volume from a planar structure but also determination of their size distribution. Unfortunately, all of these methods are applicable only to microparticles of one definite shape: spheroids. With a certain approximation they may be used for calculating the number and size distribution of spatially nonaqueous microparticles. Only approximate methods are available for the calculation of the total number of microparticles of other shapes.

Section 32. Determination of the Total Number of Flat Grains Per Unit Area of Microsection. The Planimetric Method and the Method of C. Jeffries.

The number of flat grains, determined directly under the microscope, in photomicrographs or a drawing, is usually given per one millimeter square area of the microsection; we shall adhere to this system in this article denoting the mean number of flat grains as n millimeter $^{-2}$. The only exception is the variation from the standard KSTM Table in which the number of flat grains is given per one square inch area of the microsection at linear magnification of 100, that is per area of the microsection equal to 0.0001 square inch or 0.0645 millimeter square. To convert the number of flat grains determined from this table to the number of flat grains per one millimeter square of the microsection n , it is necessary to divide the found number of grains by 0.0645 or to multiply by the factor $\frac{1}{0.0645} = 15.500$.

It is common practice to evaluate flat grains by the area of mean grain, F , usually determined in square microns. To convert this value into the number of grains n , in the case of a single-phase structure, it is possible to utilize the following relation:
(In original (32.1))

$$n = \frac{10^6}{F} \text{ MM}^{-2} \quad (32.1)$$

If the structure consists of several constituents, then the ratio of the number of flat grains to the mean area has another form:

(In original (32.2))

$$n = \frac{10^6}{F} \sum F \text{ MM}^{-2} \quad (32.2)$$

where $\sum F$ is a nondimensional quantity which expresses a section of the area of microsection occupied by the structural constituent whose grains are to be calculated, F is the mean area of one grain, micron square.

The fraction of the area $\sum F$ corresponds to the fraction of the volume called the alloy $\sum V$ occupied by the same structural constituent.

The most accurate technique for determining the number of flat grains in single-phase structures is the measuring of the area of one or several groups of grains with the aid of a planimeter outlining the outer grain boundaries bounding a given group of grains. After that the number of grains comprising the group are counted, accounting for all flat grains regardless of their size, including the most minute grains. The quotient of the calculated number of grains in a group divided by their total area, expressed in millimeter square, defines the mean number of grains per unit area of the microsection n . If for higher accuracy the calculation is done for several groups of grains, then the number of grains in the grain area are totaled separately for each group and the first number is divided by the second.

Planimetric measurements can be carried out on a photomicrograph or a drawing of the contour which bounds the given group of grains; the tracing can be made on the opaque glass of the microscope camera. In all cases it is necessary to determine accurately the magnification with the aid of an optic-micrometer and to convert the measured area to the corresponding area in the plane of polish. If the figure obtained is to express truly the mean value of the grain area and the mean number of grains, characteristic for the entire specimen, it is necessary to have photomicrographs or drawings of at least several fields of vision from different sections of the plane of polish.

The method of direct planimetric measurement is applicable only for pure metals or single-phase alloys and in those cases when the second structural constituent forms a very fine network along the grain boundaries of the principal structural constituent.

A very simple method for calculating a number of flat grains was proposed by C. Jeffries. After that it was recommended by the A.S.T.M. as E 2 (16). In the form it has been published it contains certain basic inaccuracies responsible for producing an error which in some cases is not permissible. The needed corrections, developed by us (17), make this method quite accurate and reliable without complicating it. For this reason, the corrected method of C. Jeffries is the basic method for the determination of the mean number of flat grains n and is applicable to grains of any structural constituent regardless of the total number of structural constituents.

There are two variants of C. Jeffries' method. In accordance with the first variant a circumference of 79.8 mm in diameter was drawn on the ground glass of the microscope camera or on the photomicrograph; magnification of 100 is a must. The actual area of the microsection, which at this magnification is found within the circumference, is 0.5 mm square. The number of grains g , which are entirely within the circumference (that is, are not intersected by it), is calculated; the number of grains w , which are bound by the circumference only in part, that is, intersected by it, are calculated separately. In this case the portal (reused) number in the area of the circumference is determined from the formula (in original (32.3))

$$X_1 = Z + 0.5 w \quad (32.3)$$

The number of grains n per one mm square of a microsection will be twice as large, since the area of the circle is 0.5 mm square. When other magnifications are used, the number of grains n per one mm square of the microsection is determined from the formula:

$$n = \frac{M^2}{5000} \quad X_1 = \frac{4X_1}{\pi D^2} \text{ mm}^{-2} \quad (32.4)$$

Where M is the linear magnification of the image on the ground glass or on the photomicrograph; E is the natural diameter of the circle (in the plane of polish), mm. Using the latter formula, it is possible to do calculations directly in the visible field of vision, having preliminarily measured its natural diameter D with the aid of an object-micrometer.

The method of C. Jeffries is based on the assumption that the circumference of the circle intersecting several grains on an average dissects them into two equal parts, that is, it is based on the assumption that the portal areas of grains, intersected by the circumference, within the circumference and outside of the circumference, are equal. This, however, is not quite so and because of that the formula which defines the reduced number of grains (32.3) is inaccurate.

If a considerable number of grains is intersected by a straight line drawn at random, then it is actually possible to assert in complete agreement with the theory of probabilities that the portal areas of grains, intersected by this line, was statistically equal on either side of the line. In other words, as the number of intersected grains is continuously increasing, the portal areas of these grains on either side of the straight line will be the closer approximation of the half of the area of intersected grains, the greater the number of the latter. However, by substituting a curve (circumference) for the straight line, as it was done by C. Jeffries, we create conditions which violate this postulate and which are responsible for producing a systematic error. Let us prove the aforesaid.

For the sake of simplicity we assume that the areas of all grains are equal and that the grains are of the same shape, which is a circle whose diameter is d . The number of grains, circles, in one mm square of area of the structure is n . The diameter of the circumference A , within which the grains are counted, is D (Figure 91). In this case a number of grains, circles, whose centers are within the circumference

will be: (32.5)

$$x = \frac{\pi D^2}{4} n \quad (32.5)$$

Let's denote the number of grains, circles, intersected by circumference A, as w, and their number within the circle entirely as c.

Let us draw two additional circumferences on circumference with diameter of $D + d$ and circumference B with diameter $D - d$. It is obvious that all grains, circles, whose centers are within the circumference B, will be entirely within the circumference A without being intersected by it. The number of such grains (circles) will be: (32.6)

$$z = \frac{\pi (D-d)^2}{4} n \quad (32.6)$$

Adversely, all grains (circles), with centers lying within a ring formed by two additional circumferences and B will have to be intersected by the principal circumference A. For this reason the number of intersected grains (circles) will be: (32.7)

$$w = \frac{\pi}{4} [(D+d)^2 - (D-d)^2] n \quad (32.7)$$

By totaling all of the grains (circles), which are entirely within the circumference A, and the fraction of grains k, intersected by circumference A, which as yet isn't known, and by equating this total to the number of grains (circles) x actually found within the circle whose diameter is D, we derive: (32.8)

$$x = z + kw \quad (32.8)$$

that is

$$\begin{aligned} & \frac{\pi}{4} (D-d)^2 n + k \frac{\pi}{4} [(D+d)^2 - (D-d)^2] n = (32.8a) \\ & = \frac{\pi}{4} D^2 n. \end{aligned}$$

hence we obtain

$$k = 0.5 - \frac{d}{4D} . \quad (32.9)$$

in C. Jeffries' formula (32.3) the coefficient k was arbitrarily given the value of one-half. This formula (32.9) it is apparent that this is possible only when the diameter of the grains (circles) is 0 or when diameter of the circumference, within which the calculation is made, is infinity, that is when it becomes a straight line. In all other cases, a systematic error will occur on the number of grains calculated therefrom C. Jeffries' formula (32.3) will be always greater than in reality. The error will be the greater. The larger the ratio of the grain (circle) diameter d to the diameter of the circumference D within which the calculation is made or, in other words, the smaller the number of grains within the circumference.

Let us calculate an error in the determination of the reduced number of grains (circles) using C. Jeffries' formula (32.3) instead of the corrected formula (32.8). The value of the systematic calculated error is determined in per cent from the formula:

$$\Delta = \frac{x_1 - x}{x} \cdot 100\% \quad (32.10)$$

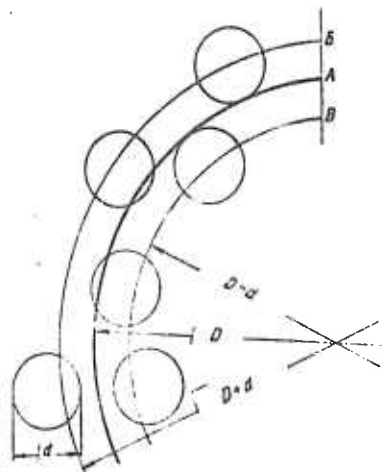


Fig. 91. Sketch to the derivation of formula (32.9)

Quantity x is calculated from formula (32.3) by substituting in it the values of z and w which for the given case are determined by precise formulas (32.6) and (32.7), respectively. Quantity x is also precisely determined by the formula (32.5). Omitting the calculation, we present the final simple relationship between the error Δ and the value of ratio $\frac{d}{D}$ or more precisely to the ratio of the areas of the grain and the circle within which the calculation is made:

$$\Delta = 100 \frac{d^2}{D} \% \quad (32.11)$$

By applying, with a certain degree of approximation, the considered case and formula (32.11) to the real single-phase polyhedral structures with equiaxed flat grains, it is possible to assume that the number of grains found within the circumference is

$$x = \frac{d^2}{D} \quad (32.12)$$

Using this relationship, we calculate the error and the value of the coefficient k in formula (32.8) for various values of the reduced number of grains found within a circumference when making the calculation using the first variant of C. Jeffries method. The data obtained are given in Table 33.

Table 33.

| 1. Количество зерен внутри окружности x | 2. Систематическая ошибка расчета, Δ % | 3. Коэффициент формулы (32.8) k | 4. Количество зерен внутри окружности x | 5. Систематическая ошибка расчета, Δ % | 6. Коэффициент формулы (32.8) k |
|---|---|-----------------------------------|---|---|-----------------------------------|
| 1 | 100,0 | 0,250 | 20 | 5,0 | 0,444 |
| 2 | 50,0 | 0,323 | 30 | 3,3 | 0,455 |
| 3 | 33,3 | 0,356 | 40 | 2,5 | 0,460 |
| 4 | 25,0 | 0,375 | 50 | 2,0 | 0,465 |
| 5 | 20,0 | 0,388 | 100 | 1,0 | 0,475 |
| 10 | 10,0 | 0,421 | 200 | 0,5 | 0,482 |

1. The quantity of grains inside circumference x .
2. Systematic calculating error $\Delta \%$.
3. Coefficient of the formula.
4. Same as 1.
5. Same as 2.
6. same as 3.

E.2-36 A.S.T.M. standard suggests that a number of grains in the area of the circle within which the calculation is made should be always not less than 50. In the meantime, if the count is made not on the photomicrograph or a drawing but visually, as it is usually done, an error can be easily committed when counting the number of intersected and, particularly, whole grains if the number of grains within a circumference is so large. Although in this case the total number of grains counted in several fields of vision may be infinitely large, the value of the systematic calculating error will be defined by the mean number of grains in one field of vision. For the convenience of the count, it is feasible to select a magnification at which the number of grains in one field of vision is 10 to 20, which predetermines the systematic error of 5 to 10 per cent without accounting for the random error common for any statistical method of analyses. This is the reason why in determining the number of grains within formula (32.3) but from the corrected formula (32.9) using the values of coefficient k given in Table 33.

The fact should be also taken into consideration that these values have been calculated approximately, inasmuch as they are also dependent upon the grain shape, and that the calculated error is valid only for the single-phase polyhedral structure with equiaxed grains. Considering the aforesaid, it is expedient to use the second variant of C. Jeffries' method for calculating the number of grains whenever it is feasible.

The second variant of C. Jeffries' method differs from the first one in that the count is made not within the circumference but within a square or a rectangle whose natural area (in the plane of polish) is 0.5 mm square. However, the latter is not obligatory. Just as in the first variant, the number of whole grains c is counted within the square or rectangle and the number of grains w intersected by their sides. After that the reduced number of grains x_1 is determined from the same C. Jeffries's formula (32.3) as in the preceding case.

Substituting a square for a rectangle for the circumference immediately prevents a systematic error which is due to the curvature of the contour bounding the area of the counted grains. However,

calculation of the reduced number of grains using formula (32.3) produces another source of systematic error. This source has the corner grains, that is those four grains which contain corners of the square or the rectangle within which the count is made. Therefore, the second variant of the method also requires a correction for C. Jeffries' formula. This correction, however, is much simpler and more accurate than for the first variant.

We have seen previously that a straight line intersecting several grains on an average dissects the grains into two sections of approximately equal areas. At the same time, the 90 degree angles at the corners of the square or the rectangle found in the plane of the grain on the average contain only 1-1/4 of the area. The latter is not accounted by C. Jeffries' Formula (32.3). In this case the error is also the greater and the smaller the number of grains found within the square or the rectangle.

In deriving the corrected formula, we took into account the fact that when taking the count of the grains within the square or the rectangle, the grains which are entirely within the boundaries of the contour must be fully taken into account (calculation factor of one); only half of the grains, which are intersected by the contour lines, should be taken into account. (The calculating factor is 0.5); one quarter of the grains, containing the surfaces of the contour should be taken into account (calculating factor is 0.25). Since the number of corner grains is always equal to 4, when taking the count in a square or a rectangle, the reduced number of grains x must be calculated from the formula:

$$x = z + 0.5w + 1 \quad (32.13)$$

where g is the number of whole grains within the rectangular contour; w is the number of grains intersected by straight lines of the contour excluding the four corner grains. This formula is the corrected formula we derived for the variant of C. Jeffries' method.

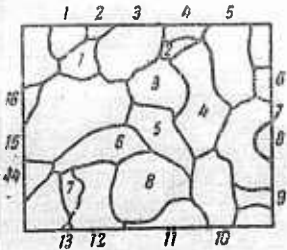


Fig. 92. Sketch of the computation of the number of flat grains on a unit of area in accordance with the corrected method of C. Jeffreys

This method and this formula are the most accurate and convenient for calculating the number of flat grains per unit area of the microsection in structures with any number of constituents and with an arbitrary shape of the grain. Let us consider its application, using as an example, the structure shown in Figure 92, magnification of 100. The actual area of the section shown in the figure is $0.6 \times 0.8 = 0.48$ mm square. The grains marked with Figures 1 and 8 are found within the rectangle in their entirety; their boundaries are not intersected by contour which bounds the area of the figure. Grains marked with Figures 1 through 16 have periphery of the figure are intersected by the sides of the rectangle. The grain marked with Figure 7 deserves attention. Although it is intersected by the contour and not the number of sections. We ignore the four grains at the corners of the rectangle contour for the formula (32.13) accounts for them. The reduced number of grains within the area of the figure is determined from C. Jeffreys' formula corrected by us: (in original marked I)

$$x = 8 + 0.5 \cdot 16 + 1 = 17$$

with the number of grains per 1 mm square of the plane of polish is correspondingly:

$$n = \frac{17}{0.48} = 35.5 \text{ mm}^{-2} \quad (\text{II})$$

To obtain a reliable mean value which characterizes the entire surfact of the plane of polish the count must be taken several times in several sections of the plane of polish uniformly distributed over its area. After that mean values of quantities of z and w are determined for all sections and substituted in

formula (32.13). In most cases a total count of 200 to 240 grains is quite adequate.

For a visual count it is possible to use a square grid ocular (Figure 14). However, this is somewhat inconvenient, for the lines of the ocular grid are superimposed on the grain boundaries and make a count difficult. It is much more convenient to use an ocular insert with a simple quadrant for a rectangle without additional lines. Grains may be also counted in a rectangular contour drawn on the ground glass of a microscope camera which makes it possible to mark down already counted grains.

Another technique of counting in a rectangular contour employs an ocular with a scale (Figure 13). During the examination the plane of polish is traversed in the direction directly perpendicular to the modular scale and its pass is recorded by the micrometric screw of the microscope stage. As the count is made in an elongated rectangle (*strip*) whose width is equal to the length of the ocular scale and whose length is equal to the path of the plane of polish with the microscope stage. The numbers of grains of two groups are continually and separately recorded while the plane of polish is being traversed on a. all grains that cross the ocular scale without touching its ends are counted and b. all grains that cross the end points of the scale aren't counted.

The grains of the first group are entirely within the contour of the examined strip and the number of these grains is equal to the value of c in formula (32.12). The grains of the second group are the grains intersected by the contour of the rectangle. For these grains it is necessary to add grains intersected by the ocular scale at the initial and final positions of the plane of polish, in order to obtain the value of w . Having examined the plane of polish of only one strip it is possible to repeat the examination and the count along another strip, etc. This method is particularly convenient for counting the grains of any one of the two or more structural constituents (carbide grains in steel, graphite precipitates in cast iron, dtc.).

S. 33. Determination of the Total Number of Flat Grains per Unit Area of Microsection. The Points-of-Juncture Method and Approximate Methods. p. 263.

In counting the number of grains per unit area difficulties arise due to the fact that some grains are found within the area enclosed within their regular contour (circle, square, rectangle), are invariably intersected by the contour lines which hinders the determination of the actual number of grains in this section, although the area of the section itself can be readily determined. If, however, a group of grains is enclosed within a contour drawn along their grain boundaries, a section with a complex contour is obtained whose area may be determined only with the aid of a planimeter, whereas the number of grains in the area may be calculated readily and accurately. If it were possible to substitute counting of some points for the counting of the number of elementary areas (grains), these difficulties would be automatically eliminated.

Consequently, the problem is reduced to finding such points in a plane of the polyhedral structure whose number would be correlated to the number of flat grains by a definite, singular relation. We shall demonstrate further in this section that such points are the junction points of flat grains. The method for determining the number of grains per unit area of the plane of polish proposed by us is based precisely on counting the number of these junction points. This method is applicable in the case of single-phase structures, as well as in those cases when the secondary structural constituent forms a fine network along the periphery of grains of the first constituent, which network does not hinder the determination of the location of the points-of-juncture of the grains.

The points-of-juncture method for counting grains is based on two postulates. The first one states that the number of converging flat grains at each juncture point is always equal to three. This is due to the mechanism of grain growth and is valid for all cases of real single-phase structures. The second initial postulate of the method is as follows: If straight lines are substituted for curved

pairs

boundary lines by connecting the corresponding points, the resulting system would be a system of convex polygons as shown in Figure 93. This is also due to the mechanics of the grain growth. However, in some instances it is not valid, particularly when the configuration is complex. Violations of this preface, that is, the fact that not always convex polygons are obtained, occur quite seldom and they can be ignored without essentially affecting the accuracy of determination. However, when the shapes of flat grains are complex, the error can be appreciable, and this must be kept in mind when using the points-of-juncture method.

Let us assume that we have a system of convex polygons which entirely fill the area subject to analyses and that three polygons always converge on one juncture point (Figure 93). Our reasoning runs as follows. From the elementary geometry it is known that the sum of angles of any convex polygon is: (In original marked II)

$$\pi (q - 2)$$

where q is the number of angles or a number of sides of the polygon.

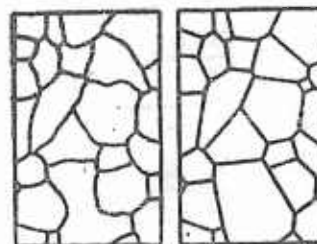


Fig. 93. Sketch to the derivation of the formula of the method of junction points

Let us assume that the number of triangles, quadrangles, pentagons, etc., in one mm square area of the plane of polish is n_1 , n_2 , n_3 , etc., respectively. The total number of all polygons in one mm square of the plane of polish we shall denote as n and the number of juncture points in the same area as M . The sum of angles of all n polygons is obviously $2M$. It is also true that this sum must be: (In original marked III)

$$2 M = \pi(3-2)n_1 + \pi(4-2)n_2 + \pi(5-2)n_3 + \dots \\ 2M = 3n_1 + 4n_2 + 5n_3 + \dots - 2(n_1 + n_2 + n_3 + \dots) = \\ = 3n_1 + 4n_2 + 5n_3 + \dots - 2n$$

Since three angles converge on each juncture point, the total number of angles per one mm square of polish is $3M$. At the same time, this number is: (In original marked IV)

$$3M = 3n_1 + 4n_2 + 5n_3 + \dots$$

By substituting this sum in the previously derived equation, we finally obtain: (In original marked 33.1)

$$\underline{M} = 2n \text{ mm}^2$$

From this formula it follows that having counted the number of juncture points M per unit area of the plane of polish and having divided this number by two, it is possible to determine the number of grains n per unit area of the plane of polish. If we were to observe a single-phase polyhedral structure, in which four flat grains would converge on each juncture point instead of three, as is the case, then the number of grains per unit area of the plane of polish would be equal to the number of juncture points in the same area.

Let us find the number of flat grains by the points-of-juncture method in structures shown in Figures 92 and 93 and compare the resulting figures with the values determined by the C. Jeffries' method. In Figure 93 the number of juncture points is 35. Consequently, the number of flat grains must be equal to one-half of this number, that is, 17.5. By using C. Jeffries' method we find: $c = 9$, $w = 15$. Consequently, the reduced number of grains from equation, (32.13) is: (In original marked V)

$$x=9+0.5 \cdot 15+1 = 17.5$$

Hence, the figures determined by both methods are in complete agreement.

In Figure 92 the number of juncture points is 33. Consequently, the number of grains is 16.5. Previously, by using C. Jeffries' method, we have found that the reduced number of grains for this pattern is 17.0. Here the difference of 0.5 of the grain is due to the presence of grain 8, which in C. Jeffries' method is accounted by the coefficient 0.5, but not accounted in our method, inasmuch as this grain has no juncture points within the confines of the figure. Generally speaking, a deviation is due to the complex grain shape.

For the calculation of juncture points, the contour of the area, within which the count is made, is of no significance. For this reason, the count may be made directly in the field of vision of the microscope, in a square, rectangle, or on a long strip by traversing the plane of polish as shown previously. When making a count in the microscope ocular, it is recommended to select magnification at which the field of vision contains not more than 10 to 12 juncture points. To obtain good accuracy, the total number of counted juncture points in a given analyses must be approximately 200 to 250; this requires about 5 to 6 minutes of observation. In those cases when not 3 but 4 grains appear to converge on the juncture point, it should be considered as two points, for this is the case of a very close location of two juncture points.

The points-of-juncture method is simpler and requires minimum time as compared with methods reviewed above. In accuracy it is inferior only to the planimetric method and to the second variant of C. Jeffries' method using the formula (32.13) corrected by us. The area of its application is single-phase polyhedral structures with not too complete configuration of flat grains.

In addition to above described methods, approximate methods for determining the number of flat grains are also widely used in metallographic examinations. These methods make use of standard

tables, chiefly GOFT 5639-51 table and E-19 A.S.T.M. table which approximates the former. For these methods the structures are divided into groups, each group being characterized by definite limits of the number of grains per unit area of the plane of polish and is evaluated by an arbitrary number of points or a number. The determination is usually made by a visual comparison of the analyzed structure against a set of standard photomicrographs or drawings.

The relation between the arbitrary number of the structure (number) and the natural area F of the mean grain, expressed in micron², is defined by the formula: (In original marked 33.2)

$$F = 500 \cdot 2^{(8 - N_2)} \text{ MM}^2 \quad (33.2)$$

For a single-phase structure this relation corresponds to the formula which correlates the number of grains per one mm square of the plane of polish to the number of the grain in the standard table: (In original marked 33.3)

$$n = 2000 \cdot 2^{(N_2 - 8)} \text{ MM}^{-2}$$

The variation limits of the mean grain size and of the mean number of grains per unit area are of greater significance than the values themselves for each number in the standard table, inasmuch as the parameters of real structures can correspond with a certain degree of precision to the mean values, determined by formulas (33.2) and (33.3) for whole values of the grain number only in exceptional cases. In the inch A.S.T.M. table the minimal and maximal limits for the number of grains is obtained by multiplying the mean number of grains for each number by 0.75 and by 1.5, respectively. In the GOFT 5639-51 table for the grain numbers from 1 to 6 the mean number of grains, determined by the formula (33.3), is multiplied by 0.8 in order to obtain a minimal limit for the number of grains of a given number and by 1.6 for the maximal limits. For grain numbers from 6 to 10 these factors are somewhat different: they are 0.833 and 1.667, respectively.

In Table 34 are given the mean values and the variation

limits for the area and the number of grains from the GOFT 5639-51 table. We have somewhat refined the figures for the number of grains; these figures are given with areas of grain of corresponding numbers. This was necessitated by the fact that a certain error was committed in GOFT 5639-51, which we have already mentioned in Section 3.

A variation using standard tables and, in particular, GOFT 5639-51 table, is the most inaccurate and rough of all methods reviewed above, since the number of grains doubles within the limits of each number in the table.

The only merit of determination in using a table is the rapidity of determination which is achieved at the expense of accuracy. In the three-dimensional micron analyses the application of evaluation using standard tables is quite limited.

It should be pointed out that methods for estimating the number of grains, proposed by Snyder and G. Graff (152, 153) and also by P. V. Konporshchikov (154) are in principle erroneous and should not be practiced in metallographic studies. The inaccuracy of the aforementioned methods is quite clear from the above considerations.

(End of tape)

Table 34

| № серии по ГОСТ 5639-51 | 2. Площадь зерна $F, \text{мк}^2$ | | | 3. Количество зерен $n, \text{мк}^{-2}$ | | |
|----------------------------------|-----------------------------------|----------------|-----------------|---|----------------|-----------------|
| | минимум мкм | среднее мкм | максимум мкм | минимум мкм | среднее мкм | максимум мкм |
| -1 | 160000 | 256000 | 320000 | 3,1 | 3,9 | 6,3 |
| 0 | 80000 | 128000 | 160000 | 6,3 | 7,8 | 12,5 |
| 1 | 40000 | 64000 | 80000 | 12,5 | 15,6 | 25,0 |
| 2 | 20000 | 32000 | 40000 | 25,0 | 31,3 | 50,0 |
| 3 | 10000 | 16000 | 20000 | 50,0 | 62,5 | 100,0 |
| 4 | 5000 | 8000 | 10000 | 100 | 125 | 200 |
| 5 | 2500 | 4000 | 5000 | 200 | 250 | 400 |
| 6 | 1200 | 2000 | 2500 | 400 | 500 | 833 |
| 7 | 600 | 1000 | 1200 | 833 | 1000 | 1667 |
| 8 | 300 | 500 | 600 | 1667 | 2000 | 3333 |
| 9 | 150 | 250 | 300 | 3333 | 4000 | 6667 |
| 10 | 75 | 125 | 150 | 6667 | 8000 | 13333 |

1. №. of grains according to GOST 5639-51
2. The area of grain $F, \text{мк}^2$.
3. Quantity of grains $p, \text{мк}^{-2}$.
 - a. minimum
 - b. average
 - c. maximum
 - d. same as a.
 - e. same as b.
 - f. same as c.

S. 34. Differentiation of Flat Grains by Size and Quantity.

The value of the total number of flat grains per one mm square of the plane of polish, n , particularly with certain other parameters of the planar microstructure make it possible to determine only the total number of microparticles for a given structural constituent per one mm cube of an alloy or pure metal from approximation formulas. A more precise determination of the total number of grains in a volume and particularly the calculation of the data for plotting a curve showing the size distribution of volumetric grains require a more detailed characteristic of planar grains, mainly classification of flat grains with respect to size with separately calculated number of grains in each size group.

The size of an individual flat grain may be characterized in two ways: either by its area or linear dimension. Grains are evaluated by the size of their areas singularly and various methods of this variation may differ only by the units of area (micron square, mm square, arbitrary units). The evaluation of linear dimensions of grains may have various approaches besides the difference in chosen linear limits of measurement. Thus, for example, standard E2-36 A.S.T.M. suggests that the size of flat grains of nonferrous metals be evaluated by the diameter of average grain in millimeters; this value is understood to mean the size of the side of a square whose area is equal to the area of average grain (16). At one time the author proposed that flat grains be evaluated by the diameter of a circle whose area is equal to the area of average grain (155). Finally, F. I. Smolenskiy and M. M. Zamyatin evaluated grains by the height of a regular hexagon whose area is equal to the area of the grain (156).

As we have already mentioned all methods of precise determination of the number of microparticles in a volume were designed for spheroidal microparticles whose intersection by a plain produces flat grains on the plane of polish; the flat grains are shaped as more or less regular circles. The mathematical calculation in all cases is also based on the spherical shape of

microparticles, whose circular sections are classified either with respect to the size of the diameter (E. Scheil and author's method) either with respect to the area (W. Johnson's method). Therefore, we shall consider the differentiation of flat grains based precisely on these parameters.

In both cases flat grains observed under the microscope or on photo-micrographs are grouped by size; the number of these groups is usually 5 to 15. The larger the number of groups, the more accurate and reliable is the picture of distribution of grains with respect to size or planer and spatial structures. This is the reason why it is desirable to have not less than 7 or 8 groups; the highest number of groups is rarely chosen higher than 12 or 13 in view of difficulties involved in a fine differentiation of grains. The grain count on any section of the plane of polish must include all grains without any exception: each grain must be evaluated by the size of the area or the diameter and placed in a proper group of grains. As we shall see further in this section, the role of fine grains is quite important. This is why this group of grains should not be ignored under any circumstances.

The fact that the visible number of grains is essentially dependent upon the magnification used should be taken into account. It is obvious that when the magnification is not sufficient, the finest grains become lost. In Figure 94 is shown the relationship of the number of all grains per unit area, n , and the mean area, F , through the linear magnification used during the count; this relationship was derived by Kostron and Dederichs (157) and quoted from (158). One and the same region of the microstructure was examined in each of four magnifications and the arithmetic mean value of the grain area was reduced from 214 micron square at the magnification of 100 down to 164 micron square at the magnification of 1000 due to the fact that new fine grains were revealed at higher magnification. At the same time, the use of high magnifications hinders the count of large grains which in this case are only partially in the field of vision. Because of that, in

a case of wide variation range of grain size, it is necessary to count the grains of different groups separately using two and even sometimes three different magnifications.

Direct classification of grains by the size of the diameter is possible only in those cases when the grain shape is sufficiently closely approximates the shape of a circle; this occurs relatively seldom (graphite precipitates in cast iron treated with magnesium or forgeable cast iron with pearlite base, cementite grains or grains of other carbides, etc.). When the count is made directly under a microscope, it is expedient to use an ocular micrometer with a scale divided into 100 parts (Figure 13). This scale is placed in a horizontal position in the field of vision. The magnification is selected such that the diameter of largest grains, subject to measurement, would be not less than 7 to 8 divisions of the scale and still better if it is 10 to 12 divisions. One division on the scale is taken as the size range of the diameter for each group. If, for example, the diameter for the largest grains is equal to 10 divisions of the scale, then the first group will comprise grains whose diameters range between 0 and 1 division, the second group will comprise grains whose diameters range from 1 to 2 divisions, the third group will comprise grains whose diameters range between 2 and 3 divisions, etc., and the last, the tenth group, will have grains whose diameters range between 9 and 10 divisions of the scale. Thus, the choice of the magnification also predetermines the number of groups. If the grain size range for one group, or the value of grouping, is denoted as Δ , then generally speaking the number of groups will be equal to the diameter of the largest grains divided by Δ . Initially the variation is carried out in arbitrary units, divisions of the ocular scale. After that (or previously) these units are mm in millimeters or microns with the aid of an object micrometer.

The microsection is traversed with the aid of the micrometric screw of the microscope stage or a two-way specimen traverse in

the direction strictly perpendicular to the ocular scale. During the movement of the microsection, as the centers of planes cross the ocular scale, each grain is evaluated by the side of the diameter, placed in a proper size group and recorded either on paper or by pressing the button of mechanical counter intended for counting grains of a given group. Those grains whose centers crossed the ocular scale during the examination along the one strip, the count is repeated along another strip, etc. Each time it is also necessary to take into account the length of strips, that is, the length of the traverse of the microsection right on the scale of the microscope stage or on the scale of the specimen traverse. Having obtained these values and having determined the length of the ocular scale in the plane of polish, we find the area of the grain counted.

Let us consider the figures of a concrete example of the differentiated count of the number of graphite grains precipitated in magnesium cast iron. The diameter of the largest precipitates is equal to 12 divisions of the ocular scale. Because of that and the value of breakdown equal to one division on the scale, we obtain 12 groups. The distribution of 346 precipitates, measured by this method, by the groups is presented in Table 35. This number of grains was counted in the area of microsection equal to 1.50 mm square (the length of the ocular scale is 0.476 mm, the length of the microsection traverse, 3.15 mm). Recalculating the numbers of grains for one mm square of the plane of polish and taking into consideration the fact that one division of the scale is equal to 4.76 microns, we derive a final data of the differentiated variation of flat grains of graphite shown in Table 36. These data can be used to plot a systogram for flat grains of graphite showing their distribution as to the size of the diameter, or the frequency curve can be plotted. These data completely characterize the planer structure of graphite.

On photomicrographs, drawings, or on the ground glass of microscope cameras grains are measured with the aid of an ordinary

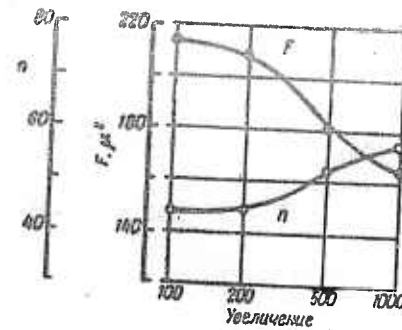


Fig. 94. Dependence of the visible number of grains on a slide \bar{n} and the average area of the grain F on the magnification in computing the grain (H. Kostron and Dederichs)

Table 35

| № группы зерен | 2. Диаметр зерен в делениях шкалы | 3. Количество зерен в группе |
|------------------------|-----------------------------------|------------------------------|
| 1 | 0-1 | 9 |
| 2 | 1-2 | 27 |
| 3 | 2-3 | 53 |
| 4 | 3-4 | 57 |
| 5 | 4-5 | 57 |
| 6 | 5-6 | 45 |
| 7 | 6-7 | 39 |
| 8 | 7-8 | 28 |
| 9 | 8-9 | 20 |
| 10 | 9-10 | 8 |
| 11 | 10-11 | 2 |
| 12 | 11-12 | 1 |
| <i>Total Всего</i> | 0-12 | 346 |

1. Nr. of groups of grains.
2. Diameter of grains in divisions of a scale.
3. Nr. of grains in a group.

1. Nr. of groups of grains
2. Diameter of grains
3. Nr. of grains in 1 mm^2
4. Nr. of grains %.

| № группы зерен 1. | 2. Диаметр зерен мк | 3. Количество зерен на 1 mm^2 | 4. Количество зерен % |
|----------------------------|---------------------|---|-----------------------|
| 1 | 0-4,76 | 6,0 | 2,6 |
| 2 | 4,76-9,52 | 18,0 | 7,8 |
| 3 | 9,52-14,28 | 35,3 | 15,2 |
| 4 | 14,28-19,04 | 38,0 | 16,5 |
| 5 | 19,04-23,80 | 38,0 | 16,5 |
| 6 | 23,80-28,56 | 30,0 | 13,0 |
| 7 | 28,56-33,32 | 26,0 | 11,3 |
| 8 | 33,32-38,08 | 18,7 | 8,1 |
| 9 | 38,08-42,84 | 13,3 | 5,8 |
| 10 | 42,84-47,60 | 5,3 | 2,3 |
| 11 | 47,60-52,36 | 1,3 | 0,6 |
| 12 | 52,36-57,12 | 0,7 | 0,3 |
| <i>Total Всего ...</i> | 0-57,12 | 230,6 | 100,0 |

Table 36

ruler with a mm scale. In the course of counting, the counted grains are marked in order to avoid a repetitious count of one and the same grains. Counting of the number of grains by groups can be accelerated by using the measuring caliper with counter device recently described by K. Chmutov (159).

In some instances it is expedient to break down the grains into groups where the variable value of breakdown Δ . Inasmuch as fine flat grains have a more appreciable effect on the results of calculation of the number of grains in a volume, then large grains, their relatively finer differentiation is applied to finer grains and a coarser one to large grains. For this purpose, the value of the breakdown Δ continually increases with increasing diameter of grains in each group. This increase in the value of the breakdown Δ a certain and definite lull. Thus, for example, in the method of "Inverse Diameters", developed by us, a table for diameters is used in which the value inverse to the diameter of a flat grain is a linear function.

If the grain shape deviates from the circular shape, then it is possible to determine the arithmetic mean value of the diameter of each grain by measuring the cross section of the grain in several directions. However, this procedure is not acceptable because it is laborious and doubles the number of measurements. For this reason, when there is a notable deviation of the grain shape from the shape of a circle, it is necessary to substitute visual evaluation for direct measurement of the diameter. For this evaluation it is more reliable to compare not the linear grain dimensions but its area against the area of figures in the appropriate table; the diameter should be determined as a diameter of an equivalent circle. Inasmuch as the area of the grain is proportional to the square of its diameter, the operator is more apt to distinguish the difference in the area than in the size of the diameter during the visual evaluation. Consequently, although it is disadvantageous to substitute a variation by visual comparison for the direct measurement of linear grain size, the

sensitivity of measuring grain area is greater than measuring diameter.

Different scales are used for evaluating the area of individual grains. These tables differ as to the type of shapes against which the grains are compared, variation of the area of shapes from one group to another and the limits of variation of areas of shapes in each group. After a group has been determined, within whose limits the area of the grain which is being evaluated falls, we can at will characterize the grain either by the size of the area or by the diameter of a circle of equal area.

W. Johnson's table is the same A.S.T.M. table modified for the individual variation of grains and has a somewhat modified notation. Thus, the area of the grain, designated in the A.S.T.M. table as No. 1, is equal to one square inch. In W. Johnson's table it is given as two square inches; the area of grain No. 2 is given as one square inch, No. 3 as one-half square inch, etc. The comparative table represents a series of squares arranged of one within another in such a manner that all squares have a common center and their sides are parallel. The areas of the squares correspond not to whole numbers but halves: -0.5, +0.5, 1.5, 2.5, 3.5, 4.5, etc. The effect of the side of each consecutively larger square is derived by multiplying the length of the side of the preceding square by the factor of 2 to $\frac{1}{2} = 1.41$ and the areas by the factor of 2. The area bound by each pair of consecutive squares corresponds to the definite number in the table with variation limits of the mean area between 0.71 and 1.41 of its value. For example, the larger square, which is the upper limit of the area of the grain No. 5, at the same time near the lower limit of the area of the grain No. 4, etc. For the variation of nonequiaxed grains a table is used which is compiled in the same way but which consists of rectangles with the ratio of sides 1 to 2. We are not giving W. Johnson's table because it employs an inch scale and we shall not need it further in this section; however, the principle of its construction will be utilized.

In the A.S.T.M. table and in almost identical W. Johnson's table the factor by which the areas of each consecutive group varies is 2 or $\frac{1}{2}$. Because of that these tables are two coarse for the purposes of quantitative micro-analyses. Tables described by H. Kostron and D. Derichs (157), W. Dickenscheid (158), et al, provide the possibility of a finer differentiation.

In H. Kostron and D. Derich's table the ratio of areas of the figures in adjacent grain groups is one to $10^{\frac{1}{4}} = 1$ to 1.78.

Practice shows by visual comparison it is possible to classify reliably areas of grains if the variation factor of the area is given smaller than in the H. Kostron's scale. Because of that W. Dickenscheid uses the coefficient of $10^{1/3} = 1.33$. The comparative table of the latter is made up of squares and rectangles whose sides are in ratios of 1/2, 1/4, 1/8, and 1/16, and is drawn for several magnification variants: 1X, 10X, 100X, and 1,000X; 2X, 20X, 200X, and 2,000X; and 5X, 50X, 500X, and 5,000X. This table can be used for classification of grains not only with respect to the size of their areas but also with respect to their shapes; it is used for differentiating a variation of grain of deformed metal (158, 160).

Attention should be paid to the fact that all of the tables described are logarithmic, that is, logarithms of the areas of grains of consecutive groups are linear functions. In Kostron and Derich's and in W. Dickenscheid's tables the variation factor of the area is 10 to the power of 1/4 and 1/8, respectively. This is why the exponent of each number in the table is also a common logarithm of the mean area of the grain expressed, for example, in micron square.

As an example we shall give a differentiating evaluation of a number of grains of a fine aluminum, rolled with reduction of 50 per cent, and then annealed at 300 C for 150 hours (for Dickenscheid (158)). The results of this evaluation, given in Table 37, account separately for grains with different ratio of width to length. This makes it possible to determine the relative area of the plane of polish filled with grains with various degrees of deformation.

By classifying isolated grains, with sufficiently round shapes,

by the size of the diameter, we obtained, as it has been previously described, the numbers of grains of each size in a definite area of the plane of polish. These numbers were recalculated for 1 mm square (see Tables 35 and 36). In single-phase polyhedral structures, by classifying grains by areas we found the size of the area of the plane of polish, in which the count was made as a total area of all counted grains under *compulsory* condition that all grains were counted. Thus, for the data in Table 37, the figures above indicate that the count was made in the area of the plane of polish equal to 1.99 mm square. Having divided the number of grains in each group by this value, we obtained the absolute distribution of grains per one mm square of the plane of polish.

| Grain size mm ² | 2. Number of grains mm ² | 2. Numbered width & length mm ² | | | 3. Number of grains mm ² |
|-------------------------------|--|--|-----|-----|--|
| | | 1/4 | 1/2 | 1/6 | |
| 2 ^{1/2} | 133 | 5 | — | — | 3 |
| 2 ^{2/3} | 178 | 1 | 5 | — | 6 |
| 2 ^{3/4} | 237 | 3 | 2 | — | 5 |
| 2 ^{4/5} | 316 | 4 | 4 | 2 | 10 |
| 2 ^{5/6} | 422 | 5 | 10 | — | 15 |
| 2 ^{6/7} | 562 | 4 | 8 | 1 | 13 |
| 2 ^{7/8} | 750 | 10 | 5 | 3 | 18 |
| 3 ^{1/2} | 1000 | 14 | 19 | — | 33 |
| 3 ^{1/3} | 1330 | 15 | 25 | 5 | 45 |
| 3 ^{1/4} | 1780 | 15 | 25 | 2 | 42 |
| 3 ^{1/5} | 2370 | 25 | 19 | — | 44 |
| 3 ^{1/6} | 3160 | 19 | 21 | — | 40 |
| 3 ^{1/7} | 4220 | 22 | 24 | — | 46 |
| 3 ^{1/8} | 5620 | 14 | 16 | — | 30 |
| 3 ^{1/9} | 7500 | 14 | 28 | 4 | 46 |
| 4 ^{1/2} | 10000 | 8 | 6 | — | 15 |
| 4 ^{1/3} | 13300 | 7 | 10 | — | 17 |
| 4 ^{1/4} | 17800 | 2 | 7 | — | 9 |
| 4 ^{1/5} | 23700 | 2 | 6 | — | 8 |
| 4 ^{1/6} | 31600 | — | 3 | — | 3 |
| <i>Total</i> | | 189 | 243 | 18 | 450 |
| <i>Bcero</i> | — | | | | |

1. Logarithms of the surface of grains.
2. Grain surface in MK^2 .
3. No. of grains with a ratio of width to length
4. Total no. of grains.

Table 37

If the grain shape is not round, which necessitates a visual evaluation, but the structure is not single-phase, we shall obtain as a result of evaluation of a definite number of grains only a relative distribution with respect to size. In this case it is necessary to carry out an independent determination of the total number of grains per one mm square of the plane of polish, using methods described in Sections 32 and 33. If the differential count of grains accounts only for c grains and the total number of grains per mm square of the plane of polish is found to be n , then the number of

grains in each group is multiplied by the ratio $\frac{N}{G}$ and the absolute distribution of grains per one mm square of the plane of polish is determined.

Further processing of the initial data, obtained by differentiation of grains by the size of the diameter or the area, can be accomplished by various methods determined by the technique of calculating the total number and distribution of grains in the volume or metal or alloy. The most important parameters of the planer structure for the purpose of quantitative micro-analyses are the following:

- A. Arithmetic mean values of the diameter d or of the area F of grains, determined respectively in millimeters or in micron square.
- B. The root mean square deviation of these values, determined in the same units, $\sigma(d)$ or $\sigma(F)$.
- C. The total number of flat grains per one mm^2 square of the plane of polish, n .
- D. The total area of all flat grains per one mm^2 square of the plane of polish, $\sum F$, which is identical to the total volume of corresponding microparticles in one mm^3 cube of the alloy, $\sum V$.

All these values can be readily calculated if the initial data, similar to the data shown in Tables 35, 36, and 37, are available. Simultaneously with the differentiation of grains we also determine the fraction of the volume of the alloy filled with microparticles of the constituent which is being analyzed. In single-phase structures this fraction is one. To obtain reliable data it is necessary in general to count at least 200 grains measured in various regions uniformly distributed over the area of the plane of polish. All grains must be evaluated and counted within the confines of each region. For the differentiation analyses of grains the surfact finish of the micro-section is of great importance. It must have a minimum relief.

Section 35. Systems of Spheres and Their Intersections with a Plane.

S. A. Saltykov's Method of Invers Diameters.

As has been mentioned, with the exception of certain approximate methods, all methods developed for the calculation of the number of microparticles in a volume have applied only to spherical-shaped microparticles (31). For this reason, let us consider the relationship between the 3-dimensional parameters of a system of spheres and parameters of their cross sections on a plane randomly intersecting the system.

A monodispersed system of spheres is a multitude of spheres of the same diameter D , the centers of which are randomly but statistically uniformly, arranged in space. If N is the mean number of spheres per unit volume, then it is possible to state that two values, D and N , completely characterize the spatial system of spheres. Let us intersect a monodispersed system by a random plane and designate as n the number of sections of spheres per unit area. It is quite obvious that this plane can and must intersect all those spheres whose centers are found on both sides of the plane at a distance not exceeding half of the sphere diameter D . Consequently, the centers of all n spheres, intersected by a plane the area of which is equal to unity, are found within the volume of a rectangular prism the base of which is equal to the unit of area and the height is equal to the diameter of spheres, D . It is obvious that the volume of such a prism is equal to D cubic units. Inasmuch as there are n spheres in a volume equal to D , their number per unit volume N must be:

$$N = \frac{n}{D}.$$

The relationship (35.1), derived for the first time by I. L. Mirkin, [33] (35.1).

Now let us go on to a more complex polydispersed system of spheres having different diameters. Such a system may be characterized by three parameters: the mean number of spheres, \bar{N} , and root-mean-square deviation of the diameter, $\sigma\{D\}$. Separating spheres as to size, let us assume that spheres of the following sizes are found in unit volume:

N_1 number of spheres of diameter D_1

N_2 number of spheres of diameter D_2

.....

N_k number of spheres of diameter D_k .

Let us designate the number of sections of spheres per unit area, as n_1, n_2, \dots, n_k , which belong respectively to spheres of the first, second, ... k -th size. Then, regarding each group of spheres of the same diameter as a monodispersed system, we can write a number of equations in conjunction with Formula (35.1) of I. L. Mirkin:

$$n_1 = N_1 D_1$$

$$n_2 = N_2 D_2$$

.....

$$n_k = N_k D_k$$

Summing up separately all right and left halves of these equations, and having designated the total number of sections of spheres of all sizes per unit area as n , we derive:

$$n = n_1 + n_2 + \dots + n_k = N_1 D_1 + N_2 D_2 + \dots + N_k D_k .$$

The right half of the latter equation, divided by the total number of spheres of all sizes per unit volume N , represents the arithmetic mean value of the diameters of spheres \bar{D} of a polydispersed system.

This is quite apparent. Therefore, finally we derive:

$$\bar{D} = \frac{N_1 D_1 + N_2 D_2 + \dots + N_k D_k}{N} = \frac{n}{N} . \quad (35.2)$$

This formula, derived by us, establishes the relationship among the number of spheres per unit volume, the number of their sections per unit area, and the arithmetic mean value of diameter of spheres for polydispersed systems of spheres and, consequently, for real systems of spherical microparticles.[17]. Formula (35.2) is a relationship between the aforementioned parameters in a general form, whereas Formula (35.1) is its specific case for a monodispersed system of spheres. However, the Formula (35.2) itself is also a specific case for an even more general relationship which we established previously for a system of convex bodies of any shape and any dimensions and expressed by the Formula (31.2). In a case

of a system of spheres, their mean diameter is obviously equal to the mean height of the body, \bar{H} , which is found in Formula (31.2).

Let us utilize the obtained relationship (35.2), and also other general relationships which correlate spatial and planar structures, in particular those relationships which have been established by us previously under the name of "The rule of summed projections for three-dimensions" (Section 27) for the case of a polydispersed system of spheres. Beside the already mentioned symbols for spatial quantities, let us designate the diameters of cross-sections of spheres on a secant plane as $d_1, d_2\dots$, and the corresponding number of sections per unit of its area as $n_1, n_2\dots$.

A. In conformity with the Cavalieri-Akera Acer principle, the relative amount (fraction) of a given phase in 1 mm³ of alloy and on 1 mm² of area of microsection must be one and the same. Therefore, the principle of Cavalieri-Akera makes it possible to correlate the sum of volumes of all spheres in 1 mm³ of space to the sum of areas of sections of these spheres on 1 mm² of the area, equating these values to each other. By introducing the abbreviated symbols for these sums, we can write:

$$\begin{aligned} \sum_i D_i^3 N_i &= \sum_j d_j^2 n_j \\ \sum_i D_i^3 N_i &= \frac{3}{2} \sum_j d_j^2 n_j. \end{aligned} \quad (35.3)$$

B. According to the law of total projection for space, the mean number of intersections, m with surfaces of a system, per 1 mm length of the secant, is equal to the total projection of all surfaces of the system found in 1 mm³ onto the plane perpendicular to the direction of the secant. (Section 27). In our case directions of the secant and of the plane are insignificant inasmuch as the system is isometric. Taking into consideration the fact that the total projection of the sphere is equal to twice the area of its central section (great circle) we can write:

$$m = 2 \sum_i \frac{D_i^2}{4} N_i = \sum_i D_i^2 N_i.$$

According to the law of total projection for the plane, the mean number of intersects m between the secant and lines of a

2-dimensional system, per 1 mm length of the secant is equal to the total projection of all lines of the system onto the line perpendicular to the secant (Section 23). In this case, the direction of the secant and of the line is also of no importance, inasmuch as the 2-dimensional system in question is isometric. Taking into account the fact that the total projection of a circumference is equal to twice the diameter, we can write:

$$m = 2 \sum_j d_j n_j.$$

For isometric systems, such as polydispersed system of spheres in space and a system of their sections on a plane, the mean numbers of intersects m per unit length of secants are equal in both instances. For this reason:

$$\begin{aligned} \sum_i D_i^2 N_i &= 2 \sum_j d_j n_j \\ \sum_i D_i^2 N_i &= \frac{4}{\pi} \sum_j d_j n_j. \end{aligned} \quad (35.4)$$

C. Finally, let us apply I. L. Mirkin's formula (35.2), which was generalized by us, according to which

$$\sum_i D_i N_i = n.$$

Here the total number of sections of spheres per 1 mm^2 , n , may be represented as the sum of zero powers of diameters of sections of all sizes, that is

$$n = \sum_j n_j = \sum_j d_j n_j.$$

Therefore,

$$D_i N_i = \sum_j d_j n_j. \quad (35.5)$$

Comparing the derived equations (35.3), (35.4), and (35.5), a definite regularity of structure may be noted in all three formulas: in each formula the sum of a given power of diameters of spheres, found in unit volume, corresponds to the sum of diameters of sections of spheres, found in unit area, whose power is one less, and also there are different coefficients of proportionality in each case. The total number of spheres per unit volume N is of interest to us. It may be represented as the sum of zero powers of diameters of all spheres in this volume, that is,

$$N = \sum_j N_j = \sum_i D_i^0 N_i.$$

In analogy with preceding equations, it is possible to assume that this value is proportional to the sum of diameters of sections of

spheres found in unit area, taken to the power of minus 1, or, in other words, proportional to the sum of inverse values of diameters of all sections in unit area. The formula which correlates these values has the following form:

$$\sum D_i N_i = \frac{2}{\pi} \sum d_j^{-1} n_j . \quad (35.6)$$

(the value of the coefficient of proportionality is discussed later in this article). To provide a more visual illustration of the analogy between the four considered equations they are listed in one table (Table 38).

| 1. Равенство | Коэффициент Σ | Размерность | Основание равенства |
|--|-------------------------|-------------|---|
| $\sum D_i^3 N_i = \frac{3}{2} \sum d_j^3 n_j$ | 1,500 | — | 5. Принцип Кавальерии дополненный Акером |
| $\sum D_i^3 N_i = \frac{4}{\pi} \sum d_j^3 n_j$ | 1,273 | mm^{-1} | 6. Метод случайных секущих, предложенный С. А. Салтыковым |
| $\sum D_i N_i = \sum d_j^3 n_j$ | 1,000 | mm^{-1} | 7. Обобщенная формула И. Л. Миркина |
| $\sum D_i^3 N_i = \frac{2}{\pi} \sum d_j^{-1} n_j$ | 0,637 | mm^{-1} | 8. Аналогия с предыдущими тремя равенствами |

7. The Ilmarkin generalized formula.

8. An analogy with the 3 previous equations.

Table 38

Let us prove the validity of equation (35.6) for the case of

a monodispersed system of spheres with diameter D , a number per unit volume, N , and a number of sections per unit area, n . The diameter of a section of a sphere, d_x , is determined by the distance x between the secant plane and the center of the sphere which it intersects. From elementary geometrical postulates it follows that the inverse value of the diameter d_x , depending upon the distance x , will be expressed by the equation:

$$\frac{1}{d_x} = \frac{1}{2\sqrt{\frac{D^2}{4} - x^2}} .$$

Any distance from the center of the sphere to a randomly drawn plane is equally probable. Therefore, we find the mean value of $\frac{1}{d_x}$ as the mean value of the aforementioned function integrated within the limits of possible values of quantity x , at which the

- 1. Equation
- 2. Coefficient
- 3. Dimension
- 4. Base of the equation.
- 5. Cavalier principle supplemented by Aker.
- 6. The method of random secants suggested by S.A. Saltykov.

sphere is actually intersected by the plane:

$$(M.O.) \frac{1}{d} = \frac{1}{D} \int_0^D \frac{dx}{\sqrt{\frac{D^2}{4} - x^2}} = \frac{\pi}{2D}. \quad (35.7)$$

Thus we have determined the inverse value of the diameter of a section of a sphere cut by a plane. We can find the sum of inverse values of diameters of all sections of spheres per unit area of the microsection by multiplying the derived value of the mathematical expectation by the number of cross sections n . Taking into consideration the fact that according to Formula (35.1) the ratio $\frac{n}{D}$ is equal to N , we derive:

$$\sum d_j^{-1} n_j = \frac{\pi n}{2D} = \frac{\pi N}{2},$$

hence, finally,

$$N = \frac{2}{\pi} d_j^{-1} n_j \text{ mm}^{-3}. \quad (35.8)$$

This equation has been derived under the supposition that diameters of all spheres are equal. However, inasmuch as the value of the diameter of spheres, D , does not enter the final formula (35.8), it is valid both for mono- as well as polydispersed systems of spheres. For example, let us assume that we actually have several groups of spheres of different diameters (however, diameters within each group are the same) and that we have a possibility for determining to which group belongs each of cross sections of spheres on a plane. Then it becomes absolutely immaterial whether we sum up separately all inverse diameters per unit area to find the total number of spheres of all groups, or sum inverse values of diameters for sections of each group of spheres, find separately the number of spheres in each group, and adding the derived numbers find the total number of spheres.

By way of analyses of obtained relationships, we can first of all state that all of them are mathematically rigorous. All formulas, beginning with (35.1) and terminating with (35.5), do not provide the possibility for determining the number of spheres or spherical microparticles in a volume, inasmuch as they contain other

parameters of the spatial structure which are not known to us.

Only the last formula (35.8) correlates the value N only with parameters of a plane structure, which parameters may be measured directly on a microsection.

This latter formula is precisely the formula of the method of inverse diameters, derived by us, which permits determination of the total number of spherical microparticles per unit volume of an alloy [68]. This method has been evaluated as distinguished by high accuracy [118], and its basic formula has been recently confirmed by A. G. Spektor, who analyzed a system of spheres by the method of distribution moments [161]. In the most general case, when all microparticles of the alloys are of different dimensions, having, however, at least approximately spherical shape, the total number of microparticles per 1 mm^3 of an alloy is defined as a sum of inverse diameters of all sections of microparticles (flat rings) found on 1 mm^2 on the area of microsection, multiplied by the coefficient, which is equal to 0.6366.

Having at our disposal a value of N found by the method of inverse diameters, and having experimentally determined on the microsection the mean number of sections per 1 mm^2 of the microsection, n , we can also find the second important parameter of the same structure: the mean diameter of spherical microparticles, \bar{D} , using Formula (35.2). ($\bar{D} = \frac{n}{N}$)

Now let us find a method for evaluating a third important parameter, which characterizes the distribution of spherical microparticles with respect to size: the root-mean-square deviation of the diameters of microparticles, σ_D . This value, in conformity to formulas of the theory of probabilities, is defined by the following expression:

$$\sigma^2(D) = \bar{D}^2 - (\bar{D})^2 \quad (35.9)$$

the arithmetic mean value of the squares of diameters of spherical microparticles, \bar{D}^2 . From the basic formula of the method of random secants for space (25.1), for the case of a polydispersed system of spherical microparticles, it follows that:

$$\sum S = \pi E d_i^2 N_i = 2m,$$

hence we find the unknown arithmetic mean value of the square of the diameters of microparticles:

$$\bar{D}^2 = \frac{1}{N} \sum d_i^2 N_i = \frac{2m}{\pi N}. \quad (35.10)$$

In the right half of the latter equation, in addition to already known quantity N there is also found the mean number of intersections m between random secants and boundary lines of sections of spherical microparticles, which we can easily determine experimentally on the microsection. Considering that in accordance with the law of total projection for a plane, $m = 2 \bar{d}n$ (35.10) we can somewhat modify the Formula (35.10):

$$\bar{D}^2 = \frac{4dm}{\pi N} = \frac{4}{\pi} \bar{d} \cdot \bar{D}. \quad (35.11)$$

In this case, instead of m it will be necessary to determine experimentally the mean diameter of sections of microparticles on the microsection, \bar{d} . Finding the value of \bar{D} from Formula (35.10) or Formula (35.11), we further determine from Formula (35.9) the value of the root-mean-square deviation of diameters of spherical microparticles, $\sigma \{D\}$, itself, inasmuch the value of the mean diameter of microparticles, \bar{D} , is already known.

Thus, to determine the three principal parameters which characterize a polydispersed system of spherical microparticles, we will have to determine experimentally, on a microsection, also three parameters of a plane structure:

A. The arithmetic mean of the reciprocal values of diameters of sections of microparticles on the microsection or, in other words, the mean harmonic value of these diameters, $\bar{d}^{-1} \text{ mm}^{-1}$.

B. The mean number of sections of microparticles per unit area of the microsection, $n, \text{ mm}^{-2}$.

C. The mean number of intersections between secants and boundary lines of sections of microparticles on the microsection, $m, \text{ mm}^{-1}$ or the mean value of diameters of these sections, $\bar{d}, \text{ mm}$.

From these three parameters of a plane structure the parameters of a spatial structure are calculated, using the following working

formulas:

$$N = 0.6366 \bar{d}^{-1} n \quad (35.12)$$

$$\bar{D} = 1.5078 (\bar{d}^{-1})^{-1}$$

$$\sigma^2_D = \sqrt{\frac{4}{\pi} \bar{d} \bar{D} - \bar{D}^2}$$

$$\sigma^2_D = \sqrt{\frac{2m}{\pi N} - \bar{D}^2}$$

An additional evaluation of the characteristic of a polydispersed system of spherical microparticles, just as in the case of any other system, is their total volume per mm^3 of alloy, equal to the total area of sections of microparticles per mm^2 of the micro-section.

The method of inverse diameters does not permit the experimental plotting, from points, of the distribution curve of spherical microparticles with respect to sizes (for example, with respect to diameters). However, we have the possibility, with minimum expenditure of effort as compared with other precision methods, of determining the basic parameters which characterize this statistical distribution.

In practice, the determination of the number of microparticles in a volume of alloy, N , is done in the following way. Diameters of sections of microparticles, observed through the ocular, on ground glass, photomicrographs or sketches, are measured with the aid of the ocular-micrometer scale or an ordinary scale and the figures obtained are converted to true values expressed in mm. When counting is done through the ocular, it is desirable to have a magnification in which five to seven sections (not more) are found in the field of vision. Measurements are not random: it is necessary to measure all sections, with the exception of those the centers of which lie outside the area which is being analyzed. Values, inverse to those and this produces the mean harmonic value of the diameters of sections, \bar{d} . Further, the derived mean harmonic value expressed in mm^{-1} is multiplied by the total number of sections, per unit area n , mm^{-2} the method of determination of which is known, and by the coeffi-

cient 0.6366 in conformance with Formula (35.12).

The technique may be somewhat modified. In a number of regions which have a similar area, or in a single region, the area of which is sufficiently large, reciprocal values of the mean diameters of all sections of microparticles found in the area which is being analyzed, are added. The obtained sum is recalculated for the true size; that is it is expressed in mm^{-1} then divided by the unit area of the microsection (1 mm^2) and multiplied by the coefficient 0.6366 in conformance with Formula (35.8). This method of determination is simpler than the preceding one. However, we derive only the value of N and cannot calculate other parameters without having at our disposal the mean harmonic value and the number of sections.

A portion of the structure of malleable cast iron, with spheroidal graphite precipitated on annealing, is shown in Figure 95. Measured diameters and their inverse calculated values are presented in Table 39. The actual area of the microsection used for measurements, is 0.325 mm^2 and the sum of inverse values of diameters on this area is 110.5 mm^{-1} . By dividing the unit area of the microsection into this sum we have $\frac{110.5}{0.325} = 340 \text{ mm}^{-3}$. The number of graphite centers precipitated on annealing per unit volume of cast iron will be

$$N = 0.6366 \cdot 340 = 216 \text{ mm}^{-3}.$$

If simultaneously with this we are to take into account the number of measured sections, which in the given example is 7, it is possible to determine the mean harmonic and the arithmetic mean values of the diameters of cross sections and their number per 1 mm^2 of the microsection, which makes it possible also to calculate the other parameters of the spatial structure, which characterize the size and distribution of microparticles of graphite.

In our example the number of sections of microparticles of graphite per unit area is:

$$m = 7/0.325 = 21.5 \text{ mm}^{-2}$$

The mean harmonic value of the inverse diameters of sections is

$$\bar{d}^{-1} = 110.5/7 = 15.8 \text{ mm}^{-1}$$

The arithmetic mean of the diameters of sections

$$\bar{d} = 0.58/7 = 0.083 \text{ mm.}$$

Having at our disposal all needed values, we find from Formulas (35.13) and (35.14):

$$\sigma \{D\} = \frac{\bar{D} = 1.5708/15.8 = 0.099 \text{ mm}}{\sqrt{\frac{4}{\pi} 0.083 \cdot 0.099 - (0.099)^2}} = 0.0266 \text{ mm.}$$

All spatial parameters calculated by us are naturally not reliable inasmuch as calculations are based on measuring only seven sections of microparticles. To obtain reliable results it is necessary to analyze an area of microsection which contains at least 200 to 250 sections of microparticles all of which must be measured and taken into account. The example, cited above, shows the great effect that cross-sections of small size have upon the results of calculation of the number of microparticles in a volume. This is the reason why in the microanalysis particular attention should be paid to thid group of sections.

From the data in Table 39 it is not difficult to compute the total area of sections of graphite precipitates on annealing and divide the obtained sum by 1 mm² of the microsection. This value will be equal to the volume fraction of the cast iron occupied by graphite.

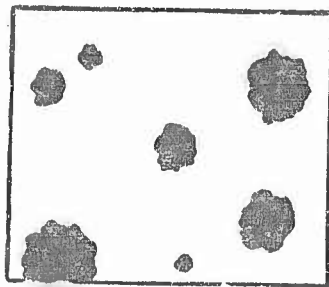


Fig. 95. Structure of wrought iron (sketch)

| A. Диаметр сечения d, мк | B. Обратная диаметру сечения единице d ⁻¹ , мк ⁻¹ |
|--------------------------------|--|
| 0,14 | 7,1 |
| 0,12 | 8,3 |
| 0,10 | 10,0 |
| 0,09 | 12,5 |
| 0,07 | 14,3 |
| 0,04 | 25,0 |
| 0,03 | 33,3 |
| 0,58 | 110,5 |

- 1. Diameter of a cross-section.
- 2. Dimension is opposite to the diameter of the cross-section.

Table 39

Section 36. Calculating the Size Distribution of Microparticles by
E. Scheil - G. Schwarz-S. A. Saltykov Method

Any polydispersed system of spheres may be regarded as consisting of several monodisperses systems. The larger the number of monodisperses systems into which we shall break down the spheres of the polydispersed system, the more complete will be the correspondence between the two. However, generally speaking, a complete correspondence between a polydispersed system and several monodisperses systems requires an infinitely large number of the latter. For practical purposes of steriometric microanalysis, breakdown of a polydispersed system of spheroid microparticles into 10 to 12 monodisperses systems would suffice.

Let us imagine a polydispersed system of spheres, in which spheres of maximum size are characterized by the diameter D_{\max} or D_m . Let us break down this system into, let us say, 10 monodisperses systems uniformly changing the size of the diameter of each of them. In that case all of the spheres of the first monodisperses system will have a diameter of $0.1 D_m$; that of the second will be $0.2 D_m$; the diameter of the third will be $0.3 D_m$, etc., and the diameter of the last system, of the tenth system, will be D_m . Each sphere of the polydispersed system we shall regard as belonging to that monodisperses system whose spheres' diameter is the closest approximation of the actual diameter of the sphere.

On a random secant plane, which intersects a system of spheres, we shall be able to observe their sections; moreover, it will be possible to note that the maximum possible diameter of a section will be also limited then by the value of D_m . Let us break down all the sections on the plane with respect to the size of their diameters also into 10 groups. Sections with diameters ranging between 0 and $0.1 D_m$ will fall into the first group; those with diameters ranging between $0.1 D_m$ to $0.2 D_m$ will fall into the second group; those with diameters ranging between $0.2 D_m$ and $0.3 D_m$ will fall into the third group, etc., and the diameters of sections of the last, tenth group, will range between $0.9 D_m$ and D_m . Let us

designate the number of sections of each size group per unit area as

$$n_1, n_2, n_3, \dots, n_{10}.$$

respectively.

By comparing the sizes of sections against the sizes of spheres, it is possible to conclude that all sections of the last group may belong only to spheres with the maximum diameter D_m , that is, to the spheres of the tenth group. Besides the largest sections, many others, with smaller diameters, may belong to the spheres of the tenth group. For spheres of diameter D_m to form on a plane sections with diameters ranging between $0.9 D_m$ and D_m , the mean distance between the centers of these spheres and secant plane must range between 0 and

$$\frac{D_m}{2} \sqrt{1 - (0.9)^2}$$

on both sides of the plane, i.e., within the volume equal to

$$D_m \sqrt{1 - (0.9)^2}$$

Since the number of sections in the tenth group is known to us and is n_{10} , using I. L. Mirkin's formula (35.1), we can readily find the number of spheres of the maximum size, D_m , per unit volume, which we shall designate as N_{10} :

$$N_{10} = \frac{n_{10}}{\sqrt{D_m \sqrt{1 - (0.9)^2}}} = 2.2941 \frac{n_{10}}{D_m}$$

Having determined the number of spheres of maximum size, we can calculate what number of sections in groups between the first and ninth, inclusive, belongs to these spheres. Let us subtract from the number of sections of the ninth group those sections which belong to spheres of maximum size, that is those of the tenth group. It is obvious that the remainder may belong only to the spheres of the ninth group, whose diameter is $0.9 D_m$. Applying this logic further, we can calculate the number of spheres of the ninth group and successively the number of spheres in all other groups.

The method of successive calculation of the number of spheroidal microparticles per unit volume of metal or alloy, the principle of which has been presented above, was developed for the first time by

E. Scheil [62, 63, 64], by using this method it is possible not only to determine the total number of microparticles in the volume but also to differentiate the particles with respect to size and plot experimentally by using points, a statistical curve of the distribution of microparticles with respect to the size of their diameter.

A shortcoming of E. Scheil's method is the need for successive calculation in the course of the determination itself, also the cumbersome aspect of the calculation.

The random error in calculating the number of microparticles of a given size predetermines incorrect results also for the number of microparticles of all smaller sizes. Therefore, numerous attempts were made at simplifying and improving the method by the author of the method himself as well as by other investigators.

Changing the sequence of calculations, proposed by G. Schwarz [65, 150], is effective. The method of E. Scheil-G. Schwarz makes it possible to calculate directly and independently the number of microparticles of any group with respect to size, using tables of previously calculated coefficients. Unfortunately, each group requires an independent table of coefficients. However, the latter have been calculated by G. Schwarz only for two variants of different shaded calculation: when microparticles are subdivided into five or ten groups. Division into five groups, as we shall demonstrate later, is insufficient and essentially affects the accuracy of determination. However, prerequisite division into ten groups is frequently difficult due to conditions of microanalysis.

A further rationalization of the method of E. Scheil-G. Schwarz was done by us [66]. This variant has the above enumerated advantages of E. Scheil-G. Schwarz's method, but at the same time it is free of its shortcomings. In our variant a direct calculation of the number of microparticles of any size group may be accomplished regardless of whether the number of microparticles of all other groups is known or not. Any number of groups can be used; only one table of coefficients, calculated by us for the number of groups up to 15, inclusive, is applicable for all cases (a larger number of

groups is generally not used). Taking into consideration the advantages of our variant, we shall describe only the procedure which has been improved by us, without cluttering the exposition by the description of the original methods of E. Scheil, and of E. Scheil and G. Schwarz.

Applying E. Scheil's principle of calculation, we regard the polydispersed system as consisting of a limited number of monodispersed systems of spheroidal microparticles; that is, we base our reasoning on the assumption that the diameters of microparticles of an alloy subject to analyses do not vary continuously but in steps, by jumps. We also assume that the maximum section, visible in the plane of polish, belongs to microparticles also with maximum diameter, the centers of which coincide with the plane of polish or are located very close to it. For this reason the maximum diameter of sections on the plane of polish is at the same time the diameter of microparticles of the maximum size, D_m . We break down all of the microparticles into groups, the number of which we choose depending upon the required accuracy of determination (this will be discussed later) and depending upon whether it is convenient to measure sections of microparticles under a microscope or on a photomicrograph. The magnification of the latter complies with the requirement that the largest diameter D_m would be expressed by an integer number of scalar divisions on the ocular-micrometer or measuring rule of not less than 7 or 8.

The term Δ , which is called "the factor for breaking down into groups" and which is equal to the ratio of the maximum diameter D_m to the number of groups K , is introduced into our calculations. It is obvious that the diameter of minimum microparticles of the first group will be equal to Δ , that of the second group will be equal to 2Δ , etc., and the diameter of maximum microparticles $K\Delta = D_m$. In Table 40 are listed designations of diameters and the numbers of microparticles with respect to groups, which we use when deriving the method of calculations.

As a result of intersection of microparticles of various sizes by the plane of polish, their sections formed on this plane are

shaped as circles, the maximum diameters of which may be equal to D and their minimum diameter may be equal to 0. Sections of microparticles on the plane of polish are subdivided with respect to the size of diameter into the same number K of groups into which all of the volumetric microparticles have been subdivided. The number of sections of each size and their diameters we shall designate in accordance with Table 41.

| № размечной группы микроочисток | Диаметр микрочисток мм | Количество в 1 см ³ |
|------------------------------------|---------------------------|--------------------------------|
| 1 | Δ | N_1 |
| 2 | 2Δ | N_2 |
| 3 | 3Δ | N_3 |
| ... | ... | ... |
| i | $i\Delta$ | N_i |
| ... | ... | ... |
| k | $k\Delta$ | N_k |

1. №. of dimensional groups of microparticles.
2. Diameter of microparticles. mm
3. №. in 1 cubic mm.

Table 40

| № размечной группы сечений микрочисток | Диаметр сечений микрочисток, мм | Количество на площади 1 см ² |
|---|---------------------------------|--|
| 1 | 0— Δ | n_1 |
| 2 | $\Delta—2\Delta$ | n_2 |
| 3 | $2\Delta—3\Delta$ | n_3 |
| ... | ... | ... |
| i | $(i-1)\Delta—i\Delta$ | n_i |
| ... | ... | ... |
| k | $(k-1)\Delta—k\Delta$ | n_k |

1. №. of dimensional groups of microparticle cross-sections.
2. Diameter of microparticle cross sections, mm
3. №. in a 1 cm² area.

Table 41

The microparticles, whose diameters are Δ , may form on the plane of polish sections of only minimum size (of the first group) whose diameters range between 0 and Δ . The microparticles, whose diameters is 2Δ , form on the plane of polish sections of both first groups, that is from 0 to Δ and from Δ to 2Δ , etc. The microparticles of the maximum size of K-th group form on the plane of polish sections of all K groups. In our further discourse the number of sections of microparticles per 1 mm^2 of the plane of polish will be designated as n with a subscript and superscript, namely: $j n_i$. The superscript j on the left designates the group of microparticles which has formed the given sections on the plane of polish. Subscript i designates the size group of sections of microparticles according to Table 41. Thus, for example, designation $3 n_2$ indicates the number of sections of the second size group (that is ranging in diameter from Δ to 2Δ), formed exclusively by the microparticles of the third size group, whose diameter is 3Δ .

From the aforesaid it follows that the total number of sections of the first size group, with diameters ranging between 0 and Δ , formed by microparticles of all sizes, will be

$$n_1 = {}^1 n_1 + {}^2 n_1 + {}^3 n_1 + \dots + {}^j n_1 + \dots + {}^k n_1.$$

The total number of sections of the next group, having diameters between Δ and 2Δ , formed by microparticles of all K groups with exception of the first, is

$$n_2 = {}^2 n_2 + {}^3 n_2 + {}^4 n_2 + \dots + {}^j n_2 + \dots + {}^k n_2$$

Let us examine the formation of sections on a plane by micro-particles of the j group having diameters equal to $j\Delta$. Sections of k -th group, having diameters ranging between $(i-1)\Delta$ and $i\Delta$, will be formed if the distance between the plane of polish and the center of microparticles which it intersects is between h_i and h_{i-1} , as illustrated in Figure 96. Consequently, the centers of microparticles must be inside of the volume limited by planes passing parallel to the plane of polish, at a distance of h_i and h_{i-1} on both sides of the plane of polish. If the area of the plane of polish in question is equal to 1 mm^2 , then in order to have

sections formed with diameters ranging between $(i-1)\Delta$ and $i\Delta$, the volume containing the centers of microparticles with diameter $j\Delta$, must be

$$2(h_i - h_{i-1}) 1 \text{ mm}^3$$

If 1 cubic millimeter contains N_j number of microparticles, the diameter of which is $j\Delta$, then the form on the area of the plane of polish equal to 1 mm^2 the number of sections with diameters ranging between $(i-1)\Delta$ and $i\Delta$, defined by the equation:

$$jn_i = 2(h_i - h_{i-1}) \cdot N_j$$

Terms h_i and h_{i-1} may be expressed readily geometrically through the values of diameters of microparticles and their sections in accordance with diagrams shown in Figure 96. Hence we derive:

$$jn_i = N_j \Delta \left(\sqrt{j^2 - (i-1)^2} - \sqrt{(j^2 - i^2)} \right) \quad (36.1)$$

Now we shall calculate the number of microparticles with respect to size, assuming that they are broken down into 1, 2 and 3 groups, so that the regularity of the formation of equations and coefficients can be determined for the calculation of the number of particles in each group.

A. Breaking down into one group. We assume that all microparticles are of one and the same size equal to maximum diameters of sections on the plane of polish, that is $D_m = \Delta \text{ mm}$. The number of microparticles per 1 mm^3 is N_1 and the number of their sections per 1 mm^2 of the plane of polish is n_1 .

In Formula (36.1) we assume that j and i are equal to unity and derive the following relationship:

$$n_1 = N_1 \Delta,$$

hence we find the number of microparticles per 1 mm^3 :

$$N_1 = \frac{n_1}{\Delta}. \quad (36.2)$$

B. Breaking down into two groups. All particles are broken down into two groups: N_1 microparticles have a diameter equal to Δ ; N_2 microparticles have twice as large a diameter, 2Δ .

Particles of the first group form on the plane of polish sections of the first size only, having diameters ranging between 0

and Δ . The number of sections which belong to them per 1 millimeter square of the plane of polish we can find from the formula (36.1), equating $j = 1$ and $i = 1$. We derive

$${}^1n_1 = N_1 \Delta .$$

The microparticles of the second group form sections of the first size (from 0 to Δ) as well as of the second size (from Δ to 2Δ). The number of both sections may be determined by substituting the values of subscripts and superscripts $j = 2$, $i = 1$, and $j = 2$, $i = 2$ into Formula (36.1). We derive

$${}^2n_2 = N_2 \Delta \sqrt{3} = 1.73205 N_2 \Delta = n_2 .$$

$${}^2n_1 = N_2 \Delta (2 - \sqrt{3}) = 0.26795 N_2 \Delta ,$$

From the latter equation we determine the number of microparticles of the second group, N_2 , in 1 mm^3 , for we know both the factor of breaking down into groups, Δ , and the number of sections of the second size (diameters from Δ to 2Δ), n_2 , determined from the plane of polish:

$$N_2 = 0.5774 \frac{n_2}{\Delta} .$$

(36.3)

The total number of sections of the first size (diameters from 0 to Δ), formed by microparticles both of the first and the second groups, is

$$n_1 = {}^1n_1 + {}^2n_1 = N_1 \Delta + 0.26795 N_2 \Delta .$$

Inasmuch as we already know the values of Δ , n_1 and N_2 (from Equation 36.3), we can also determine the number of microparticles of the first size in 1 mm^3 of an alloy:

$$N_1 = \frac{n_1}{\Delta} - 0.1547 \frac{n_2}{\Delta} .$$

(36.4)

Further there is no need for calculations similar to those cited above: in knowing Formulas (36.3) and (36.4) and having determined the values of n_1 , n_2 and Δ from the plane of polish

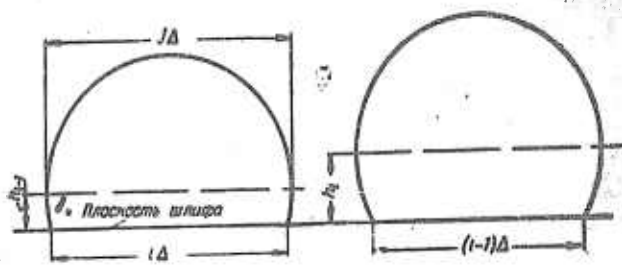


Fig. 96. Sketch to the derivation of the formulas for computing the number of spherical microparticles in a volume by the Sabsili-Saltykov method.

1. Surface of a micro-section.

we can calculate directly the number of microparticles both of the first and second groups, independently of each other.

C. Breaking down into three groups. Microparticles of the minimum size of the first group (diameter Δ), whose number is N_1 , form sections only of the first size (from 0 to Δ) on the plane of polish. Their number is defined by the Formula (36.1):

$$^1n_1 = N_1 \Delta.$$

The microparticles of the second group, whose number is N_2 , form sections both of the first and second sizes. Their numbers are respectively:

$$^2n_1 = 0,26795 N_2 \Delta \quad ^2n_2 = 1,73205 N_2 \Delta.$$

The microparticles of the third group, whose number is N_3 , forms sections of the first, second and third sizes. Their numbers are defined by the Formula (36.1):

$$^3n_1 = N_3 \Delta (3 - \sqrt{8}) = 1,17157 N_3 \Delta,$$

$$^3n_2 = N_3 \Delta (\sqrt{8} - \sqrt{5}) = 0,59236 N_3 \Delta,$$

$$^3n_3 = N_3 \Delta \sqrt{5} = 2,23607 N_3 \Delta.$$

By summing up the number of sections of the same size, formed by microparticles of different groups, we derive:

$$n_1 = ^1n_1 + ^2n_1 + ^3n_1 = N_1 \Delta + 0,26795 N_2 \Delta + 0,17157 N_3 \Delta,$$

$$n_2 = ^2n_2 + ^3n_2 = 1,73205 N_2 \Delta + 0,59236 N_3 \Delta,$$

$$n_3 = ^3n_3 = 2,23607 N_3 \Delta.$$

In the last of the three equations we know all terms with the exception of the number of microparticles of the third group, N_3 . Hence having determined N_3 and substituting the value obtained into the second equation we can also determine the value of N_2 .

and after that the value of N_1 from the first equation. Having carried out appropriate operations, we derive formulas which make it possible to determine the values of N_1 , N_2 , and N_3 not successively but directly and independently of each other, with n_1 , n_2 , n_3 and Δ determined from the plane of polish:

$$N_1 = \frac{n_1}{\Delta} - 0,1547 \frac{n_2}{\Delta} - 0,0360 \frac{n_3}{\Delta}, \quad (36.5)$$

$$N_2 = 0,5774 \frac{n_2}{\Delta} - 0,1529 \frac{n_3}{\Delta}, \quad (36.6)$$

$$N_3 = 0,4472 \frac{n_3}{\Delta}. \quad (36.7)$$

By comparing the formulas for the calculation of the number of microparticles of different sizes, when breaking down into 1, 2 and 3 groups, that is Formulas (36.2); (36.3), (36.4); (36.5), (36.6) and (36.7), common regularities in their form may be noted. The number of microparticles of each group is equal to the difference between the number of sections of the same size and the and the numbers of all sections are found in formulas with corresponding coefficients. Further it may be noted that for any number of groups, coefficients of numbers of sections n_1 , n_2 , n_3 are identical in formulas which define the number of particles of one and the same group. Actually, the coefficient of n_1 is equal to unity in Formulas (36.2), (36.4) and (36.5); the coefficient of n_2 is 0.5774 in Formulas (36.3) and (36.6), etc. Therefore, having once calculated the coefficients for breaking down into any number of groups, as it has been previously stated, we can use these coefficients in all cases and determine directly the number of microparticles of the group which is of interest to us, regardless of whether we know the number of microparticles in other groups. It is possible also to calculate directly the total number of microparticles of all

sizes.

From the formulas presented above which determine numbers N_1 , N_2 and N_3 for a different number of groups, we can conclude that all of these formulas in a general case have the following form:

$$N_x = \frac{A_k s_k - A_{k-1} s_{k-1} - \dots - A_1 s_1}{\Delta}$$

(36.8)

The values of coefficients A_k , A_{k+1} ..., calculated by us, are listed in Table 42 to 4 decimal points for the number of groups up to 15, inclusive. Breaking down into a greater number of groups in practice is difficult and is not needed. Breaking down into a number of groups less than 7 is not desirable and less than 5 is not permissible, although coefficients for such numbers of groups are listed in Table 42, inasmuch as they are used for breaking down into a greater number of groups. As an example let us consider the calculation procedure for a statistical curve of size distribution of cementite grains of spheroidized steel containing 1% C. The diameter of the largest section of grains in the photomicrograph, taken at the magnification of 2000, is 8 mm. For this reason we apply breaking down into 8 groups. Inasmuch as the actual diameter of maximum sections of grains in the plane of polish, D_m , is equal to 8 divided by 2000 equals 0.004 mm or 4 microns, the factor of breaking down:

$$\Delta = \frac{D_m}{K} = \frac{0.004}{8} = 0.0005 \text{ mm}$$

or 0.5 micron. Having measured a total of 500 grain sections and having determined their number per 1 mm^2 of the plane of polish, we obtain the initial data for the calculation of the number of grains in the volume, presented in Table 43.

The number of grains of the maximum size, whose diameter is 4 microns, is:

$$N_8 = 0,2582 \frac{n_8}{\Delta} = 0,2582 \frac{600}{0,0005} = 310000 \text{ mm}^{-3}.$$

Here the coefficient 0.2582 was taken from Table 42 for the eighth group of microparticles.

For example, the number of grains in the third group (grain diameter 1.5 microns) will be defined by the Formula (36.8) with coefficients taken from the third horizontal line in Table 42.

$$N_3 = \frac{1}{0,0005} (0,4472n_3 - 0,1382n_4 - 0,0408n_5 - 0,0178n_6 - 0,0093n_7 - 0,0057n_8) = 18780000 \text{ mm}^{-3}.$$

The number of cementite grains and grains of all other sizes is determined in the same way. The data obtained are presented in Table 44. The total number of cementite grains of all sizes is the formidable figure 45.45×10^6 per 1 mm^3 of steel.

If we were concerned only with this latter figure, that is with the total number of microparticles without subdivision into sizes, we could calculate it directly using Formula (36.8) and coefficients listed in the bottom horizontal line in Table 42. Tables of coefficients calculated by us, identical to those in Table 42, have also been presented in papers [66, 17 and 118].

On the basis of data of planar distribution, similar to those listed in Table 43, the calculation may be done quickly and accurately using coefficients of Table 42 and an adding machine. All negative products are summed up in an adding machine without an intermediate recording discarding the results of multiplication; only their total sum is recorded and subtracted from the positive product. The result is divided by the factor of breaking

down or multiplied by its reciprocal. Calculations with breaking down into ten groups, for example when using an adding machine "Feliks" takes about 25 to 30 minutes. It should be noted that quite frequently the number of calculated sections of minimum sizes happens to be low. This circumstance is revealed when calculating the number of microparticles in the volume, when the total of negative products in the right half of Formula (36.8) are greater than the positive product and the result due to that is negative. For this reason, cross sections of minimum sizes should be quite carefully taken into account.

Table 42

Coefficients

| | a_0 | a_1 | a_2 | a_3 | a_4 | a_5 | a_6 | a_7 | a_8 | a_9 | a_{10} | a_{11} | a_{12} | a_{13} | a_{14} | a_{15} | a_{16} | a_{17} | a_{18} | a_{19} | a_{20} | a_{21} | a_{22} | a_{23} | a_{24} | | | | | |
|----------|---------|---------|---------|---------|---------|---------|---------|---------|---------|---------|----------|----------|----------|----------|----------|----------|----------|----------|----------|----------|----------|----------|----------|----------|----------|---------|---------|---------|---------|---------|
| N^2 | +1.0000 | -0.1547 | -0.0350 | -0.0130 | -0.0051 | -0.0005 | -0.0005 | -0.0009 | -0.0013 | -0.0015 | -0.0015 | -0.0015 | -0.0015 | -0.0015 | -0.0015 | -0.0015 | -0.0015 | -0.0015 | -0.0015 | -0.0015 | -0.0015 | -0.0015 | -0.0015 | -0.0015 | | | | | | |
| N^3 | | +0.5774 | -0.1529 | -0.0490 | -0.0171 | -0.0057 | -0.0005 | -0.0011 | -0.0015 | -0.0015 | -0.0015 | -0.0015 | -0.0015 | -0.0015 | -0.0015 | -0.0015 | -0.0015 | -0.0015 | -0.0015 | -0.0015 | -0.0015 | -0.0015 | -0.0015 | -0.0015 | | | | | | |
| N^4 | | | -0.1382 | -0.0408 | -0.0176 | -0.0058 | -0.0017 | -0.0026 | -0.0026 | -0.0018 | -0.0018 | -0.0018 | -0.0018 | -0.0018 | -0.0018 | -0.0018 | -0.0018 | -0.0018 | -0.0018 | -0.0018 | -0.0018 | -0.0018 | -0.0018 | -0.0018 | | | | | | |
| N^5 | | | | -0.1263 | -0.0395 | -0.0179 | -0.0055 | -0.0017 | -0.0029 | -0.0029 | -0.0027 | -0.0027 | -0.0027 | -0.0027 | -0.0027 | -0.0027 | -0.0027 | -0.0027 | -0.0027 | -0.0027 | -0.0027 | -0.0027 | -0.0027 | -0.0027 | | | | | | |
| N^6 | | | | | -0.1263 | -0.0395 | -0.0179 | -0.0055 | -0.0017 | -0.0029 | -0.0029 | -0.0027 | -0.0027 | -0.0027 | -0.0027 | -0.0027 | -0.0027 | -0.0027 | -0.0027 | -0.0027 | -0.0027 | -0.0027 | -0.0027 | -0.0027 | | | | | | |
| N^7 | | | | | | -0.1161 | -0.0395 | -0.0179 | -0.0055 | -0.0017 | -0.0029 | -0.0029 | -0.0027 | -0.0027 | -0.0027 | -0.0027 | -0.0027 | -0.0027 | -0.0027 | -0.0027 | -0.0027 | -0.0027 | -0.0027 | -0.0027 | -0.0027 | | | | | |
| N^8 | | | | | | | -0.3015 | -0.1081 | -0.0346 | -0.0163 | -0.0091 | -0.0053 | -0.0032 | -0.0016 | -0.0016 | -0.0016 | -0.0016 | -0.0016 | -0.0016 | -0.0016 | -0.0016 | -0.0016 | -0.0016 | -0.0016 | -0.0016 | -0.0016 | | | | |
| N^9 | | | | | | | | +0.3015 | +0.1081 | +0.0346 | +0.0163 | +0.0091 | +0.0053 | +0.0032 | +0.0016 | +0.0016 | +0.0016 | +0.0016 | +0.0016 | +0.0016 | +0.0016 | +0.0016 | +0.0016 | +0.0016 | +0.0016 | | | | | |
| N^{10} | | | | | | | | | -0.2773 | +0.2773 | +0.2582 | +0.2582 | +0.2582 | +0.2582 | +0.2582 | +0.2582 | +0.2582 | +0.2582 | +0.2582 | +0.2582 | +0.2582 | +0.2582 | +0.2582 | +0.2582 | +0.2582 | +0.2582 | | | | |
| N^{11} | | | | | | | | | | -0.2425 | -0.2425 | -0.2425 | -0.2425 | -0.2425 | -0.2425 | -0.2425 | -0.2425 | -0.2425 | -0.2425 | -0.2425 | -0.2425 | -0.2425 | -0.2425 | -0.2425 | -0.2425 | -0.2425 | -0.2425 | | | |
| N^{12} | | | | | | | | | | -0.2294 | -0.2294 | -0.2294 | -0.2294 | -0.2294 | -0.2294 | -0.2294 | -0.2294 | -0.2294 | -0.2294 | -0.2294 | -0.2294 | -0.2294 | -0.2294 | -0.2294 | -0.2294 | -0.2294 | -0.2294 | | | |
| N^{13} | | | | | | | | | | | -0.2182 | -0.2182 | -0.2182 | -0.2182 | -0.2182 | -0.2182 | -0.2182 | -0.2182 | -0.2182 | -0.2182 | -0.2182 | -0.2182 | -0.2182 | -0.2182 | -0.2182 | -0.2182 | -0.2182 | -0.2182 | | |
| N^{14} | | | | | | | | | | | -0.2085 | -0.2085 | -0.2085 | -0.2085 | -0.2085 | -0.2085 | -0.2085 | -0.2085 | -0.2085 | -0.2085 | -0.2085 | -0.2085 | -0.2085 | -0.2085 | -0.2085 | -0.2085 | -0.2085 | -0.2085 | | |
| N^{15} | | | | | | | | | | | | -0.2030 | -0.2030 | -0.2030 | -0.2030 | -0.2030 | -0.2030 | -0.2030 | -0.2030 | -0.2030 | -0.2030 | -0.2030 | -0.2030 | -0.2030 | -0.2030 | -0.2030 | -0.2030 | -0.2030 | -0.2030 | |
| N^{16} | | | | | | | | | | | | -0.1925 | -0.1925 | -0.1925 | -0.1925 | -0.1925 | -0.1925 | -0.1925 | -0.1925 | -0.1925 | -0.1925 | -0.1925 | -0.1925 | -0.1925 | -0.1925 | -0.1925 | -0.1925 | -0.1925 | -0.1925 | |
| N^{17} | | | | | | | | | | | | | -0.1857 | -0.1857 | -0.1857 | -0.1857 | -0.1857 | -0.1857 | -0.1857 | -0.1857 | -0.1857 | -0.1857 | -0.1857 | -0.1857 | -0.1857 | -0.1857 | -0.1857 | -0.1857 | -0.1857 | -0.1857 |
| N | +1.0000 | +0.4227 | +0.2583 | +0.1847 | +0.1433 | +0.1170 | +0.0988 | +0.0856 | +0.0753 | +0.0672 | +0.0610 | +0.0553 | +0.0511 | +0.0472 | +0.0441 | | | | | | | | | | | | | | | |

| Группа | Диаметр сечений зерен мк | Количество сечений зерен на 1 см ² шлифа |
|----------|-----------------------------|--|
| 1. | 0.0-0.5 | $n_1 = 4500$ |
| 2. | 0.5-1.0 | $n_2 = 16500$ |
| 3. | 1.0-1.5 | $n_3 = 26550$ |
| 4. | 1.5-2.0 | $n_4 = 15600$ |
| 5. | 2.0-2.5 | $n_5 = 4350$ |
| 6. | 2.5-3.0 | $n_6 = 1050$ |
| 7. | 3.0-3.5 | $n_7 = 600$ |
| 8. | 3.5-4.0 | |
| Всего .. | 0.0-4.0 | $n = 78000$ |

1. group
2. diameter
of grains
Cross - sec-
tions
3. Nr. of grains
Cross - sec-
tions in 1
cm² area,

Table 43

| Группа 1. | Диаметр зерен мк | Количество зерен в 1 мм ³ 2. | Распределение, % 3. |
|--------------------|---------------------|--|------------------------|
| 1 | 0,5 | $N_1 = 1480000$ | 3,0 |
| 2 | 1,0 | $N_2 = 9340000$ | 20,5 |
| 3 | 1,5 | $N_3 = 18780000$ | 41,3 |
| 4 | 2,0 | $N_4 = 9930000$ | 21,8 |
| 5 | 2,5 | $N_5 = 2800000$ | 6,2 |
| 6 | 3,0 | $N_6 = 2350000$ | 5,2 |
| 7 | 3,5 | $N_7 = 460000$ | 1,0 |
| 8 | 4,0 | $N_8 = 310000$ | 0,7 |
| Всего . . Total | 0,5—4,0 | $N = 45450000$ | 100,0 |

1. Group
2. Diameter of grains
3. No. of grains in 1 cubic mm.
4. Distribution % .

Table 44

Section 37. Calculating the Size Distribution of Microparticles
by the W. Johnson-S. A. Saltykov Method

W. Johnson's method also retains the principle of E. Scheil, in accordance with which it is assumed that the size of microparticles varies steplike, discontinuously. However, W. Johnson uses the characteristic of the grain area for the initial differentiated evaluation of planar grains. In dividing planar grains into groups, a logarithmic scale of grain areas is used, that is, when going from the grain area of the maximum group to preceding ones this area is reduced each time by a definite number but not by a constant value. This number for W. Johnson's coefficient is taken as 2, just as in the ASTM scale. W. Johnson's evaluation scale, plotted on the inch scale, was briefly described in Section 34. Further, W. Johnson's reasoning is correct according to Cavalieri-Acer's principle that the total volume of microparticles, belonging to a definite size group and found per unit volume of metal, is equal to the total area of sections of these microparticles per unit volume of metal, is equal to the total area of sections of these microparticles per unit area of the plane of polish.

Using these premises, W. Johnson developed an experimentally simple method in which the calculation is done not by means of repeated multiplication, as in E. Scheil's method, but basically is limited to the subtraction operation, which, naturally substantially accelerates and simplifies the calculation. W. Johnson gives only the description of the application of the method, in the nature of instruction, and, in the words of the author, "leaving aside the involved mathematical analysis on which it (the method) is based". W. Johnson's method[18] has a definite value and interest, inasmuch as calculations are considerably less laborious than the calculation by the method described in the preceding paragraph, particularly when using tables of coef-

ficients compiled by the author of the method. Our experience confirms the data of the author that the time of calculations (excluding the derivation of initial data) is about 10 minutes; that is, one-third of the time when using E. Scheil's method, even when an adding machine is used in the latter case.

However, W. Johnson's method cannot be recommended in the form in which it was presented, for it has a number of shortcomings. The volumetric size of microparticles is evaluated by W. Johnson by arbitrary numbers similar to numbers of the standard ASTM scale for planar grains. The variation coefficient of the grain area of successive groups, which he assumes as two, makes the evaluation too rough, which has been noted previously (see also [158]). The inch scale apparently must be replaced by the millimeter scale. The method is applicable only to single-phase polyhedral structures or to structures in which the second constituent forms on the plane of polish an insignificantly fine network along the grain boundaries of the principal constituent. The mathematical calculation of the method contains certain inaccuracies.

However, the main, as to principle, shortcoming of W. Johnson's method consists in that the variation coefficient of the grain area in groups is represented by various powers of two and not by bases of the common and natural systems of logarithms.

We have demonstrated on several structures of various types that the statistical distribution of microparticles with respect to size is well described by the formula of logarithm-normal distribution [162]. In other words, the common (Gaussian) curve of the normal distribution provides a fine characteristic for the distribution of logarithmic values of the diameters of spheroidal microparticles. Therefore, the most rational scale for the classification of microparticle sizes is the linear logarithmic scale of their diameters. In contrast to the method of E. Scheil, the method of W. Johnson made it fully possible to introduce precisely this scale. However, the author of the method did not utilize this possibility.

In connection with the shortcomings of the W. Johnson's method, as noted above, we have introduced the required modifi-

cation and radically modified the method. In its new form it is being presented further in this section.

We break down the spheroidal microparticles into groups using the linear common logarithmic scale of diameters of microparticles measured in microns (in order that negative values of logarithms can be avoided in most cases). Inasmuch as microparticles, whose diameters are greater than 1 mm, are generally of no interest, the scale begins with the logarithm of the diameter equal to 3.0 and follows a descending order. The scale division was chosen as 0.1 of the common logarithm, so that all microparticles are divided into 30 groups in which the logarithms of the diameters of microparticles are 3.0, 2.9, 2.8, 2.7...0.4, 0.3, 0.2, 0.1. It does not mean, of course, that any real structure should be differentiated into the entire ³⁰ groups. In most cases the microparticle sizes of one object contain 7 to 10 and maximum 12 to 15 groups of the proposed logarithmic scale. This scale encompasses microparticles of spheroidal shape whose diameters range between 1 and 1000 microns. If necessary it may be easily extended both in the direction of large as well as small diameters. The division value, expressed as a common logarithm equal to 0.1, corresponds to the coefficient of transition of an area of a planar grain of one group to the next, higher group equal to 1.5849. If this value is compared with coefficients used in the ASTM and W. Johnson's (2.0) scales or in the scale of H. Kostron and Dederichs (1.78), it may be concluded that the scale chosen by us assures a finer differentiation of planar grains than these scales, although the coefficient in W. Dickenscheid's scale is even less (1.33).

The limits of the diameters of sections of spheroidal microparticles, corresponding to the logarithmic scale of diameters of microparticles themselves, chosen by us, are distributed by groups according to norms given in Table 45.

Now let us consider how the sections of a single sphere, the diameter of which is taken as 1000 microns, are distributed into the groups. From the diagram shown in Figure 97, it is apparent that

| № группы | Пределы логарифма диаметра сечений в группе | Пределы диаметра сечений в группе, мк | № группы | Пределы логарифма диаметра сечений в группе | Пределы диаметра сечений в группе, мк |
|-------------|---|---------------------------------------|-------------|---|---------------------------------------|
| 1. | 2. | 3. | 4. | 5. | 6. |
| 30 | 3,0-2,9 | 1000,0-794,3 | 18 | 1,8-1,7 | 63,10-50,12 |
| 29 | 2,9-2,8 | 794,3-631,0 | 17 | 1,7-1,6 | 50,12-39,81 |
| 28 | 2,8-2,7 | 631,0-501,2 | 16 | 1,6-1,5 | 39,81-31,62 |
| 27 | 2,7-2,6 | 501,2-398,1 | 15 | 1,5-1,4 | 31,62-25,12 |
| 26 | 2,6-2,5 | 398,1-316,2 | 14 | 1,4-1,3 | 25,12-19,95 |
| 25 | 2,5-2,4 | 316,2-251,2 | 13 | 1,3-1,2 | 19,95-15,85 |
| 24 | 2,4-2,3 | 251,2-199,5 | 12 | 1,2-1,1 | 15,85-12,59 |
| 23 | 2,3-2,2 | 199,5-155,5 | 11 | 1,1-1,0 | 12,59-10,00 |
| 22 | 2,2-2,1 | 155,5-125,9 | 10 | 1,0-0,9 | 10,00-7,943 |
| 21 | 2,1-2,0 | 125,9-100,0 | 9 | 0,9-0,8 | 7,943-6,310 |
| 20 | 2,0-1,9 | 100,0-79,43 | 8 | 0,8-0,7 | 6,310-5,012 |
| 19 | 1,9-1,8 | 79,43-63,10 | ... | ... | ... |

1. №. of groups.
2. Range of logarithms of the diameters of cross-sections in a group.
3. The range of cross-section diameters in a group
4. same as 1.
5. " " 2.
6. " " 3.

Table 45

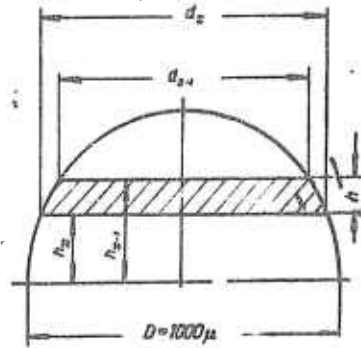


Fig. 97. Sketch to the derivation of the formulas for the computation of the number of spherical micro particles in a volume by the Johnson-Saltykov method

the height h of a spherical band, limited by parallel sections whose diameters d_x and d_{x-1} correspond to the upper and lower limits of the diameter value of any group in the scale shown in Table 45, will be defined by the expression

$$h = \frac{1}{2}(\sqrt{D^2 - d_x^2} - \sqrt{D^2 - d_{x-1}^2}).$$

The ratio of the number of sections of a sphere, whose diameters lie between d_x and d_{x-1} , to the number of all other possible sections of this sphere, is the same as the ratio of the height of the spherical band h to the radius of the sphere, equal to $\frac{1}{2}D$. This postulate is absolutely rigorous as a case of geometrical probability and does not require additional proofs. Therefore, by calculating the heights of spherical bands for all groups of the scale and by dividing the obtained values of h by the radius of the sphere (500 microns), we can find the relative distribution of planar sections of the sphere with respect to the groups of the scale. These data, also expressed in per cent, are given in Table 46.

The fact that the derived distribution is of a universal nature and is valid for a sphere of any size, if sections are grouped in accordance with the logarithmic scale presented by us (Table 45), is of extreme importance to us. For example, if the diameter of a sphere is not 1000 but 199.5 microns, will contain 60.75 per cent of all possible sections, and the group of the next size (whose diameters range between 125.9 to 158.5) will contain 16.83 per cent of sections, etc. This is the reason why the size distribution of sections, shown in Table 46, is valid both for any single sphere and for any monodispersed system of spheroidal microparticles.

After that, we have to determine the same scale group distribution of the areas of sections of each group expressed in fractions or per cent of the total area of all sections. In other words, we have to determine what fraction of the total area of sections of more dispersed spheroid microparticles on a plane would

Table 46

| No. groups | Номера групп сечений в группах, № | | |
|---------------|--------------------------------------|--------|--------|
| | 1. | 2. | 3. |
| 30 | 1000,0-794,3 | 0,0075 | |
| 29 | 794,3-631,0 | 0,1632 | |
| 28 | 631,0-501,2 | 0,0145 | |
| 27 | 501,2-399,1 | 0,0050 | |
| 26 | 399,1-316,2 | 0,0314 | |
| 25 | 316,2-251,2 | 0,0192 | |
| 24 | 251,2-199,5 | 0,0120 | |
| 23 | 199,5-158,5 | 0,0075 | |
| 22 | 158,5-125,9 | 0,0046 | |
| 21 | 125,9-100,0 | 0,0030 | |
| 20 | 100,0-79,43 | 0,0018 | |
| 19 | 79,43-63,10 | 0,0012 | |
| 18 | 63,10-50,12 | 0,0007 | |
| 17 | 50,12-39,81 | 0,0005 | |
| 16 | 39,81-31,62 | 0,0003 | |
| 15 | 31,62-25,12 | 0,0002 | |
| 14 | 25,12-19,95 | 0,0001 | |
| Total | | | 0,9998 |
| B.cero | | | 99,98 |

1. No. of groups
2. The range of cross-section diameters in a group.
3. Distribution of cross-sections of a ball according to size groups.
4. Portions of the total no. of cross-sections.

Table 47

| No. groups | Средняя пло- щадь сечения в группе $\bar{F}_i, \text{м}^2$ | Относитель- ное количе- ство сечений на поверхности | Произведение $F_i n_i$ | Относительное количе- ство сечений в группе номером | |
|------------|---|--|---------------------------|--|---------|
| | | | | 5. | 6. |
| 30 | 688794 | 0,0075 | 418442 | 0,79916 | 79,916 |
| 29 | 407832 | 0,1633 | 68638 | 0,13109 | 13,109 |
| 28 | 258040 | 0,0895 | 22916 | 0,04377 | 4,377 |
| 27 | 161253 | 0,0520 | 8385 | 0,01601 | 1,601 |
| 26 | 101646 | 0,0314 | 3192 | 0,00610 | 0,610 |
| 25 | 64101 | 0,0192 | 1231 | 0,00235 | 0,235 |
| 24 | 40439 | 0,0120 | 485 | 0,00093 | 0,093 |
| 23 | 25494 | 0,0075 | 191 | 0,00036 | 0,036 |
| 22 | 16091 | 0,0046 | 74 | 0,00014 | 0,014 |
| 21 | 10160 | 0,0030 | 30 | 0,00006 | 0,006 |
| 20 | 6412 | 0,0018 | 12 | 0,00002 | 0,002 |
| 19 | 4053 | 0,0012 | 5 | 0,00001 | 0,001 |
| | | | 523604 | 1,00000 | 100,000 |

5. Relative area occupied by cross-sections of a given group.
6. Portions of the total area of cross-sections.

be occupied by sections of each size group. Inasmuch as we do know the relative number of sections of each group (see Table 46), all we have to do is to find the mean area of section for each group on our scale. These values are calculated by dividing the volume, of a circular corresponding to a given group, by its height, and are presented in Table 47. Further, we multiply separately for

1. No. of groups
2. Average area of cross-section in group n_i
3. Relative no. of cross-sections on the surface n_i
4. Product $\bar{F}_i n_i$.

each group the relative number of sections in a group n_i by the mean value of the area of cross section F_i . The quotient of the product $F_i n_i$, will give us the size of the relative area occupied on a plane by sections of a given size group of the scale. These values are given in the last two columns in Table 47, in fractions of area and in per cent. The derived distribution of relative areas of the total of sections in each group, as well as previously derived distribution of the number of sections, are independent of the absolute dimensions of the sphere.

In summing up the calculations made for a single sphere, which means the same as for a monodispersed system of spheres or a system of spheroidal microparticles, it is possible to state the following. By distributing the sections of spheroidal microparticles of a monodispersed system on a plane, using the groups of our logarithmic scale (in accordance with norms in Table 45), by totaling after that the areas of sections within the limits of each group, and by dividing the totals derived by the total area of sections of all groups, we shall derive in all instances the distribution defined by the figures in the last two columns in Table 47. Regardless of the diameter of a microparticle of a monodispersed system, the sections of the corresponding maximum size will occupy the area equal to 79.916 per cent of the total area occupied by the sections of microparticles on the plane of polish. Cross sections of successive groups of smaller sizes will occupy respectively, areas equal to 13.109 per cent, 4.377 per cent, 1.601 per cent, etc. Thus, the distribution of total areas of sections with respect to the groups of the scale, derived by us, is a sliding distribution independent of absolute sizes of spheroidal microparticles of a monodispersed system. From the data presented it follows that division into 12, 10 and 7 groups exhausts the distribution up to 0.001 per cent, 0.01 per cent and 0.1 per cent of the area, respectively.

The aim of the calculations presented above was to establish the relative distribution of total areas of sections of each group, which is universal for any monodispersed system of spheres. It

is presented in Table 47 in the right-hand column.

For practical application of the method we use two working tables, the first of which is Table 48.

| Число груп. групп | Пределы логарифмов диаметров плоских зерен в группе | Пределы площадей плоских зерен в группе, мк ² | Средняя площадь плоского зерна мк ² | Объем зерна мк ³ | 1. Representative nr. of groups. |
|----------------------|---|--|--|-----------------------------|---|
| | | | | | 2. Range of diameter logarithms. of flat grains in a group. |
| 30 | 2,9--3,0 | 495556--785308 | 634918 | 523599000 | 3. |
| 29 | 2,8--2,9 | 312671--495556 | 400625 | 262421000 | |
| 28 | 2,7--2,8 | 197212--312671 | 252798 | 131521000 | |
| 27 | 2,6--2,7 | 124477--197212 | 159491 | 65917000 | |
| 26 | 2,5--2,6 | 78540--124477 | 100621 | 33037000 | |
| 25 | 2,4--2,5 | 49556--78540 | 63492 | 16558000 | |
| 24 | 2,3--2,4 | 31267--49556 | 40062 | 8299000 | |
| 23 | 2,2--2,3 | 19721--31267 | 25280 | 4159000 | |
| 22 | 2,1--2,2 | 12448--19721 | 15949 | 2084000 | |
| 21 | 2,0--2,1 | 7854--12448 | 10062 | 1045000 | |
| 20 | 1,9--2,0 | 4956--7854 | 6349 | 523599 | |
| 19 | 1,8--1,9 | 3127--4956 | 4006 | 262422 | |
| 18 | 1,7--1,8 | 1972--3127 | 2528 | 131521 | |
| 17 | 1,6--1,7 | 1245--1972 | 1595 | 65917 | |
| 16 | 1,5--1,6 | 785--1245 | 1006 | 33037 | |
| 15 | 1,4--1,5 | 496--785 | 635 | 16558 | |
| 14 | 1,3--1,4 | 313--496 | 401 | 8299 | |
| 13 | 1,2--1,3 | 197--313 | 253 | 4159 | |
| 12 | 1,1--1,2 | 124--197 | 159 | 2084 | |
| 11 | 1,0--1,1 | 78,5--124 | 101 | 1045 | |
| 10 | 0,9--1,0 | 49,6--78,5 | 63,5 | 524 | |
| 9 | 0,8--0,9 | 31,3--49,6 | 40,1 | 282 | |
| 8 | 0,7--0,8 | 19,7--31,3 | 25,3 | 132 | |
| 7 | 0,6--0,7 | 12,4--19,7 | 15,9 | 65,9 | |
| 6 | 0,5--0,6 | 7,85--12,4 | 10,1 | 33,0 | |
| 5 | 0,4--0,5 | 4,96--7,85 | 6,35 | 16,6 | |
| 4 | 0,3--0,4 | 3,13--4,96 | 4,01 | 8,30 | |
| 3 | 0,2--0,3 | 1,97--3,13 | 2,53 | 4,16 | |
| 2 | 0,1--0,2 | 1,24--1,97 | 1,59 | 2,08 | |
| 1 | 0,0--0,1 | 0,785--1,24 | 1,01 | 1,04 | |

Table 48

In accordance with the norms of this table, graphical comparative scales are compiled for the individual evaluation of each planar grain from its area. The table may be easily extended in both directions, since the same values of the limits of area are repeated every ten groups with the coefficient 10 or 0.1, and the values of the mean area reoccur with the same coefficient every five groups. The latter values, calculated by Simpson's law, differ somewhat from the values shown in Table 47, calculated for a single sphere.

Now let us discuss real polydispersed systems, limiting ourselves for the time being only to single-phase polyhedral structures with spatially equiaxed microparticles which fill space, although in the first approximation we assume them to be spheroidal. Let us consider the course of the analysis of a concrete structure of austenite grain of steel, developed by standard carburization.

Using norms of Table 48, we distribute the planar grains, which are being observed, into groups, visually estimating the area of each grain (not randomly). Having estimated all total 258 grains, we derive their distribution with respect to the groups of the logarithmic scale, shown in Table 49. The maximum planar grains, and consequently, the maximum microparticles correspond to the 25th group of the scale; that is, their diameter is $10^{2.5} = 316.2$ microns. We multiply the number of planar grains of each group by the mean area of the grain of this group (the value of it we find in the working Table 48). The product, preliminarily multiplied by 100, is divided by the total of products for all groups. The operations of this preliminary calculation are sufficiently clear in Table 49.

| Условный № группы 1. | Количество измеренных зерен* 2. | Средняя площадь плоского зерна, мк ² 3. | Суммарная площадь зерен 4. | Площадь зерен в % от плохости 5. |
|-------------------------|------------------------------------|--|-------------------------------|-------------------------------------|
| 25 | 4 | 63492 | 253968 | 9,25 |
| 24 | 12 | 40962 | 481744 | 17,60 |
| 23 | 17 | 25280 | 429760 | 15,65 |
| 22 | 38 | 15949 | 606062 | 22,07 |
| 21 | 44 | 10662 | 442728 | 16,12 |
| 20 | 45 | 6349 | 285705 | 10,40 |
| 19 | 34 | 4006 | 136204 | 4,96 |
| 18 | 27 | 2528 | 68256 | 2,49 |
| 17 | 17 | 1595 | 27115 | 0,99 |
| 16 | 11 | 1006 | 11066 | 0,43 |
| 15 | 5 | 635 | 3175 | 0,12 |
| 14 | 4 | 401 | 1604 | 0,06 |
| Всего | 258 | — | 2746387 | 100,00 |

1. Representative number of groups.
2. No. of measured grains
3. Average area of a flat grain.
4. Total grain area.
5. Area of the group of grains
% in all areas.

Table 49

Fractions of the area of the plane of polish, occupied by planar grains of each size group and expressed in per cent of the total area, are the initial data for further calculation of the number of microparticles in the volume. These initial data, for the example at hand, are listed in the extreme right column in Table 49.

From the previous discourse we know that planar grains of maximum size (in our case grains of the 25th group) are also formed by microparticles of the maximum size, belonging to the same group; they are formed only by those microparticles. We also know that if the entire 100 per cent of the steel volume were filled only with microparticles of the 25th group, then the planar grains of the same group would occupy 79.916 per cent of the total area of the plane of polish (see Table 47). In our case, the planar grains of this group occupy only 9.25 per cent of the area of the plane of polish, which follows from the initial data in Table 49. For this reason the total volume of microparticles of the 25th group in the volume of steel, expressed in per cent, is found very simply:

$$100 \Sigma V_{15} = \frac{9.25 \cdot 100}{79.916} = 11.57\%.$$

Some of the planar grains of other groups also belong to microparticles of the maximum group. This fraction may be readily found for each group using the same distribution of Table 47.

For example, the area of planar grains of the 24th group, belonging to the microparticles of the 25th group, will be equal:

$$\frac{11.57 \cdot 13.109}{100} = 1.52\%.$$

The area of planar grains of the 23rd group, belonging to the same microparticles of the 25th group, equals

$$\frac{11.57 \cdot 4.377}{100} = 0.50\%$$

etc.

Now we can go on to microparticles of the next, 24th, group. The area of planar grains of this group, excluding the edge portion belonging to microparticles of the 25th group (which we found to be 1.52 per cent) is formed entirely by microparticles

only of the 24th group. This area is

$$17,50 - 1,52 = 15,98\%.$$

We proceed with our reasoning. If the microparticles of the 24th group were to occupy 100 per cent of the volume of steel, the area of the planar grains of the 24th group would be 79.916 per cent of the plane of polish. Inasmuch as we found that it is only 15.98 per cent of the area, the total volume of microparticles of this group in the volume of steel, expressed in per cent, is

$$100 \Sigma V_{24} = \frac{15.98 \cdot 100}{79.916} = 20.00\%.$$

By means of successive calculations we can thus find the fractions of the volume of steel occupied by microparticles of each group. Knowing the volume of a microparticle of each group, it is possible also to calculate their number per unit volume of steel.

However, the course of successive calculation is quite cumbersome and laborous. Therefore, in order to avoid the successive calculation, in part presented previously, W. Johnson and auxiliary table. When using this table the calculation is basically reduced to a number of successive subtractions. The same kind of a table, calculated by us, is intended for the logarithmic scale proposed by us. This second working table is presented below (Table 50).

Relative areas on the plane of polish, occupied by planar grains of the largest size, in per cent, are listed in the first column of the table. As the maximum group of grains drops out, each remaining group in turn becomes maximum. Corresponding volumes, occupied by maximum microparticles, in volume per cent of steel, are listed in the second column. In next columns are given the relative areas of planar grains of successively smaller sizes, belonging to microparticles of the maximum size (also in per cent area). K signifies the maximum group of microparticles and sections

| Number of grain dimensions, K. No. | Percentage of grains with size K, % | 3. Площадь зерен K размера, % | | | | | | | | |
|--|--|-------------------------------|------|------|------|------|------|------|------|-----|
| | | R=1 | R=2 | R=3 | R=4 | R=5 | R=6 | R=7 | R=8 | R=9 |
| 1 | 1,25 | 0,16 | 0,05 | 0,02 | 0,01 | — | — | — | — | — |
| 2 | 2,50 | 0,33 | 0,11 | 0,04 | 0,02 | 0,01 | — | — | — | — |
| 3 | 3,75 | 0,49 | 0,16 | 0,06 | 0,02 | 0,01 | — | — | — | — |
| 4 | 5,01 | 0,65 | 0,22 | 0,08 | 0,03 | 0,01 | — | — | — | — |
| 5 | 6,26 | 0,82 | 0,27 | 0,10 | 0,04 | 0,01 | 0,01 | — | — | — |
| 6 | 7,51 | 0,98 | 0,33 | 0,12 | 0,05 | 0,02 | 0,01 | — | — | — |
| 7 | 8,76 | 1,15 | 0,38 | 0,14 | 0,05 | 0,02 | 0,01 | — | — | — |
| 8 | 10,01 | 1,31 | 0,44 | 0,16 | 0,06 | 0,02 | 0,01 | — | — | — |
| 9 | 11,26 | 1,48 | 0,49 | 0,18 | 0,07 | 0,03 | 0,01 | — | — | — |
| 10 | 12,51 | 1,64 | 0,55 | 0,20 | 0,08 | 0,03 | 0,01 | — | — | — |
| 11 | 13,76 | 1,80 | 0,60 | 0,22 | 0,08 | 0,03 | 0,01 | — | — | — |
| 12 | 15,02 | 1,97 | 0,66 | 0,24 | 0,09 | 0,04 | 0,01 | 0,01 | — | — |
| 13 | 16,27 | 2,13 | 0,71 | 0,26 | 0,10 | 0,04 | 0,02 | 0,01 | — | — |
| 14 | 17,52 | 2,30 | 0,77 | 0,28 | 0,11 | 0,04 | 0,02 | 0,01 | — | — |
| 15 | 18,77 | 2,46 | 0,82 | 0,30 | 0,11 | 0,04 | 0,02 | 0,01 | — | — |
| 16 | 20,02 | 2,62 | 0,88 | 0,32 | 0,12 | 0,05 | 0,02 | 0,01 | — | — |
| 17 | 21,27 | 2,79 | 0,93 | 0,34 | 0,13 | 0,05 | 0,02 | 0,01 | — | — |
| 18 | 22,52 | 2,95 | 0,99 | 0,36 | 0,14 | 0,05 | 0,02 | 0,01 | — | — |
| 19 | 23,77 | 3,12 | 1,04 | 0,38 | 0,15 | 0,06 | 0,02 | 0,01 | — | — |
| 20 | 25,03 | 3,28 | 1,10 | 0,40 | 0,15 | 0,06 | 0,02 | 0,01 | — | — |
| 21 | 26,28 | 3,44 | 1,15 | 0,42 | 0,16 | 0,06 | 0,02 | 0,01 | — | — |
| 22 | 27,53 | 3,61 | 1,20 | 0,44 | 0,17 | 0,06 | 0,03 | 0,01 | — | — |
| 23 | 28,78 | 3,77 | 1,26 | 0,46 | 0,18 | 0,07 | 0,03 | 0,01 | — | — |
| 24 | 30,03 | 3,94 | 1,31 | 0,48 | 0,18 | 0,07 | 0,03 | 0,01 | — | — |
| 25 | 31,28 | 4,10 | 1,37 | 0,50 | 0,19 | 0,07 | 0,03 | 0,01 | — | — |
| 26 | 32,53 | 4,26 | 1,42 | 0,52 | 0,20 | 0,08 | 0,03 | 0,01 | — | — |
| 27 | 33,79 | 4,43 | 1,48 | 0,54 | 0,21 | 0,08 | 0,03 | 0,01 | — | — |
| 28 | 35,04 | 4,59 | 1,53 | 0,56 | 0,21 | 0,08 | 0,03 | 0,01 | — | — |
| 29 | 36,29 | 4,76 | 1,59 | 0,58 | 0,22 | 0,09 | 0,03 | 0,01 | 0,01 | — |
| 30 | 37,54 | 4,92 | 1,64 | 0,60 | 0,23 | 0,09 | 0,03 | 0,01 | 0,01 | — |
| 31 | 38,79 | 5,09 | 1,70 | 0,62 | 0,24 | 0,09 | 0,04 | 0,01 | 0,01 | — |
| 32 | 40,04 | 5,25 | 1,75 | 0,64 | 0,24 | 0,09 | 0,04 | 0,01 | 0,01 | — |
| 33 | 41,29 | 5,41 | 1,81 | 0,66 | 0,25 | 0,10 | 0,04 | 0,01 | 0,01 | — |
| 34 | 42,54 | 5,58 | 1,86 | 0,68 | 0,26 | 0,10 | 0,04 | 0,02 | 0,01 | — |
| 35 | 43,80 | 5,74 | 1,92 | 0,70 | 0,27 | 0,10 | 0,04 | 0,02 | 0,01 | — |
| 36 | 45,05 | 5,91 | 1,97 | 0,72 | 0,27 | 0,11 | 0,04 | 0,02 | 0,01 | — |
| 37 | 46,30 | 6,07 | 2,03 | 0,74 | 0,28 | 0,11 | 0,04 | 0,02 | 0,01 | — |
| 38 | 47,55 | 6,23 | 2,08 | 0,76 | 0,29 | 0,11 | 0,04 | 0,02 | 0,01 | — |
| 39 | 48,80 | 6,40 | 2,14 | 0,78 | 0,30 | 0,11 | 0,05 | 0,02 | 0,01 | — |
| 40 | 50,05 | 6,56 | 2,19 | 0,80 | 0,31 | 0,11 | 0,05 | 0,02 | 0,01 | — |
| 41 | 51,30 | 6,73 | 2,25 | 0,82 | 0,31 | 0,12 | 0,05 | 0,02 | 0,01 | — |
| 42 | 52,56 | 6,89 | 2,30 | 0,84 | 0,32 | 0,12 | 0,05 | 0,02 | 0,01 | — |
| 43 | 53,81 | 7,05 | 2,36 | 0,86 | 0,33 | 0,13 | 0,05 | 0,02 | 0,01 | — |
| 44 | 55,06 | 7,22 | 2,41 | 0,88 | 0,34 | 0,13 | 0,05 | 0,02 | 0,01 | — |
| 45 | 56,31 | 7,38 | 2,46 | 0,90 | 0,34 | 0,13 | 0,05 | 0,02 | 0,01 | — |
| 46 | 57,56 | 7,55 | 2,52 | 0,92 | 0,35 | 0,14 | 0,05 | 0,02 | 0,01 | — |

1. Overall dimension of grain areas

2. Volume of grains of the greatest size

3. The area of grains of K dimension

Table 50

at a given stage of calculations. In our case at the first stage K is 25, at the second it is 24, etc., all the way to 14. In order to reduce the working Table 50, first are listed only the integer numbers of per cent, after that tenths and hundreds of 1 per cent, separately.

It is convenient to carry out calculations in the order proposed by W. Johnson, writing down successive results in a special calculating table. Below we present an example illustrating the calculation using the second working table (Table 50). From the initial data for the austenite grains in steel which we have already used previously (see Table 49, the column on the extreme right). The calculating table for this case is presented further in this section (Table 51).

| Площадь, % помесячно менее 1 мк N, % | Область измерения расстояния, % | Площади зерен K размера, % | | | | | | | | |
|---|------------------------------------|----------------------------|------|------|------|------|------|------|------|------|
| | | K=1 | K=2 | K=3 | K=4 | K=5 | K=6 | K=7 | K=8 | K=9 |
| 47 | 58,81 | 7,71 | 2,57 | 0,94 | 0,36 | 0,14 | 0,05 | 0,02 | 0,01 | — |
| 48 | 60,06 | 7,87 | 2,63 | 0,96 | 0,37 | 0,14 | 0,06 | 0,02 | 0,01 | — |
| 49 | 61,31 | 8,04 | 2,68 | 0,98 | 0,37 | 0,14 | 0,06 | 0,02 | 0,01 | — |
| 50 | 62,57 | 8,20 | 2,74 | 1,00 | 0,38 | 0,15 | 0,06 | 0,02 | 0,01 | — |
| 51 | 63,83 | 8,37 | 2,79 | 1,02 | 0,39 | 0,15 | 0,06 | 0,02 | 0,01 | — |
| 52 | 65,07 | 8,53 | 2,85 | 1,04 | 0,40 | 0,15 | 0,06 | 0,02 | 0,01 | — |
| 53 | 66,32 | 8,69 | 2,90 | 1,06 | 0,40 | 0,16 | 0,06 | 0,02 | 0,01 | — |
| 54 | 67,57 | 8,86 | 2,96 | 1,08 | 0,41 | 0,16 | 0,06 | 0,02 | 0,01 | — |
| 55 | 68,82 | 9,02 | 3,01 | 1,10 | 0,42 | 0,16 | 0,06 | 0,02 | 0,01 | — |
| 56 | 70,07 | 9,19 | 3,07 | 1,12 | 0,43 | 0,16 | 0,07 | 0,03 | 0,01 | — |
| 57 | 71,32 | 9,35 | 3,12 | 1,14 | 0,44 | 0,17 | 0,07 | 0,03 | 0,01 | — |
| 58 | 72,58 | 9,51 | 3,18 | 1,16 | 0,44 | 0,17 | 0,07 | 0,03 | 0,01 | — |
| 59 | 73,83 | 9,68 | 3,23 | 1,18 | 0,45 | 0,17 | 0,07 | 0,03 | 0,01 | — |
| 60 | 75,08 | 9,84 | 3,29 | 1,20 | 0,46 | 0,18 | 0,07 | 0,03 | 0,01 | — |
| 61 | 76,33 | 10,01 | 3,34 | 1,22 | 0,47 | 0,18 | 0,07 | 0,03 | 0,01 | — |
| 62 | 77,58 | 10,17 | 3,40 | 1,24 | 0,47 | 0,18 | 0,07 | 0,03 | 0,01 | — |
| 63 | 78,83 | 10,33 | 3,45 | 1,26 | 0,48 | 0,19 | 0,07 | 0,03 | 0,01 | — |
| 64 | 80,08 | 10,50 | 3,51 | 1,28 | 0,49 | 0,19 | 0,07 | 0,03 | 0,01 | — |
| 65 | 81,34 | 10,66 | 3,56 | 1,30 | 0,50 | 0,19 | 0,08 | 0,03 | 0,01 | — |
| 66 | 82,59 | 10,83 | 3,61 | 1,32 | 0,50 | 0,19 | 0,08 | 0,03 | 0,01 | — |
| 67 | 83,84 | 10,99 | 3,67 | 1,34 | 0,51 | 0,20 | 0,08 | 0,03 | 0,01 | 0,01 |
| 68 | 85,09 | 11,15 | 3,72 | 1,36 | 0,52 | 0,20 | 0,08 | 0,03 | 0,01 | 0,01 |
| 69 | 86,34 | 11,32 | 3,78 | 1,38 | 0,53 | 0,20 | 0,08 | 0,03 | 0,01 | 0,01 |
| 70 | 87,59 | 11,48 | 3,83 | 1,40 | 0,53 | 0,21 | 0,08 | 0,03 | 0,01 | 0,01 |
| 71 | 88,84 | 11,65 | 3,89 | 1,42 | 0,54 | 0,21 | 0,08 | 0,03 | 0,01 | 0,01 |
| 72 | 90,09 | 11,81 | 3,94 | 1,44 | 0,55 | 0,21 | 0,08 | 0,03 | 0,01 | 0,01 |
| 73 | 91,35 | 11,97 | 4,00 | 1,46 | 0,56 | 0,21 | 0,08 | 0,03 | 0,01 | 0,01 |
| 74 | 92,60 | 12,14 | 4,05 | 1,48 | 0,56 | 0,22 | 0,09 | 0,03 | 0,01 | 0,01 |
| 75 | 93,85 | 12,30 | 4,11 | 1,50 | 0,57 | 0,22 | 0,09 | 0,03 | 0,01 | 0,01 |
| 76 | 95,10 | 12,47 | 4,16 | 1,52 | 0,58 | 0,22 | 0,09 | 0,03 | 0,01 | 0,01 |
| 77 | 96,35 | 12,63 | 4,22 | 1,54 | 0,59 | 0,23 | 0,09 | 0,03 | 0,01 | 0,01 |
| 78 | 97,60 | 12,79 | 4,27 | 1,56 | 0,60 | 0,23 | 0,09 | 0,04 | 0,01 | 0,01 |
| 79 | 98,85 | 12,96 | 4,33 | 1,58 | 0,60 | 0,23 | 0,09 | 0,04 | 0,01 | 0,01 |
| 80 | 100,11 | 13,12 | 4,38 | 1,60 | 0,61 | 0,24 | 0,09 | 0,04 | 0,01 | 0,01 |
| 0,1 | 0,13 | 0,02 | 0,01 | — | — | — | — | — | — | — |
| 0,2 | 0,25 | 0,03 | 0,01 | — | — | — | — | — | — | — |
| 0,3 | 0,38 | 0,05 | 0,02 | 0,01 | — | — | — | — | — | — |
| 0,4 | 0,50 | 0,07 | 0,02 | 0,01 | — | — | — | — | — | — |
| 0,5 | 0,63 | 0,09 | 0,03 | 0,01 | — | — | — | — | — | — |
| 0,6 | 0,75 | 0,10 | 0,03 | 0,01 | — | — | — | — | — | — |
| 0,7 | 0,88 | 0,11 | 0,04 | 0,01 | 0,01 | — | — | — | — | — |
| 0,8 | 1,00 | 0,13 | 0,04 | 0,02 | 0,01 | — | — | — | — | — |
| 0,9 | 1,13 | 0,15 | 0,05 | 0,02 | 0,01 | — | — | — | — | — |
| 1,0 | 1,25 | 0,16 | 0,05 | 0,02 | 0,01 | — | — | — | — | — |
| 0,01 | 0,01 | — | — | — | — | — | — | — | — | — |
| 0,02 | 0,03 | — | — | — | — | — | — | — | — | — |
| 0,03 | 0,04 | — | — | — | — | — | — | — | — | — |
| 0,04 | 0,05 | 0,01 | — | — | — | — | — | — | — | — |
| 0,05 | 0,06 | 0,01 | — | — | — | — | — | — | — | — |
| 0,06 | 0,08 | 0,01 | — | — | — | — | — | — | — | — |
| 0,07 | 0,09 | 0,01 | — | — | — | — | — | — | — | — |
| 0,08 | 0,10 | 0,01 | — | — | — | — | — | — | — | — |
| 0,09 | 0,11 | 0,01 | — | — | — | — | — | — | — | — |
| 0,10 | 0,13 | 0,02 | 0,01 | — | — | — | — | — | — | — |

Table 50 cont.

The numbers of groups of microparticles, which are actually observed in the object subjected to investigation, are written down in the first line in order of descending sizes. In our case these numbers range from 25 to 14. Corresponding areas of the plane of polish, in per cent, are written down in the second line; that is, the initial data which we find in the extreme

right column in Table 49.

The first figure in the second line (9.25 per cent) we break down into integers, tenths and hundredths of 1 per cent; that is into 9, 0.2 and 0.05. We find these figures in the first column in Table 50 and write down the corresponding 3 rows of figures from all columns of the table:

| | | | | | | | |
|------------------|-------|------|------|------|------|------|------|
| Для 9 | 11,26 | 1,48 | 0,49 | 0,18 | 0,07 | 0,03 | 0,01 |
| » 0,2 | 0,25 | 0,03 | 0,01 | — | — | — | — |
| » 0,05 | 0,06 | 0,01 | 0,00 | — | — | — | — |
| » 9,25 | 11,57 | 1,52 | 0,50 | 0,18 | 0,07 | 0,03 | 0,01 |

The obtained totals are written in the third line of the calculating Table 51.

| 25 | 24 | 23 | 22 | 21 | 20 | 19 | 18 | 17 | 16 | 15 | 14 | Cip. |
|-------|-------|-------|-------|-------|-------|------|------|------|------|------|------|------|
| 9,25 | 17,50 | 15,65 | 22,07 | 16,12 | 10,40 | 4,96 | 2,49 | 0,99 | 0,40 | 0,12 | 0,05 | 2 |
| 11,57 | 1,52 | 0,50 | 0,18 | 0,07 | 0,03 | 0,01 | — | — | — | — | — | 3 |
| | 15,98 | 15,15 | 21,89 | 16,05 | 10,37 | 4,95 | 2,49 | 0,99 | 0,40 | 0,12 | 0,05 | 4 |
| 20,00 | 2,62 | 0,87 | 0,32 | 0,12 | 0,04 | 0,02 | 0,01 | — | — | — | — | 5 |
| | 12,53 | 21,02 | 15,73 | 10,25 | 4,91 | 2,47 | 0,98 | 0,40 | 0,12 | 0,05 | 0,05 | 6 |
| 15,69 | 2,05 | 0,69 | 0,25 | 0,09 | 0,04 | 0,01 | 0,01 | — | — | — | — | 7 |
| | 18,97 | 15,04 | 10,00 | 4,82 | 2,43 | 0,97 | 0,39 | 0,12 | 0,05 | 0,05 | 0,05 | 8 |
| 23,79 | 3,11 | 1,04 | 0,38 | 0,15 | 0,05 | 0,02 | 0,01 | — | — | — | — | 9 |
| | 11,93 | 8,96 | 4,44 | 2,28 | 0,92 | 0,37 | 0,11 | 0,05 | 0,05 | 0,05 | 0,05 | 10 |
| 14,93 | 1,95 | 0,65 | 0,24 | 0,09 | 0,03 | 0,01 | — | — | — | — | — | 11 |
| | 7,01 | 3,79 | 2,04 | 0,83 | 0,34 | 0,10 | 0,05 | — | — | — | — | 12 |
| 8,77 | 1,15 | 0,38 | 0,14 | 0,05 | 0,02 | 0,01 | — | — | — | — | — | 13 |
| | 2,64 | 1,66 | 0,69 | 0,29 | 0,08 | 0,04 | — | — | — | — | — | 14 |
| 3,30 | 0,44 | 0,14 | 0,05 | 0,02 | 0,01 | — | — | — | — | — | — | 15 |
| | 1,22 | 0,55 | 0,24 | 0,06 | 0,03 | — | — | — | — | — | — | 16 |
| 1,53 | 0,19 | 0,06 | 0,02 | 0,01 | — | — | — | — | — | — | — | 17 |
| | 0,36 | 0,18 | 0,04 | 0,02 | — | — | — | — | — | — | — | 18 |
| 0,46 | 0,06 | 0,02 | 0,01 | — | — | — | — | — | — | — | — | 19 |
| | 0,12 | 0,02 | 0,01 | — | — | — | — | — | — | — | — | 20 |
| 0,16 | 0,00 | 0,00 | — | — | — | — | — | — | — | — | — | 21 |

Table 51

The first figure of the third line, 11.57, gives directly the per cent of the volume of steel occupied by the microparticles of the 25th group. We subtract the other figures in line 3 from figures in line 2 and write them in the fourth line.

The first figure of the fourth line (15.98 per cent) is also broken down into integers (15), tenths, and hundreds of 1 per cent (0.9 and 0.08). These figures are found in the first column of the working Table 50. After that the corresponding three rows of figures in all columns are written down and added, as previously:

| | | | | | | | | |
|-------------------|-------|------|------|------|------|------|------|------|
| Line 15 | 18.77 | 2.46 | 0.82 | 0.30 | 0.11 | 0.04 | 0.02 | 0.01 |
| * 0.9 | 1.13 | 0.15 | 0.05 | 0.01 | 0.01 | — | — | — |
| * 0.08 | 0.10 | 0.01 | — | — | — | — | — | — |
| * 15.98 | 20.00 | 2.62 | 0.87 | 0.32 | 0.12 | 0.04 | 0.02 | 0.01 |

The totals are written in the fifth line of the calculating Table 51, so that the first figures would be directly under the index of Group 24. The first figure of the fifth line, 20.00 per cent, also gives directly the volume of steel occupied by microparticles of the next, now 24th, group. Other figures in line 5 are subtracted from figures in line 4 and the obtained differences are written in line 6.

After that the calculation procedure is repeated in the order described until all groups are exhausted, as shown in Table 51. It is of interest to note that in the course of calculation the microparticles of two groups, 15th and 14th, disappear. This signifies that all planar grains of these groups are formed by microparticles of larger size. As each stage of the calculation is completed, we derive a successive value of the volume of steel occupied by microparticles of successive size groups and the length of the line in the calculating table is reduced by 1 column. Figures at the bottom of each column in Table 51 give the volumetric content of microparticles of a given size in steel. If the calculation has been done correctly, the sum of these figures

should be obviously 100 per cent. In our case the sum is 100.2 per cent, which is explained by rounding off the figures to two decimal points when calculating the working Table 50. A calculation error of this kind is naturally quite permissible.

We believe that it is necessary to stress the point that the example cited of the different shape of the calculation of volumes of austenite grains is one of the most laborious encountered in practice, both with respect to choosing large numbers of groups and calculations from Table 50 with accuracy to 0.01 per cent of the area. In the original W. Johnson's method, division was made only to six groups, and the sixth group incorporated there to all grains of successive smaller dimensions. The auxiliary table of W. Johnson has been calculated with accuracy of 0.1 per cent of the area and not 0.01 per cent as calculated by us. Reducing the number of groups to 7 or 8 is quite permissible in many cases, as well as the calculation with accuracy up to 0.1 per cent of the area. In this case the calculating table is reduced to 15 lines and 7 columns and the time of calculation approximately down to 10 minutes. We believe that it is expedient to provide the more accurate Table 50, which for the purpose of concrete microanalysis, anyone can reduce if so desired by rounding off the figures in the table to 0.1 per cent of the area.

From the description presented above it follows that the calculation is reduced to writing down appropriate number of figures from the working Table 50, adding them and subtracting the totals from the preceding line in the calculating Table 51. Having derived the final distribution of total volumes with respect to groups, it is necessary to use the division operation for the determination of the number of microparticles of each size in volume. Final data of calculated numbers of microparticles in the volume are given in Table 52. They are derived by dividing the total volume of microparticles of each group, expressed in per cent, by the volume of 1 microparticle of this group, the value of which is found in Table 48 and multiplied by 10^{-7} . The total

number of microparticles of austenite, N , happens to be 853.7 mm^{-3} .

From the data in Table 49 it follows that 258 measured grains occupy 2.746 mm^2 of the area of the plane of polish, which makes it possible to determine the mean number of planar grains:

$$n = 258 : 2.746 = 93.9 \text{ mm}^{-2}$$

Applying Formula (35.2), we find the mean arithmetic value of the diameter of austenite microparticles:

$$\bar{D} = 93.9 : 853.7 = 0.110 \text{ mm.}$$

The method modified by us makes it possible to determine the absolute size and amounts of volumetric microparticles. The specific surface area of grains, as we already know, may be simply and accurately determined by the method of secants.

As it has been previously mentioned, the original method of W. Johnson is limited to single-phase polyhedral structures. Let us consider the possibility of calculating the number of spheroidal microparticles for any one of the structural constituents of complex structures. Evaluating the sections of microparticles in accordance with the norms of our logarithmic scale, we simultaneously must determine the total number of sections per unit area of the plane of polish, which was unnecessary in single-phase polyhedral structures. From experimental data, having found the number of sections of each size group per 1 mm^2 on the plane of polish, we multiply these numbers by the mean areas of sections of corresponding groups, expressed in micron 2 (see Table 48) and by 10^{-4} , in order to obtain the total areas of sections of each group expressed in per cent of the area of the plane of polish. This distribution is the initial one, using it we proceed with our calculations exactly as described previously, using the working Table 50, compiling the calculated table similar to Table 51.

Advantages over W. Johnson's method are the simplicity of calculating operations, reduced in the first two operations to arithmetic and also a finer differentiation of small sections, which, as we know, have a great influence on the results of calculating the number of microparticles in a volume. Moreover, the use of our logarithmic scale makes it possible to obtain the distribution of logarithms of the diameters of microparticles and to determine their actual sizes and numbers. An example of a comparative scale is shown in Figure 98 for the evaluation of the area of grains.

| Числовой нр группы | Логарифм диаметра микрочастин | Суммарный объем микрочастин % объема стали | Количество микрочастин м^{-3} | Распределение по размерам |
|-----------------------|-------------------------------------|---|--|------------------------------|
| 1. | 2. | 3. | 4. | 5. |
| 25 | 2,5 | 11,57 | 7,0 | 0,82 |
| 24 | 2,4 | 20,00 | 24,1 | 2,82 |
| 23 | 2,3 | 15,69 | 37,7 | 4,42 |
| 22 | 2,2 | 23,79 | 114,2 | 13,37 |
| 21 | 2,1 | 14,93 | 142,9 | 16,74 |
| 20 | 2,0 | 8,77 | 167,5 | 19,62 |
| 19 | 1,9 | 3,30 | 125,8 | 14,74 |
| 18 | 1,8 | 1,53 | 116,3 | 13,62 |
| 17 | 1,7 | 0,46 | 69,8 | 8,18 |
| 16 | 1,6 | 0,16 | 48,4 | 5,67 |
| Bсero .. | — | 100,00 | 853,7 | 100,00 |

1. Representative nr. of groups.
2. Diameter of logarithms of micro particles.
3. Total volume of micro particles %
of steel volume.
4. nr. of micro particles mm^3
5. Distribution by dimensions.

Table 52

Section 38. Calculation of the Distribution of Microparticle Size by A. T. Spektor's Method of Chords

In the discussed method of W. Johnson, the evaluation criterion of cross sections of spherical microparticles on the plane of polish are areas of cross sections and in the method described earlier by E. Scheil their diameters. In contrast to those methods, a method was developed by A. T. Spektor based on the measurements of the size of chords obtained when intersecting spherical cross sections of microparticles on the plane of polish by straight lines. The diagram shown in Figure 99 illustrates the variety of measured parameters of the three methods for the determination of the number of microparticles in volume and their distributions according to size.

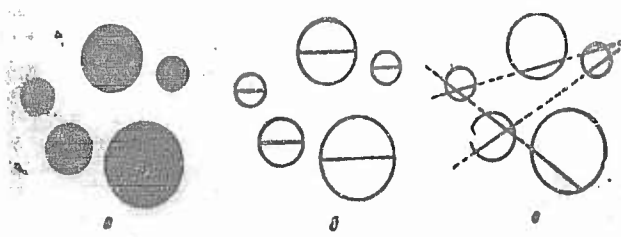
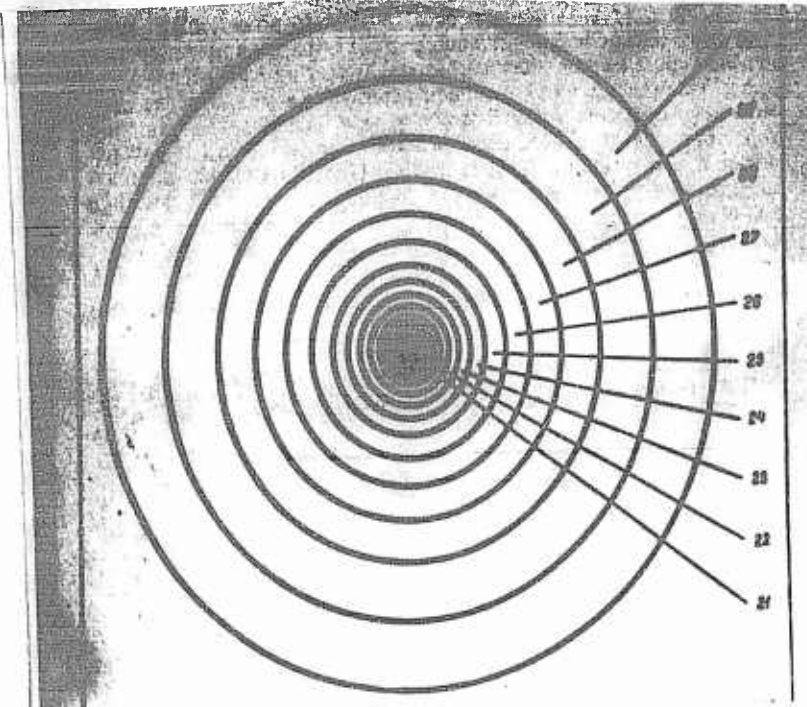


Fig. 99

Fig. 98. Scale of comparison for evaluation of the area and diameter of the grain according to the logarithmic scale with a magnification of 100

Fig. 99. Sketch showing the difference in the original parameters with methods of computation of the amount of the spherical micro particles in a column according to:
a--W. Johnson (area); b--E. Scheil (diameter); c--A. G. Spektor (chord)

We can consider it, a priori, self evident that the concrete statistacal distribution of spheroidal microparticles by a poly-dispersed system will give us a single valued predetermination of the distribution of lengths of chords obtained during random intersection of microparticles by straight secants. Therefore, starting with the distribution of lengths of chords, which are determined experimentally, we can find the distribution of microparticles according to size. The advantage of this method is the fact that we can determine simultaneously the size of the specific area of miceoparticles because the number of chords obtained per unit of length of the secant equals the mean number of intersections m , in the case of a single-phase polyhedral structure, and $\frac{1}{2}$ of this number in any other case. There are no objections in regard to mathematical rigor of Spiktor's method as derived for the case of monodisperse and polydisperse systems of spheres. Calculations conducted on the basis of the initial distribution of chords according to size are simple.

However, we must note that during the analysis by the method of chords the most difficult task is to obtain accurate initial data taking into account the microrelief of the polish of any real structure. The influence of the microrelief counts also during the measurements of other parameters as diameter or area which characterize the size of the flat grain but it is especially unfavorable for the measurement of chords.

Figure 100A gives us a schematic diagram of the structure of carbides of hypereutectoid steels given by A. T. Spektor to illustrate the use of the method of chords (67). As it is noticeable even in a very small microrelief, carbide grains are surrounded by a shadow ring the width of which is approximately constant for all the grains. Therefore, a ratio of the width of the shadow ring to linear dimensions of grains will increase if the size of carbide grains decreases. Figure 100B shows a similar diagram by M. E. Blanter (118) which corresponds to a larger microrelief than Figure 100A.

As we have mentioned before, a most accurate agreement between data of the quantitative microanalysis and between data of chemical analysis will take place if the center line of the shadow ring is taken as the true contour of carbide grains. Let us analyze the diagram in Figure 101.

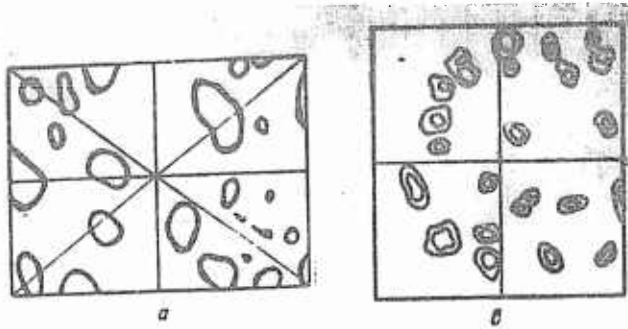


Fig. 100. Actual structure of carbides in steel with a shaded ring produced by the MM microrelief of the slide

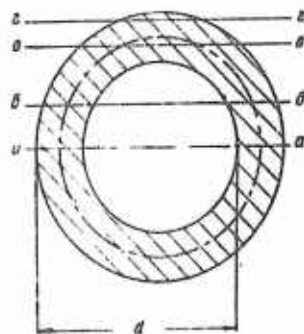


Fig. 101. Sketch explaining the origin of error in measuring the lengths of the chords as a result of the presence of a shaded ring

The diagram shows the external and internal contours of the grain and they set the boundary for the area of the shadow ring. The diagram shows also the imaginary center line of this ring. If we measure the diameter of the grain on the line aa, the width of the shadow ring on this line is relatively small and the measured value (diameter) is big. When we move the secants away from the center of the grain the width of the shadow ring on the secant (for instance, bb) will increase and the measured value (chord) will decrease.

Therefore, the ratio of the width of the shadow ring on the intersecting line to the length of the chord determines the error of measurement and grows rapidly. As long as the secant is placed only partly in the light central field of the grain, we can correct measurement of chords as it is done in Figure 101. If we measure the diameter, d will equal the diameter of the middle line of the shadow ring; but if the secant leaves the limits of the light field and intersects only the shadow ring, as is the case for lines vv or for lines gg (Figure 101), a more or less correct determination of the length of the chords will not be possible. When we measure cross sections of other types of microparticles a relatively small error stipulated for instance by an obstruction at the edge of the cross section will be found also during the measurement of the diameter and will grow if the secant moves away from the center of the cross section. The stated facts should be kept in mind during analysis by the method of chords which requires a very accurate determination of initial data. However, the simplicity of the calculation will compensate for the additional time taken for an accurate measurement of the length of chords.

Chords can be measured on the photomicrograph or directly under the microscope. It is evident that the maximum possible size of chords is determined by the maximum diameter of flat grains. Measured chords are grouped according to their length and the division factor, Δ , is chosen in such a manner that the total number of groups will amount to approximately 10. A diagram of the division of chords into groups according to their lengths is shown in Figure 102⁽⁶⁷⁾. The number of measured chords in each group pertains to one millimeter of the secant.

The working formula for the method of chords, derived by A. T. Spektor, is used to calculate the distribution of microparticles according to their size and to divide them into a limited number of groups. The diameter of microparticles of the K th group equals $K\Delta$. N_K is number of microparticles with a diameter of $K\Delta$. Δ is a

division factor in mm, and U is the number of chords per 1 mm of the length of the secant. The index of U designates the corresponding dimensional group of chords.

$$N_K = \frac{4}{\pi \Delta^2} \left(\frac{U_K}{2K-1} - \frac{U_{K+1}}{2K+1} \right) \text{ mm}^{-3},$$

(38.1)

Let us analyze the use of this method and application of Formula (38.1) on the concrete example of the distribution determination of the number of ferrite grains in low-carbon steels. This determination was made by the author of this method (67). The division factor of chords according to their lengths, Δ , is 0.0025 mm. Limits of lengths of chords and their distribution according to groups are given in Table 53.

Formula (38.1) permits us to calculate directly the number of microparticles of each group without knowing the number of microparticles of the sixth group, the diameter of which is 0.015 mm, will equal

$$N_6 = 2,04 \cdot 10^5 \left(\frac{8}{12-1} - \frac{5}{12+1} \right) = 0,70 \cdot 10^5 \text{ mm}^{-3}.$$

Table 54 gives us the number of ferrite grain in volume calculated for all dimensional groups by Formula (38.1).

| 1. Nr. of K groups | 2. Range of chord lengths mm | 3. Nr. of chord in a 1 mm secant. |
|----------------------|---------------------------------|-----------------------------------|
| 1 | 0,0-2,5 | 1 |
| 2 | 2,5-5,0 | 17 |
| 3 | 5,0-7,5 | 24 |
| 4 | 7,5-10,0 | 19 |
| 5 | 10,0-12,5 | 18 |
| 6 | 12,5-15,0 | 6 |
| 7 | 15,0-17,5 | 5 |
| 8 | 17,5-20,0 | 4 |
| 9 | 20,0-22,5 | 3 |
| 10 | 22,5-25,0 | 2 |
| <i>Sum</i> | | |
| <i>Bzero</i> | 0,0-25,0 | 101 |

Table 53

| № группы К 1. | Диаметр микрочастиц, мк 2. | Количество микрочастиц | |
|------------------|-------------------------------|-----------------------------|--------------|
| | | мк ⁻³ | % |
| 1 | 0,0025 | 0,68·10 ⁸ | |
| 2 | 0,0050 | 1,77·10 ⁸ | 5,7 |
| 3 | 0,0075 | 4,26·10 ⁸ | 14,7 |
| 4 | 0,0100 | 2,59·10 ⁸ | 35,4 |
| 5 | 0,0125 | 1,46·10 ⁸ | 21,5 |
| 6 | 0,0150 | 0,70·10 ⁸ | 12,1 |
| 7 | 0,0175 | 0,24·10 ⁸ | 5,8 |
| 8 | 0,0200 | 0,19·10 ⁸ | 2,0 |
| 9 | 0,0225 | 0,14·10 ⁸ | 1,6 |
| Total | | | |
| Total | | 12,03·10⁸ | 100,0 |

1. №. of K groups.

2. Diameter of micro-particles, мк

3. №. of micro-particles.

Table 54

At the same time, we can determine the specific area of micro-particles. Inasmuch as we deal with a single-phase structure, the number of chords of all dimensions per 1 mm of the secant will be the same as the average number of intersections of the secant with boundary lines of ferrite grains on the polish m. Therefore, the specific area can be found by the basic formula of the method of random secants for space, Formula (25.1):

$$\Sigma S = 2m = 2 \cdot 101 = 202 \text{ мк}^2/\text{мк}^3.$$

Another version of the method of chords will allow us to plot an integral curve of the distribution of grains according to their size, that is, a curve showing the relation between the diameter of grains and the number of grains, the diameter of which is larger than the given diameter. By graphical differentiation of the integral curve, we can construct also an ordinary distribution curve of grains according to the size of the diameter.

In the case of finite differences of diameter and chord values (with which we deal in practice) the number of grains, the diameter of which exceeds the value h, will be determined by Spektor's Formula:

$$N_h = \frac{2}{\pi \Delta} \frac{U_h}{h} \text{ mm}^{-3}, \quad (38.2)$$

where

h is the length of the chord or the diameter of the grain in mm

Δ is the division factor of chords according to length, mm

U_h is the number of chords with the lengths from $h - \frac{1}{2}$ to $h + \frac{1}{2}$ per 1 mm of the secant.

Table 55 shows an example of the calculation of an integral curve of the distribution of diameters of carbide microparticles of annealed hypereutectoid steel according to method of the author (67).

Lengths of chords were measured on a photoprint with the total magnification of 8000 (magnification in microphotography was 1500, followed by magnification of 2.35). Total true length of secants was

| Средняя длина хорды, мм h | Количество хорд на 1 мм секущей прямой U_h | Количество микрочастин, диаметр которых больше h , $N_h \text{ mm}^{-3}$ |
|-----------------------------|--|--|
| 1. | 2. | 3. |
| 0,16 | 34,2 | $110,0 \cdot 10^7$ |
| 0,28 | 62,1 | $110,0 \cdot 10^7$ |
| 0,40 | 65,0 | $83,0 \cdot 10^7$ |
| 0,53 | 51,0 | $49,0 \cdot 10^7$ |
| 0,66 | 46,5 | $36,0 \cdot 10^7$ |
| 0,78 | 32,8 | $21,0 \cdot 10^7$ |
| 0,91 | 22,6 | $13,0 \cdot 10^7$ |
| 1,03 | 10,3 | $5,1 \cdot 10^7$ |
| 1,16 | 11,0 | $4,8 \cdot 10^7$ |

1. Average chord length h .
2. Nr. of chords in 1 mm straight secant. U_h
3. Nr. of microparticles, the diameter of which is greater than h . $N_h \text{ mm}^{-3}$

Table 55

1.46 mm, and the division factor, Δ , was 0.125 micron. Figure 103 shows the obtained integral curve of the distribution of diameters of microparticles. The same figure shows data of a check calculation by

the method of E. Scheil which are very satisfactory. The number of microparticles in each diametersize interval can be obtained easily as the difference of two ordinates limiting this interval. If we divide the entire axis of abscissas (Figure 103) into many equal intervals and determine differences of each pair of ordinates, we will be able to construct an ordinary statistical curve on the distribution of microparticles according to the size of the diameter. In the construction of such a curve, the obtained values of the difference of ordinates refer to the center of the corresponding interval.

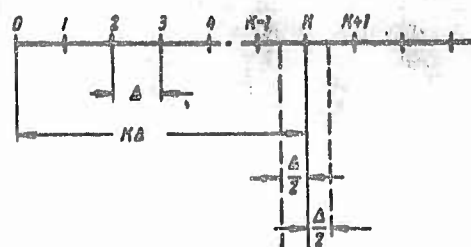


Fig. 102. Sketch of the layout of the chords by groups in accordance with the length (A. G. Spektor)

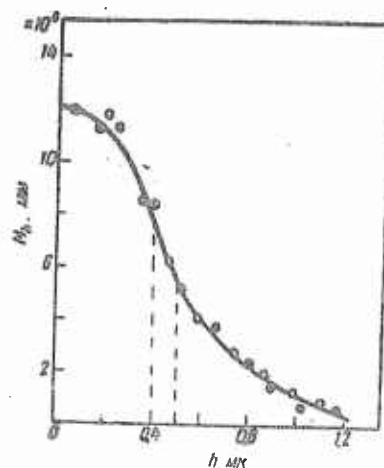


Fig. 103. Integral curve of the distribution of the dimensions of the microparticles of cementite in eutectic steel according to data obtained by the method of E. Scheil (circles) and by the method of the chords (dots) per A. G. Spektor [67].

Section 39. The Type of Distribution Curve for Sizes of Equiaxed Microparticles and the Determination of their Parameters by the Method of Combined Indices

When making a qualitative study of relationships, on the one hand, between statistical distribution of microparticles and size and, on the other hand, between indices of properties and factors which characterize the working and behavior of metals or alloys, we have to deal without tables or statistical distribution graphs, but with definite numerical values of its parameters. Previously we have demonstrated a method for calculating the three basic parameters, which characterize any polydispersed system of spheroidal microparticles, such as their number per unit volume, N , the mean diameter, \bar{D} , and the root-mean-square deviation of the diameter, D (see Section 35). However, inasmuch as we do not know the general law of statistical distribution of microparticles with respect to size (if such a law does exist), we cannot determine all the parameters of spatial structure, which are of interest to us, such as the total volume of microparticles or their surface, from the aforementioned parameters. However, if we knew the general type of statistical curves or the distribution formula for sizes of microparticles, we would be able to compute their parameters, determining the minimum number of parameters from a plane microstructure.

It has been noted for quite some time that the size of microparticles fit very smooth assymetrical distribution curves with one maximum [3, 163]. Attempts to find a mathematical expression for these curves were made by G. Tammann [38], S. Z. Roginskiy and O. M. Todes [164, 165], W. Johnson and R. Mehl, D. Meijering [130], et al. According to Tammann, two types of distribution of microparticles occur in metallic structures: in cast metal this distribution conforms to a normal symmetrical (Gaussian) curve and in recrystallized metal it corresponds to a Maxwell distribution. Roginskiy and Todes analyzed the relationship between the shape of the distribution curve for microparticles and the kinetics of crystallization, examining different variants of phase formation. Although the authors do not give any

mathematical expression for the distribution curves, they arrived at a conclusion, important to us, that "not a single variant of the kinetics of phase formation yields anything resembling the Gaussian distribution" [164]. In particular, as has been pointed out by S. C. Roginskiy, the distribution of microparticle resulting from a constant linear growth rate and rate of nucleation of crystallites per unit of volume per unit time, "has nothing in common with a Gaussian distribution" [165].

Experimental data confirm the conclusions of Roginskiy and Todes. Literally all distribution curves, which we have had an opportunity to observe, are asymmetrical. Moreover, no major difference is noted between the distribution of microparticles formed as a result of primary or secondary crystallization or as a result of recrystallization. [Translator's note: In Russian usage primary crystallization is the formation of crystals coincidental with the phase change from the liquid to the solid, whereas secondary recrystallization is coincidental with allotropic transformation]. For this reason, we have to consider the second hypothesis of G. Tammann.

As is known, the Maxwell distribution is characterized by the following formula:

$$N_i = \frac{N \Delta \sqrt{\frac{2}{\pi}}}{\sigma_0^3} D_i^3 e^{-\frac{D_i^3}{2\sigma_0^2}} \text{ mm}^{-3},$$

(39.1)

where Δ is the group interval, in mm; D_i is the diameter of microparticles of the i -th group, mm; N_i is the number of microparticles of the i -th group in 1 mm³; N is the total number of microparticles of all sizes in 1 mm³.

Quantity σ_0 , which is found in Formula (39.1), is related to the values of the mean diameter of microparticles, \bar{D} , and the root-mean-square deviation of the diameter, $\sigma \{D\}$, by the formulas:

(39.2)

$$\sigma_0 = \frac{\sigma(D)}{\sqrt{3 - \frac{8}{\pi}}}.$$

(39.3)

From these formulas it follows that the variation coefficient of Maxwell distribution is

$$\sigma = \frac{\sigma(D)}{D} = \frac{\sqrt{3\pi - 8}}{2\sqrt{2}} = 0.422$$

that is, it is a constant value for any distribution of this type. Extensive experimental data from different authors which have been analyzed by us, show that the variation coefficient of real distributions is a quantity which is far from being constant and that it generally varies between 0.2 to 0.5 [162]. For several structures, the characteristic of microparticles distribution of which was given by A. G. Spektor [161], the variation coefficient varies between 0.14 and 0.63. Among these structures, are microparticles of carbides in annealed and hardened steel, microparticles of ferrite and mild steel of O8 type, microparticles of cementite and tempered carbon steel. It is apparent that both works confirm the fact that the variation coefficient is not constant; the ranges of its variations found in real structures were very similar.

But even in the case when the actual variation coefficient of a

real distribution is very close to the value corresponding to Maxwell's formula, the experimental curve does not coincide with the theoretical Maxwell curve. Figure 104 shows a typical distribution curve for the diameters of cementite particles in carbon steel (1% c), plotted by points found experimentally by Scheil's method (Curve 1). The distri-

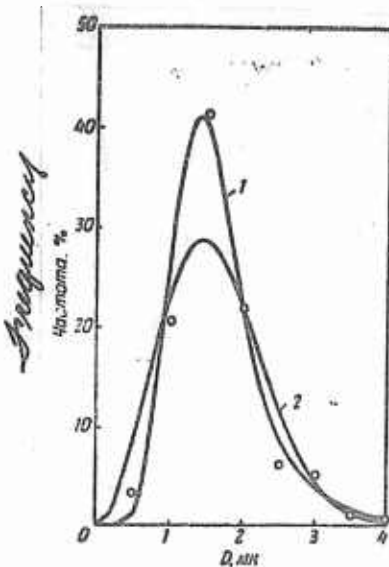


Fig. 104. Actual distribution of the diameters of the micro particles of cementite in carbon steel (1) and corresponding curve of Maxwell (2)

bution is characterized by the following parameters:

| | |
|---|------------|
| The average diameter of microparticles, microns | 1.645 |
| The root-mean-square deviation, microns | 0.678 |
| The variation coefficient | 0.412 |
| The number of microparticles in 1 mm ³ | 45,450,000 |

The Maxwell distribution curve, shown in the same figure (Curve 2) has been plotted using the same parameters. It may be seen that the shape of the experimental curve differs essentially from the shape of Maxwell's curve. The experimental curve (1) and Maxwell's curve (2) for the distribution of diameters of austenitic grains in steel, developed by standard carburization, are presented in Figure 105.

In this case, the mean diameter $\bar{D} = 69.7$ microns; the root-mean-square deviation of the diameter $\sigma \sqrt{D} = 23.3$ microns; the variation coefficient $\delta = 0.334$ and the number of microparticles in 1 mm³ $N = 4188$. The relationship between the experimental and the calculated

curves in Figure 105 is the same as in the preceding case. Not having the opportunity of citing the scores of distributions for diameters of microparticles, which we have studied, we wish to note that not in a single case do the experimentally found data coincide with calculated Maxwell's distribution curves characterized by identical parameters.

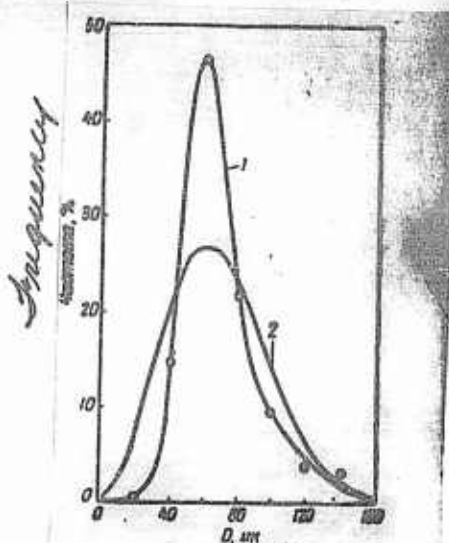


Fig. 105. Actual distribution of the diameter of the grains of austenite (1) and corresponding curve of Maxwell (2). Figure 105

The aforesaid illustrates convincingly that the distribution curves for microparticle sizes in metallic structures do not obey either the Maxwell's distribution law or the normal Gaussian law.

Attempts have been undertaken at different times at mathematical computation of the distribution curve for microparticle size, which attempts have been based on the Tammann scheme of crystallization process. Different variants of the kinetics of crystallization are predicated either on the constancy of crystallization parameters in time, their regular change in the course of the process, or, finally, on the presence of rating centers of crystallization. However, in all cases it is being assumed that the growth of microparticles ends at the moment they impinge and that the interface boundary, which has formed, remains stationary after that, which as it is well known does not correspond to reality. Moreover, calculations of this kind do not take into account the process of coagulation of microparticles, which process begins and proceeds simultaneously with crystallization and does not even require the direct contact between microparticles. By imposing

the process of coagulation into the crystallization process essentially changes the picture of size distribution of microparticles. It is natural that the distribution curves, obtained by the method described, differs so much from the real curves that they cannot be used for our purposes. Therefore, the only method for the development of the general law of size distribution of microparticles is the study of empirical relationship based on reliable metallurgical data.

A very convenient method for the verification of the law of distribution is the method of plotting the so-called straightened-out curve of frequencies. Let us assume that we have data at our disposal obtained experimentally, which show the distribution of diameters of microparticles with respect to a certain finite number of groups. If N is the total number of distributed microparticles and $\sum N_i$ is the total number of microparticles, whose diameters does not exceed the value of D_i , then for each dimensional group we determine the ratio $\frac{N_i}{N}$. After that the obtained values of this ratio we equate to the normalized function of normal distribution, $\psi(t)$, consecutively for each dimension of microparticles, that is we assume:

$$\frac{\sum N_i}{N} = \psi(t) = \frac{1}{\sqrt{2\pi}} \int_{-\infty}^t e^{-\frac{t^2}{2}} dt.$$

(39.4)

Appropriate values of the normalized deviation t are found in tables given in textbooks on the theory of probabilities, inasmuch as the integral (39.4) is not chosen. In the case of a normal Gaussian distribution of the value which is being observed (in our case the diameter of microparticles), the relationship between it and found values of t must be expressed by a straight line. We shall give an example of plotting a straightened out curve of frequencies for the distribution of diameters of microparticles of partially transformed austenite. The order of preliminary calculations is clear in Table 56. In the first two columns of this table there are given the original data which char-

acterize the distribution. The total number of microparticles in the distribution $N = 13,077$. Further, we plot a graph showing the relationship between the diameter of microparticles, D , and normalized deviation, t , shown in Figure 106. Here it is apparent that the de-

| Диаметр зерна D_i , мк | Количество зерен N_i , мк ⁻¹ | $S N_i$ | $\frac{N_i}{N}$ | t |
|-----------------------------|---|---------|-----------------|-------|
| 6,87 | 634 | 994 | 0,076 | -1,43 |
| 13,74 | 6901 | 7285 | 0,504 | 0,25 |
| 20,61 | 3456 | 11351 | 0,860 | 1,13 |
| 27,48 | 1320 | 12871 | 0,959 | 1,57 |
| 34,35 | 262 | 12933 | 0,989 | 2,29 |
| 41,22 | 124 | 13057 | 0,998 | 2,88 |
| 48,09 | 20 | 13077 | 1,000 | ∞ |

1. Grain diameter
2. Nr. of grains

Table 56

rived relationship substantially deviates from the rectilinear relationship and that it rather resembles a logarithmic curve. In order to verify the supposition on the presence of a logarithmic relationship between the two values in question, we plot the same graph in Figure 107 , but using logarithmic scale on x axis. In this case we obtain a clearly manifested rectilinear relationship between the logarithm of the diameter of microparticles and normalized deviation t . This lends evidence that it is not the diameter of microparticles but its logarithm which obeys the law of normalized distribution. We plot a similar linearized diagram of frequencies for the distribution of microparticles of cementite, shown in Figure 104, and for the distribution of austenitic grains of steel, developed by standard carburization, according to data published by M. Ye. Blanter [166]. The examples cited show with sufficient conviction that for the cases reviewed the law of distribution of diameters of microparticles is expressed by the formula of logarithmic normal distribution, which has the following form:

$$N_i = \frac{N_A}{\sqrt{2\pi} D_i \sigma \{\ln D\}} e^{-\frac{(\ln D_i - \bar{\ln D})^2}{2\sigma^2 \{\ln D\}}} \quad (39.5)$$

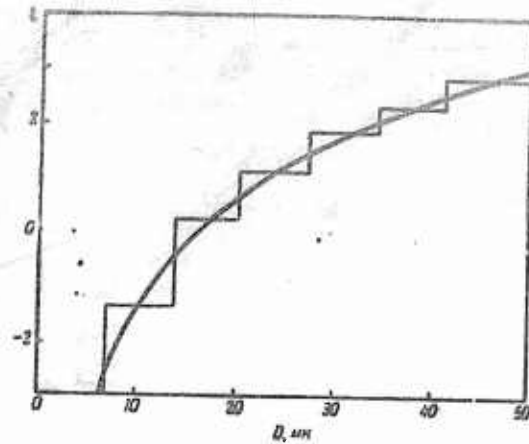


Fig. 106. Dependence of the normalized deviation on the diameter of the micro particles in ordinary coordinates

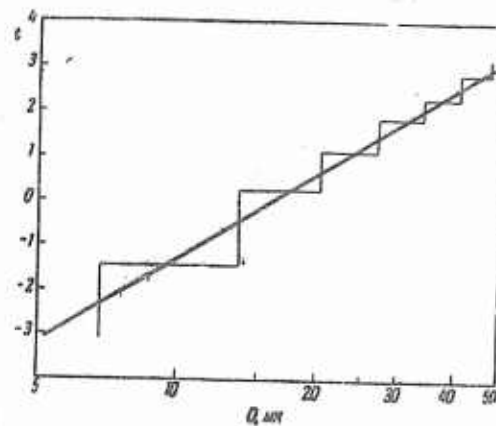


Fig. 107. The same dependence as in Fig. 106 with a logarithmic scale along the axis of the abscissae (straightened curve of frequencies)

Where Δ is the group interval (multiplying factor), mm; D_i is the diameter of microparticles of the i -th group, mm; N_i is the number of microparticles of the i -th group in 1 mm^3 ; N is the total number of microparticles of all sizes in 1 mm^3 ; $\overline{\ln D}$ is the mean logarithm of the diameter of microparticles; $\sigma \{ \ln D \}$ is the root-mean-square deviation of the logarithm of the diameter of microparticles.

Further in this article we present a number of experimental statistical distribution curves for spheroidal microparticles of different structural constituents compared with theoretical curves calculated

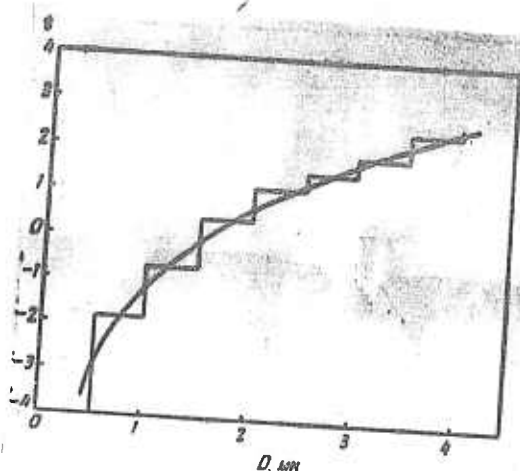


Fig. 108. Dependence of the normalized deviation on the diameter of the micro particles of cementite in ordinary coordinates

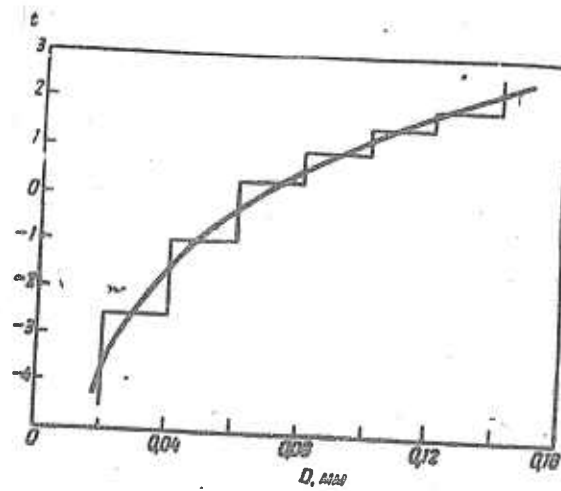


Fig. 109. Dependence of the normalized deviation on the diameter of the grains of austenite in ordinary coordinates

from actual parameters of each distribution in accordance with the formula of logarithmic normal distribution (39.5). In order to have an absolutely objective judgment as to the validity of the derived law of distribution of the diameters of microparticles, we shall use the experimental data of a great number of investigators who calculated the distribution of diameters of microparticles using different methods (E. Scheil, W. Johnson, A. G. Spektor).

A distribution of diameters of microparticles of cementite in carbon steel (0.86% C) following quenching and 6-hour tempering at 700°C is shown in Figure 113. The points coincide with the experimen-

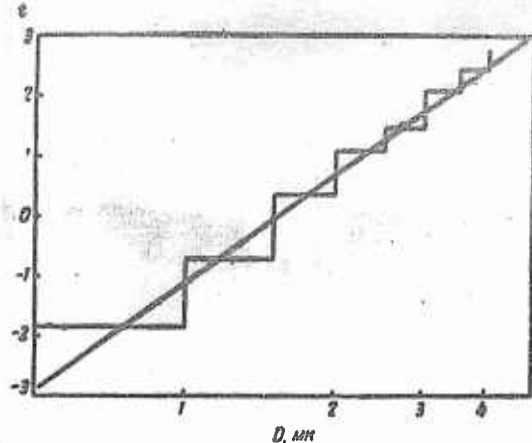


Fig. 110. The same dependence as in Fig. 108 with logarithmic scale along the axis of the abscissae

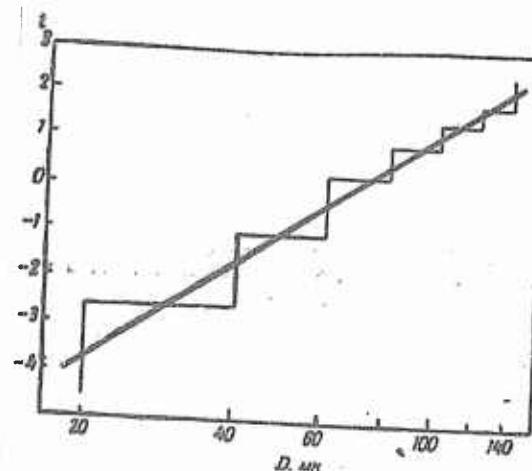


Fig. 111. The same dependence as in Fig. 109 with logarithmic scale along the axis of the abscissae

tal data of M. E. Blanter [166]. The curve has been calculated from actual parameters of distribution described by him: $\bar{D} = 3.48$ divisions of the scale, $\sigma \{D\} = 1.20$ divisions of the scale, $\ln \bar{D} = 1.18272$ and $\sigma \ln \bar{D} = 0.35671$. The total number of microparticles in the distribution is taken as 100%.

Two distributions of microparticles of cementite in steel containing 0.4% C and 3% N₁, subjected to quenching and subsequent isothermal tempering at 630°C, are shown in Figure 114. The curve on the left characterizes the distribution produced by the 30-minute tempering and the one on the right characterizes the distribution produced by 25-hour tempering. Both curves have been plotted on the basis

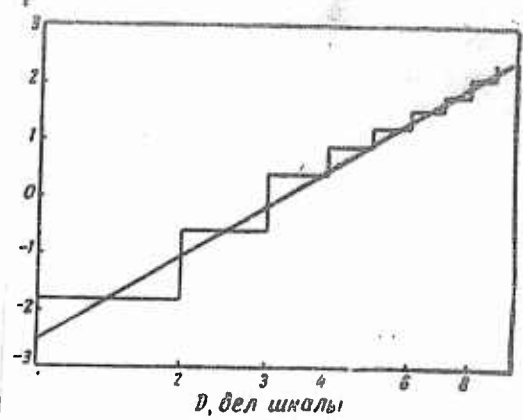
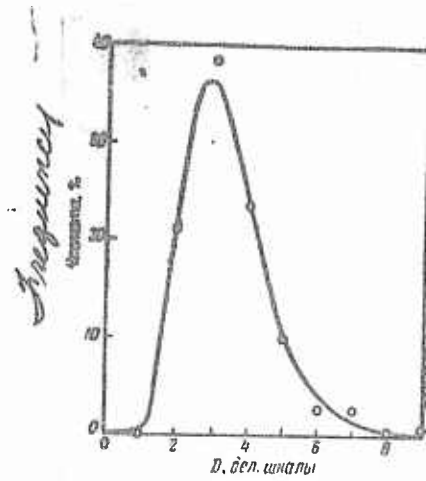


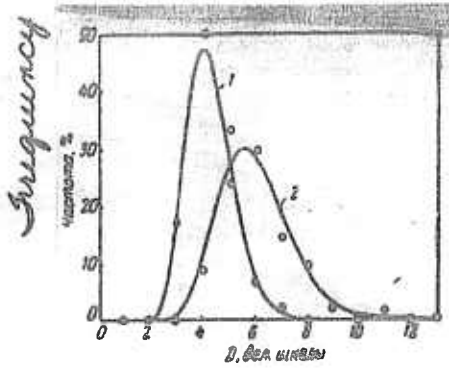
Fig. 112. Straightened curve of the frequencies of the diameters of the grains of austenite according to data published by M. Ye. Blanter [166].

of experimental data published by S. F. Bokshteyn [167]. Distribution parameters following the 30-minute tempering are: $\bar{D} = 4.27$ divisions of the scale; $\sigma \{ D \} = 0.90$ divisions of the scale; $\ln \bar{D} = 1.42919$ and $\sigma \{ \ln D \} = 0.20782$. Following the 25-hour tempering, the distribution parameters are: $\bar{D} = 6.00$ divisions of the scale; $\sigma \{ D \} = 1.42$ divisions of the scale; $\ln \bar{D} = 1.76490$ and $\sigma \{ \ln D \} = 0.23336$. The total number of microparticles in each distribution has been taken as 100%.

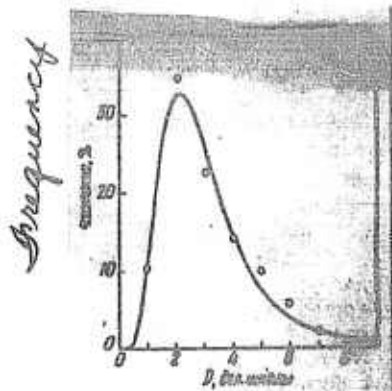


D-Division of scale

Fig. 113. Distribution of the diameters of micro particles of cementite of carbon steel (0.86% C) according to experimental data published by M. Ye. Blanter [116].



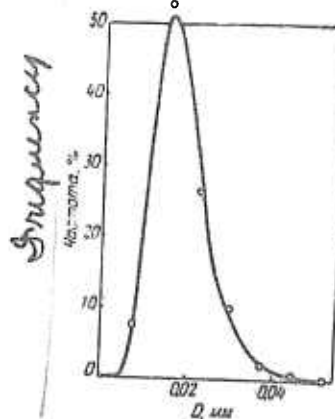
114



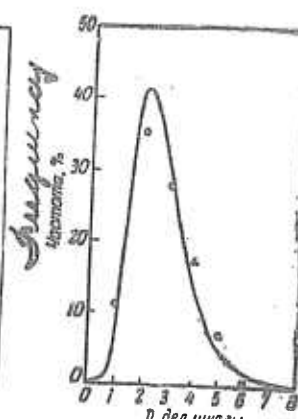
115

Fig. 114. Distribution of the diameters of the micro particles of cementite of carbon steel (0.4% C) after hardening and annealing at 630° for 30 min (1) and 25 hours (2), according to experimental data of S. Z. Bokshteyn [167]

Fig. 115. Distribution of the diameters of the grains of partially converted austenite (0.8% C), according to experimental data of M. Ye. Blanter [166]



116



117

Fig. 116. Distribution of the diameters of the grain of partially converted austenite of steel 40 with the addition of boron, according to experimental data of S. M. Vinarov [15]

Fig. 117. Distribution of the diameters of the spherical micro particles of the graphite of magnesium iron

Distribution curves, which characterize the structure of partially decomposed austenite at low degree of supercooling are of great interest. The distribution of microparticles of partially transformed austenite of carbon steel with 0.8% C is shown in Figure 115. The temperature of isothermal decomposition is 600 C. The distribution curve has been plotted from the experimental data of M. Ye. Blanter [166]. The parameters of the distribution curve are: $\bar{D} = 3.09$ divisions of the scale; $\sigma \{ D \} = 1.56$ divisions of the scale; $\ln \bar{D} = -4.05660$ and $\sigma' \{ \ln D \} = 0.36139$. The total number of microparticles in the distribution has been taken as 100%.

The distribution of spheroidal graphite precipitates in magnesium cast iron, according to the data of the author, is shown in Figure 117. The distribution parameters are: $\bar{D} = 2.755$ divisions of the scale, $\sigma \{ D \} = 1.1890$ divisions of the scale, $\ln \bar{D} = 0.92810$, $\sigma' \{ \ln D \} = 0.41312$. The total number of microparticles in the distribution has been taken as 100%.

The distribution curve of diameters, shown in Figure 118, has been obtained for grains of polyhedral structures of cast magnesium. The distribution parameters are: $\bar{D} = 0.087$ mm, $\sigma \{ D \} = 0.028$ mm, $\ln \bar{D} = -2.44566$ and $\sigma' \{ \ln D \} = 0.31960$. The total number of grains in the distribution has been taken as 100%. The distribution has been plotted from the data of the author.

We have used the data of A. G. Spektor, who computed the distribution of grain sizes of ferrite in mild steel by the method of chords,

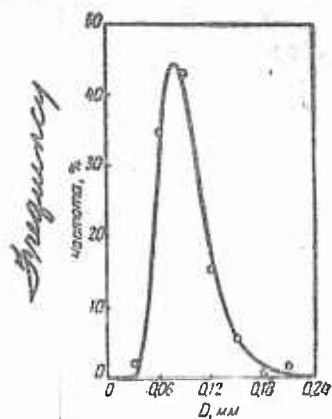


Fig. 118. Distribution of the diameters of the grains of cast magnesium

in contrast to all above cited data calculated by Scheil's method.

Figure 119 shows the distribution which we have plotted from the data of A. G. Spektor [67]. The distribution parameters are: $\bar{D} = 9.12$ microns, $\sigma \{ D \} = 3.99$ microns, $\ln \bar{D} = 1.20705$ and $\sigma \{ \ln D \} = 0.41808$.

The total number of microparticles in the distribution have been taken as 100%.

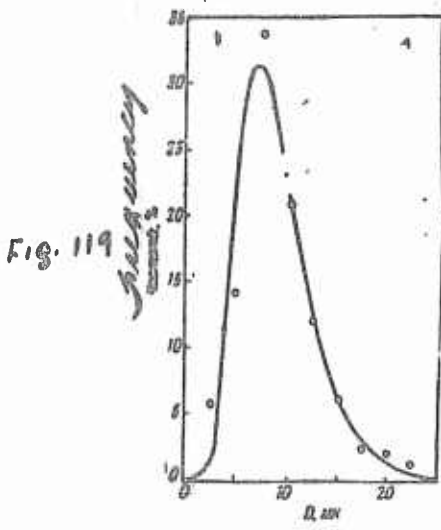


Fig. 119

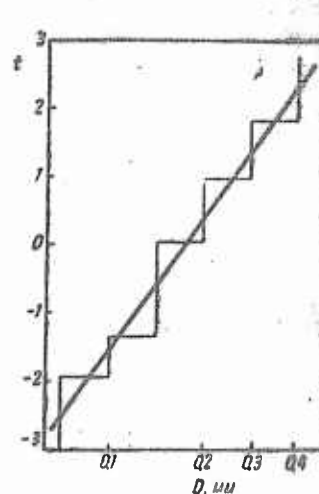


Fig. 120

Fig. 119. Distribution of the diameters of the grains of ferrite computed by the method of chords, per experimental data of A. G. Spektor [67]

Fig. 120. Straightened curve of frequencies of diameters of grains of steel computed by the method of W. Johnson [18]

Finally, a linearized curve of frequencies for the distribution of diameters of grains of steel having a polyhedral structure is shown in Figure 120 (experimental data of W. Johnson, obtained by his method [18]).

The cited statistical curves of distribution and linearized graphs of frequencies of structural constituents of various types convincingly demonstrate that the distribution of diameters of microparticles are based on the law of logarithmic normal distribution expressed by the formula (39.5). The results obtained are absolutely objective, inasmuch as we have used experimental materials obtained by the investigations of M. Ye. Blanter, S. Z. Bokshteyn, S. M. Vinarov, A. G. Spektor, W. Johnson, and ours. Moreover, the original distribution of diameters was determined by the methods of Scheil and A. G. Spektor and W. Johnson.

One cannot insist that the observed law of distribution of diameters of microparticles is universal for all cases, for this requires

experimental verification from a large number of various polydispersed systems of spheroidal microparticles. However, the law of the logarithmic normal distribution undoubtedly is applicable to a quite large number of structural constituents of various types, both polyhedral, single-phase (microparticles of austenite in steel, microparticles of magnesium (and structural constituents which form separated spheroidal microparticles (cementite grains in steel, graphite grains in magnesium cast iron, microparticles of a partially transformed austenite).

The curve of the logarithmic normal distribution and formula (39.5) are conclusive quantitative characteristics of spatial structure of systems of spheroidal microparticles. This curve is completely defined by three parameters found in the Formula (39.5):

- a. The mean logarithmic diameter of microparticles, $\overline{\ln D}$.
- b. The root-mean-square deviation of logarithms of diameters of microparticles, $\sigma \{ \ln D \}$.
- c. The total number of microparticles in 1 mm^3 of metal or alloy, N.

The advantage of W. Johnson's method of differential distribution of the number of spheroidal microparticles in volume, modified by us, lies in the fact that we obtain directly the values which characterize the distribution of logarithms of diameters of microparticles, which facilitate the calculation of the values of $\overline{\ln D}$ and $\sigma \{ \ln D \}$. When computing the distribution by Scheil's or A. G. Spektor's methods, we derive the values which characterize the distribution of diameters of microparticles from which the parameters, \bar{D} and $\sigma \{ D \}$, may be readily calculated. In this case, it is possible to recalculate these parameters to parameters of logarithmic normal distribution, using relationships:

$$\sigma^2 (\ln D) = \ln \left[1 + \frac{c^2 (D)}{(\bar{D})^2} \right] \quad (39.6)$$

$$\overline{\ln D} = \ln \bar{D} - 0.5 \sigma^2 (\ln D). \quad (39.7)$$

Other important parameters, which characterize the structure and which are of great practical importance, may be derived by rigorous mathematical calculations from Formulas (39.5), (39.6) and (39.7). In view of cumbersome derivations, we cite only several final exact formulas. The total volume of spheroidal microparticles per unit volume of metal or alloy is found from the formula:

$$\Sigma V = \frac{\pi}{6} N \left[\bar{D} + \frac{\sigma^2(D)}{\bar{D}} \right]^3 \text{ MM}^3/\text{MM}^3.$$

(39.8)

The specific surface of microparticles, that is, the total surface of all spheroidal microparticles which are not in contact with each other and which are found in the unit volume of metal or alloy, is

$$\Sigma S = \pi N [(\bar{D})^2 + \sigma^2(D)] \text{ MM}^2/\text{MM}^3.$$

(39.9)

By simultaneous solution of Equations (39.8) and (39.9) we can exclude from them the quantity $\sigma^2(D)$. After that, substituting the ratio of $\frac{n}{N}$ for the mean diameter of microparticles, \bar{D} which is equal to it, we derive the following simple relationship between the total number of microparticles in unit volume and three parameters of the structure, which can be the most readily determined from the microsection:

$$N = 6\pi^2 \left(\frac{n}{\Sigma S} \right)^2 \Sigma V \text{ MM}^{-3}.$$

(39.10)

The latter relationship is precisely the basic formula of the method of combined indices, developed by us, which makes it possible to de-

termine all parameters of size distribution for spheroidal microparticles in a volume and their distribution with respect to size, it is not necessary to evaluate differentially the cross sections of microparticles. Thus, the need for doing the most effort-consuming and tedious operation, measuring dimensions of sections on a micro-section (diameters, areas or chords), is eliminated. Parameters found in Formula (39.10) are found with the minimum effort: n by the corrected method of C. Jeffries (Section 32), ΣS by the method of random secants for space (Section 25) and ΣV by the linear method of A. Rosiwal or by the point method of A. A. Glagolev (Sections 14 and 16).

The latter two parameters are in themselves important parameters of the spatial microstructure of an alloy. Moreover, knowing their values and also the value of n we have the possibility for calculating all parameters of logarithmic normal size distribution of microparticles of a given structural constituent and, when it is necessary, to construct the statistical distribution curve itself.

One of the parameters of distribution, the number N , is directly defined by the Formula (39.10). Further, we find a mean value of the diameter of microparticles, \bar{D} , which is exactly equal to the ratio of n . After that, from Formula (35.15), which is valid for any poly-

dispersed system of spheroidal microparticles, we find the value of $\sigma \{ D \}$:

$$\sigma(D) = \sqrt{\frac{\sum S}{\pi N} - (\bar{D})^2} \text{ mm.} \quad (39.11)$$

Knowing the values of \bar{D} and $\sigma \{ D \}$ we find the parameters of the logarithmic normal distribution from formulas, as it has been shown previously. By substituting the obtained values of parameters into Formula (39.5), it is possible to compute the data needed for plotting the graph of the distribution curve, which is needed to verify whether the actual distribution corresponds to the logarithmic normal curve.

It should be noted that the quantity $\sum S$, found in Formulas (39.10) and (39.11), expresses the total surface of spheroidal microparticles in 1 mm^3 of metal or alloy. If microparticles (grains) are in contact with each other forming a common interface, then this surface must be doubled in order to obtain the correct results from the same formulas. (Note: That is, each grain must be considered separately, as if it were a particle). Thus, for example, if the object of microanalyses is a single-phase polyhedral structure with equiaxed grains in space, all boundary surfaces simultaneously belong to two grains. Therefore, for such structures the value determined by the method of random secants must be doubled before being inserted into Formulas (39.10) and (39.11). Inasmuch as in a single-phase polycrystalline aggregate the total volume fraction of grains is 1, the Formula (39.10) to be applied to this case must be modified as follows:

$$N = 6 \pi^2 \left(\frac{n}{2 \sum S} \right)^3 \text{ MM}^{-3}. \quad (39.12)$$

Let us consider the case of using the method of combined indices for the calculation of the number of grains of ferrite in 1 mm³ of mild steel. In this case, Formula (39.12) is applicable. The number of flat grains, determined by the method of C. Jeffries, is 1175 per 1 mm² of the microsection, and the specific surface, measured by the method of random secants, is 71.4 mm²/mm³. By inserting these values into Formula (39.12) we derive:

$$N = 6\pi^2 \left(\frac{1175}{2 \cdot 71.4}\right)^3 = 32958 \text{ mm}^{-3}.$$

The control calculations by the method of E. Scheil, which was done when dividing ferrite grains and their sections into 15 size groups, produces a somewhat high figure of 34,992 mm⁻³, which exceeds the value determined by us by 5.8%. Taking into account the fact that the structure is single-phase and that microparticles of ferrite definitely cannot be spheroidal, because of that, the agreement of results should be considered quite satisfactory. The deviation from the results of calculations by E. Scheil's method is even less than that, if the number of groups is less (10 to 5).

From the original value of n and from the value just found, N , we determine the mean value of the diameter of ferrite grains:

$$\bar{D} = 1175 : 32958 = 0.0356 \text{ mm.}$$

If we take the value of N , as calculated by the method of E. Scheil, we derive $\bar{D} = 0.0336 \text{ mm.}$

To compute the root-mean-square deviation, $\sigma\{D\}$, we use Formula (39.11) but instead of the experimentally determined value of the specific surface, 71.4 mm²/mm³, we insert its doubled value, 142.8. We derive:

$$\sigma(D) = \sqrt{\frac{142.8}{32958}} - (0.0356)^2 = 0.0106 \text{ mm.}$$

The root-mean-square deviation, computed directly from the distri-

bution of diameters, calculated by E. Scheil's method, happened to be 0.0111 mm.

From the data presented it is apparent that the deviation in values of all three parameters, calculated by the method of combined indices and by E. Scheil's method, is approximately 6 per cent in the most advantageous case, that is, polyhedral structure.

Section 40. The Accuracy of Methods for Determining the Number of Microparticles. Approximation Methods.

All methods, reviewed in this chapter, of determining both the over-all number, as well as the number, differentiated with respect to size, of spheres in polydispersed system are rigorous from the mathematical viewpoint or may be rendered as accurate as desired by dividing into a larger number of size groups (for example, the method of E. Scheil). This is why the basic and, so to speak, principal source of the error is the deviation between the actual shape of real microparticles and ideal spheroidal shape. Secondary errors arise in practical applications of the methods described, which errors are due to random inaccuracies in measurements taken on the microsection or photomicrograph.

The actual volumetric size of grains was investigated in works of E. Scheil and G. Wurst [63][64]. Specifically, they applied the method of successive grindings, each removing a layer of metal 0.008 mm thick. From the time the plane of polish exhibited the trace of a reoccurring grain, areas of its successive sections were subject to planimetric measurements. As a result, it was possible to form a notion of the true shape and volume of several microparticles. The object of the investigation was a specimen of Armco iron with a relatively complex shape of sections of grains on the plane of polish. Curves 1 and 2 in Figure 121 show variations in the area of sections with height of 2 microparticles of ferrite, according to data presented by E. Scheil and H. Wurst as typical [64]. The total height of the microparticle in the direction perpendicular to the plane of polish was taken by us as unity. Actually it was equal 0.112 mm for Specimen 1 and 0.250 mm for Specimen 2. In the same figure Curve 3 shows similar distribution of areas of sections of a sphere, whose diameter is 1. Just as it should have been anticipated, sections of microparticles, beginning with the maximum, decrease more rapidly than sections of the sphere; in the lower section in Figure 121. The curvatures of the graphs for the microparticles and for the sphere are of opposite sign. E. Scheil and H. Wurst concluded that by assuming microparticles

are spheres, we commit a considerable error.

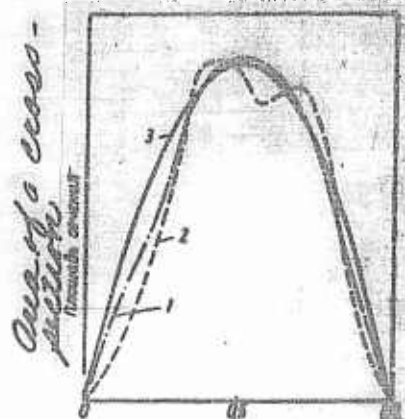


Fig. 121. Typical change of area of section of two grains as to height.
Obtained by the method of successive grinding off of soft steel
by E. Scheil and H. Wurst

The actual magnitude of the error apparently cannot be determined inasmuch as we do not have the possibility of breaking down a polycrystalline aggregate into separate microparticles, to calculate their number and separately evaluate with respect to size (volume, weight), so as to compare the figures thus obtained against the results calculated from the data of quantitative microanalyses of a plane section of the aggregate subject to investigation (on the plane of polish). Even if we possessed this possibility, in each separate case and conforming to one and the same procedure of stereometric microanalyses the error will vary, for it is determined by the concrete "mean shape" of microparticles and by its dispersity.

A certain notion of the order of error is possible if two values of the specific surface area are compared: one calculated as the sum of surface areas of spheres of the obtained distribution of diameters of microparticles and another measured directly by the method of random secants.

The distribution of diameters of microparticles of ferrite in mild steel, calculated by the method of E. Scheil using division into 15 groups, is given in Table 57. The parameters which characterize this distribution have been previously given in Section 39. Calculating the specific surface as a total surface area of spheres, we derive:

$$\Sigma D(N) = 137.4 \text{ mm}^2/\text{mm}^3$$

Inasmuch as the structure is a single-phase and polyhedral, the grain boundary surface in any of its points simultaneously belongs to two microparticles. For this reason the specific surface area will be equal to one-half of the derived value, that is

$$\Sigma S = 137.4 \cdot 2 = 68.7 \text{ mm}^2/\text{mm}^3$$

The true specific surface area, determined by the method of random secants, happened to be $71.4 \text{ mm}^2/\text{mm}^3$ and, consequently, the error was 3.8 per cent.

| μ | Number of groups in diameter range, μ | Approximate number of microparticles in group |
|--------------|--|--|
| 1 | 0.005 | 9 |
| 2 | 0.010 | 26 |
| 3 | 0.015 | 700 |
| 4 | 0.020 | 3120 |
| 5 | 0.025 | 7216 |
| 6 | 0.030 | 8300 |
| 7 | 0.035 | 6016 |
| 8 | 0.040 | 3500 |
| 9 | 0.045 | 2220 |
| 10 | 0.050 | 1440 |
| 11 | 0.055 | 960 |
| 12 | 0.060 | 600 |
| 13 | 0.065 | 400 |
| 14 | 0.070 | 240 |
| 15 | 0.075 | 152 |
| <i>Total</i> | | |
| Bero | 0.005–0.075 | 34992 |

1. No. of groups
2. Diameter of microparticles
3. No. of microparticles in

Table 57

Very tentative limits of error of determining the number of microparticles, which is due to the deviation between their actual shape and spherical shape, may be established only approximately. For a single-phase polyhedral structure this error may be estimated by values of the order of 5 to 10 per cent. The lower limit refers to structures whose planar grains are equiaxed, each separately and in any

section, and which are characterized by the minimum curvature of grain boundaries. As the contour of planar grains becomes more complex and their individual shapes deviate from equiaxed (although as a whole the isometricity of the system of boundary lines is maintained in any section), the error is increased and, generally speaking, cannot be limited more or less rigidly by the upper limit of 10 per cent.

A relatively smaller error occurs in "granular" constituents of complex structures, when microparticles of spheroidal shape do not come in contact with each other. In some cases microparticles of this type are capable of assuming almost an ideal spherical shape, for example, graphite precipitates in low-silicon malleable cast iron annealed at low temperatures and having a pearlite base. When analyzing isolated microparticles, the error may be tentatively estimated by the values of 3 to 6 per cent or higher, if the shape of microparticles notably deviates from the spatial equiaxed.

When the number of microparticles is determined by the method of E. Scheil, using divisions into a smaller number of size groups, the error of the method may exceed a great deal the error which is due to the deviation between the shape of microparticles and spherical shape. In order to determine the influence of the number of groups on the result of calculations, we have employed the distribution of ferrite microparticles, the characteristic of which is given in Table 57. Initially sections of microparticles were divided into 15 size groups and figures, given in Table 57, have been calculated using this division. After that, the groups were gradually incorporated and calculations by the method of E. Scheil were carried out for 9 variants of breaking down into various number of groups. The summary of results is given in Table 58. Although the total number of microparticles continually increases with an increasing number of groups, all the way to 15, the figure which is derived for 15 groups may be accepted as the true value of the number of microparticles, arbitrarily assuming that the error of the method in this case is equal to zero. The data in the table show that the error of calculations begins to increase particularly rapidly when the number of groups is five or less than

that. This is particularly apparent in the graph shown in Figure 122.

| Число групп разбики | Количество микро частиц в 1 м ³ | Ошибка расчета, % | Средний диаметр, мк |
|------------------------|--|----------------------|------------------------|
| 2. | 3. | 4. | 5. |
| 1 | 15040 | 56,9 | 0,078 |
| 2 | 27339 | 22,5 | 0,043 |
| 3 | 36758 | 12,5 | 0,032 |
| 4 | 34760 | 9,4 | 0,027 |
| 5 | 32625 | 6,4 | 0,026 |
| 6 | 31705 | 3,9 | 0,026 |
| 7 | 31316 | 2,0 | 0,026 |
| 8 | 30201 | 0,3 | 0,025 |
| 9 | 29592 | 0 | 0,024 |

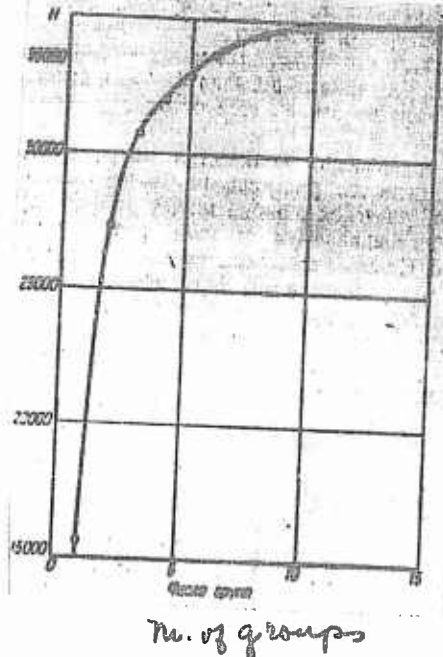
1. №. of division groups

2. №. of micro particles in 1 m³.

3. Calculation error %.

4. Average diameter, mic.

Table 58



No. of groups

Fig. 122. Number of micro particles in a unit of volume, computed by the method of E. Scheil as depends on the number of groups of МММ layout

Therefore it is desirable to have at least seven groups; breaking down into a number of groups, which is less than five, is not permissible. At the same time increasing the number of groups above 10 to 12 is not practically expedient, for there is no sense in trying to attain the accuracy of calculations up to tenths or hundreds of 1 per cent, while the deviation of the shape of microparticles from the shape of a sphere is responsible for an error the minimum of which is estimated in several per cent.

All these conclusions refer also to the method of W. Johnson. However, in the latter breaking down into 7 to 8 groups is quite acceptable and breaking down into 6 groups permissible, for the logarithmic scale assures a finer differentiation of sections of small diameter, which have a greater effect on the results of calculations than the large sections. The method of inverse diameters is free from this type of error, inasmuch as the breaking down into groups is not made and Formula (35.8) is rigorous from the mathematical viewpoint.

Approximate methods for calculating the number of microparticles are applicable not only to microparticles of spheroidal shape, but also to particles of other configurations more or less geometrically regular. To apply approximation formulas, it is sufficient to determine 2 and sometimes only 1 parameter of a planar structure. Let us consider some of these methods.

A. Formula of I. L. Mirkin for Spheroidal Microparticles

The exact formula of I. L. Mirkin (35.1) correlates the diameter of spheres in a monodispersed system D, their number per unit volume, N, and the number of sections of spheres per unit area, n. Of these values only one, n, can be determined directly from the plane of polish. Therefore, in order to be able to determine the number of spheres, N, I. L. Mirkin substitutes the mean diameter of sections of spheres, \bar{d} , visible on the plane of polish, for the diameter of spheres, D, introduces the correction coefficient K, and obtained:

$$N = K \frac{n}{\bar{d}} \text{ mm}^{-3}.$$

(40.1)

I. L. Mirkin estimates the value of the coefficient K within the limits of the 0.87 and 1.25 [168]. Its value obviously is dependent upon the fluctuation of actual sizes of diameters of microparticles of an actual polydispersed system. We have a possibility of estimating the accuracy of Formula (40.1) and the validity of the coefficient K.

From Formulas (35.9) and (35.11), which are valid for any poly-dispersed system of spheres and which have been derived by rigorous mathematical operations, we obtain the following relationship:

$$\frac{\bar{d}}{\bar{D}} = \frac{\pi}{4} \left(1 + \frac{\sigma^2(D)}{(\bar{D})^2} \right) = \frac{\pi}{4} (1 + \delta^2),$$

(40.2)

where δ is the coefficient of variation of the diameters of spheres. Identical formula was previously obtained by somewhat different method A. G. Spektor [161]. By substituting term \bar{D} from Formula (40.2) into exact formula of I. L. Mirkin, which we generalized for the case of the polydispersed system of spheres (35.6), we obtain a relationship which contains the same terms as the approximation formula (40.1), but with an exact expression for the coefficient K:

$$N = \frac{\bar{d}}{\bar{D}} = \frac{\pi}{4} (1 + \delta^2) \frac{\bar{d}}{d} MM^{-\frac{1}{2}}.$$

(40.3)

Comparing Formulas (40.1) and (40.3), we derive:

$$K = \frac{\pi}{4} (1 + \delta^2).$$

(40.4)

Previously we mentioned that the values of the coefficient of variation of diameters for real polydispersed systems of spheroid microparticles are more frequently found between the limits of 0.2 and 0.5. In Table 59 we give the values of the coefficient K, calculated for various values of the coefficient of variation δ from Formula (40.4).

| Коэффициент вариации диаметров микрочастиц | Коэффициент K | Коэффициент вариации диаметров микрочастиц | Коэффициент K |
|--|---------------|--|---------------|
| 1. | 2. | 3. | 4. |
| 0 | 0,785 | 0,6 | 1,000 |
| 0,1 | 0,783 | 0,7 | 1,179 |
| 0,2 | 0,817 | 0,8 | 1,280 |
| 0,3 | 0,856 | 0,9 | 1,422 |
| 0,4 | 0,911 | 1,0 | 1,571 |
| 0,5 | 0,932 | | |

- 1. Variation of microparticle diameter
- 2. Coefficient K.
- 3. Same as 1.
- 4. Same as 2.

Table 59

The data in the table indicate that the limits of values of the coefficient K , cited by I. L. Mirkin, are somewhat exaggerated. For the most frequently encountered values of the coefficient of variation of diameters, the values of the coefficient K are found in the limits of 0.82 and 0.92. We believe it is expedient to accept $K = 0.9$ for approximate calculations. In this case the formula of I. L. Mirkin will have the following form:

$$N = 0.9 \frac{n}{d} \text{ nm}^{-3}$$

(40.5)

The error of the method when using this formula for calculations is determined by the actual value of the coefficient of variation of the diameters of microparticles of the structure which is being investigated. Accepting the ordinary limits of the values of the coefficient of variation of diameters between 0.2 and 0.5, we derive the values of the error of the method, when calculating from Formula (40.5), respectively equal to plus 10.2 and minus 8.4 per cent. In isolated instances, for values of the coefficient of variation beyond the ordinary limits, the error will be correspondingly higher.

B. The First Formula of S. A. Saltykov for Spheroidal Microparticles

The total volume of spheres of a monodispersed system is precisely defined by the expression:

$$\Sigma V = \frac{\pi D^3}{6} N^2 \text{ nm}^3/\text{nm}^3$$

(40.6)

From the exact formula of I. L. Mirkin (35.1) for a monodispersed system of spheres we have:

$$n = DN \text{ nm}^{-3}$$

(40.7)

By eliminating from these two formulas the term D , which is known to us, we obtain the possibility of calculating the number of spheroidal microparticles per unit volume from the formula:

$$N = \sqrt{\frac{\pi}{6\pi V}} n^{1/2} = K_0 n^{1/2} \text{ MM}^{-3}.$$

(40.8)

The derived expression is rigorous only for a monodispersed system of spheres. When using this expression for the analysis of polydispersed systems of microparticles, the accuracy of the formula is determined by the value of the coefficient of variation of diameters of microparticles. The number of sections per 1 mm^2 is determined from the plane of polish as well as the fraction of the area of the plane of polish occupied by these sections, which fraction corresponds to the fraction of the volume of the alloy occupied by corresponding microparticles.

Let us consider the error of the method predetermined by the application of Formula (40.8) to the analysis of polydispersed systems of spheroidal microparticles, when this formula is derived for monodispersed systems in which the coefficient of variation of diameters of microparticles is zero. If the distribution of diameters of microparticles corresponds to the law of logarithmic normal distribution, the total volume of microparticles is precisely expressed by the formula:

$$\Sigma V = \frac{\pi}{6} N \left[\bar{D} + \frac{\sigma^2(D)}{\bar{D}} \right]^3 \text{ MM}^3/\text{MM}^3$$

(40.9)

(see Section 39) by applying the formula of I. L. Mirkin, generalized by us for the case of a polydispersed system of spheres (35.6), by substituting the coefficient of variation, σ , for the ratio of $\sigma \{ D \}$ to \bar{D} , and by determining the value of N , we derive the following rigorous relationship valid for polydispersed systems of spheroidal microparticles, whose diameters follow a logarithmic normal distribution:

$$N = \sqrt{\frac{\pi}{6 \Sigma V}} (1 + \delta^2)^{1/2} n^{1/2} \text{ mm}^{-3}$$

(40.10)

The derived exact formula differs from the approximate formula (40.8) in that it contains an additional factor the value which is singularly determined by the coefficient of variation δ and is always greater than unity. The values of this factor for various values of δ are given in Table 60. From the data found in the table it follows that for the middle range of the more common values of the coefficient of variation (0.8 to 0.5), the value of the factor is approximately 1.2. It is expedient to introduce an appropriate correction into Formula (40.8), in order to avoid a one-sided error. For this reason we accept:

$$N = 1.2 k_0 n^{1/2} = k_1 n^{1/2} \text{ mm}^{-3}$$

(40.11)

Table 60

| Коэффициент вариации диаметров микрочастиц | Множитель $(1 + \delta^2)^{1/2}$ | Коэффициент вариации диаметров микрочастиц | | Множитель $(1 + \delta^2)^{1/2}$ |
|--|-------------------------------------|--|------|-------------------------------------|
| | | 1. | 2. | |
| 0 | 1.000 | | 0.6 | |
| 0.1 | 1.015 | | 0.61 | |
| 0.2 | 1.031 | | 0.62 | |
| 0.3 | 1.039 | | 0.63 | |
| 0.4 | 1.048 | | 0.64 | |
| 0.5 | 1.057 | | 0.65 | |

1. Variation coefficients of micro-particle diameter δ .
2. Multiple $(1 + \delta^2)^{1/2}$.
3. Same as 1.
4. Same as 2.

Table 61

| Суммарный объем микрочастиц | Коэффициент формулы (40.11) | Суммарный объем микрочастиц | | Коэффициент формулы (40.11) |
|--------------------------------|-----------------------------------|---|------|-----------------------------------|
| | | Σ V, мкм ³ /мкм ² | % | |
| 0.01 | 1 | 0.603 | 0.35 | 0.6 |
| 0.02 | 2 | 0.640 | 0.40 | 0.573 |
| 0.03 | 3 | 0.613 | 0.45 | 0.554 |
| 0.04 | 4 | 0.613 | 0.50 | 0.536 |
| 0.05 | 5 | 0.633 | 0.55 | 0.517 |
| 0.06 | 6 | 0.645 | 0.60 | 0.498 |
| 0.07 | 7 | 0.658 | 0.65 | 0.479 |
| 0.08 | 8 | 0.670 | 0.70 | 0.460 |
| 0.09 | 9 | 0.683 | 0.75 | 0.441 |
| 0.10 | 10 | 0.706 | 0.80 | 0.422 |
| 0.15 | 15 | 0.746 | 0.90 | 0.375 |
| 0.20 | 20 | 0.795 | 0.95 | 0.338 |
| 0.30 | 30 | 1.047 | 1.00 | 0.267 |
| 0.50 | 50 | 1.767 | 1.00 | 0.196 |

1. Total volume of microparticles.
2. Formula coefficient (40.11) K2.
3. Same as 1.
4. Same as 2.

This is the formula which we assume approximates the working formula. When using this formula, our calculations produce an error of the method, the highest values of which, corresponding to the extreme limits of ordinary values of the coefficient of variation of the diameters, are +13.1 and -14.1 per cent. To facilitate the application of the formula (40.11) we have listed the values of the coefficient k_1 in Table 61. These values have been computed for various contents of the substance of microparticles, expressed in fractions or in volume per cent of the alloy.

The relationship between the number of microparticles of graphite of spheroidal shape per 1 mm^3 of malleable cast iron, determined by the method of E. Scheil, and the number of their sections per 1 mm^2 of the plane of polish, is plotted in logarithmic coordinates in Figure 123. It confirms the acceptability of our approximate Formula (40.7). Experimental data of H. Schwarz [169] and ours [178] have been used in plotting the graph. Two parallel lines on the graph correspond to the relationship, defined by the Formula (40.11), at 5 and 7 per cent content of the substance of the microparticles in the volume of the alloy. These limits correspond to an ordinary volumetric content of carbon in malleable cast iron.

Let us also compute the number of grains of ferrite in mild steel, whose diameter distribution has been given in Table 57. The total volume of grains per 1 mm^3 is 1, inasmuch as the structure is single phase, and the number of planar grains is 1175 mm^{-2} . Therefore we obtain:

$$N = 0.000(1175)^{1/2} = 0.000 \cdot 3427 = 3427 \text{ mm}^{-2}$$

Calculation by E. Scheil's method with division into 15 groups yields $34,992 \text{ mm}^{-3}$, which is very close to the figure found above. This high accuracy, produced by the approximation formula, is explained by the fact that the coefficient of the variation of diameters of grains of ferrite is 0.330, that is, it differs very little from the value of , on the basis of which we have determined the correction coefficient

for Formula (40.8). We must note that it is sufficient to determine experimentally only one parameter of a planar structure, the number n , in order to compute the number of grains of a single-phase structure.

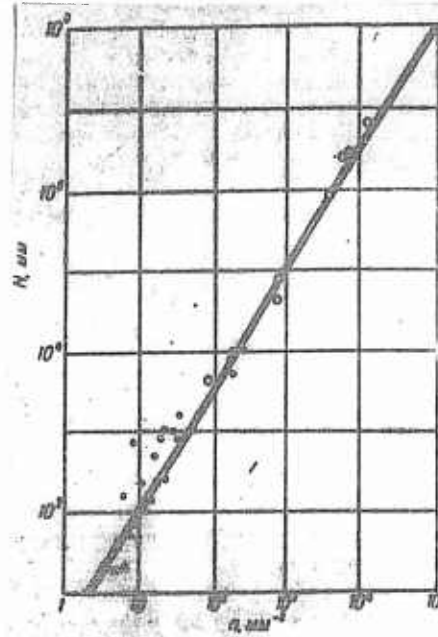


Fig. 123. Interdependence between the number of spherical graphite divisions in a unit of volume and on a unit of area of the slide, per data of H. Schwartz (dots) and S. Saltykov (circles)

C. The Second Formula of S. A. Saltykov for Spheroidal Microparticles

The total surface of microparticles of any polydispersed system of spheres is defined exactly by the formula: (see Section 39)

$$\Sigma S = \pi N [(\bar{D})^2 + e^2(D)] \cdot \pi R^2 / M M^2$$

(40.12)

Using the formula of I. L. Mirkin, generalized by us, and by substituting the coefficient of the variation of diameters, δ^2 , for the ratio of D to \bar{D} , we derive the exact formula:

$$N = \pi (1 + \delta^2) \frac{n^3}{\Sigma S} M M^{-3},$$

(40.13)

from which, arbitrarily assuming that the term in parentheses is con-

stant, we can derive the approximation working formula. Inasmuch as ordinary limits of the values of the coefficient of variation of diameters are confined to values of 0.2 and 0.5, the middle of this range corresponds to the value of δ equals 0.35. This is the reason why the mean value of the factor, which is dependent upon the coefficient of variation, found in Formula (40.13), will be:

$$1 + \delta^2 = 1.1225$$

and the approximation formula will have the following form:

$$N = 3.53 \frac{r^3}{ES} \text{ mm}^{-3}$$

(40.14)

this formula contains two parameters whose determination from a planar structure is a very simple matter.

The error in the method when using the approximation working formula (40.14) in calculations, corresponding to the extreme limits of ordinary values of the coefficient of variation of diameters of microparticles, will be +7.9 and -10.2 per cent. It should be kept in mind that Formula (40.14) contains the total surface area of spheroidal microparticles and therefore, if they have a partial or complete contact between each other, this circumstance must be taken into consideration. For example, in a single-phase structure, the value of the specific surface area determined by the method of random secants must be doubled. In a case of partial contact, is counted as two intersections.

Let us apply this formula to the same structure of mild steel that we had before. The specific surface area, determined by the method of random secants, is 71.4; by doubling its value (in view of the single-phase structure) we derive $142.8 \text{ mm}^2/\text{mm}^3$. The number of planar grains is 1175 per 1 mm^2 . Therefore

$$N = 3.53 \frac{(1175)^3}{142.8} = 34129 \text{ mm}^{-3}$$

The result obtained is approximately 2.5 per cent less than the figure

resulting from the same calculation by A. Scheil's method, which is $34,992 \text{ mm}^{-3}$.

D. Formulas for Microparticles the Shape of Which is Not Spheroidal

Let us employ relationships between the parameters of spatial structure and planar structure, derived by us previously, in order to derive approximate formulas permitting the determination of the number of microparticles shaped as a cube or cubic octahedron. Microparticles shaped as quite regular cubes are encountered in real structures (see for example Figure 4), and the cubic octahedron approximately corresponds to the shape of microparticles of a single-phase polyhedral structure with spatially equiaxed microparticles. Formulas presented further in this article, just as those previously derived approximation formulas for spheroidal microparticles, are based on the assumption that all microparticles in the volume are of equal size. Inasmuch as we do not have an opportunity to introduce a correction for the dispersity of sizes of microparticles shaped as cubes or cubic octahedrons, the formulas presented below are less accurate than the formulas for the calculation of the number of spheroidal microparticles.

Let us consider microparticles, shaped as a cube, whose edge is a . The surface area of one cube is $6a^2$ square and the total surface area of N number of cubes, isolated from each other, will be defined by the equation:

$$\Sigma S = 6a^2 N \text{ mm}^2/\text{mm}^3.$$

(40.15)

The length of the edge of the cube is a . Therefore the length of all edges of 1 cube is $12a$, and the total length of edges of cubes, isolated from each other, will be defined by the expression:

(40.16)

where M is the mean number of apexes of sections of cubes per 1 mm^2 of the plane of polish. The simultaneous solution of these two equations eliminates the term a from them, and we derive:

(40.17)

In practice it is more convenient to substitute the number of sections of cubes per 1 mm^2 of the plane of polish, n , for M . Let us visualize a system of close packed cubes of equal size, which we intersect by a number of planes randomly oriented in space. The obtained sections will have three to six angles. Inasmuch as each edge in this system will be common to four adjacent cubes, four boundary lines will join in each load on the plane, i. e., four adjacent sections will be joined. Consequently, although the number of apexes of separate sections of the cube may differ, the mean number of apexes of sections of cubes must be equal to four. Now if all the cubes in our system are separated and oriented randomly in space, the reasoning and the conclusions presented above will be still in force and, consequently, the random sections of cubes on an average always have four apexes and therefore, the number of apexes of sections of cubes, M , may be replaced by an equal value of $4n$. By appropriate modification of Formula (40.17), we derive an approximate working formula for the calculation of the number of cubic microparticles isolated from each other.

$$N = \frac{16n^3}{625} = 2.67 \frac{n^3}{25} \text{ mm}^{-3}.$$

(40.18)

Now we shall carry out similar computations for a system of cubic octahedrons, of equal size, whose edge is a . The surface area of a separate cubic octahedron, S , is defined by the expression:

$$S = 6a^2(1 + 2\sqrt{3}) = 36a^2 + 24a^2\sqrt{3}$$

Therefore, the specific surface area of cubic octahedrons which are not in contact with each other will be:

$$\Sigma S = 20.765 \cdot N \text{ mm}^2/\text{mm}^3$$

(40.19)

A cubic octahedron has 36 edges, for this reason the total length of edges per unit volume will be:

$$\Sigma L = 36N \text{ mm}/\text{mm}^3$$

(40.20)

where M is the number of apexes of sections of cubic octahedron per 1 mm^2 .

By eliminating the term a from equations (40.18) and (40.19), we get formula:

$$M = 2.00 \frac{N^2}{S} \text{ mm}^{-3}$$

(40.20)

It is more convenient to substitute the number of sections of cubic octahedrons per 1 mm^2 on the plane of polish, n , for the term M . We take into account the fact that each edge in a system of a close packed cubic octahedrons simultaneously belongs to three of them. By reasoning as in the case of cubes, it is possible to demonstrate that sections of cubic octahedrons produced by a plane have on an average six apexes, that is, the same number of apexes which on an average have the planar grains of single-phase structures. By substituting $6n$ for M in Formula (40.20), we derive an approximation working formula for microparticles shaped as cubic octahedrons and isolated from each other:

$$N = 2.00 \frac{n^2}{S} \text{ mm}^{-3}$$

(40.21)

If the formula is applied to a single-phase structure, the value of the specific surface area, found experimentally by the method of random secants, has to be doubled and only after that substituted into Formula (40.21).

The proposed approximation Formulas (40.18) and (40.21) contain two parameters, which can be most simply determined experimentally. The number of microparticles of the shapes in question per 1 mm³, N, may be also correlated with other parameters of the structure, for example with the specific volume, as it has been proposed by us in one of our preceding papers [17]. If we are to analyze the error of the method of approximation calculation of the number of spheroidal microparticles, using formulas correlating the term N and the specific volume of the substance of microparticles (40.11) and the specific surface area of microparticles (40.14), we shall see that in the second case this error is considerably smaller, therefore, Formulas (40.18) and (40.21) should be preferred for the calculations; these formulas are similar to Formula (40.14) for spheroidal microparticles by the method of the approximation calculation proposed by us previously and described in paper [17].

CHAPTER V
QUANTITATIVE DETERMINATION OF FORM OF MICROPARTICLES

Section 41. Methods of Defining the Shape of Microparticles

In metal-working practice, the form of sections of microparticles (or of the microparticles themselves) is determined mainly by purely qualitative concepts. For instance, the form of microparticles of ~~MX~~ cementite in pearlite is defined as granular, beaded, or lamellar, the form of graphite deposits in ~~gray~~ gray iron is defined as rectilinear and curled (GOST 3443 - 46), etc. Often there is used a semiquantitative determination using conventional index points (balls) with the aid of scales of structures, representing to a sufficient degree an arbitrary set of the same qualitative ~~determinations~~ determinations, arranged in fixed sequence. Only in ~~XXX~~ individual cases is the construction of scale based on a fixed quantitative parameter, characterizing the element of the form of two-dimensional section of microparticles. For instance, in GOST 3443 - 46, the shape of graphite deposits is typified by the ratio of ~~XXX~~ length of their sections, visible on the cut, to thickness (more exactly, to ~~width~~).

Let us examine several methods which have already been used in quantitative metal-working analysis, which can be recommended for use as adequately ~~effective~~ effective.

According to purely qualitative criterion, we can divide microparticles into three main groups from the viewpoint of their shape:

1. Equiaxed microparticles, in which the dimensions on an average are the same in all directions or, speaking more precisely, in which there is no prevalence of dimensions in any one or two fixed directions over the remaining ones. Microparticles of this group are often typified as ~~equiaxed~~ equiaxed grains or polyhedrons, globules, spheroids, ~~etc.~~ clusters etc. The ~~equiaxed~~ equiaxiality of microparticles does not mean that ~~they~~ they should have the form of a sphere or one close to it. The surface of microparticles can have any degree of roughness, and their actual shape can be very complex, similar to a rosette-shaped one (crab shaped,

~~etc.~~ chrysanthemum shaped) of graphite deposits, occurring in gray irons.

2. Plane microparticles, in which the dimensions in two directions prevail markedly over the dimension in the third direction (small leaves, scales, plates, lenses etc.). These microparticles can be both flat, as well as spatially bent in any shape and degree.

3. The linear microparticles, the dimension of which in one direction prevails sharply over the dimensions in all other directions (needles, rods, ~~etc.~~ threads etc.). These microparticles also can have any steric curvature.

Understandably, this classification is to a considerable degree provisional, since there can exist all possible intermediate and transitional forms. For instance, the junction of small leaf-shaped deposits of graphite, having externally equiaxed lamellar outlines, can also be referred to the first and to the second group.

A. Determination with the Aid of the Factor Form

Examining the total surface of grains or of microparticles in a unit volume of metal, changing in the process of collective recrystallization or coagulation, we can state that, at given conditions, this value tends toward a certain marginal minimum of specific surface. The decrease in specific surface is accomplished both owing to combination of individual grains and microparticles, as well as owing to change in the form of each of them.

The process of form modification is manifested in a decrease of curvature faces and edges, of facets and vertices, in changes of contact ~~between~~ two-facet and solid angles, in acquisition of ~~new~~ equiaxed, rounded outlines. All these changes in form are reflected fairly distinctly by dimensionless ~~relationships~~ ratios between values of volume and surface of microparticles or, accordingly, of area and perimeter of their flat (plane) sections.

In geometry, the definition of the form of plane figures is conducted with coefficient of ~~proportion~~^{uniformity} the aid of the coefficient of form, which is defined as the ratio of area of rectilineal figure F to the square of its perimeter, P. For instance, for various ~~figures~~^{rectilinear} polygons, independently of their absolute dimensions, the coefficients of form equal:

| | |
|---|--------|
| rectilineal | |
| For RIGHT triangle | 0.0481 |
| For a square | 0.0625 |
| For a rectilineal hexagon | 0.0722 |
| For a circle | 0.0796 |

In analogy with the coefficient of form of plane figures, the form of

steric bodies may be determined by the dimensionless value being defined as the ratio of the volume of the body with respect to its surface in powers of $3/2$.

For metal-working quantitative analysis, we consider it more convenient

to replace the coefficient of form by another parameter connected with it in a

wholly well-defined manner, i.e. completely determined by the area and perimeter of the

plane figure. The two-dimensional factor of form proposed by us is determined

by the value of ratio of the perimeter of the circle, of equal size over the

area of the figure being considered, to the perimeter of this figure. Otherwise

expressed, the factor of form indicates which part of the perimeter of the

figure can encompass a circle of equal size to it. From the very definition of

factor of form it is clear that for a circle, its value equals 1, while for other

figures it is the less, the more their form deviates from one which is ideally

round. Therefore an estimation with the aid of the factor of form is very graphic

in comparison with the estimation by the coefficient of form. By way of simple

calculations, we find that the value of two dimensional factor of form Φ_2 is

determined by the expression:

$$\Phi_2 = 2 \frac{\sqrt{\pi F}}{P} = 3,545 \frac{\sqrt{F}}{P} . \quad (41.1)$$

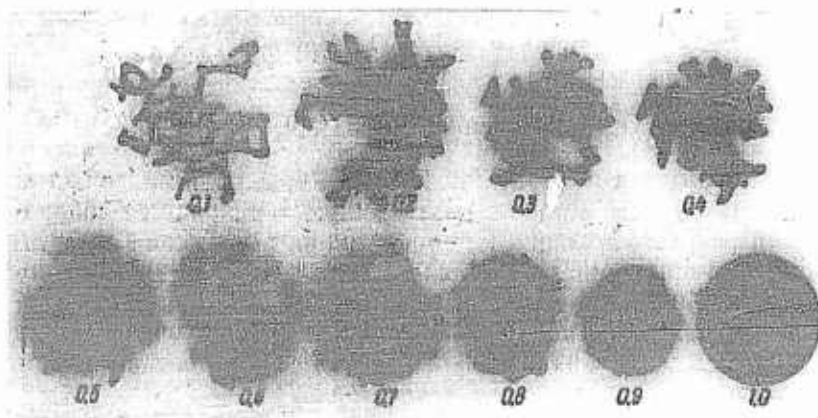


Fig.124 - Scale for Estimating Forms of Graphite Deposits of Malleable Iron by Value of Factor of Form δ

Understandably, the measurement of areas and perimeters of individual sections of microparticles on a cut or on a microphotograph, with a subsequent calculation of form factor based on eq.(41.1) would be too prolonged and unwieldy. It is ~~unadvantageous~~ advantageous to estimate the form of sections of microparticles or of plane grains by method of visual comparison with figures of special scales. In Fig.124, we show such a scale developed by ~~GIST~~ for ~~estimating~~ estimating the graphite formations of malleable iron. The numbers at each figure of the scale signify the value of the form factor, calculated exactly for each figure based on ~~MAXX~~ eq.(41.1). For figures of the scale, we used forms of graphite formations of actual structures, modified only slightly to get rounded values for the form factor. Externally, this scale is similar to many scales, usually in use for visual semiquantitative estimation of the form of various structural formations.

For instance, in Fig.125 there is presented our scale, frequently reproduced, intended for estimation of the same graphite formations of malleable iron (Bibl.171). The chief difference between the scales shown in Figs.124 and 125 is that in the first of them, estimation is ~~XX~~ conducted by fixed geometric parameters, changing regularly from one figure to the next, whereas in the second scale the form is estimated by a conventional index point, wherein the choice of figures is arbitrary and random. Estimation based on the first scale is quantitative (although approximate, since the XX estimation is done visually), while based on the second scale, in the optimum case it is semiquantitative.

For determining the shape of various structural components, scales should be used which are constructed to resemble the scale in Fig.124, but taking into account the specifics of form of sections of microparticles of the given component. Best of all, in the construction of the scales drawn, one should proceed from actual structures, appraising in a strictly quantitative manner the form of sections by the form factor. For each value of the form factor, there can be given not one but two and more figures. Estimating according to the microsection a number of sections of microparticles in conformity with the scale, one computes the arithmetic mean of the form factor which also characterizes the form of the given structural component.

In ~~XXX~~ constructing the scales of comparison, the perimeter and area of each of the figures of the scale can be measured respectively by a curvometer and a planimeter. For this purpose, it is very convenient to use the method of random secants and the Glagolev method (point counting method). A figure, the outline of which is drawn with thin lines on tracing paper or cellophane, is placed on a grid as shown in Fig.126. One can also use a grid drawn on the tracing paper or cellophane, superimposing it on the figure (for instance, on the ~~photomicrograph~~ photomicrograph). Following the outline of the figure, we calculate in how many points it is intersected by the lines of the grid (both vertical as well as horizontal), and, separately, how many nodal points of the grid fell within the outline. We repeat the calculation, moving in succession the contour of the figure relative to the grid, wherein this displacement should be random in nature.

In Table 62 are adduced the results of computing the number of intersections of the outline of the figure in Fig.126 with lines of the grid at 22 positions of the figure. In the second column are given numbers of intersections for each position, in the third column the increasing sum of these numbers, and in the fourth column is given the ~~cumulative average~~ cumulative average number of intersections, which as we quite see, stabilizes ~~XXXXX~~ rapidly. The total number of intersections for the given cutline depends upon distance between lines of the grid (network) and the number of displacements of the figure. It is desirable that it be not less than 400 - 500,

Table 62

| a) | b) | c) | d) |
|----|----|------|------|
| 1 | 75 | 75 | 75,0 |
| 2 | 77 | 152 | 76,0 |
| 3 | 80 | 232 | 77,4 |
| 4 | 76 | 308 | 77,0 |
| 5 | 91 | 399 | 79,9 |
| 6 | 79 | 478 | 79,4 |
| 7 | 79 | 557 | 79,6 |
| 8 | 82 | 639 | 79,9 |
| 9 | 79 | 718 | 79,8 |
| 10 | 73 | 791 | 79,1 |
| 11 | 84 | 875 | 79,5 |
| 12 | 81 | 956 | 79,6 |
| 13 | 78 | 1034 | 79,9 |
| 14 | 85 | 1119 | 79,9 |
| 15 | 76 | 1195 | 79,7 |
| 16 | 76 | 1271 | 79,5 |
| 17 | 76 | 1347 | 79,4 |
| 18 | 89 | 1436 | 79,9 |
| 19 | 84 | 1520 | 80,1 |
| 20 | 75 | 1595 | 79,8 |
| 21 | 83 | 1678 | 80,0 |
| 22 | 82 | 1760 | 80,0 |

a) No. in series; b) Number of intersections of outline with lines of grid;
 c) Cumulative total of numbers of intersection; d) Cumulative average, \bar{x}

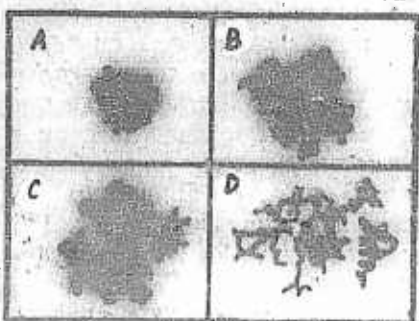


Fig.125 - Conventional Scale for
 Estimating Form of Graphite Deposits
 of Malleable Iron (Bibl.171)

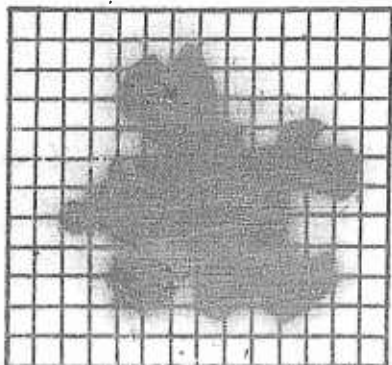


Fig.126 - Determination of Form Factor
 of Plane Figure with Aid of Grid

which assures a sufficiently accurate result. If the average number of intersections of outline of figure with lines of the grid (both vertical and horizontal) is signified by x , the perimeter of the figure will then equal

$$P = \frac{\pi}{4} x \Delta, \quad (41.2)$$

where Δ is the distance between lines of the grid. Equation (41.2) is easily derived from a solution of the Buffon problem "concerning a needle". In our case, using the data in Table 62, we find the perimeter of the figure shown in Fig.126:

$$P = \frac{\pi}{4} 80,0 \Delta = 62,83 \Delta.$$

In Table 63, we show a calculation of ~~the~~ number of nodal points of the grid, falling within the outline of the figure in Fig.126 in case of 30 positions for it. In this case, the cumulative average also rapidly stabilizes. If the average number of nodal points, falling ~~XXXXXX~~ within the cutline, is signified by z , the area of the figure is then determined by the equality:

$$F = z \Delta^2. \quad (41.3)$$

As follows from data in Table 63, in our case the mean number of points falling within the outline of the figure equals 42.0; therefore, its area will equal:

$$F = 42,0 \Delta^2.$$

Using the derived values for perimeter P and area F , we compute on the basis of eq.(41.1) the value of ^{the} two-dimensional factor of form for the figure shown in

Table 63

| a) | b) | c) | d) | a) | b) | c) | d) |
|----|----|-----|------|----|----|------|------|
| 1 | 44 | 44 | 44,0 | 16 | 41 | 673 | 42,1 |
| 2 | 44 | 88 | 44,0 | 17 | 43 | 716 | 42,1 |
| 3 | 40 | 128 | 42,7 | 18 | 44 | 760 | 42,2 |
| 4 | 39 | 167 | 41,8 | 19 | 40 | 800 | 42,1 |
| 5 | 44 | 211 | 42,2 | 20 | 43 | 843 | 42,1 |
| 6 | 45 | 256 | 42,6 | 21 | 41 | 884 | 42,1 |
| 7 | 43 | 299 | 42,7 | 22 | 40 | 924 | 42,0 |
| 8 | 42 | 341 | 42,6 | 23 | 45 | 969 | 42,1 |
| 9 | 38 | 379 | 42,1 | 24 | 40 | 1009 | 42,1 |
| 10 | 42 | 421 | 42,1 | 25 | 44 | 1053 | 42,2 |
| 11 | 41 | 462 | 42,0 | 26 | 39 | 1092 | 42,1 |
| 12 | 43 | 505 | 42,0 | 27 | 41 | 1139 | 42,0 |
| 13 | 45 | 550 | 42,3 | 28 | 44 | 1177 | 42,1 |
| 14 | 38 | 588 | 42,0 | 29 | 42 | 1219 | 42,1 |
| 15 | 44 | 632 | 42,1 | 30 | 40 | 1259 | 42,0 |

- a) No. in series; b) Number of nodal points of grid within outline;
 c) Cumulative total of number of nodal points; d) Cumulative average, z

Fig.126:

$$\Phi_3 = 3,545 \frac{\sqrt{42,0}}{62,83} = 0,365.$$

The value assigned to a division of the grid Δ , as we see, is reduced and does not have significance during the calculation. Therefore for the case of the described method of computing the form factor with the aid of the grid, it is feasible to use the transformed eq.(41.1), namely:

$$\Phi_3 = \frac{8}{\sqrt{\pi}} \cdot \frac{\sqrt{x}}{x} = 4,51 \frac{\sqrt{x}}{x}. \quad (41.4)$$

The denotation of values z and x is the same as above in the text. Determination of value of form factor of the figure, required for including it in the scale of comparison, is conducted by the described method, including the calculations, in about 12 - 15 min. Estimation of the structure based on the scale of comparison, being conducted visually, is also accomplished simply and quickly. The magnification being used for the comparison does not have substantial significance and is selected in such a way that the form of sections of microparticles is differentiated quite clearly and so that not more than 8 - 10 sections being subjected to determination, are located in the field of view. If the microparticles have a spatially complex form, ~~the~~ the value for the form factor being determined by the indicated method can prove erroneous. Because of this, we cannot establish ~~in~~ (in any case, with the necessary simplicity and reliability) the belonging of several sections to one and the same microparticle. For instance, we assume that the microparticle forms, in the plane of the cut, two sections which are typified by the values of areas F_1 and F_2 , and of perimeters of sections P_1 and P_2 . If we know that both sections belong to the same microparticle, we calculate the form factor, using the following expression:

$$\Phi_s = 3,545 \frac{\sqrt{F_1 + F_2}}{P_1 + P_2}$$

Since in most cases, we usually do not know whether both sections belong to the same microparticle, we conduct a calculation independently for each section, using eq.(41.1), and we then determine the mean value of the form factor. The error resulting therefrom is determined by the difference between values of the left and right ~~sides~~^{parts} of the corresponding inequality:

$$\frac{\sqrt{F_1 + F_2}}{P_1 + P_2} \neq \frac{1}{2} \left(\frac{\sqrt{F_1}}{P_1} + \frac{\sqrt{F_2}}{P_2} \right).$$

The use of a two-dimensional form factor in metal-working analysis is all the more feasible and valid, the higher its significance as of a ~~known~~ parameter characterizing not only the form of plane sections of microparticles, but also their spatial form. There are certain bases for assuming that the two-dimensional form factor not only is unequivocally connected with the similar parameter, computed for spatial bodies, but also coincides with them numerically, or, in any case, is sufficiently close to them.

For estimating the form of steric bodies, we select a dimensionless ~~relationship~~^{ratio} between the volume and surface of a body, which we will call the three-dimensional form factor. To obtain absolute values for this last factor, comparable with the ~~known~~ values of two-dimensional form factor, we proceed as in the first case ~~in~~^{from} from the dimensionless ~~relationship~~^{ratio} of linear values, i.e. from the ratio of volume of body, taken in the degree of 1/3, to the surface of body to the degree 1/2 we ~~known~~

get the expression:

$$\Phi_3 = K \frac{V^{1/3}}{S^{2/3}},$$

where V is the volume of individual microparticle;

S is the surface of individual microparticle.

We determine the value of coefficient K , assuming that for a sphere, the

three-dimensional form factor Φ_3 equals 1. We get a final equation, determining

the value of three-dimensional form factor as a function of volume and surface of

the
body:

$$\Phi_3 = \sqrt{36\pi} \frac{V^{1/3}}{S^{2/3}} = 2,199 \frac{V^{1/3}}{S^{2/3}}. \quad (41.5)$$

We shall attempt to compare the values of three-dimensional and two-dimensional form factors, computed respectively for spatial bodies and for random plane sections of these bodies. Having chosen a body of fixed form, we should intersect it with a large number of randomly directed planes and, having obtained a number of plane sections, we should determine for each of them the two-dimensional form factor. Then we need to find ~~the~~ its average value for all derived sections and compare this value with that of the three-dimensional form factor computed for the original body. The fulfillment of such a calculation encounters considerable ~~mathematical~~ mathematical difficulties in calculating the distribution of the random sections according to values of area, perimeter and

form factor. Therefore, we will limit ourselves to a consideration of ~~such~~ bodies that have equiaxed sections, and in first approximation their averaged form can be regular assumed as ~~rectangular~~ polygons. First of all, we note that for a sphere and as three-dimensional plane-sections, the values of ~~tridimensional~~ and two-dimensional factors of form exactly coincide and equal 1. Then let us consider a number of ~~regular~~ polygons and parallelohedrons.

At the intersection of a dihedral angle by a random plane, we get in the section a plane angle, the value of which, being determined by direction of secant the faces and edges of plane relative to ~~faces and edges~~ of the dihedral angle, can turn out to be either smaller or larger than its true value. However, as the analysis conducted by Parker has shown, the values of plane angles most often ~~are very close~~ close to the true value of dihedral angle, and the deviations from this value are all abrupt, the higher they are (Bibl.174). The calculations the more ~~are conducted~~ conducted by us using other methods in report (17), and also presented in Section 40 of the present book, confirm this proposition.

Therefore, it can be considered that the averaged form of plane section of an equiaxed convex polyhedron is constituted by a ~~rectangular~~ polygon, of which the ~~vertices~~ inside angle at the ~~vertices~~ coincides in value with the ~~averaged~~ ~~regular~~ ~~averaged~~ (relative to the edges) of the value of dihedral angles of the polyhedron. For instance, for ~~a~~ a cube such an averaged section is constituted by a square, for a cubooctahedron, by a ~~regular~~ ~~averaged~~ ~~regular~~

hexagon, etc. It is quite evident that, in a general case, ~~a~~ rectilineal polygon,

representing an averaged section of a given polyhedron, may prove to be ~~the~~ weighted mean (relative to the edges).

imaginary, if the ~~value~~ value of dihedral angles of

the polyhedron will not correspond exactly to values of angles of real polygons,

varying continuously.

Table 64

| a) | b) | c) |
|---|-------|-------|
| Tetrahedron | 71 | 0,820 |
| Cube | 90 | 0,898 |
| Hexahedral prism, drawn around a sphere | 104 | 0,920 |
| Octahedron | 109 | 0,920 |
| Dodecahedron | 117 | 0,954 |
| Cubooctahedron | 120 | 0,954 |
| Icosahedron | 138 | 0,969 |
| Sphere | (180) | 1,000 |

weighted value (by edges) mean (relative to the edges) of the

a) Polyhedron; b) Average angle between sides;

c) Three-dimensional factor of form F_3

rectilineal

In Table 64, we present for a number of ~~rectilineal~~ polyhedrons, parallelohedrons

and a sphere, the mean values of angles between the faces, averaged on the basis of

the lengths of corresponding edges, and values of three-dimensional form factor. In

Fig. 127, we show the dependence of three-dimensional form factor of ~~rectilineal~~ polyhedrons upon

their ~~mean~~ weighted value of dihedral angles (points) and dependence between the

mean the included between the faces of two-dimensional form factor and value of angle between faces of

regular
hexagons (curve).

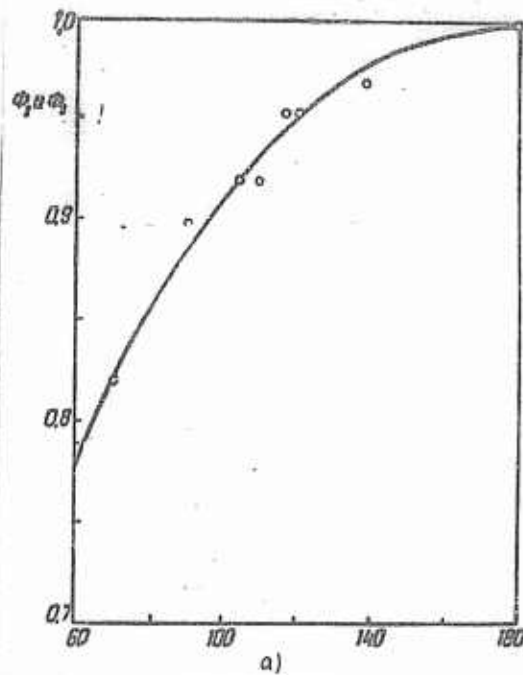


Fig.127 - Dependence of Two-Dimensional Form Factor of ~~hexagonal~~ Polygons upon Value of Angle between ~~the~~ ^{the faces} Sides (Curve) and of Three-Dimensional Form Factor of Rectilineal ~~Ex~~ Polyhedrons and Parallellohedrons upon Mean Value ^{the} of Angle between ~~the~~ ^{the faces (Data)} Sides (~~points~~)

a) Angle, in degrees

The close coincidence obtained for values of three-dimensional and two-dimensional form factors provides us with a sufficient base for assuming that this parameter, being determined by plane random sections of microparticles, simultaneously also characterizes quantitatively the spatial form of the microparticles themselves. It needs to be specially emphasized that for this, the sections should be random. In isometric structures, this mandatory condition is assured at any position of the

^{the}
plane of microsection. In actually oriented structures, random sections of
^A
microparticles are considerably more difficult to obtain; for this, it is necessary
to have not one but many cuts, the planes of which are variously directed relative
^{to}
to the axes of orientation of structure. As follows from Table 64, the value of
^A
the form factor for convex and equiaxed bodies is fairly high, namely not below
0.8. For nonconvex bodies and for nonequiaxed bodies, it quickly decreases.

B. Evaluation of Nonequiaxed Microparticles

lamellae,
Plane microparticles, having the shape of plates, ~~small leaves~~, disks, lenses
etc. form on the cut nonequiaxed sections, the maximum linear ~~measurement~~ of which
more or less considerably exceeds the ~~maximum~~ minimum ~~measurement~~. Such a type
of nonequiaxed sections are formed by nonlinear microparticles (~~elongated~~ grains,
threads etc.), if the plane of cut is parallel to direction of their larger
dimension
~~measurement~~ (axis). Most often, the nonequiaxed sections occur in deformed
~~hexagonal~~ structures, in which the directions of maximum and minimum cross sections
(of plane grains) are common for all sections and are oriented in a definite way
relative to the direction of deformation. In other cases, these directions can
be disoriented, for instance in the structure of graphite deposits of gray iron,
lamellar
martensite, ~~stratified~~ pearlite etc.

In the quantitative evaluation of form of nonequiaxed sections of microparticles,
of (cross) section
we often use the dimensionless ratio of least dimension ~~(or diameter)~~ of section

to its maximum dimension, or vice versa. For evaluating the deformed structures based on lengthwise cut, this method of evaluation was first used by Ye.Geyn (Bibl.136).

In GOST 3443 - 46, the configuration of graphite deposits is determined by ^{the} ratio of ^{the} length of their sections in the cut to the width and is subdivided according to this criterion into six subgroups (see Table 65). At such a method of evaluation, the parameter, equal to 1, corresponds to the equiaxed ~~XX~~ section, and in all remaining cases it is greater.

Table 65

| a) | b) |
|-----|----------|
| Gp1 | below 3 |
| Gp2 | 3-7 |
| Gp3 | 8-14 |
| Gp4 | 15-24 |
| Gp5 | 25-40 |
| Gp6 | above 40 |

a) Subgroup; b) Ratio of length to thickness (width)

According to M.Ye.Blanter the form of sections is typified by a reciprocal, namely by the ratio of least linear dimension of section l_2 to its maximum section l_1 . Naturally in such an evaluation, the units of measurement are neutral. For sections of a given structural component, there is a correlational relationship between the values l_1 and l_2 . In Fig.128 is shown an example of such a connection, obtained ^{the} for structure of granular pearlite with nonequiaxed sections of carbide particles

*(Bibl.118). The points expressing the results of measurements of 100 sections
of carbide microparticles in a microsection, ~~on the curve~~, form an ellipse of
dispersion, the axis of which passes through the origin of coordinates, since ΣX
 $b_1 = 0$ and $b_2 = 0$. According to M.Ye.Blanter, the form of the investigated
aggregate (set) can be characterized by the index of form I_f , which ΣX equals
the tangent of angle θ (see Fig.128) and corresponds to the most probable value
of the ratio of the minimum and maximum dimensions of nonequiaxed sections of
microparticles. For the given case (granular pearlite) the index of the form*

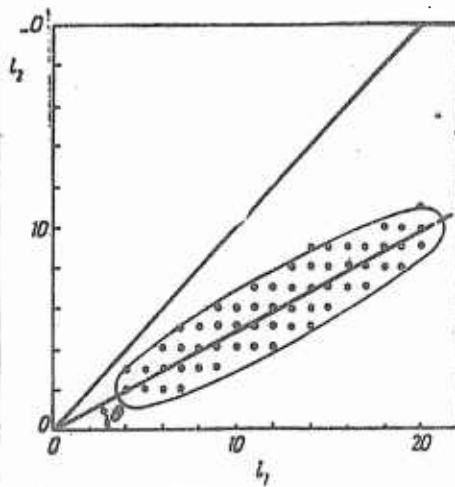


Fig.128 - Correlation between Minimum and Maximum Dimensions of Carbide Particles
~~(M.Ye.Blanter)~~ (M.Ye.Blanter) (Bibl.118)
 $L_2 = 0.5$

$$\frac{l_2}{l_1} = 0.5$$

by the form index R_{α} . Therefore it would be more correct to call this parameter an

equals 0.5. The boundary values of the form index comprise zero (in the case of sections, the length of which is infinitely great in comparison with their width) and 1 (at equiaxed sections of microparticles). If the sections of microparticles are equiaxed, as for instance the figures in Fig. 124, the form index in all cases equals 1 and hence the actual difference in ^{the} form of figures or sections is not detected.

index of ~~nonequiaxiality~~ nonequiaxiality instead of a form index.

In quantitative microanalysis of deformed structures, the direction of ~~the dimension~~ measurement of diameters of plane grains is connected with fixed directions, chosen in conformity with the forces in effect during deformation. For instance, at deformation ~~by~~ by rolling or drawing, the nonequiaxiality of plane grains in ~~lengthwise~~ the lengthwise cuts is estimated by the ratio of diameters, ~~being~~ measured perpendicularly and parallelly to the direction of rolling or drawing.

B.B.Chechulin ~~investigated~~ investigated the nonequiaxiality of plane grains of nondeformed and deformed metal in samples of three smeltings of low-carbon ~~steel~~ steel (0.04 - 0.05% C) of two smeltings of carbonic (0.15% and 0.26% C) and austenitic steel (Bibl.175). The diameters of grains a and b were measured along and across a fixed direction. For nondeformed metal, the construction of frequency diagrams for the ratio $a/b = \alpha$ showed that the maximum occurs at the value $\alpha = 1$, which is a proof of the absence of ~~nonequiaxiality~~ orientation of nonequal axiality or of isometric state of structure. In ~~opinion~~ Chechulin's opinion, in the evaluation of ~~nonequiaxiality~~ the nonequiaxiality of plane grains, it is feasible to use the statistically mean value $\epsilon = \ln \alpha = \ln (a/b)$, and also the variance of this value. In nondeformed metal, the distribution diagram for the ϵ value is close to normal, ^{the} Gauss law of distribution (coefficient of asymmetry ranging from -0.2 up to +0.28 at measurement of 150 - 200 grains and decreases at increase of this number). The

variance $\sigma^2\{\epsilon\}$ characterizes the nonequiaxiality of grains of nondeformed metal.

During deformation, both the mean value ϵ as well as its variance increase, since on the distribution curve, characterizing the initial nonequiaxiality of grains, there is superimposed the curve typifying the nonequiaxiality caused by deformation.

According to difference in indexes, determined for ~~the~~ structure of initial and deformed metal, one can find the values ϵ and $\sigma^2\{\epsilon\}$. The first of these values characterizes the true average deformation, while the second indicates the degree of heterogeneity of deformation by individual grains. The Chechulin method is a development of ~~the~~ first proposed by P.O.Pashkov, who determined the local deformation and revealed the periodicity of flow in metal being deformed, measuring the ratio of diameters of plane grains, directed in a fixed manner relative to the effective forces (Bibl.145).

Let us discuss the various types of evaluating the form of nonequiaxial microparticles by the value of ratio of diameters of their plane sections. We will call this ratio the two-dimensional coefficient of nonequiaxiality.

As a number of investigations of deformed metal have shown, the coefficient of nonequiaxiality is ~~nonequivalently~~ unequivocally connected with the degree of deformation of ~~the~~ given type and can be effectively used in a study of the process of plastic deformation in general, of local deformation and of its distribution in the deformed volume and by individual grains. However, it is noteworthy that at various types of

~~AXISYMMETRIC~~ deformation, one can get identical values for the coefficient of ~~nonequiaxiality~~ nonequiaxiality of plane sections, whereas the spatial form of microparticles differs greatly. For instance, in swaging and ~~XX~~ in drawing, we can note plane grains with a uniform coefficient of nonequiaxiality on the cuts, the planes of which pass through the axis of symmetry of the ~~STRUCTURE~~ structure or else are parallel to it. Moreover, in swaging, the spatial grains have the shape drawing, fibers of a disk or "lobe", while in ~~XX~~ they have the form of ~~WIPERS~~ or of rods. based on the Therefore, an evaluation ~~without~~ coefficient of nonequiaxiality does not ~~XX~~ provide a full concept of the form of spatial grains, if it is not supplemented either by ~~XXX~~ its qualitative characteristics, or by an indication of the type of deformation, causing the nonequiaxiality.

The actual process of measuring diameters of grains is ~~XXXX~~ painstaking and laborious. As a rule, the shape of plane grains is complex. Therefore, the measurement of diameters of grains, especially those having a ~~XXXXXX~~ variable width, is a problem which is to a known degree arbitrary, which for the same object of analysis can be solved by various observers in various ways. At the same time, it can be assumed with a high degree of ~~REPRODUCIBILITY~~ certainty that the mean value of ratio of diameters is identical to the ratio of average numbers of intersections of straight lines, located respectively parallel and perpendicular to the axis of orientation of plane

structure, i.e. to the ratio m_{\parallel}/m_{\perp} . The determination of these last values is conducted very simply and quickly, and requires much less effort than the separate measurement of diameters, and the valuation obtained is more objective and more accurate. Using the values m_{\parallel} and m_{\perp} , one can compute the coefficients of the degree of orientation of any given type, which yield a fixed concept of the spatial form of microparticles, and also one can determine the average and local deformation no less accurately than this is done with the aid of the coefficient of nonequiaxiality.

The evaluation of ~~XXXX~~ form with the aid of the coefficient of nonequiaxiality is feasible only in the study of the distribution of deformation by individual grains.

In the other case, if the object of microanalysis is constituted by nonequiaxial microparticles, characterized by the isometric state of their boundary surfaces, a markedly expressed nonequiaxiality of their sections can occur only at formations of stratified form (graphite deposits of gray iron, layers of ferrite and cementite in the pearlite, layers of martensite etc.). Formations of linear shape (rods, threads, needles, linearly ~~extended~~ ^{elongated} microparticles), which formed a ~~XX~~ markedly expressed nonequiaxial state at mutually parallel orientation of their major axes and at coincidence of ^{the} plane of cut with their direction, under conditions of random distribution of axes of microparticles, ^{will} form sections with a relatively weakly

manifested nonequiaxiality.

In an evaluation of the nonequiaxiality of sections of stratified formations, everything stated above concerning the unwieldiness and arbitrariness of measurements of diameters of sections also applies. In the given case, in comparison with the ~~unusual~~ deformed structures in the lengthwise cuts, additional difficulties arise in measuring the lengths of sections of microparticles, since they are often considerably bent. For instance, the graphite deposits can be greatly curled and, moreover, have a V-shaped, Y-shaped, or even a more complex shape ("crablike" deposits, Fig.129).

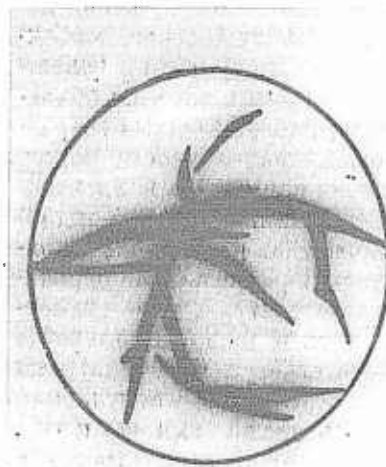


Fig.129 - Crablike Deposits of Graphite
in Iron (after L.A.Dolinskaya) (Bibl.177)

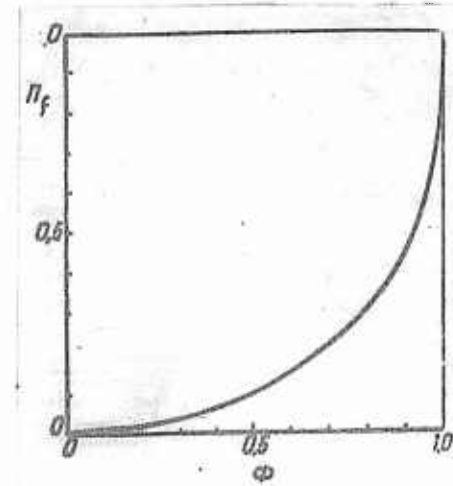


Fig.130 - Dependence between Values of
Form Factor Φ and Coefficient of
Nonequiaxiality Φ for Ellipses Having
Ratios
Varying Relationship of Lengths of
Semiaxes

This circumstance imparts a considerable indefiniteness to the evaluation using the coefficient of nonequiaxiality.

Comparing the estimation by two-dimensional form factor and by coefficient of nonequiaxiality, it is noteworthy that for geometrically monotypical plane figures, these values are unequivocally interconnected. In Fig. 130 we show an example of such a connection for ellipses having a varying ~~relationship~~ ratio of lengths of axes.

The positive ~~sense~~ ^{and} of the estimation using the form factor is the fact that it is determined by fully concrete values of ^{the} area and perimeter of section of a

microparticle, whereas estimation of dimensions of diameters of ~~section~~, at ~~the~~ variation in width, curvature,

~~microparticles with complex configurations~~ and complexity of configuration, turns out ~~to be~~

to be debatable. At the same ratio of diameters of given sections, the form factor also reflects the complexity of the outline bounding the section. Therefore, ~~it~~

it seems to us, in isometric structures it is more feasible to estimate the

shape of sections of microparticles ~~by~~ by the form factor (based on specialized scales, by the visual estimation method) instead of by the nonequiaxiality coefficient.

This evaluation must be supplemented by ~~by~~ a qualitative characteristic of the form (equiaxed, lamellar, of microparticles ~~homogeneously stratified~~, linear). Neither the form factor nor the

nonequiaxiality coefficient reflect the degree of bending of the ~~the~~ nonequiaxed sections ("degree of curling" of graphite deposits, etc.); therefore, when necessary,

this element of form should be regarded as a supplemental parameter.

Understandably, the advantage of the evaluation by the form factor does not exclude the feasibility of using the nonequiaxiality coefficient in individual special cases, when for some reasons it can EX prove more indicative and more in response to the purposes of microanalysis.

C. Estimation of Angular Elements of Form of Microparticles

Of considerable interest are the values of dihedral angles, forming intersecting faces of microparticle-polyhedrons. In a single-phase polyhedral structure, along the lines of edges, three microparticles are always in contact.

Therefore the mean value of the contact angle in such a structure (both of the dihedral one as well as in the plane of the cut), always equals 120° , although the values of dihedral angles, being formed by various pairs of faces, can deviate considerably from this mean value both to one and to the other side. Let us consider (according to Parker) the contact angles φ_1 , φ_2 and φ_3 , being formed on the line of juncture of three microparticles I, II, and III (Fig. 131). The cross-hatched area delimits the zone of effect of interatomic forces upon the atoms which are located along the juncture line (or in the point of juncture - in the drawing). The atoms located at the juncture line and belonging to the lattice of microparticle I, have the relatively greatest number of neighbors and therefore are connected more stably with its own lattice in comparison with the atoms

belonging to microparticle II and especially III. Therefore, under conditions favoring the mobility of atoms, there will occur ~~the~~ displacement of atoms and a change in the contact angles in the direction indicated in Fig. 131 (Bibl. 176, 177). Thence it follows that in the process of recrystallization, there should occur an equalizing ~~approximating~~ of the values of ^{the} dihydral contact angles, which occurs in actuality. From the viewpoint of quantitative change ⁱⁿ form of microparticles, this process should be accompanied by a decrease in the variance of values of ^{the} dihedral angles.

As Parker indicated, the mean value of a plane section of a dihedral angle also determines its actual value. As can be ~~supposed~~ hypothesized, the variabilities in values of dihedral angles and of their plane sections are interconnected in a well-defined manner. Therefore, based on ^{the} variability of values of contact angles in the plane of the cut, one can also judge the variability in values of ^{dihedral} angles. As far as we know, neither the form of connection of variabilities of dihedral and plane angles, nor the change in variability in the process of recrystallization have been subjected to investigation.

In the presence of microparticles of second phase, the value of ^{the} dihedral contact angle is determined by ^{the} relative energy of ~~the~~ boundaries. This creates the possibility of determining the relationship of values of

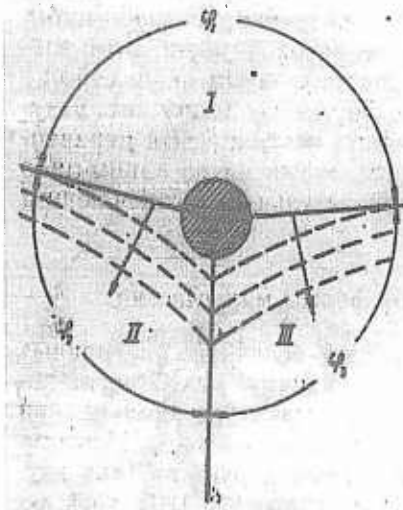


Fig.131 - Diagram of Displacement of
Boundaries of Grain at Inequality of
Contact Angles [after Parker and
Darker (Bibl.176)]

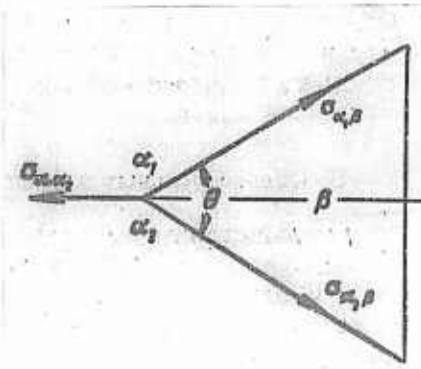


Fig.132 - Diagram Indicating the
Conditions of Formation of Equal
Boundaries of Grain in the Juncture
of Two Phases [after S.Smith (Bibl.174)]

surface tension at the boundary ~~between~~ of microparticles of various phases according

to value of contact angle, being formed at the juncture of these microparticles.

In Fig.132, we show (after Smith) the formation of contact angles at the juncture

of two microparticles of phase α and of one microparticle of phase β , under

conditions of equilibrium. The surface tension, effective on a unit ~~length~~ length of

surface, is ~~not~~ portrayed by vectors. Under conditions of equilibrium, the vector

~~the~~ common edge of sum in a plane perpendicular to the line of ~~between~~ three microparticles,

should equal zero. From this condition we get a relationship between ~~the~~ values of

~~the~~ surface tension at boundaries of microparticles of the same and of different phases:

$$\zeta = \frac{\sigma_{\alpha\beta}}{\sigma_{\alpha\alpha}} = \frac{1}{2\cos(\theta/2)}, \quad (41.6)$$

where $\sigma_{\alpha\alpha}$ is the surface tension at boundary of microparticles of phase α , the lattices of which are oriented differently, and $\sigma_{\alpha\beta}$ is the surface tension at the boundaries of microparticles of various phases. Determining, on basis of the microsection, the value of contact angle θ , one can compute the relationship between the values of surface tension (Bibl.174). If the contact angle θ comprises about 60° , the ratio of surface tensions ζ , determined by eq.(41.6), equals 0.57. Therein the second phase is located in the zones of juncture of three microparticles of the basic phase and its formations acquire the form of trihedral prisms with almost flat sides, extended along the lines of edges of microparticles of basic phase. In the plane of cut, the sections of formations of second phase have the shape of triangles, mainly rectilineal, located in the junctures of the three microparticles of the basic phase. An example of such a structure is an alloy of copper containing 3% Pb, annealed at 900° (the second phase is melted in the annealing process). At a decrease in the ratio ζ from 0.57 to a value close to 0.50, the formations of the second phase are distributed to an increasing degree along the boundary surfaces of the basic phase, wherein the contact angle decreases from 60° to a value close to 0° , and the interphase boundary surface acquires a concavity facing towards the microparticles of the basic phase.

An example of a structure of such a type is the formations of phosphoric eutectic in gray iron, hardening along the juncture lines of microparticles of primary austenite. In the boundary, when the ratio of surface tensions γ equals 0.50, while the contact angle equals 0° , the second phase is located completely along the boundary surfaces of microparticles of basic phase [eutectics in alloy of copper containing 15% Ag(Bibl.179)]. However, if the actual ratio γ is greater than 0.57, the formations of second phase located along the lines of edges of microparticles of basic phase acquire a convexity \rightarrow toward these microparticles. Therein the contact angle increases and when it is close to 180° , the formations of second phase become spherical. From this viewpoint, the obtainment of ~~globular~~ globular graphite is explained by the increase of ratio γ under the effect of magnesium, which either decreases the surface tension at the boundary of austenite and graphite, or increases the surface tension at the boundary of austenitic microparticles. At formation of microparticles of a given type, significance is also acquired by the quantity of second phase and dimensions of microparticles of the basic phase.

The statements made above indicate quite convincingly that the study of the form of microparticles, being typified by values of \rightarrow contact dihedral angles, deserve attention. Having accumulated sufficient test data and observations in this field, we can again approach a consideration of the process of structure

formation or, more exactly, the formation of microparticles.

Unfortunately this branch of stereometric metallography is the only one in which the leading role does not yet belong to Soviet metallurgists; one can note only a number of serious reports conducted in this area by foreign scientists (Bibl.178 - 181 and others).

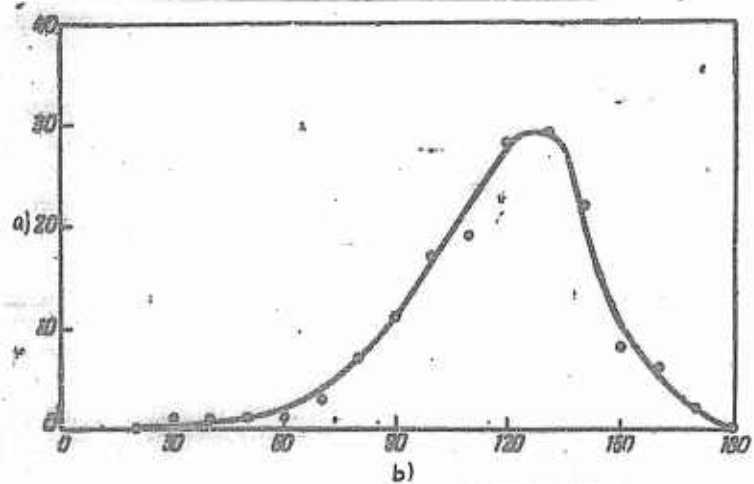


Fig.133 - Frequency Curve of Distribution of Values of Contact Angles

of Plain Grains of Austenite in Steel

a) Frequency, %; b) Angle θ

The experimental determination of values of contact angles do~~not~~ meet with difficulties, although it is fairly ~~expensive~~ painstaking and laborious.

Measurements are conducted relatively simply in microphotographs. Therein one can use the ~~expensive~~ simplest devices for measuring the angles: a transparent protractor or even a standard protractor equipped with a filament. In most cases, values of

angles being measured can be estimated as whole tenths of degrees, since a more accurate measurement is meaningless. Only if the mean value of angles is small (for instance, in case of graphite formations of gray iron), is a more accurate

estimation of each angle being measured necessary. The value of ^{the} angle is determined by ^{the} direction of ~~lines of boundary~~ along the point of ^{vertex} ~~of~~ angle,

wherein a change in direction in proportion to distance from this point, caused by boundary lines

curvature of ~~lines of boundary~~ is not taken into consideration. To obtain a

a well expressed statistical distribution curve and curve of reliable average value

for the angle, it is sufficient to measure 150 - 250 angles, which requires from

1 to 2 hrs. In Fig. 133 we show a distribution obtained by us for values of plane

were revealed as a contact angles for austenite microparticles, which ~~XXXXXX~~ fine cementite

network. A total of 156 angles was measured. The average value of ^{the} contact angle
the

coinciding with the actual value of ~~XXX~~ dihedral angle of microparticles of

austenite was found to equal $118^{\circ}2'$, while the mean ^{-square} deviation of the

plane angle was $46^{\circ}2'$. Since in the structure being analyzed, the value of the

dihedral angle should equal 120° , the error in measurement amounted to 1%.

In measurement of angles under a microscope, the/point ^{vertex} ^{the} ~~of apex~~ of angle is placed

in the center of the eyepiece with the cross hairs(or with one diagonal). A pointer

tubus
is fastened on the eyepiece, and on the jacket of the microscope, a dial equipped with

attaining
a graduated scale is mounted. Turning the eyepiece and ~~WEEKEING~~ superposition
(or parallel ~~state~~) of the diagonal line alternately with the first and
second sides of the angle, its value is noted from the dial.

()

CHAPTER VI
STO~~M~~METRIC STRUCTURE AND PROPERTIES OF METALS
AND ALLOYS

Section 42. Tamman Parameters of Crystallization and Their Determination

Describing the process of crystallization of steel, D.K.Chernov noted two stages of this process, namely the formation of "embryos of crystals" and their subsequent "growth" [1898 (Bibl.4)]. G.Tamman introduced two geometric parameters, characterizing quantitatively these two aspects of the crystallization process:

a) the rate of nucleation of crystallization (frequency of growth), being measured by the number of nuclei originating per unit ~~of~~ time ~~per~~ unit ~~of~~ volume

~~of~~ mother phase ($\text{mm}^{-3} \cdot \text{min}^{-1}$);

b) linear rate of growth of crystals, being measured by ~~the~~ value of linear displacement of ~~the~~ face of growing crystal in ~~the~~ direction perpendicular to it, per

~~time~~ unit ($\text{mm} \cdot \text{min}^{-1}$).

G.Tamman studied the kinetics of crystallization of transparent, mainly organic, materials (salol, benzophenone, piperine, and others). Subsequently, the parameters proposed by Tamman were used for describing the kinetics of transformations in metals and in metal alloys. In the course ~~XXV~~ of more than 50 yrs, these two

~~KINETICS~~

parameters have been widely used for quantitative characteristic of processes
of crystallization from liquid state, of phase transformations in solid state,
processes of separation into solid solutions, recrystallization, etc.

Against the background of a vast ~~number~~^{amount} of research devoted to the kinetics of crystallization and phase formation, a marked contrast is made by the almost complete absence of reliable test data on the actual values of Tamman parameters, obtained from experience for one or another process and conditions. Exact data determined for three-dimensional structures by ^{of} direct method, without any assumptions or approximations, are completely lacking.

Let us consider the conditions and potentialities of direct ~~experimental~~
^{the} determination of rates of nucleation and growth of crystals and, in particular, the
use for this purpose of methods of stereometric metallographic analysis.

If we proceed from the assumption of the constancy of rates of nucleation and growth, the dependence upon the total number of particles forming per unit ~~the~~ of ~~the~~ crystallization ~~the~~
~~MX~~ volume of alloy, upon duration ~~the~~ isothermal process of ~~MX~~
or phase formation is expressed by the curve, for which a concept is provided
in Fig.134. The initial sector of the curve, corresponding to that stage of the
process in which the decrease in volume of ~~the~~ mother phase owing to ~~the~~ formation of a
new phase is trivial, is very close to a straight line. Then, under condition of

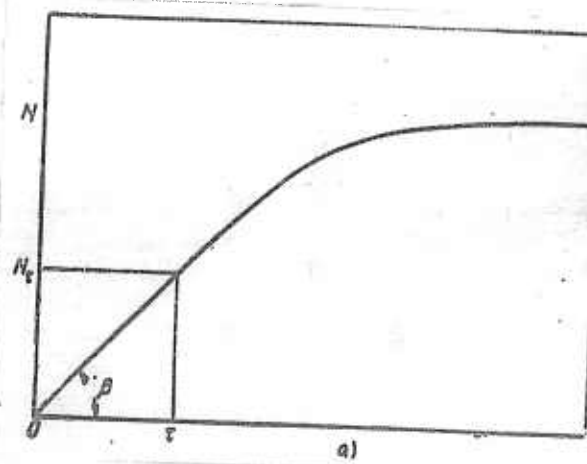


Fig.134 - Diagram of Determining the Rate of Nucleation in the Initial Period of Phase Formation under Conditions of Its Temporal Constancy
a) Time

constancy of rate of nucleation and ~~time~~ under consideration of only the initial phase of the process, we can get a very simple dependence between the quantity of particles per unit ~~of~~ volume of alloy N and duration of ~~the~~ isothermal ~~process~~ holding τ :

$$N = a\tau, \quad (42.1)$$

where a is the rate of nucleation. Under maintenance of the above-indicated conditions, it is sufficient to determine experimentally the number of particles per unit ~~of~~ volume N for one single sample, subjected to isothermal holding in ~~time~~ the ~~process~~ course of time τ , and then from (42.1) to find the rate of nucleation a .

A method of determining this parameter was used in a number of reports.

However, investigations of recent years have indicated that in a general case we have no bases for considering the rate of nucleation as a constant, not changing temporally in the process of isothermal holding during crystallization, phase formation, or recrystallization. Moreover, up to the moment of beginning of the isothermal process in the alloy, there can already exist stable embryos of a new phase, i.e. process of crystallization may proceed at prepared nuclei. Therein the quantity of nuclei may either remain constant or increase owing to the formation of new nuclei, or decrease owing to the absorption of thermodynamically unstable small embryos by more stable larger ones. It is natural that under these conditions, the rate of nucleation can be described only as a variable, being determined as a function

XXXXXX

of time:

$$G = \varphi(t). \quad (42.2)$$

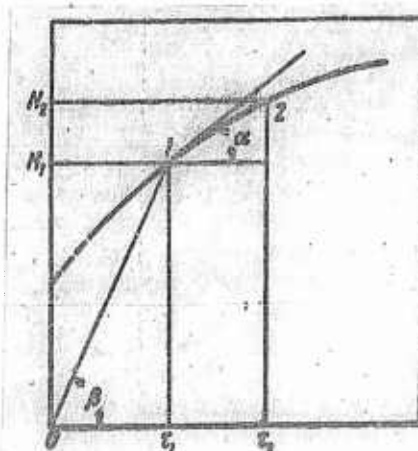


Fig.135 - Diagram of Determining the Rate of Nucleation, Based on Kinetic Curve of Change in Quantity of Particles in Time

Hence our problem reduces to finding the form of this function for the given transformation and actual conditions in which they are fulfilled.

Let us assume that the total number of particles occurring per unit volume of alloy, changing as a function of time,

is expressed by the relationship:

$$N = \psi(\tau) \quad (42.3)$$

and is portrayed graphically, generally speaking, by some given curve, not necessarily passing through the origin of coordinates, as this was shown in Fig.135. If the particles are sufficiently large and are accessible to observation and measurement ~~under~~ a microscope, and their shape is ~~far~~ close to a spherical one, one can find the dependence (42.3) by experiment. For this it is necessary to have at one's disposal a number of samples, the structure of which is fixed at various isothermal transformation, and to determine in stages of ~~the~~ ~~the~~ ~~the~~ ~~the~~ ~~the~~ them the quantity of microparticles by one of the methods described in Chapter IV of the present book.

The first derivative based on time from function (42.3) determines the rate of nucleation, referred to a unit ~~of~~ volume of ~~the~~ alloy (but not to a unit volume of ~~the~~ starting phase, i.e. not the value a):

$$a' = \frac{dN}{d\tau} \quad (42.4)$$

As is clear from Fig.135, the rate of nucleation a'_1 at the moment τ_1 is fixed by the tangent of ~~the~~ angle α , ~~made~~ by the tangent to the curve at point 1 with the x-axis. It would be a gross error to estimate the rate of nucleation by the value of the ratio N_1/τ_1 , i.e. by the value of tangent of ~~the~~ angle β , as we did ~~the~~ above, proceeding from the assumption of the constancy of the temporal rate of nucleation.

This ratio can produce quite an erroneous concept of the rate of nucleation, wrong not only in absolute value but also in sign. For instance, if the quantity of particles in the volume does not ~~increase~~ increase, but decreases in time (see Fig.8) and hence, the rate of nucleation is a negative value, the ratio N/τ , determined for a certain moment of time, is always positive. We consider it necessary to mention this circumstance specially, since errors of such a type are sometimes admitted.

If the dependence between N and τ , i.e. the function (42.3), obtained from experience, can be satisfactorily described empirically or by a more precise formula, the rate of nucleation, referred to a unit ^{of} volume of alloy a' , is then determined ~~in a time~~ ^{of time} function by expression (42.4).

However, if the mathematical expression of dependence (42.3) cannot be established, the ~~KX~~ test curve obtained, expressing this ~~KX~~ dependence, is divided into a number of segments. Assuming the segment of the curve between points (1) and (2), for instance, to be a straight line (see Fig.135), we can find the mean rate of nucleation, referred to a unit volume of alloy, for the given segment ^{the} ~~KX~~ of time of ~~KX~~ the isothermal process:

$$a'_{1-2} = \frac{N_2 - N_1}{\tau_2 - \tau_1} . \quad (42.5)$$

The value obtained from eq.(42.5) refers to the center of the sector between τ_1

and τ_2 . Having accomplished the described operation for a sufficiently great number of segments of the curve, we get a dependence of ~~the~~ rate of nucleation ~~as~~
~~as~~ function of time, which we can extrapolate to the zero value τ .

Thus, using one of the methods ~~XXXX~~ described, we get a dependence of ~~rate~~
of nucleation referred to ~~a~~ unit ~~MM~~ volume of ~~alloy~~, from the duration of isothermal exposure (holding). Our final problem is the determination of ~~the~~ dependence of ~~rate~~
of nucleation, ~~referred~~ to unit volume of ~~the~~ starting phase, upon time, i.e. of the function (42.2). Therefore we should divide the value a' , found for the time moment τ , by ~~relative~~ volume of starting phase, which it occupied in the volume of alloy at that exact ~~moment~~ ~~instant~~ of time. The amount of new phase ~~changes~~ ~~in~~ function ~~of~~ varies as a function / of time, which is determined by the rate of nucleation, linear rate of growth and syngony of growth. The experimental determination of ~~the~~ amount of new phase ~~is~~ as a function of time does not encounter difficulties. It is conducted either by the methods described in Chapter II, or by ~~the~~ totaling of the volumes of spherical microparticles, whose total number N_τ and ~~the~~ distribution ~~of~~ according to dimensions is determined by the methods of ~~XXXXXX~~ V. Johnson, A.G. Spektor or the author. The relative amount of starting phase (i.e. the volume occupied by it in ~~MM~~ 1 mm³ of alloy) is found by way of deducting from one the relative amount of the new phase. The calculation of rate of nucleation ~~referred to~~ ~~unit~~ ~~volume~~ of

starting phase is conducted for a number of instants of the isothermic process, whereupon there is constructed a final dependence of this value upon time, and we determine the form of this dependence and its parameters.

On the basis of what has been presented, the method of experimental determination of the time-variance of the rate of nucleation is comprised of the following stages and operations:

a) In the process of isothermic transformation, at its various stages, there is fixed the structure of a number of samples chosen in sufficient quantity to

reveal the regularity of the process over its entire extent (or in a certain segment);

b) In each of the samples, there is determined the total number of microparticles per unit volume N_τ , their average diameter \bar{D}_τ , the mean-square quadratic deviation of diameter $\sigma^2(D)$, the relative volumes of transforming (old) and forming (new) phase;

c) There is found the mathematic expression of dependence of total quantity of microparticles N_τ per 1 mm^3 , upon duration of isothermic delay τ [eq.(42.3)], or a curve is constructed for this dependence;

d) There is found the dependence of rate of nucleation, relative to unit volume of alloy, upon duration of isothermic holding, in conformity with expressions (42.4) or (42.5);

e) A curve is plotted the the
of the dependence of relative volume of starting

the phase upon duration of isothermal holding;

f) The dependence is found of rate of nucleation, relative to unit
the time of starting phase, upon duration of isothermal holding.

The mathematic derived,
expression of this is found, i.e. function (42.2), and its parameters are found

for actual conditions of the occurrence of the given transformation.

Let us recall that the derived dependence of a upon τ will not be

with the accomplished, since existing means of microscopic analysis, we can observe the

embryos not at the instant of their formation, but only after the lapse of a

certain time, when they reach microscopic sizes. Therefore the obtained experimental

curve of dependence a upon τ reflects the process of nucleation with a certain

delay and is somewhat displaced to the right in comparison with the

actual dependence.

The conditions of obtaining more accurate values of the rate of nucleation

D.Khollomon and D.Tarnball were presented by (Bibl.182). We assume that within the

initial phase α there are formed regions of new phase β . The value of each

region of β -phase D is a function of time: $D = f(\tau)$. For an experimental

determination of rate of nucleation, we should construct curves of dependence D upon τ or a large number of regions of β -phase for the given stage of transformation,

XXXXXX

extrapolate the obtained curves to the zero dimension D, determine the number of intersections of curves with the x-axis per unit of time, and refer the number derived to the volumes of α -phase, corresponding to the given time. It is quite clear that we do not have the chance to determine the gradual ~~change in size~~^{time rate of change in size of} of the same particle ~~inclusion~~ under conditions of studying the three-dimensional structure of a nontransparent object. Therefore ~~X~~^{XXX} this method with reference to metals and alloys is not realizable at present, if one does not proceed to some kind of assumptions and simplifications, for instance to a limitation of the examination to a two-dimensional problem.

As Khollomon and Tarnball correctly remark, the quantitative data on the rate of nucleation are necessary for checking the conclusions of presently existing theories of formation of nuclei and in order to aid the further development of the theory. Taking into account that the quantitative data obtained from experience for actual three-dimensional structures are now lacking, it is noteworthy that the problem of studying the rate of nucleation by stereometric metallographic methods acquires an exclusively great significance and actuality.

Let us examine conditions of measuring the second parameter of the crystallization process, namely the linear growth ~~X~~^{XXX} rate.

The conditions of growth of crystals, taking place in the tests of Tamman, are quite remote from real conditions of spatial growth of microparticles in metal

~~X~~^{XXX}

alloys. Nevertheless, the conclusion of Tamman on the constancy of ^{the} linear rate of growth in time was confirmed by a number of researches for processes of primary and secondary recrystallization [D.Burke and D.Tarnball (Bibl.182)]. In many other cases however, there is proved the inconstancy of the linear growth rate in time.

It was shown that in the growth of crystals in liquid phase, the linear growth rate in most cases decreased with the passage of time. It is possible that this is caused ~~by~~ by the release of latent heat of melting (Bibl.187). At diffused growth of particles of new phase, the linear growth rate changes in the process of isothermal holding, initially increasing to a maximum and then gradually decreasing (Bibl.188).

As follows from the data obtained by I.N.Bogachev, for the process of graphitization in particular, the linear growth rate does not remain constant in time (Bibl.189). D.Burke noted the jumplike displacement of ~~WW~~ boundaries in time during the primary recrystallization of zinc (Bibl.182), etc.

Taking into account the data listed above, we should proceed from the possibility of inconstancy of linear growth rate in time and, basing on this, develop a method of measuring this parameter. The test data obtained in conformity with the above-described program of determining the rate of nucleation, are quite sufficient for computing the linear growth rate and its ^{Variation} ~~change~~ in the course of the isothermal process. However, it is worth noting that the discussion can deal

only with an average, provisional value for this parameter. In reality, at any moment of the isothermal process, each microparticle and, moreover, individual sectors of surface of the same microparticle, are characterized by a differing growth rate. In this connection, the growth rate can be different not only in amount but also in sign, namely thermodynamically more stable microparticles or sectors individual ~~elements~~ of their surfaces grow, while the less stable ones are absorbed (are dissolved or melted). The growth of microparticles of new phase does not stop at the moment of their contact, but is replaced by the growth of one of the microparticles at the expense of another, which is less stable thermodynamically. Naturally, therein the rate of free growth owing to the mother (starting) phase is replaced by the rate of collective recrystallization, i.e. by a value differing sharply from the initial one both in amount as well as in sign (for one of the two microparticles). The difference in rate of growth of individual microparticles is determined not only by their size# and shape of surface (curvature, roughness, angularity), but also by the location of a microparticle relative to the other microparticles. For instance, K.P.Bunin and A.V.Chernovol showed that if a graphite deposit in magnesium iron was in contact with carbide on one side, and on the other with austenite, there is then observed an abrupt difference in rates of growth: on the side of the austenite, the deposit grows rapidly, while on the side of the carbide it hardly grows at all, i.e. the growth rate in one direction is

considerable, while in the other it is close to zero (Bibl.190).

Based on what has been said, we can consider only a certain average value of linear growth rate. In this connection, it is possible to use a different approach to a determination of this mean value: it can be regarded as the mean linear rate of growth, weighted either by quantity of microparticles, or according to their surface.

Let us examine two successive moments of isothermal holding τ_1 and τ_2

and determine the mean linear growth rate of spherical microparticles in this

segment of time, weighted according to quantity of microparticles. Let us ~~denote~~

the quantity of microparticles per unit volume, corresponding to the chosen ~~moment~~

~~moments~~,

~~moments~~ by N_1 and N_2 , and the values of mean diameters of microparticles, by D_1

and D_2 . Let us assume that the quantity of microparticles increases temporally,

i.e. $N_2 > N_1$. We get the linear growth rate as an ~~increment~~ of the total radius

relative to
of all microparticles ~~moment~~ for the given time interval, ~~referenced~~ its

the
duration and to final quantity of microparticles, i.e.:

$$v_{1-2} = \frac{D_2 N_2 - D_1 N_1}{2(\tau_2 - \tau_1) N_2}. \quad (42.6)$$

Expression (42.6) is solved in a very elementary way, as the ~~increment~~ (or,

the the relative to unit time
generally speaking, change) in radii of microparticles, ~~referred to time~~

and to one microparticle, participating in the process in the given time interval. Therefore if the quantity of microparticles decreases in time, i.e. if $N_2 < N_1$, in the denominator of expression (42.6), the number of microparticles N_2 is replaced by the number N_1 .

Comparing the numerator of eq.(42.6) with the earlier introduced dependence (35.2), we can state that it represents the difference in quantities of sections of microparticles (of flat grains), occurring per unit area ΔX of cut in the initial and final ~~moments~~^{instants} of the time interval being considered. Thence it follows that the increase in ^{the} quantity of flat grains in time corresponds to the positive ~~average weighted~~^{mean} (by quantity of particles) linear growth rate, and its decrease corresponds to a negative one.

The obtainment of negative values of ~~average weighted~~^{the mean of} linear growth rate is explained in that ΔX in the processes of phase transformations or ^{the} processes of deposition, simultaneously and parallelly, there transpire two independent processes: the growth of one part of microparticles points ΔX to ~~a separation of~~^{an increment in the} quantity of new phase and dissolving (or melting) of the other ~~part~~^{part} ~~of~~^{mean of} microparticles, which are less stable thermodynamically. Depending upon which of these processes prevails, the ~~mean weighted~~^{increment} linear growth rate can either be positive or negative. Obviously, in processes of collective recrystallization or exchange coagulation, when the ~~appearance~~^{absence} of new phase is lacking, the mean

linear growth rate, weighted on basis of ^{the} quantity of particles, is always negative. Having determined on the basis of (46.2) this parameter for various stages of the isothermal process, we can find its dependence upon time ~~the~~ confirm the constancy of the average linear growth rate.

The method of measuring the mean linear growth rate, weighted according

to ^{the} surface of transforming phase, was developed by Spektor (Bibl. 237). This method is suitable for any form of microparticles, but for its use requires changes in the quantity of transforming phase, ^{as} function of time or temperature. If there is no such change (recrystallization, exchange coagulation), the method is unsuitable, which is quite understandable: in similar processes, the average linear growth rate, weighted according to ^{the} value of surface, equals zero.

Let us assume that ~~at the instant~~ of time τ in a unit ^{the} volume of alloy, the microparticles of ^{the} given phase are characterized by ^{the} total volume V_τ and by ^{the} specific surface S_τ . At increase (or decrease) of ^{the} total volume of microparticles by a slight time interval $d\tau$, all points of the surface of ^{the} given phase are displaced along a perpendicular to this surface by a distance ^{the} ~~the~~ ^{the} dx on ^{the} average.

Then the ~~area~~ ^{the} increment (or decrement) of volume of ^{the} phase for the time $d\tau$ is expressed by the ~~value~~ quantity

$$dV = S_\tau dx. \quad (42.7)$$

Thence we find the linear rate of displacement of surface, i.e. the ~~average~~ average

growth rate (or rate of diffusion) of microparticles in the considered time

moment τ :

$$v_t = \frac{dx}{d\tau} = \frac{1}{S_t} \cdot \frac{dV_t}{d\tau}. \quad (42.8)$$

For experimental determination of mean linear growth rate (or rate of diffusion)

based on eq.(42.8), it is necessary to have access to kinetic

change of curves of relative volume V_t and of specific surface S_t of the

considered phase, in function of time. For a short time interval $d\tau$, there is

determined (from the curve) the increment (or decrement) of volume of given phase

relative to phase dV_t , which is determined by the value of the interval $d\tau$ and to the specific surface S_t , corresponding to the given instant of the process of transformation.

Having repeated the determination for a series of successive instants of the

process, one can find the dependence of mean linear growth rate (or rate of diffusion),

weighted according to value of surface of considered phase, as a function of time of isothermal holding.

The method also remains effective when the process of transformation occurs

at variable temperature. For instance, Spektor determined the mean linear

rate of dissolving of carbides in type ShKh15 steel in the process of its heating

at a rate of around $4^{\circ}/sec$. The values found by him are presented below (Bibl.237):

(Bibl.237):

| Temperature °C | Mean Linear Rate of Dissolving, A°/sec |
|-------------------|--|
|-------------------|--|

| | |
|-----|----|
| 820 | 18 |
| 845 | 19 |
| 860 | 20 |
| 895 | 22 |
| 920 | 24 |
| 945 | 26 |
| 975 | 30 |

The above-described methods of determining the rate of growth (or of diffusion) make it possible to measure only the average value of this parameter, weighted according to quantity of particles or according to their surface. At the same time, the particles of various sizes grow at a rate which differs both in absolute value as well as in sign. In connection with this, of considerable interest is the differentiated measurement of linear rate of growth (dissolving), conducted separately for microparticles of various size groups. Solution of this problem was recently proposed by Spektor (Bibl.239).

In any stage of the process, the system of microparticles is characterized as a function of their distribution by sizes. As a result of the growth (or diffusion) of microparticles at various rates, the distribution function changes becomes time-variant distribution (temporally) (see, e.g., the two ~~XXXXXX~~ curves in Fig.114). Ya.I.Frenkel proposed an equation, connecting the rate of this change with the growth rate, by whose use ~~using published~~ Spektor obtained a formula permitting a determination of the

diffusion)
individual growth rate (rate of ~~formation~~ of microparticles of a given size.

Let us assume that we are interested in microparticles, the diameter of which equals x , and let us examine two distributions ~~of~~ of microparticles, obtained for the start and end of a short segment of time $\Delta\tau$. We determine the mean quantity of microparticles of given size x in ~~a~~ unit ~~volume~~ volume for the initial and final moment of interval $\Delta\tau$ and ~~divide~~ this value by \bar{N}_x . Then we find separately for each of the two distributions the numbers of microparticles, the diameter of which exceeds the size x , and we find the difference of these numbers (increase or decrease) namely $\Delta\Sigma N_x$. Then the linear rate of growth or diffusion of microparticles of size x of interest to us, which occurred in the considered interval of time, is determined by the Spektor equation:

$$v(x, \tau) = \frac{\delta}{2N_x} \cdot \frac{\Delta\Sigma N_x}{\Delta\tau}, \quad (42.9)$$

where δ is the width of interval in distributions of microparticles according to their size (to value of diameter).

As follows from what has been said, ~~for~~ for determining the individual rates of growth (~~and~~ diffusion) of particles, it is necessary to have available the functions of/distribution ~~of~~ ^{their size} ~~by~~ (value of diameter), obtained for a series of ^{instants} ~~moments~~ of the process of phase formation, recrystallization or exchange

coagulation. As we know, for an extensive group of structures, this function is expressed by the law of logarithmically standard distribution (see Section 39).

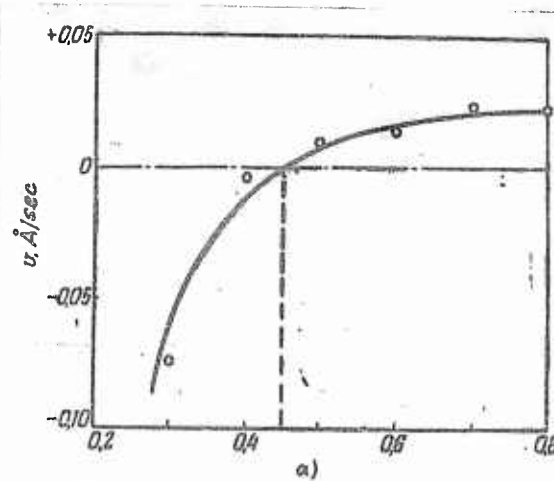


Fig.136 - Rates of Growth and Diffusion of Cementite Microparticles during Annealing (Steel with 0.4% C, annealing at 630°) [A.G.Spektor (Bibl.239)]

~~a) (b) (c) (d) (e) (f) (g) (h) (i) (j) (k) (l) (m) (n) (o) (p) (q) (r) (s) (t) (u) (v) (w) (x) (y) (z)~~ Diameter of particles x , microns

Spektor measured the individual rates of growth (\downarrow diffusion) of cementite microparticles of tempered carbon steel (0.4% C) in the range from 1 to 6 hr holding at 630° , having used for this the test data of Bokshteyn. In Fig.136 we show the derived dependence of rate of growth of cementite microparticles upon their size (diameter). The dependence found shows that the microparticles having a diameter of 0.3 and 0.4 microns are characterized by ~~negative~~ ^{an} negative rate of growth, i.e. are diffused, while the rate of growth of microparticles with diameter

ranging from 0.5 to 0.8 micron is positive and hence they grow. Under the given conditions, as the drawing shows, the dimension of microparticles equaling 0.45 micron is a critical one.

The method developed by Spektor for determining individual growth rates of microparticles is quite promising in our opinion.

At the same time, it is noteworthy that the parameters proposed over 50 yrs ago by Tamman are not the best and are not convenient enough, since they proved to be values, changing (generally speaking) in time at constancy of temperature of the transformation process. In order to be able to compare the rates of nucleation at various temperatures under these conditions, it is proposed, e.g., to express the constants, appearing in expression (42.2) as a function of temperature [R.Meyl and others (Bibl.182)]. Otherwise expressed, characterizing the kinetics of crystallization by Tamman parameters, we forced at the same time to characterize even these latter values with the aid of some kind of supplemental ^{values} parameters, which are independent of time. Thence one can conclude that the Tamman parameters are not those primary physical values with the aid of which one could describe in a well-defined and detailed way the kinetics of the isothermal recrystallization process, phase transformation etc. Considerable ~~experimental~~ difficulties arise ~~exist~~ in the path of determining the actual values of these parameters

for processes occurring in metal alloys. In particular, a more or less strict determination of these parameters can be conducted only at equiaxed form of the growing microparticles.

Among the large number of geometric values, being used for evaluating the stereometric structure of metal alloys, the most important in value and undoubtedly the most frequently used are the Tamman parameters, specifically the rate of nucleation. Therefore we consider ~~XX~~ that it is especially necessary to dwell upon the principal error connected with the choice of this parameter and with its use for describing the kinetics of transformations in heterogeneous systems, which are comprised by metals and alloys in a solid and (almost always) in liquid states. The value of the nucleation rate is determined as the first derivative in time from the expression (42.3), characterizing the change in quantity of particles per unit ~~XX~~ volume of alloy ^{as a} function of time. Therefore the prepared nuclei, which can exist in a heterogeneous alloy at the initial moment of isothermal transformation are not taken into account at all by this parameter of G.Tamman. In the following ~~XX~~ section, we shall try to show that the existence in the initial phase of prepared nuclei of new phase is an occurrence which is not only quite actual but very widespread. Therefore we can by no means disregard it during a quantitative study of phase transformation.

Section 43. Boundary Zones and Phase Transformations in Them

distinguished
In the metals, ~~exist~~ by the degree of purity available to us, and occurring in both liquid and solid states, there exist numerous sectors, distinguished by ~~increased~~ increased energy. These sectors can have both a fluctuational and a structural origin. Their role in the process of formation of structures, transformations in ^{the} solid state, and in determination of properties of solid metal is decisive.

The general cause of all disruptions of the energy homogeneity of metal, having a structural origin, is the presence of various boundary interfaces of phases or variously oriented crystalline formations.

In a general case both in metals and in alloys, the boundary surfaces are formed by microparticles of various phases (among which one may be liquid, gaseous, or vacuum) or of variously oriented crystalline formations of the same phase. The boundary surfaces are physical surfaces and possess a definite thickness, although it is quite trivial ~~in~~ in comparison with their maximum measurements. The ~~in~~ mutual intersection of boundary surfaces creates boundary lines and points. In view of the fact that the boundary surfaces, ~~exist~~ lines and ~~exist~~ points have a spatial extent, we will call them boundary zones, distinguishing ~~the~~ two-dimensional zones (boundary surfaces of two contacting microparticles or blocks), ~~single~~ -

dimensional zones (boundary lines of juncture of three microparticles) and point zones (points of juncture of four microparticles).

The extent of boundary surfaces and lines per unit volume of alloy is determined simply and accurately by methods of stereometric metallography; the number of boundary points is determined less precisely. Determination of relative volume of boundary zones is made difficult owing to the lack of reliable data on the thickness of boundary layer. Proceeding from the basis that the forces between atoms of solid bodies have a closely related effect, V.D.Kuznetsov (Bibl.191), Din and Grig (Bibl.45), Ke Tin-suy (Bibl.192), F.Zeyts (Bibl.184) and others estimate this thickness ~~with~~ values running from one to several interatomic distances.

Localization of admixtures at the boundaries cause a considerably greater thickness of boundary layer in actual metals and alloys, which according to V.I.Arkhakov comprises from several hundred to several thousand Å (Bibl.46, 193). The direct measurement of average thickness of boundary layer in technical iron, first carried out by A.I.Gardin by way of electron-microscopic analysis with the use of the method of ~~XX~~ random secants, gave a figure of the same order, namely 2500 Å.

The structure of iron studied by Gardin is shown in Fig.137. The relative volume of intercrystallite zones comprises a considerable amount, namely ~~XXXX~~ around 3% of the volume of the iron (Bibl.87).

Atoms of the boundary zone, occurring under the simultaneous influence of arrangements of atoms of two, three, or four crystalline lattices, contacting in the region of the zone, occupy some intermediate, compromise position. The boundary zones are characterized by the presence of irregular groups of atoms and by a large number of vacancies. Here the atoms are arranged less compactly,

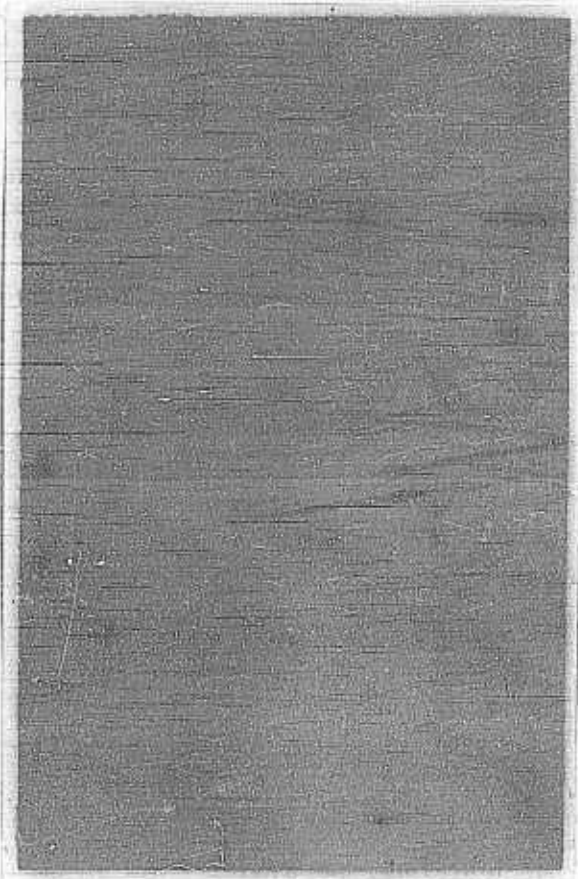


Fig.137 - Electron Photomicrograph of Boundaries of Grains of Technical Iron [after A.I.Gardin (Bibl.87)]

occurring at greater distances from each other and being less firmly interconnected than within the crystallites, blocks and, what is more, within the regular crystal

lattice. The energy of activation of atoms of ^a~~the~~ boundary zones is known to be lower than ~~for~~ ^{that of} atoms within the crystals or blocks, while the surface energy referred to ^a unit ~~of~~ volume is higher. Therefore the ~~heat~~ processes, the intensity of which is caused by mobility of ^{the} atoms, proceed considerably more actively in the boundary zones than within the volume of ^a crystallite or block, and at ~~maximum~~ expenditure less of energy. For instance, S.Z.Bokshteyn, S.T.Kishkin and L.M.Moroz recently determined by test that the rate of self-diffusion of γ -iron at 1000° ^{the grain} at boundaries ~~of grains~~ is 12,000 times greater than within the grains. The energy of activation of volumetric ^(intragranular) ~~within grain~~ self-diffusion proved to be more than twice greater than for boundaries ~~of grains~~ of γ -iron (64,000 and 30,600 cal/gm-atom respectively) (Bibl.276).

P.Klemm and D.Fisher computed the value of critical energy ~~heat~~ necessary for forming a nucleus in various sectors of polyhedral structure, taking into account the gain in free ~~energy~~ ^{the} energy owing to disappearance of part of boundaries between the crystallites. In particular, the calculation was conducted for values of critical energy of nucleation of ferrite from austenite at temperature of around 1000° K. The values derived for critical energy are presented in Table 66 (Bibl.194). As metallographic practice indicates, the relative activity of various boundary zones increases at the same magnitude as that obtained by Klemm and Fisher.

Table 66

| Location of Nucleus | Critical Energy of Formation, erg |
|--|-----------------------------------|
| Within crystallite | $1,913 \cdot 10^{-8}$ |
| At contact point of two crystallites | $0,220 \cdot 10^{-8}$ |
| At contact point of three crystallites | $0,0436 \cdot 10^{-8}$ |
| At contact point of four crystallites | $0,0096 \cdot 10^{-8}$ |

As V.I.Arkharov indicates, in the process of thermal ~~motion~~^{attraction} of atoms of impurities dissolved in the metal, ~~there~~ there can occur the predominating displacement of atoms both into the boundary zones as well as in the reverse direction, namely into the ~~innermost~~^{The} layer of crystallite. Direction of displacement is fixed by the type of atoms: if the departure of atoms of the given element from the boundary zone lowers its ~~surplus~~^{excess} energy, these atoms ("horophobic") will migrate ~~into~~^{measured} into the layer of crystallites; if, on the other hand the enrichment of the boundary zone by atoms of a definite element decrease its ~~surplus~~^{excess} energy, it will then be enriched by the same atoms ("horophilic") (Bibl.46). This phenomenon of intercrystallite internal adsorption may be revealed experimentally, although we do not yet have the possibility of determining the chemical composition of the boundary zone. Arkharov, by way of pickling the surface of ^{the} lithoidal fracture of type 18KhNMA steel and the surface of a microsection of the same steel showed that in the first case the content of molybdenum proved to ~~be~~ be twice ~~greater~~^{more} than in the second case, although the thickness of the layer being pickled exceeded

by 1000 times the thickness of the boundary zone (Bibl.46). An exemplary pattern

of distribution of concentrations of various elements in the center and at the

boundaries of microparticles was revealed by the method of autoradiography in

~~another~~

report (Bibl.195). In Fig.138, we show the distribution of 0.007% ~~of~~ niobium

the intensity of blackening of an emulsion layer.
in a grain of nickel, ~~revealed by density of blackening of emulsion layer.~~

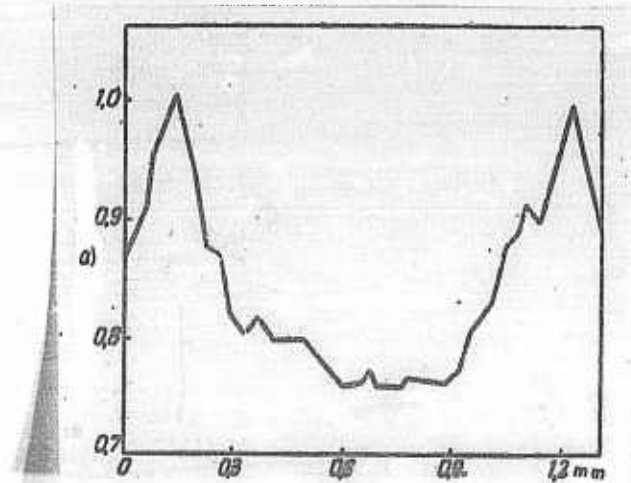


Fig.138 - Distribution of Niobium (0.007%) in a Grain of Nickel,

Revealed by the Method of Autoradiography [after S.Z.Bokshteyn
and others (Bibl.195)]

a) ~~Density of blackening~~ Photographic density

Constituting, comprising in relation to nickel, a ~~genetic~~ element, niobium concentrates

at the boundaries of microparticles. In Fig.139, we show the distribution of iron

(3%) in a grain of nickel. In this case, iron in ~~relation to~~ nickel constitutes a

comparison to the horophbic element, ~~causing~~ ^{increasing} the concentration of iron within the crystallite

of nickel is higher than at its boundaries.

The X-ray data presented testify to the fact that the boundary zones are differentiated from the intracrystallite zones both in composition and in energy structure. As Fig.137 shows, the boundary intercrystallite zone is separated by a sharply ~~manifested~~ ^{defined} interface from the ~~XXXX~~ intracrystallite zone. In conformity with the definitions of the concept "phase", given by D.Gibbs and N.S.Kurnakov, we have a basis for ~~XXXXXX~~ considering the metal of boundary zones as an independent phase, as this is also proposed by A.I.Gardin (Bibl.115), with all of the ensuing consequences. Among them, for us the most important is the conclusion to the effect that the temperature of phase transformations in the boundary zones should differ from the temperature being determined for identical transformation in the mass of metal or alloy.

The experiments of B.Chalmer, conducted on very pure tin, showed that the melting temperature at the boundaries of crystallites is 0.14° below the ~~temperature~~ ^{point} ~~melting~~ of tin (Bibl.184). According to data of S.D.Gertsriken, in a ~~polycrystal~~ of aluminum of high ~~XX~~ purity (99.998%) at the boundaries of crystallites, melting starts 4° lower than the usual melting ~~XXXX~~ temperature. According to ~~the same~~ ^{the} single crystal data, in a ~~monocrystal~~ of ~~XX~~ zinc the local melting starts at 3° below the normal temperature for melting zinc (Bibl.197).

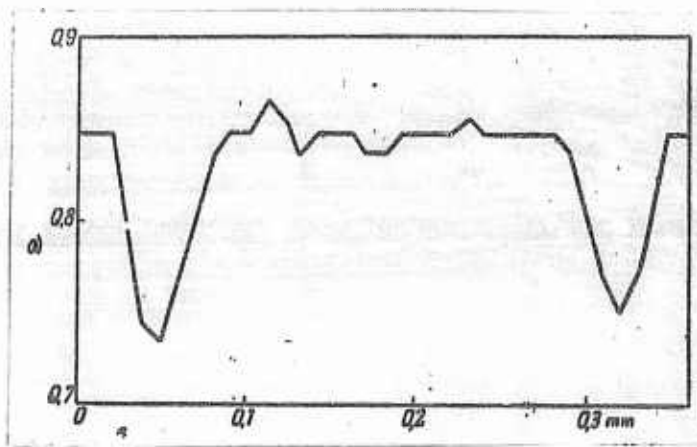


Fig.139 - Distribution of Iron (3%) in a Grain of Nickel, ~~Boring~~

Revealed by the Method of Autoradiography [after S.Z.Bokshteyn

et al (Bibl.195)]

Photographic

a) Density of darkening

G.M.Bartenev, basing ^{on} ~~on~~ ^{the} anomaly of heat capacity and coefficient of volumetric expansion near the melting point, demonstrated that in a ^{single} monocrystal of zinc for a range of 3° before the melting point, there already is a 1% liquid phase. Calculation of the anomalous part of ^{the} heat capacity and of ^{the} coefficient of volumetric expansion near the melting point leads to a satisfactory correlation with the experiment (Bibl.198). However, the author erroneously supposes that "any point of the crystal can be a center of melting", not taking into consideration the existence of interunit boundary zones with elevated free energy and possible defective ^{sites} ~~places~~ in the structure of the ^{single} monocrystal, namely of the ~~KOMMAGEN~~ boundary

zones occurring in contact with the impurities present in the metal. Therefore, for an explanation of the phenomenon ~~being~~ observed, he was attracted by the hypothesis of the possibility of phase fluctuations with the transfer of substance from ^{the} solid to liquid phase. As research ~~XXXXXX~~ conducted by V.N.Kostryukov and P.G.Strelkov has indicated, the results obtained by ~~XXX~~ G.M.Bartenev do not require a particular interpretation and are explained by the effect of impurities. Based on data of these authors, the addition to pure mercury (99.999%) of zinc in the amount of 0.04% atomic weight causes melting at 5° before the critical point, while the addition, besides the zinc, of 0.015% (atomic weight) of Tl intensifies this phenomena: the melting ~~XXXXX~~ begins 7° before the critical point (Bibl.199).

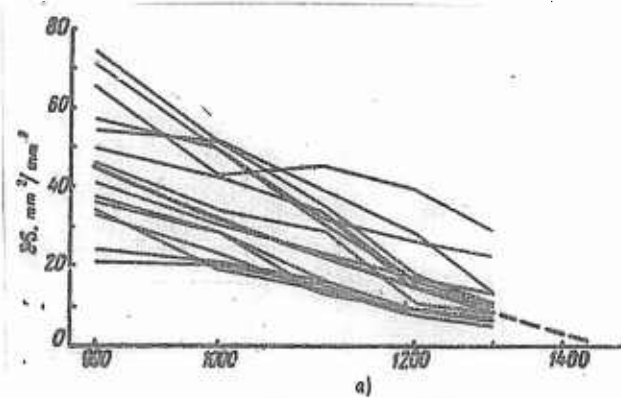


Fig.140 - Change in Specific Surface of Austenitic Grains as Function of Temperature ^{a)} Three-Hour Holding at ~~XXXX~~ Various Temperatures
a) Temperature, $^{\circ}\text{C}$

The study by S.E.Khaykin and N.P.Bene, conducted with ~~single~~ monocrystals and polycrystals of tin, convincingly show that ~~the~~ defects of structure of ~~monocrystals~~, presence of intercrystallite ~~boundary~~ boundary zones and of surface boundary layers cause ~~the~~ local melting of ~~single~~ monocrystals and ~~of~~ polycrystals (Bibl.200).

In finely grained metal, a possible considerable effect of drop in melting

temperature ~~due~~ to intercrystallite boundary zones is hidden owing to the abrupt decrease of their relative volume in proportion to ~~the~~ temperature increase, especially near the melting point. The concept of this process is shown in

Fig.140, in which is adduced the change in specific surface of austenitic grains graph as a function of the heating temperature. The ~~curve~~ is drawn on the basis of experimental data of I.S.Gayev for ~~XXXXXX~~ 15 different steels and irons, ~~XXX~~ containing 0.24 - 2.62% C (Bibl.201). The mean values of plane grains, presented in the study by Gayev, are converted by us to approximate values of specific surface. As evident from the drawing, the value of specific surface of austenite microparticles tends towards zero value at ~~the~~ melting point.

The examples adduced show that, before ~~the~~ reaching of ~~the~~ equilibrium melting temperature in solid ~~single~~ and polycrystals, there can already exist a liquid phase, which is localized in the intercrystallite boundary zones, ~~that is~~ in the zones in contact with the ~~impurities~~ in the surface boundary zone. The opposite

conclusion is fully valid: that hardening of the liquid metal, there occurs a local formation (or presence) of solid phase at temperatures somewhat higher than the equilibrium temperature. The place of localization in this case is constituted by boundary zones at the surface of liquid metal, and also zones occurring in contact with particles of solid impurities ~~XXXXXX~~ (contaminants).

It was shown long ago that G.Tamman and his school did not study the spontaneous crystallization of supercooled liquid, but the crystallizing effect of solid particles of admixtures (Bibl.47, 185). In spite of the fact that Tamman himself revealed the predominant effect of admixtures, artificially introduced into the material being studied, upon the number of nuclei, he considered that he was studying spontaneous crystallization. Moreover, the idea of nucleation in prepared surfaces, namely of solid particles, ~~being~~ confirmed by numerous and convincing tests, starting from 1865, ~~is~~ penetrating more and more into science and at present ~~is~~ quite widespread. The studies of V.I.Danilov and his school demonstrated ~~XXXXX~~ that the use of multiple filtration and centrifuging for purifying a molten substance from mechanical impurities leads finally to a complete loss of the capacity of the material (salol) for crystallization under all supercoolings, all the way to the transition to ~~a~~ solid vitreous state (Bibl.203). Obviously, under these conditions the actual concept "supercooling" becomes indefinite, since the ~~KAM~~ temperature of

crystallization proves to be dependent upon the solid admixtures present in the substance. One can say that Tamman studied the parameters of crystallization not under conditions of supercooling of ~~the~~ actual substance relative to ~~the~~ true critical temperature of pure substance, but under conditions of superheating ~~XXXXXX~~ above this temperature.

I.N.Fridlyander and Z.G.Filippova showed that during the crystallization of organic substance (benzophenone) with supercoolings ranging from 43° to 13° , the liquid ~~in front~~ of the front of crystallization ~~is heated~~ owing to the ~~separation~~ ^{evolution} ~~of latent heat~~ and therefore ~~XX~~ temperature at the front of crystallization ~~is~~ will remain ~~XXXXXX~~ close to the critical temperature (Bibl. 204). During the crystallization of a metal ingot, the latent heat being released at the crystallization front maintains a ~~XXXXXX~~ temperature here which is close to critical. It is clear ~~XXXXXX~~ that, under these conditions, ^{the} temperature of liquid metal in the inner zones of the ingot cannot be below critical under any conditions. Moreover, in these zones there occurs the formation of crystals in the boundary zones of liquid metal ~~in contact with the nonmetallic solid particles~~. This is proven convincingly, in particular for a steel ingot in the discussion concerning ~~XX~~ "rain of crystals" (Bibl. 205, 206 and others).

As O.D.Kazachkovskiy proved, in the depressions ("recesses") of insoluble

impurities present in any actual metal, there can exist small crystals of solid metal at temperatures which exceed the equilibrium temperature all the more, the narrower the "recess" (Bibl.202). As V.I.Likhtman, P.A.Rebinder and G.V.Karpenko remarked, "one considers it established that near the temperature of crystallization in liquid phase there are ~~XXX~~ already contained nuclei of future solid phase in the form of individual mobile atomic complexes, within which the spatial arrangement of atoms comprises the crystal spatial lattice" (Bibl.207, 208) (emphasized by us - S.S.).

Taking into account the immutable fact of the beginning of crystallization either from ~~the~~ external surface of liquid metal or from nonmetallic inclusions, it is necessary to suppose that these atomic complexes are localized in the appropriate boundary zones, the atoms of which have increased energy and mobility.

As the data presented show, the existence of nuclei of a new, liquid or solid phase is noted at temperatures, lying respectively/above the critical temperature of phase equilibrium. In this connection, the advancing ~~X~~ attains values ~~XXXXXX~~ ranging from tenths of a degree to several degrees (for metals). In transformations in ~~the~~ solid state, this advancing reaches ~~XXXXXX~~ maximum values and is sometimes reckoned in hundreds of degrees.

As V.N.Gridnev demonstrated, along the boundaries of grains of ferrite, upon heating it to subcritical temperatures ($500 - 720^{\circ}$), there forms a new phase,

~~NEW~~

namely the "subcritical solid solution". In nature, this phase is an austenite, which is confirmed by study of microstructure, by data of magnetic and dilatometric analyses, and by results of tests for impact strength (Bibl.209). The formation of austenite along the boundaries of grains of ferrite, hardened from temperatures below the critical one (700°) was also noted by A.Tsou, D.Nutting, and J.Menter. The alloy investigated by them contained 0.026% C, of which 0.015% was found in an oversaturated solid solution, forming films along the boundaries of the ferrite grains. It was established by the method of electron diffraction that this solid solution has a face-centered ~~hex~~ cubic lattice, the parameter of which corresponds to the content of carbon dissolved in it in the amount of 0.85 - 1.7% or 1.17 - 2.33% of nitrogen. The authors hypothesize that austenite along the boundaries of grains contains both carbon and nitrogen simultaneously (nitrogen content in alloy 0.0057%) (Bibl.210, 211).

During heating of ferrite-graphite pig iron, there occurs a dissolution of graphite with ~~hex~~ formation of austenite at temperatures lying considerably below the alpha-gamma transformation temperature, as this was indicated by M.M.Zakladnyy and the author (Bibl.212). The fixing of the structure obtained, by hardening or rapid air cooling reveals in an excellent manner the qualitative pattern of kinetics of local formation of solid solution. Initially, austenite forms at the boundaries of ferrite grains, then along the surfaces of blocks. Such a nature of the dissolving

of graphite accompanied by formation of austenite (and after cooling, of ~~troostite~~
troostite or sorbite) was first revealed for malleable iron by V.A.Savatugin (Bibl.213).
M.A.Krishtal (Bibl.214) described a similar pattern of formation of austenite in
gray ferrite-graphite iron. As is shown schematically in Fig.141, austenite having
first formed in the boundary intercrystallite zones of ferrite, spreads further
inside the crystals, forming in each of them a system of mutually parallel wedges
("of tongues", according to the terminology of Savatugin), adjoining the wide side
to the intercrystallite boundary. The distance between the "tongues" was measured
by us based on microphotographs of Savatugin and Krishtal and for both cases
proved equal 3 - 4 microns. According to research data of I.A.Oding and M.
M.G.Lozinskiy, the blocks of mosaic in γ -iron represent plates, the thickness of
which (at heating up to 1100°) comprises from 1 to 5 microns, i.e. have the same
order of size as the distances between the "tongues" (Bibl.215, 216). The stratified
structure of blocks was also noted by Gardin for α -iron (Bibl.87). Therefore it
can be assumed that the formation of a "second row" of austenite takes place in the
boundary interunit zones of ferrite. The local formation of austenite at induction
heating of ferrite-graphite malleable iron in various boundary zones, and the
alternation of formation of austenite in which is connected with temperature of
heating, were noted by P.I.Rusin (Bibl.217).

For a long time, there has been noted the presence of free carbon (graphite) in white pig irons, having been cooled during hardening with a maximum speed.

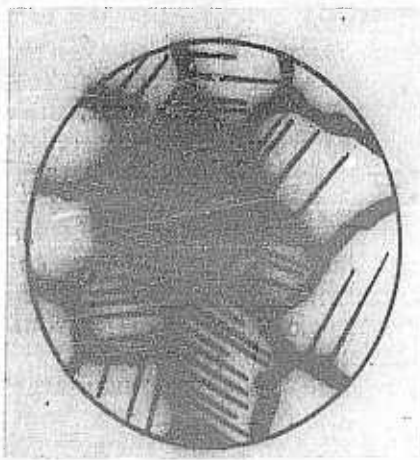


Fig.141 - Diagram of Process of Dissolving of Carbon (Graphite) during Heating of Ferrite-Graphite Malleable Iron

a) Graphite

In castings having the shape of thin plates, EX H.Schwartz and M.Barnett revealed by chemical analysis the constant presence of graphite amounting to from 0.006 to 0.009% (Bibl.218).

In connection with this, we express the proposition that the process of crystallization of graphite from solid solution (graphitization in solid state) progresses at prepared nuclei

(Bibl.170). This is confirmed by the study of formation of graphite in the graphitized steels and white pig irons which ~~WORK~~ was conducted by Ye.Z.Grayfer and I.V.Salli.

The authors concluded that the process of graphitization consists preferably in the growth of already prepared nuclei (Bibl.219).

R.Agarwala and H.Wilman described a case of phase transition, evoked by the effect ~~MICROSTRUCTURE~~ of grinding. Monocrystal of iron was developed as a surface parallel ~~to~~ (110), using emory cloth No.0000 once on a sector 250 mm long at light hand pressure (around 50 gm/cm²) at a speed of about 75 mm/sec. The cloth was soaked

with gas. Thereupon, by the method of electron diffraction, in the surface layer there was detected a certain quantity of γ -iron. Repeated study revealed the complex alternation of layers of α - and γ -iron, but confirmed the presence of the latter. ~~Repeating the same experiment, the authors~~ The authors assume that the transformation is caused by local heating of the surface up to ^{the} temperature of phase transition (900°C) (Bibl.220, ~~XXX~~ 221). This explanation is of little probability, since if it is valid, the transformation should proceed in a reverse direction. It is much simpler to assume that under the conditions described, there is created a boundary surface layer with a distorted lattice and with elevated free energy, which leads to the formation of the new phase.

E.Owen and D.Jones found that the crystal structure of cobalt with a purity of 99.9% depends upon the size of grain. In case of small size ~~XXXXXX~~ grain (cobalt sponge), ~~XX~~ the cubic face-centered lattice, typical for high-temperature modification of cobalt, proves to be of stable structure. In case of large grains (rods), there is observed the normal hexagonal lattice of α -cobalt. In the presence of a mixture of large and small grains (filings) in the range from 20 to 450° , both lattices are observed, namely K12 and G12, while above 450° only the K12 lattice occurs (Bibl.222).

P.Bridgman, having studied the plastic deformations at high hydrostatic pressure, ~~XXXXX~~ writes: "It could be expected that at such exclusively high deformations of displacement, the lattice will be disrupted to such a degree that in it the polymorphic transitions no longer can occur. It turns out, on the contrary, ~~that~~ these conditions ~~XX~~ do not obstruct, but ~~XXXXX~~ rather even promote the polymorphic transitions. Examples were found of the fact that under effect of stress of displacement at room temperature, there occur such transitions which without the stress of displacement do not take ~~XXXXX~~ place until the temperature has risen to 200°C for overcoming the internal viscosity. The existence of polymorphism under such unusual conditions indicates that the lattice is basically preserved. In order to explain how this occurs, further researches are necessary"

(Bibl.223) (our underlining - S.S.).

Examples of stable existence of phases, differing from those which are determined for a given temperature by structural diagrams, can easily be continued. In all cases, it is caused by the presence of ~~XX~~ boundary zones, possessing increased free energy in comparison with the ~~XX~~ free energy level within the regular lattice. Similar occurrences, attributable to the same ~~XXXXXX~~ reason, are observed in thin metal films, the crystal structure of which depends upon the thickness of film, since

together with it there changes the value of surface energy, referred to a unit volume of film. In the reports (Bibl. 224 - 227) and a number of others, it is shown that at room temperature there can exist high-temperature modifications, that is modifications unusual for the given metal in large samples, and finally an amorphous structure can exist.

Additional proof of the proposition that prepared nuclei of new phase are already present at the initial moment of phase transition is provided by a mathematical analysis of distribution curves ~~of sizes~~ ^{the size} of microparticles, which was carried out by S.Z.Roginskiy and O.M.Todes (Bibl. 164, 165). As primary parameters, typifying the kinetics of the phase formation process, the authors adopted the usual Tamman parameters. They examined possible forms of ~~distribution~~ ^{size} curves ~~of sizes~~ for microparticles, being obtained ~~in~~ ⁱⁿ case of the following types of change of these parameters during the phase formation process: crystallization at prepared nuclei at constant rate of growth; crystallization at ~~constant~~ ^{time-invariance} of both parameters ~~in time~~; crystallization at constant rate of nucleation and at linear rate of growth, increasing with the growth of crystals; crystallization from solution at given ~~M~~X number of nuclei in case of falling concentration; and crystallization of solution at falling concentration taking into account the dependence of rate upon sizes of forming crystals. In all cases, the authors limited themselves to an

examination of the initial crystallization stage, when the zones of crystallization, leaving the individual nuclei, still do not come into contact i.e. to a consideration of crystallization under conditions of free growth of microparticles (without collisions).

The authors concluded that the nature of primary distribution depends greatly upon ^{the} rate of formation of crystallization nuclei. If it ^{is} constant or changes ~~XXX~~ little in the crystallization process, distribution of ~~sizes~~ ^{the size} of microparticles is indicated either by a horizontal line or by a descending curve without any signs of a maximum. On the other hand, at zero rate of nucleation (i.e. during ~~XXXXXX~~ crystallization at prepared nuclei) or under a condition reducible to this case, when the rate of nucleation falls with a decrease in concentration of solution much more quickly than the linear growth rate, on the distribution curve there is an abrupt maximum, ~~XXXXXX~~ temporally being displaced.

As we pointed out above [Section 39, see also (Bibl.162)], for a large number of various kinds of crystal formations of metallic structure, there is in effect the law of logarithmically normal distribution of microparticles based on sizes, being characterized by a curve with a ^{indistinct} ~~markedly pronounced~~ maximum. The data presented above can be supplemented by research materials of N.N.Buynov and L.I.Podrezov, who obtained distribution ~~XXXXXX~~ curves of similar type for sizes of

zones of Ginzburg-Preston and particles θ' and zinc in aluminum-copper and aluminum-zinc alloys (Bibl. 228, 229). These curves are of particular interest,

since they are obtained for

particles and zones, the dimensions

of which comprise from 70 to 120 \AA ,

i.e., they approach the sizes of nuclei.

The data presented in the present paragraph indicate quite convincingly that if crystallization at prepared nuclei is not a law, it is very widespread. Therefore expression (42.3)

is more correctly replaced by another:

$$N = N_0 + \psi(\tau), \quad (43.1)$$

in which N_0 is the number of nuclei already present at the initial moment of isothermal transformation ($\tau = 0$). It is easy to ~~imagine~~ perceive that the rate of nucleation, which at the initial transformation stage can be examined as the first derivative in time from expression (43.1), does not reflect the presence of prepared nuclei, the role of which should be particularly significant at the ~~initial~~ initial period of phase formation.

In Fig.142, we show schematically several different curves, expressing relationship (43.1) at identical (in all cases) law of change ~~of~~^{time rate of change of} nucleation ~~in time~~, but at varying number of prepared nuclei, which had existed at the ~~initial~~^{instant} transformation. It is quite evident that these ~~XXX~~ curves fully reflect the kinetics of nucleation, while the Tamman parameters will prove uniform in all cases and will create a distorted or poor concept of the kinetics of nucleation, and hence also of the transformation process as a whole.

Naturally it is more feasible to use the parameter N , and not the value $dN/d\tau$, especially since the latter can be derived from the former.

Section 44. Estimation of Transformation Kinetics

Speaking of crystallization kinetics, V.D.Kuznetsov states that at present there is still no such theory of crystallization which is capable of describing the entire process or of making a forecast of its progress. Kuznetsov writes "metallurgical practice requires the development of such a theory which could: 1) define the time, in the course of which there occurs the entire crystallization process under the given conditions; 2) determine for each given moment the quantity of crystallized matter and ~~XXX~~ 3) determine the dependence of ^{the} amount of crystallized matter upon ^{the} rate of change in external conditions, basically upon the rate of temperature drop" (Bibl.185). To these requirements, it is necessary to add still ~~XXX~~

another: the possibility of the predetermination of that structure which would be obtained at the end of transformation or at any stage of it, under the given conditions. The last requirement can envisage both a purely qualitative characteristic of structure, as well as its quantitative characteristic, mainly the dispersed state.

As parameters, typifying the kinetics of the process, Kuznetsov proposes the temperature of crystallization and the amount of crystallized matter (in weight or volumetric percentages). Dispersed state can be estimated by the value of specific surface, by sizes of particles, their distribution, by quantity per unit ~~of~~ volume, etc.

Many methods and formulas were proposed for calculating the amount of crystallized phase as a function ^{of} duration of isothermal transformation. Unfortunately, all of them are based on the Tamman parameters of crystallization, which in our opinion predetermines their ~~failure~~ failure. Actually, taking the Tamman parameters as a ~~basic~~ basis, we should either consider them as being independent of time (at constant temperature), which is patently incorrect, or assign some law of their change in time, i.e. proceed from more or less ~~arbitrary~~ arbitrary assumptions. Moreover, there is excluded from consideration the possibility of presence of prepared nuclei, the actual existence of which in many cases is confirmed by data presented in Section 43.

G.Tamman derived the first equation permitting one to calculate the relative volume of transformed phase V_τ as function of time τ ; he proceeded from a number of assumptions, simplifying the conclusion: rate of nucleation was assumed constant and was ~~not referred~~ referred ~~not to a unit~~ not to a unit volume of native phase but to a unit volume of substance being considered as a whole (i.e. there was adopted the value a' , but not a , see Section 42); the linear growth rate was also assumed ~~not~~ to be constant; collision of growing particles was not taken into account; and ~~the~~ spherical syngony of growth of particles was assumed. As a result, we got the equation:

$$V_\tau = \frac{\pi}{3} a' v^3 \tau^3 (\tau + 1). \quad (44.1)$$

F.Geller and G.Zaks solved the problem at the same initial assumptions, having replaced the value a' by the rate of nucleation, referred to a unit volume of native phase a . The expression obtained by them for cubic syngony of growth has the following form (Bibl.230):

$$V_\tau = 1 - \cosh p\tau \cos p\tau, \quad (44.2)$$

where \cosh is the hyperbolic cosine, while the parameter p equals:

$$p = \sqrt[4]{12av^3}.$$

The formulas of G.Tamman, F.Geller and G.Zaks are valid only for initial stages

of transformation, since they do not take into account the phenomenon of mutual collision of growing particles.

A detailed analysis of kinetics of transformation and an analysis of it with aid of models were conducted ~~in~~ in the report by ~~XXXXX~~ B.V.Stark, I.L.Mirkin and A.N.Romanskiy (Bibl.231) and were continued by the report of Mirkin (Bibl.5). Since the final conclusions of the latter report overlap with the developed and more general solution proposed by A.N.Kolmogorov (Bibl.232), we shall consider the results of this last analysis.

A.N.Kolmogorov derives a precise formula for probability $p(\tau)$, with which the randomly selected point of volume, initially filled by ~~the~~ initial ~~XX~~ phase, will fall in the course of time interval τ within the new forming phase. It can be considered with quite sufficient approximation that the part of the volume, occupied by the new phase up to the ~~moment~~ τ , also is equal to this probability, i.e.,

$$V_\tau = p(\tau). \quad (44.3)$$

Moreover, an equation is derived determining the kinetics of variation in ~~the~~ total quantity of microparticles in the volume being considered and their final number upon completion of the transformation process.

In the conclusion, Kolmogorov proceeds from broad assumptions, assuming that

the rate of nucleation $a(\tau)$ is a function of time. Linear rate of growth is regarded as a function both of time and of direction:

$$v(\tau, n) = k(\tau) \cdot v(n). \quad (44.4)$$

However, in the latter case a certain limitation is added, reducing to the fact that, although ~~the~~ growth rate can depend upon ~~the~~ direction N , this dependence should be identical in all points. In other words, the formulas derived are valid either at uniform growth in all directions, or ~~in~~ the case of ~~hexagonal~~ crystals, of arbitrary form, uniformly oriented in space. Since the second case does not occur in practice, the Kolmogorov conclusion is valid for the case of formation of equiaxed (globular) microparticles of new phase.

The conclusion takes into ~~account~~ the occurrence of collisions of growing microparticles and a decrease in volume of ~~the~~ initial phase in proportion to development of the transformation process. In the most general case, being typified by the above-presented conclusions, the Kolmogorov equation for phase transformation kinetics has the following form:

$$V_\tau = 1 - e^{-\frac{4\pi}{3} \sigma^3 \Omega}, \quad (44.5)$$

where Ω is determined by the expression:

$$\Omega = \int_0^\tau a(\tau') \left[\int_{\tau'}^\tau k(\tau'') d\tau'' \right]^3 d\tau' \quad (44.6)$$

The kinetics of change in quantity of microparticles of new forming

phase is determined by the equation:

$$N_{\tau} = \int_0^{\tau} a(\tau') q(\tau') d\tau', \quad (44.7)$$

in which $q(\tau')$ equals:

$$q(\tau') = 1 - p(\tau'). \quad (44.8)$$

For practical use of the precise equations derived by Kolmogorov, it is

necessary to know the type of functions determining the ~~time~~ dependence

of rate of nucleation $a(\tau)$ and of linear rate of growth $k(\tau)$. Later, certain

investigators, basing on these or other concepts, assigned a definite type of

these functions (I.L.Mirkin, M.Avrami-Melvin, D.Meyering), while others consider

that they should be revealed experimentally (W.Johnson and R.Mehl)*. One should

concur unconditionally with the opinion of the latter.

A.N.Kolomogorov gives two special solutions of both equations (44.5) and

44.7. In the first of these solutions, it is assumed that the rates of

* We consider it necessary to note that Johnson and Mehl obtained for phase

transformation kinetics an expression, ~~corresponding in accuracy to the~~

~~expression obtained by Kolmogorov~~. Even though the latter was published more

than two years earlier than the study of Johnson and Mehl (Bibl.233), these

authors did not refer even once to the study of Kolmogorov (Bibl.232), furthermore

almost completely reproduced in the report (Bibl.5).

nucleation and growth are independent of time and hence:

$$a(\tau) = a \text{ and } k(\tau) = 1.$$

Then the phase transformation kinetics are determined by the expression:

$$V_\tau = 1 - e^{-\frac{\pi}{3} v^2 \sigma \tau^4}. \quad (44.9)$$

The latter formula was compared by Mirkin with special test data, and also with data of a number of researchers, obtained during the study of the isothermal transformation of austenite. Coincidence with eq.(44.9) is noted only for the data obtained by Vefer (Wefer) in chrome-nickel steel by the magnetic method.

All of the remaining test data (Mirkin, KREZN Epton, Davenport and Beyn) showed a good correspondence to the formula, analogous to eq.(44.9), but the agreement with time was not to the fourth but to the third power. Mirkin considers the following as possible causes of this circumstance: a) change in properties being determined during the test (magnetic state, electric resistance), possibly not fully proportional to the actual amount of austenite present; b)/probability of nucleation in various points of ~~the~~ volume may be dissimilar, namely it is maximum at the surface of austenite grains, which leads to ~~a~~ incomplete three-dimensional state of growth of microparticles of new phase; and c) rates of nucleation and growth may not be ~~time-invariant~~.

In connection with the fact noted by Mirkin, of great interest is the second

special solution proposed by Kolmogorov for a special case ~~KM~~ when all nuclei of crystallization are forming at the actual beginning, i.e. when the formation of microparticles of new phase occurs in prepared nuclei. In this case, the general formula (44.5) acquires the following form:

$$V_r = 1 - e^{-\frac{4\pi}{3} b^3 r^3}, \quad (44.10)$$

where b is the amount of prepared nuclei, existing per unit of volume of material

~~at~~ initial moment of transformation. As we see, ~~KM~~ eq.(44.10) is quite similar to eq.(44.9), but includes time not to the fourth, but to the third power. Therefore, Mirkin for decrease in ~~the~~ expression analogous to the three possible causes indicated by ~~KM~~ we can add a fourth: the existence, at initial/transformation, ~~moment~~ of the time exponent, ~~at~~ the instant of ~~the~~ prepared crystal nuclei.

N.N.Sirota studied the effect of dimensionality of growth of microparticles upon type of function determining the phase ~~KM~~ transformation kinetics. He established that ~~KM~~ the exponent for time in ~~KM~~ expression analogous to (44.9), equals the fourth power ~~at~~ at three-dimensional growth, the third power at two-dimensional growth (plate) and ~~at~~ the second power at ~~single~~ dimensional growth (needles, rods) (Bibl.32). In a similar way, the exponent for linear rate of growth decreases. An experimental checking of the derived formulas was conducted

"Acicular"

in a study of the process of isothermal formation of "Bainite" troostite
(Bainite)
~~experiments~~ in type U10 steel (Bibl.32). It turned out that the test ~~MIRKIN~~ curve

provides quite good coincidence with the theoretical curve expressed ~~MIRKIN~~ by the

one-

equation for ~~single~~ dimensional growth, although the spatial formations of

"Acicular"

~~theoretical MIRKIN~~ troostite, as well as of martensite, have a lamellar shape,

i.e. are two-dimensional. Hence, in addition to regularity of growth of

microparticles, other factors, the effect of which is reflected in decrease in

exponent for time in the kinetic phase transformation formula play a substantial

part. As Komolgorov indicated, one of such factors can be the existence of

instant

prepared nuclei at the initial moment of transformation.

Time variance the

As Mirkin indicates, another cause may be the ~~indefiniteness~~ of linear rate of

growth ~~isotropic~~. For instance, having assumed that the radius of a microparticle

grows in proportion to time to the ~~degree~~ of ~~MIRKIN~~ Mirkin obtained a formula

for the kinetics of phase transformation, similar to (44.9) but including time

to the power of 2.5 (Bibl.5).

Finally, as the study by M.Avrami-Melvin indicates, the decrease in exponent

the

for time can occur owing to the gradual exhaustion of number of potentially

sites

preferable places for nucleation (Bibl.182, 234).

At present we do not have enough data to select a concrete form of function

of the kinetics of phase transformation or recrystallization, the general expression

of which is given by the eqs. (44.5) and (44.6) of Kolmogorov. We need to conduct detailed experimental investigations for establishing the form of dependence of rates of nucleation and growth ~~as a~~ function of time, and also the effect of presence of prepared crystal nuclei. Therein, it needs to be taken into account that the verification of the kinetic formulas, determining the volume of transformed phase ~~as a~~ function of time by way of comparison with test curves of ~~the~~ increase of volume of new phase in time, is inadequate.

It can be shown that the extremely good coincidence of theoretical and experimental curves of ~~the time rate of change of the relative amount of new phase in function of the size distribution of microparticles~~ ~~the curve whose distribution function of microparticles~~ ~~can differ sharply from the curve~~ ~~slope~~ ~~is predetermined by initial laws of change in rates of nucleation and growth, assumed in deriving the theoretical formula. Specifically, in the initial period of formation of new phase, when its quantity is slight, the relative quantity of microparticles, depending upon their sizes are characterized by the ascending ~~curve~~ curve (if we proceed from the theoretical formulas of phase transformation kinetics). Moreover, the study of N.N.Buynov and L.I.Podrezov showed that the size distribution function of ~~new~~ microparticles is already typified by the asymmetric ~~curve~~ distribution of usual type with a sharply expressed maximum, when the ~~size~~ sizes of particles do not yet exceed several tens of angstroms (Bibl. 228, 229). Distribution function of microparticles in~~

conformity with the logarithmically normal curve evidently have a universal nature, which must be connected with the kinetics of nucleation and growth of microparticles.

The data presented above indicate that the problem of quantitative expression of kinetics of formation of new phase or of ~~recrystallization~~ recrystallization is being far from solved theoretically. The special solutions, proceeding from more or less arbitrary assumptions of ~~the~~ relative rates of nucleation and growth, do not permit one to obtain sufficiently reliable formulas. The solution of this problem in a general form requires a knowledge of the functional dependence of the Tammann parameters upon time. If these dependences become revealed, they should include some new parameters, independent of time, which greatly complicates both the kinetic formula of phase formation as well as its practical use.

At the same time, it should be noted that very often the kinetics of change in quantity of new phase can be described by empirical formulas, including the usual two or three parameters, depending upon properties of substance and temperature of the process. Therefore it is feasible, not forsaking systematic investigations, conducted for solving the general Kolmogorov equation for actual cases of phase formation and recrystallization (these studies should include at the same time the problem of determining the ~~size distribution~~ size function distribution of ~~size~~ size of microparticles at any stage and at the end of the process), to find

empirical formulas describing the kinetics of change of quantity of new phase and of basic geometric parameters, typifying the alloy structure (values of specific surface, number of microparticles, their average size and dispersion).

It is rational to accomplish the estimation of the kinetics of phase-formation process on the basis of natural parameters of actual spatial structure, which are applicable to any structures, independently of the shape of growing microparticles, and being determined experimentally with the least expenditure of effort and with the maximum accuracy. Above all, such universal parameters are: relative volume of transformed phase, specific surface of microparticles of this phase and specific surface of the separation of the old and new phases.

As an example, we present certain results, obtained by us for kinetics of the process of graphitization of ~~bound~~ carbon in white and gray pig irons based on experimental data, both developed by us and published by other researchers. The amount of carbon, capable of being graphitized at a given temperature, was assumed to be unity. Then the degree of graphitization ^{as a} function of time is determined by an integral curve, corresponding to the expression:

$$V_{\tau} = \frac{1}{\sqrt{2\pi}} \int_{-\infty}^{\tau} e^{-\frac{t^2}{2}} dt, \quad (44.11)$$

where V_{τ} is the part of graphite which had formed during isothermal holding for the time τ (degree of graphitization), and the value for t is determined by the

equality:

$$t = a \ln \tau - b, \quad (44.12)$$

in which a and b are constant coefficients, depending upon composition and structure of pig iron and upon temperature of the ~~MAX~~ annealing process.

Equation (44.11) is verified for the process of graphitization of cementite, ledeburite and pearlite at temperatures both below and above the temperature of eutectoid transformation. The degree of graphitization was determined by dilatometric method and based on data of chemical analysis. In Fig.143, ~~MAX~~ a computational curve is shown and experimentally found points are drawn in for the process of graphitization of eutectoid carbon of gray iron, containing 2.03% Si at ~~a~~ temperature of 700° .

As is known, the integral ~~to the right~~ of eq.(44.11) is not taken. Therefore it is convenient to construct a straightened curve of ~~the dependence~~ the quantity t versus the ~~abscissa~~ logarithm of duration of isothermal heating τ . Therein, one should use the tabular data of dependence of integral (44.11) upon ~~values~~ ~~on~~ (standard deviation), introduced in the courses ~~in~~ the theory of probability.

In Fig.144, we show such a straightened kinetic curve for the process of graphitization of white iron, containing 3.19% C and 1.88% Si, at 740° (the specimens ~~were cast in the form of thin rods~~ ~~5 mm~~ in diameter and had the

structure of white iron). The obtainment, in the chosen coordinates, of rectilinear dependence is a proof of its conformity to ~~to~~ eq.(44.11).

In Fig.145 is shown an analogous dependence, constructed by us based on test data of S.O.Vitenzon, obtained for white iron containing 0.7% Si at annealing temperature of 1000° (Bibl.235). The two initial points are not shown in the curve. This is easily explained by the fact that graphitization actually began during the heating process, up to the attainment of temperature of isothermal heating.

As we see, eq.(44.11) under the assigned conditions ~~XXX~~ of phase transformation, permits us to fully characterize the kinetics of the process only by two parameters, of which one (b) depends upon temperature of isothermal heating.

In a study of kinetics of collective recrystallization, a natural parameter is the value of specific surface of microparticles, since the actual process of recrystallization is caused by a tendency toward a maximum decline in the level of free energy owing to ^a decrease in specific surface of microparticles. Whether this decline progresses owing to ^{an} increase in ^{the} radius of curvature of boundary surfaces, changes in two-faced and solid angles or owing to absorption of unstable fine microparticles, it is always accompanied by ~~the~~ reduction of specific surface. typifies best and most feasibly from the Therefore, the kinetics of this reduction ~~XXX~~ recrystallization as a whole.

No less rational is the determination of the kinetics of change of this parameter and in case of formation of new phase, since it supplements the pattern of structural formation, characterizing the dispersed state of the new phase.

~~Here~~ it is noteworthy that there is practically no difficulty in determining experimentally the two values separately, namely the specific surface of the boundary of the old and new phases and the ~~surface of the division~~ ^{interface} of microparticles of new phase with ~~one another~~. The first of these values quickly increases, reaches a maximum and then decreases almost to zero toward the end of the phase formation process. The ~~surface of mutual separation~~ ^{mutual interface} of microparticles of new phase continuously increases, ~~it~~ reaches a maximum somewhat before the end of the process of formation of new phase, and then slowly declines owing to secondary processes (coagulation, collective recrystallization, spheroidization etc.). The use of specific surface of boundary of old and new phases, as a parameter typifying the ~~kinetics~~ kinetics of the crystallization process was first suggested by A.G.Spektor (Bibl.236).

In Fig.146, we show the change in specific interface of austenitic and ~~MAX~~ pearlite components of steel during the process of isothermal decay of austenite. There is a basis for assuming that the dependence of specific surface as a function of time is expressed logarithmically as a normal curve, which however requires further experimental verification.

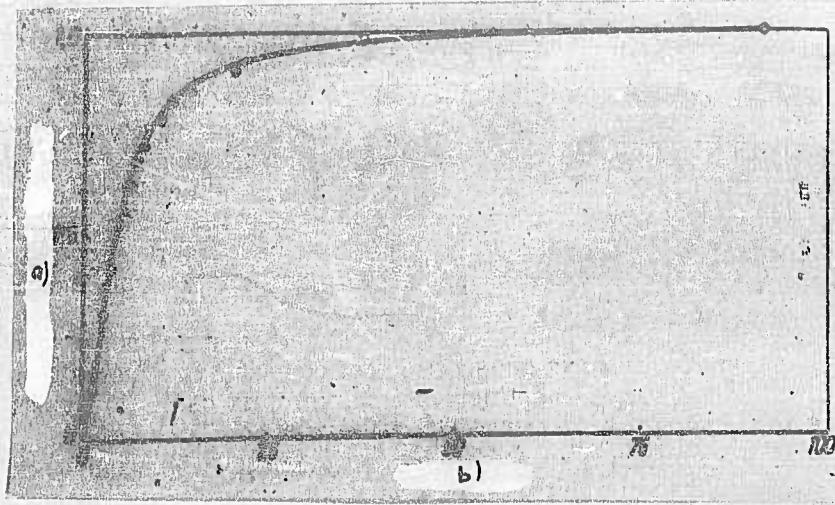


Fig.143

a) Degree of graphitization; b) Time, min

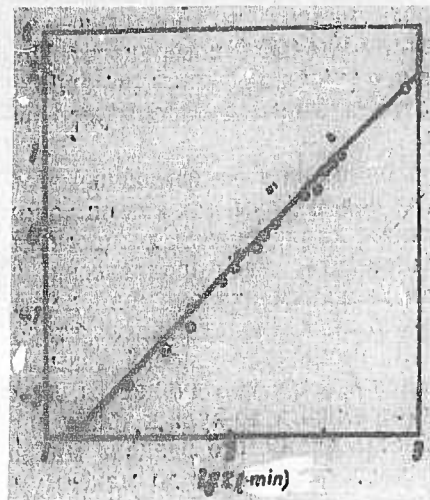


Fig.144

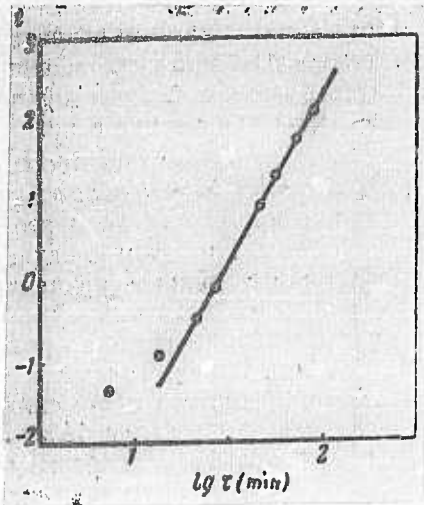


Fig.145

Section 45. Special Transitional Zones and Properties of Metals and Alloys

In polycrystalline pure metal, two-dimensional, ~~single~~^{one}-dimensional, and point boundary zones are the place of juncture of two, three, and four spatial lattice respectively, the crystallographic axes of which are oriented differently in space. Imagine that these boundary zones are geometric surfaces, lines and points, not having any third dimension. Even in such a case, the degree of saturation of metal with boundary surfaces and lines could not help but reflect upon its properties, since the properties of a crystal lattice are anisotropic, having an influence within the metal, reaching the boundaries between crystallites, changing its direction, rate of propagation or energy, and therefore the number of such changes is without doubt significantly reflected in the effectiveness of the influence.

As we know, real boundary zones have a definite volumetric extent and moreover differ from the intracrystallite (more accurately from the intrablock) metal in their structure, chemical composition, and hence in properties. Therefore they exert ~~an~~^{the} influence upon the properties of metal in the same way as if they had been affected by the presence of the corresponding quantity of second phase, being characterized by properties and external configuration, similar to the boundary zones of a polycrystal.

Depending upon the nature and character of external effect upon metal, its effectiveness (to the degree to which it is determined by ~~dispersion of~~^{the degree of dispersion of} the degree of dispersion of

^{the} polycrystalline structure) can ~~as~~ depend basically both upon the first as well as upon the second factor, or upon both of them together. However, since the thickness of boundary zones is very slight in comparison with their two-dimensional ^{one-} or ^{single} dimensional extent, the relative volume of boundary zones is proportional to their specific extent. Thence it follows that the effectiveness of external

influence (to the extent that it

^{the degree of dispersion of}
~~dispersion state of~~

/polyhedral structure) is determined
in a well-defined manner by values of the
specific surface and specific extent of
lines of boundaries, independently of
which of the two factors (various
orientation or quantity of "second
phase") proves most real under the
given conditions.

As is clear, between the relative

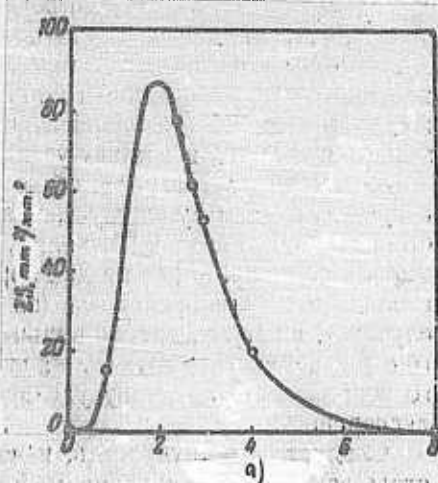
volumes of two-dimensional and ^{one-}
~~single~~

dimensional boundary zones there exist

Fig.146 - Kinetics of the Change in Specific Interface of Austenite and Pearlite Components at Isothermal Decomposition of Austenite of Austenitic Carbon Steel

a) Time, min

an approximately constant relationship. Since the actual relative volume of



flat of the one -

two-dimensional zone is about twice as great as ~~the single~~ dimensional zone, the latter can be disregarded (with the exception of certain special cases). Therefore, the degree of dispersion of the studying the effect of ~~dispersion of the~~ polyhedral structure of pure metal upon its properties, it ~~is~~ is most feasible to use the value of specific surface as an index of ~~dispersion of the~~ the degree of dispersion.

Unfortunately, ~~it~~ it must be stated that this parameter, so easily and precisely being determined experimentally, has as yet been used relatively rarely and is not determined ~~by~~ by a direct method (by the method of random secants), but indirectly through the value of a flat grain. In most of the experimental data, the polyhedral structure is typified ~~mainly~~ by this latter value, which is estimated as the mean area of grain, by mean number of grains per unit ~~of~~ area, by average by diameter of grain, or conventional number on the scale for GOST 5639-51. In order to introduce uniformity into the estimation of ~~dispersion~~, all experimental data of other ~~MX~~ authors from here on are converted by us to the value of specific surface of crystallites. In the conversion, we proceeded from the position that the specific surface is about proportional to the square root of the number of flat ~~MX~~ grains per unit ~~area~~ of cut and universally proportional to the average diameter of a flat grain or to the square root of the average area of grain. Therein, we used the relationships obtained from eqs. (40.10) and (40.13) at $\Sigma V = 1$

and a coefficient of variation $\delta = 0.35$:

$$\Sigma S = 2.05 \sqrt{n} = \frac{2.05}{\delta} = \frac{2.05}{\sqrt{F}} \text{ mm}^2/\text{mm}^2.$$

In alloys, we encounter a greater diversity of factors affecting properties.

Above all, this is the structural composition of an alloy, i.e. the relative volumetric content in it of various phases and structural components. Moreover, in connection with the presence of several phases, there appear boundary surfaces of various form, being determined by the pair occurring in/contact of structural components. There is a number of factors which, not reflecting on the structure, can significantly reflect on the properties of the alloy (differing concentration of impurities in solid solutions, cold-hardening). Finally, at the same value of specific surface of given structural component, its form of microparticles can be different, which also, generally speaking, should reflect upon the properties. Therefore, for a study of the separate influence of a definite type of boundary surface upon properties, it is necessary to assure the constancy of the remaining factors or, in any case, to take their change into consideration as well.

Below we present test data on the effect of boundary zones upon various properties of metals and alloys, obtained by a number of investigators; we have attempted to systematize these data and explain them from the viewpoint of MX stereometric structure.

A. Mechanical Properties

Hardness

As far as we know, the first writers to indicate the existence of direct relationship between hardness, being determined by the Brinell method, and the value of specific surface were H.Angus and R.Summers (Bibl.241). Both on the basis of their own observations, as well as using data published earlier by Bassett and Davis, they showed that the increase in hardness is proportional to the increase in specific surface of crystallites. In Fig.147 is shown the dependence of hardness of ~~single~~-phase α -brass upon ~~the~~ specific surface of microparticles of solid solution, based on data of Bassett and Davis, converted by us (Bibl.242). In Fig.148 is shown an analogous dependence which was obtained by Angus and ~~Summers~~ Summers. It is interesting to note that both the dependence for ~~pure~~ pure copper (Fig.148), as well as for ~~single~~-phase bronze (4.5% Sn), shown in Fig.149, was obtained by the authors during the calculation of specific surface as a tripled value of the square root from the number of flat grains per unit ~~area~~ area, which coincides closely with the formula presented earlier. Correction figures are adduced in Figs.148 and 149.

The hardness of armco-iron ~~XXX~~ in dependence upon ^{the} value of flat grain was determined by T.Ishigaki (Bibl.243). The data obtained by him, converted in a similar manner, are shown in Fig.150. Here there is observed a perceptible

rectilinear dependence at very small values of specific surface, when the dimensions of the diagram are made to coincide with the sizes of the flat grain.

As the author notes, in testing on single grains, the imprint loses its rounded form.

The distortion of the dependence can be explained by the rapid increase of the zone of relatively free plastic deformation around the imprint, in proportion to approaching the zero value of specific surface (i.e. to the ~~mon~~^{single} crystal). We shall return again to this question.

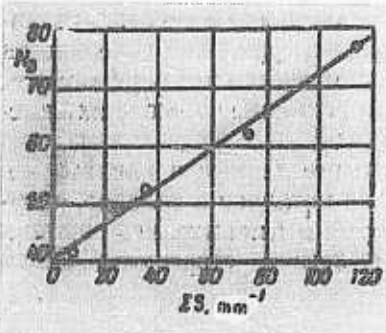


Fig.147 - Hardness of α -Brass depending upon the value of Specific Surface of Grains. Based on experimental data of Basset and Davis, converted by the author

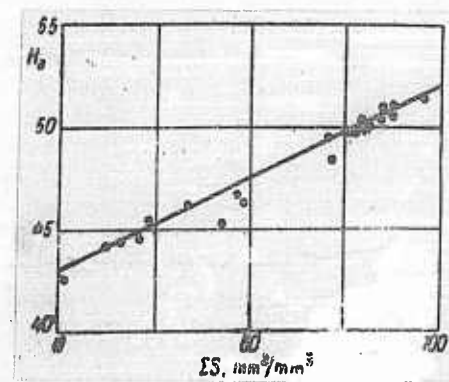


Fig.148 - Hardness of Pure Copper as a function of the value of Specific Surface of Grains. The experimental data are from Angus and Summers (Bibl.241), converted by author

The above-adduced data indicate that one can consider as established the dependence rectilinear ~~dependence~~ of hardness upon ^{the} value of specific surface for ~~pure~~ pure

single-
metals and ~~mono~~phase solid solutions, in any case for values of specific surface of ~~practical~~ practical interest. This dependence in a general case is expressed by a formula of the type:

$$H_B = H_0 + \epsilon \Sigma S \kappa / \quad ^3. \quad (45.1)$$

Typical for the given metal or alloy are the values of coefficients of this formula, where H_0 can be possibly represented as the hardness of ~~mono~~crystal, averaged for all possible directions of test relative to crystallographic axes. ~~MAXIMUM~~ The coefficient ϵ expresses the tendency of the metal towards hardening owing to boundary surfaces. The values of this coefficient for the above-described cases equal:

| | |
|------------------|-------|
| Bronze | 0.073 |
| Copper | 0.090 |
| Iron | 0.143 |
| Brass | 0.320 |

These data should be considered approximate, since the specific surface was measured not directly but by an indirect method. Evidently in the analysis of brass the twinning surface was not taken into consideration, which caused the obtainment of an elevated value for the ~~XX~~ coefficient of hardening ϵ .

Among the more complex, multiphase structures, the structure of pearlite in steel is of great practical interest. The dependence between ~~MAXIMUM~~ hardness and specific surface of cementite in stratified pearlite was studied by

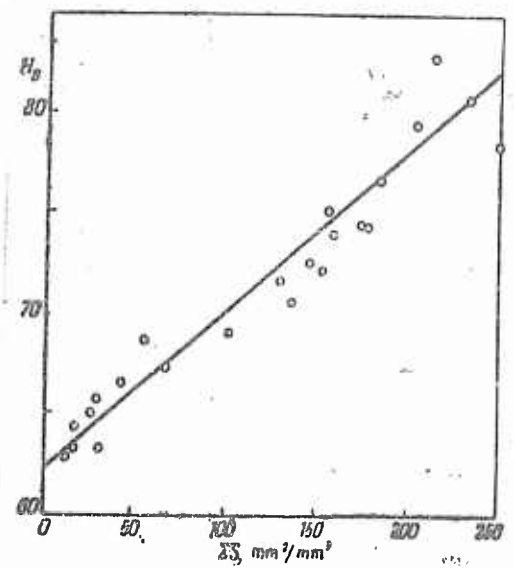


Fig.149 - Hardness of Monophase Bronze (4.5% Sn) as *the* Function of Value of Specific Surface of Grains. Based on Experimental Data of Angus and Summers (Bibl.241), Converted by Author

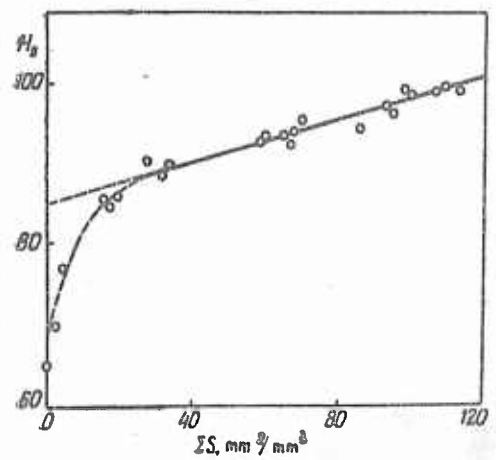


Fig.150 - Hardness of Armco-Iron as *the* Function of Value of Specific Surface of Grains. Based on experimental data of T.Ishigaki (Bibl.243), converted by author

NEXT N.T.Belyayev in a relatively narrow range of hardnesses (215 - 300)

(Bibl.48, 186). The dependence obtained by Belyayev is defined by the ~~XX~~ expression:

$$H_B = \frac{0.0796}{\Delta_0} \text{ kg/mm}^2,$$

in which it is easy to replace the ~~interstratified~~ ^{interlamellar} distance Δ_0 with a value of specific surface; using the known relationship between these values, we get:

$$H_B = 0.0398 \Sigma S_n \text{ kg/mm}^2. \quad (45.2)$$

The dependence obtained by Belyayev leads to unreal values of hardness of pearlite outside the range of dispersed state studied by him. For instance, in coarsely stratified pearlite, the specific surface of cementite comprises $1000 - 1500 \text{ mm}^2/\text{mm}^3$, but the hardness of such pearlite is approximately two - three times greater than the value obtained on the basis of the formula ($40 - 60 H_B$). On the other hand, in highly dispersed ~~stratified~~ ^{lamellar} structures, the value of specific surface of cementite attains $15,000 - 20,000 \text{ mm}^2/\text{mm}^3$ (in sorbite, troostite), but the hardness of such structures is about twice less than that which we get according to the equation (45.2) ($600 - 800 H_B$).

Worthy of confidence is the dependence obtained by S.Z.Bokshteyn in the study of structure of granular cementite of hypoeutectoid steel (0.4% C), hardened and exposed to high annealing (Bibl.125). The type of this dependence is identical to the expressed general ~~XX~~ ^{equation} (45.1) for single-phase structures. A similar

dependence was obtained by us for structures of lamellar pearlite of eutectoid steel (Bibl.151).

In a very wide range of hardnesses and values of specific surface of cementite of products of isothermal decay of ~~XXX~~ austenite, the dependence among them was studied by A.P.Gulyayev and A.I.Gardin (Bibl.196). The dependence obtained by us is expressed by two straight lines separately for the products Ar' and Ar'' transformations of austenite respectively.

We generalized the test data of N.T.Belyayev, A.P.Gulyayev and A.I.Gardin, our own data (Bibl.17), and supplemented by individual data of E.Beyn (Bibl.244), A.N.Rozanov and M.I.Fantayev (Bibl.245). These composite data are presented in Fig.151 where the circles denote the Gulyayev and Gardin data referring to products of ~~XXX~~ Ar''-transformation, while the dots represent all the remaining data. The general dependence established by us, expressed by one straight line, determines fairly reliably the connection between hardness of ~~XXX~~ pearlite (sorbite, troostite) and value of specific surface of cement phase (Bibl.246). The following formula corresponds to the straight line in Fig.151:

$$H_B = 125 + 0,02 \sum S_c \text{ mm}^2/\text{mm}^3 \quad (45.3)$$

On the basis of his own test data (Bibl.238), A.E.Ger later obtained a similar dependence with almost identical values of coefficients (122 and 0.023 respectively*). * In the published text of report (Bibl.238), there is included a misprint which cannot be doubted: 0.0023 instead of 0.023, which is confirmed by ~~XXX~~ experimental data presented by the author of the report.

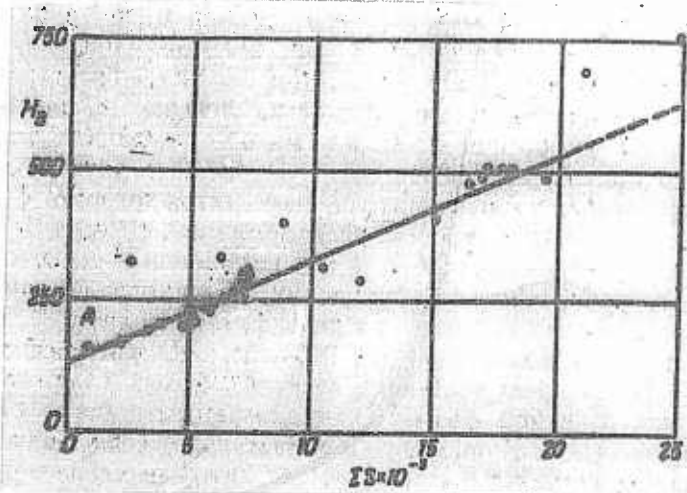


Fig.151 - Hardness of Ferrite-Carbide Mixture (Pearlite)
as Function of the Value of Specific Interface of Phases.
Composite data

As was shown by Bokshteyn (Bibl.125), Ger (Bibl.238) and others, the dependence between hardness and specific surface of carbides of granular form has the same type as eq.(45.3), with a higher value for the hardening coefficient.

In all of the studies relating to pearlite, including ours, only the specific interface of the phases "carbide-ferrite" was taken into account. Moreover, strictly speaking there should also be considered the effect of surface of pearlite grains, which can prove considerable, especially in dispersed structures of the "acicular ~~needlelike~~ troostite" type.

Worthy of attention is the significant difference in values of the strengthening coefficient ϵ for structure ~~micro~~pearlite and for polyhedral structure. For instance,

for pure iron, the strengthening coefficient equals 0.143, while for ~~short~~^{thin} lamellar pearlite, it is 0.02 in all. As it is said, this difference is caused by the construction of the boundary surfaces. The continuous spatial ~~XXXX~~ network of boundary surfaces of crystallites, typical for polyhedral structure, forms a strong framework, making ~~XX~~ quite difficult the plastic deformation in the closed (within the cells of the network) volumes of crystallites. The boundary interfaces of phases in ~~short~~^{thin} lamellar pearlite, representing mutually parallel planes, obstruct the plastic deformation to a lesser extent. Also the boundary surfaces of granular cementite, ⁱⁿ which ferrite flows around during the plastic deformation process, obstruct but little the flow of soft component (α -ferrite). It is also possible that in ~~XXXX~~ the polycrystal aggregate, the boundary zones enriched by adsorbed impurities are stronger themselves than the boundary zones of separation of phases in the pearlite.

The curves shown in ~~XXXX~~ Figs. 147 - 151 can also be regarded from the viewpoint of the effect of "second phase" (or, generally speaking, "of boundary phase"), as diagrams of the type composition-property, according to N.S.Kurnakov. Actually, if we admit that the thickness of ^{the} boundary zone either does not depend, or depends but slightly, upon sizes of microparticles, the relative volume of ^{the} boundary zone will be proportional to the value of the corresponding specific surface. Therefore the rectilinear nature of dependence does not change, if we replace the specific

surface of grains by relative volume of boundary zone between them. As we have already mentioned, the thickness of boundary zones in technical iron, according to the determination of Gardin, equals 0.25 micron. Hence the relative volume of the boundary zone will equal

$$\Sigma V_b = 0.00025 \Sigma S \text{ mm}^3/\text{mm}^2.$$

Using this relationship and the dependence of hardness of iron upon ^{the} value of specific surface, which is given by the curve in Fig. 150, we get a relationship between hardness and relative volume of ^{the} boundary zone of technical iron:

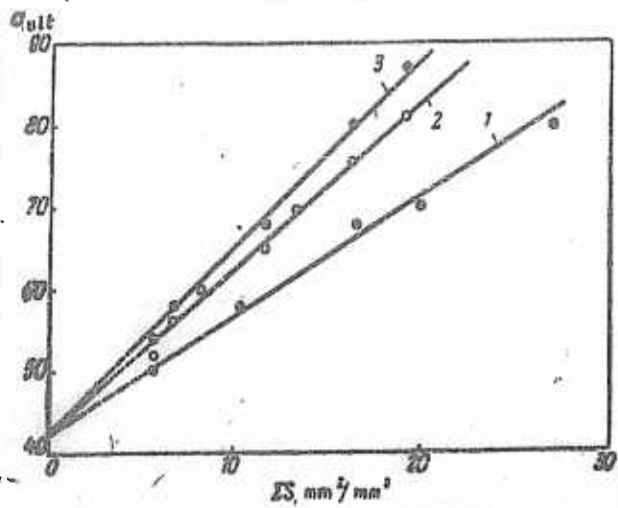
$$H_B = 85 + 572 \Sigma V_b \text{ kg/mm}^2.$$

The extrapolation of the last equation to the value ΣV_p , equaling 1, permits us to compute in first approximation the hardness of metal in the boundary zone, which proves to equal $657 H_B$. This calculation is not rigorous, since the properties of ^{the} boundary zone and the grains included in its cells are not additive. Nevertheless, the data derived confirmed the fact of considerable hardness in metal in the boundary zones, noted by a succession of studies.

Static Maximum Strength

As is known, between the hardness being measured by the Brinell method and the ⁱⁿ yield strength limit ~~under~~ there exist a direct proportionality, characterized by a high value for the correlation coefficient. Therefore we can consider that the dependence of the ~~strength limit under tension~~ upon ^{the} value of specific surface is

expressed by ^{an} ~~the~~ equation similar to dependence (45.1).



Tear (ultimate strength)

Fig.152 - ~~Strength~~ Resistance of ~~Magnetic~~ Iron Alloyed with Nickel
as ^a Function of ^{the} Value of Specific Surface of Grains:

1 - 0.9% Ni; 2 - 1.9% Ni; 3 - 3.97% Ni. Based on test data of
M.M.Shteynberg (Bibl.249), converted by author

The existence of a dependence of such a type for ~~the resistance~~ ^{the ultimate strength} is confirmed

by a number of test data. In Fig.152, we present data of M.M.Shteynberg (Bibl.249),
cited
converted by us, and ~~published~~ in (Bibl.118), obtained for ferrite alloyed with nickel.

The straight lines defining the dependence of ~~the~~ ^{the} resistance ^{to rupture} upon the value of
specific surface, corresponds to the equation:

$$\sigma_{ult} = 42 + \epsilon \Sigma S \text{ kg/mm}^2,$$

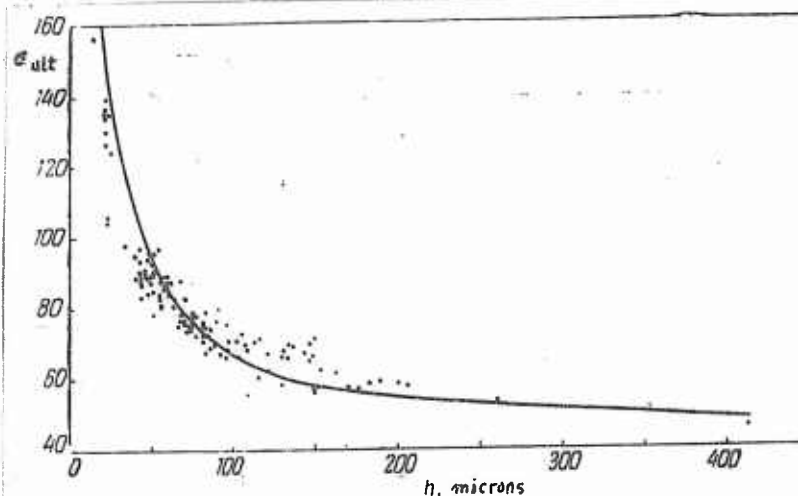
the

in which the coefficient of strengthening ϵ depends upon/degree of alloying:

| % Nickel | σ |
|----------|----------|
| 0,90 | 1,48 |
| 1,90 | 2,05 |
| 3,97 | 2,35 |

the ultimate

Ya.M.Potak, V.V.Sachkov and Ye.Bushmanov studied the effect upon shear strength a ferrite grains, resistance of linear value of ~~grain size~~ of ferrite, alloyed with a whole series of elements (Ni, Cr, Mn, W, Co, Cu, Si and others) (Bibl.250, 251). The test data obtained by us, including specimens alloyed with all of the investigated elements, are shown by dots in Fig.153. In estimating the value of grain, there was computed the



Ultimate Strength
Fig.153 - Shear Resistance of Ferrite Alloyed with Various Elements as a Function of Linear Dimension of Grain.

Points are based on test data of Potak, V.V.Sachkov and Ye.Bushmanova (Bibl.250, 251). The curve corresponds to the formula presented in the text

number of grains, ~~number of grains~~ intersected by a straight line of fixed length,

and we computed the ~~average~~^{grain} average linear dimension ~~of grain~~ in microns, which denote we signify by h . It is easy to note that the value for h , expressed in mm, in a single-phase polyhedral structure is identical to the reciprocal of ~~average~~^{the mean} number of intersections mm^{-1} , which in its turn equals half of the specific surface. The plotted curve ~~drawn~~ by us in Fig. 153 corresponds to the expression:

$$\sigma_{ult} = 42 + \frac{2600}{h} = 42 + 1.3 \Sigma S \text{ kg/mm}^2.$$

As we see, the last dependence is very close to the one computed by us based on ~~M.M.Shteynberg's~~ M.M.Shteynberg's data, which was presented above.

the degree of Relatively many studies are devoted to establishing the effect of ~~dispersed~~
dispersion of ~~state of~~^{creep} ferrite-carbide mixture upon the limit of steel. Unfortunately, each ~~researcher~~ of the authors approaches in his own way the estimation of ~~dispersion~~, which ~~which~~ deprives us of the opportunity of comparing the results of the various studies.

the N.N.Lyullicheva determined directly the value of specific surface of carbide phase of hardened and annealed steel (Bibl.84). The ~~dependence~~ dependence obtained by her of the creep limit upon value of specific ~~KN~~ surface of carbides is expressed by the equality:

$$\sigma_t = 15.5 + 0.016 \Sigma S \text{ kg/mm}^2,$$

characterized which is ~~expressed~~ by a correlation coefficient equaling 0.91.

the degree of ~~dispersed~~
~~M.Gensamer and others~~ opposed the conduct of an evaluation of ~~dispersed~~

dispersion a
 BRAKING SECANTS of ferrite-carbide mixture by the value of ~~average rectilinear distance~~
 the
 based on/main phase - ferrite (Bibl.252). Having denoted this parameter by h_f ,
 let us consider what it represents from the viewpoint of ~~XXXXXX~~ spatial structure
 and its natural parameters. A straight line drawn through a ferrite-carbide mixture
 passes mainly through the ferrite component, but at the same time also will intersect
 a number of cementite microparticles (~~if~~ grains or ~~phases~~). If the length of straight
 line equals 1, then in conformity with the proposition of Cavalieri-Aker, the
 part of this length allotted to the ferrite component equals ΣV_f . If the number of
 carbide microparticles intersecting a 1 mm length, proves to equal z , the ~~average~~
 mean
 rectilinear
 direct path through ferrite ~~XXX~~ will then equal:

$$h_f = \frac{\Sigma V_f}{z} \text{ mm.}$$

If we double the number z , we then get the ~~average~~ mean number of intersections of
~~XXXXX~~ secants by ^a straight line with surfaces of microparticles of carbide phase,
 i.e. the number $m \text{ mm}^{-1}$, which in its turn equals half the value of specific surface
 of microparticles ΣS_k . Therefore the latter equation can feasibly be ~~MX~~ rewritten
 as follows:

$$h_f = \frac{4 \Sigma V_f}{\Sigma S_k} = \frac{4(1 - \Sigma V_k)}{\Sigma S_k}.$$

The relationship derived indicates that the parameter h_f depends both upon
 the
 content of ferrite (or carbide) phase as well as upon/specific surface of carbides.

However, since the relative volume of ferrite phase in steel in practice will vary within relatively narrow limits, namely from 0.85 to 1.00 (at carbon content ranging from 0 to 1%), the parameter h_f almost unequivocally is determined by the value of specific surface of carbide. In Fig. 154, we show the dependence of the creep limit of steel upon logarithm of parameter h_f (measured in angstroms), obtained by M.Gensamer and others.

A similar dependence obtained on the basis of the test data of N.N.Lyulicheva,

~~XXXXXX~~

expressed in the equality:

$$a_t = 364.1 - 75.5 \lg h_f$$

has a correlation coefficient equaling 0.89.

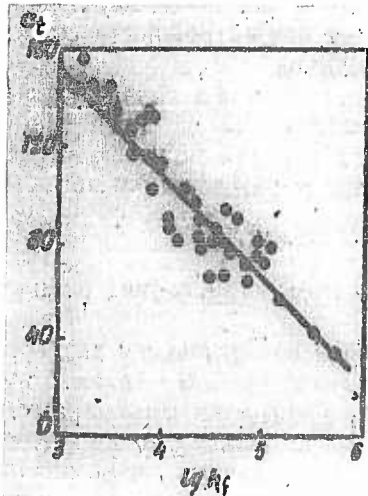


Fig. 154 - Yield Point of Ferrite-Carbide Mixture in Dependence on Mean Logarithm of Free Direct Path through Ferrite, Expressed in Angstroms [after M.Gensamer et al (Bibl.252)]

Investigating the dependence of yield point of steel upon structure, P.O.Pashkov considered that in a dispersed two-phase structure, there occurs a slowing down of plastic deformation of soft (basic)phase in its thin layer, directly adjoining the microparticles of solid (dispersed) phase (Bibl.253). In his time, S.T.Konobeyevskiy indicated that near the interface of two phases, the lattice of basic phase should be

significantly distorted and therefore in place of the actual size of small crystal of

the phase separation r ,
phase separation, one should consider a certain effective radius equaling:

$$r_1 = r + c$$

retarded

(Bibl. 254). Let us assume the width of the ~~layer~~^{layer} (in the plane of the microsection) as equal to c , the number of sections of carbide microparticles per 1 mm^2 of cut ~~is~~^{to} equal to n , and their mean diameter as equaling d . Then the part of area of cut occupied by ferrite is roughly determined, according to P.O.Pashkov, by the expression:

$$\Sigma F_f = 1 - n(d + c)^2. \quad (45.4)$$

while the yield point of steel will equal

$$\sigma_t = \frac{\sigma_s}{1 - n(d + c)^2} \text{ kg/mm}^2, \quad (45.5)$$

where σ_s is the yield point of soft phase, i.e. of ferrite.. Obviously, expression (45.4) determines not only the portion of the cut but also the portion of the

steel which can freely deformed plastically. In a somewhat modified form, the dependence (45.5) was studied by N.N.Lyulicheva for carbon steels containing

0.3% - 1.06% C, and alloyed steels type 45G2 and 60S2, in structures of granular type, obtained by hardening with subsequent annealing in the temperature range of

450 - 600°C. It turned out that the empirical formula:

$$\sigma_t = \frac{\sigma_s}{1 - \frac{\% \text{ Fe}_3\text{C}}{100} - c \Sigma P} \text{ kg/mm}^2 \quad (45.6)$$

is typified by a very high ~~correlation~~ correlation coefficient, equaling 0.97.

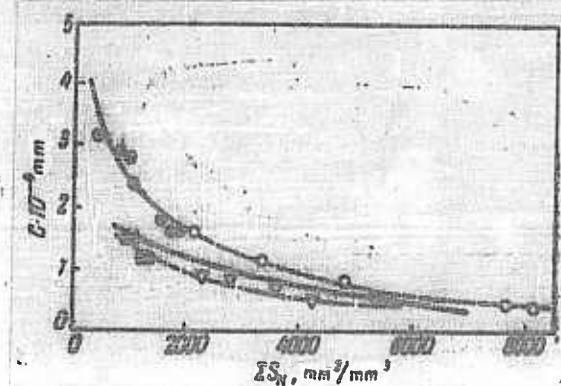


Fig.155 - Width of Retarded Layer in Ferrite-Carbon Mixture as Function
of Value of Specific Surface of Carbides [after N.N.Lyulicheva (Bibl.84)]
—○— O-60S2; —■— 45G2; — carbon steel

The deviation of actual result from the computed one does not exceed 1.3 kg/mm^2
(relative error 3.1%) for structures studied with the aid of an optical microscope.

For more dispersed structures being solved by electron microscope, the error amounted to 2.7 kg/mm^2 or 4.85%. In Fig.155, we indicate the dependence of ~~the~~ width of ~~the~~ retarded layer c upon ~~the~~ value of specific surface of carbide phase (Bibl.84). Replacing in eq.(45.6) the parameters of plane structure by the corresponding parameters of spatial structure, we get the formula:

$$\sigma_t = \frac{\sigma_0}{1 - \Sigma V_k - c_0 \Sigma S_k} \text{ Kg/mm}^3, \quad (45.7)$$

$$c_0 = \pi/4c$$

in which the coefficient ~~XXX~~. The physical nature of this coefficient possibly corresponds to the concept of it as ~~representing~~ the thickness of ~~the~~ retarded or boundary layer, which however is not mandatory. It suffices to assume that this coefficient reflects the degree of obstruction of deformation on the part.

of interfaces of phases, being characterized by differing curvature.

In the case of ~~sheet~~ structures, as was shown by N.N.Lyulicheva, there

occurs a ~~XXXX~~ rectilinear dependence of ^{the} yield point upon ^{the} value of specific surface of carbide phase.

L.S.Moroz proposed an empirical formula connecting the yield point with the conventional parameter, called the "volume of ferrite". By this parameter is meant the elementary ~~XX~~ volume of ferrite in which mechanical obstructions to plastic displacements are lacking (Bibl.128). As Moroz indicated, the yield point is defined ~~XXXXXXX~~ clearly by the value of "volume of ferrite", wherein the dependence between these values for granular structures is typified by a high correlation coefficient, i.e. 0.97 (for steels containing 0.25% - 1.03% C). However, one should consider that in the calculations of "volume of ferrite", ~~XX~~ Moroz proceeded from the assumption of the equal size of carbide microparticles, which lowers the reliability of the result obtained.

The introduction of "volume of ferrite" into natural parameters of spatial structure indicates that it is connected by a complex exponential dependence with ~~the~~ relative volume of carbide phase and with its specific surface.

Considering all of the data presented above, referring to the dependence of ~~the~~ yield point of steel upon ~~dispersed state~~ ^{the degree of dispersion} of ferrite-carbide mixture, we can state that in all cases the yield point is connected with two natural parameters of

spatial structure, namely with the relative volume and with ^{the} specific surface of carbide phase. However, a reliable dependence between these parameters and the yield point has not yet been established. In our opinion, this is explained by the experimental difficulties involved in measuring the specific surface of dispersed phases of ~~granular~~ granular type, especially when working with an electron microscope, as was discussed above. These difficulties are caused by the presence of inevitable microrelief of ^{the} microsection, the effect of which is all the greater, the more the structure is dispersed. In ~~structured~~ structures, the microrelief hardly ~~MX~~ affects the accuracy of measurement of specific surface, and in this case, there is established a reliable ~~straight-line~~ ^{rectilinear} dependence of yield point upon value of specific surface of carbide phase (at constant content of C in the steel). It is very probable that the same type of dependence can be established also for granular structures upon elimination of ^{the} effect of microrelief upon results of measuring the specific surface.

Plastic Properties. Creep

The mechanism of plastic deformation of intracrystallite and boundary zones is accomplished in quite different ways. While within the crystallite, the deformation occurs by way of displacement formation, in the boundary zones this type of deformation is not realizable in view of the absence in them of any crystallographic planes or directions. Therefore the sole possible type of deformation for boundary zones is viscous flow, typical for amorphous bodies. In a polycrystal, both types of

deformation are closely interconnected, namely the displacement deformation cannot occur without ~~the~~ corresponding viscous flow of metal in the boundary zones, and vice versa.

As is known, the high plasticity of a ~~single~~ crystal is abruptly limited upon ~~the~~ appearance of boundary surfaces. Qualitatively, this is clearly illustrated by the pattern of deformation of samples consisting of a few crystallites (~~of~~ two or three). Upon expansion of such samples in the zone of boundary surfaces, deformation hardly occurs and it acquires a unique angular (jointed) form. On the other hand it is known that finely grained metals are more viscous than coarsely grained ones and hence the boundary zones promote the increase in viscosity of ~~the~~ metal.

In Fig.156, we show the effect of specific surfaces of grains upon ^{the} impact strength of eutectoid steel, processed to a hardness of $50 R_C$, manifested by test data of E.Beyn, converted by us (Bibl.244). At static tests, the effect of ^{the} value of specific surface is noted to be considerably weaker than during dynamic tests, but is also positive. The studies conducted by A.D.Danielyan (in the metallurgical ~~INSTITUTE~~ laboratory of the Yerevan Polytechnic Institute ~~IMI~~ imeni ~~KARAGAM~~ K.Marx) on technical iron and type 45 steel, indicate that the dependence of viscosity (reduction in area) ^{on} ~~the~~ value of specific surface has the appearance shown in Fig.157. In examination of dependences of a similar type, one should take into account the circumstance that a polycrystal sample has zones ~~but~~ characterized by

a varying degree of free displacement deformation. The relative ~~volume~~ volumes of these zones at the assigned value of specific surface (or at value of crystallites) depend upon ~~the size of the sample, and at the assigned size of the sample, they depend upon the~~ the value of specific surface. This is shown schematically in Fig. 158, in which are shown the cross sections of two samples differing in value of crystallites. In unshaded internal ~~zone~~ zone, each of the crystallites is completely surrounded by others, the displacement deformation in it is fully blocked and cannot be accomplished without the appropriate viscous flow of metal of boundary zones and displacement deformation in the surrounding crystallites. In the outer shaded zone, the displacements are blocked only on one side and the displacement can occur much more freely. The relative volume of zone of free deformation is ~~all the greater,~~ the less the specific surface (at ^a given size of sample). In finely grained metal, the role of the zone of free deformation is slight, since it becomes decisive at grain sizes which are comparable with sizes of the sample. Hence the increase in specific surface, decreasing the relative volume of zone of free deformation, promotes the decrease in indexes of plasticity of the sample as a whole.

At the same time, it is necessary to consider that displacive deformation of crystallites of the internal zone of a sample, occurring under conditions of blocking on all sides, is limited by viscous flow of the boundary metal. The greater the extent of boundary surfaces, occurring per unit ~~of~~ area of possible planes of displacement (i.e. in a unit ~~of~~ volume of metal), the more intense there can

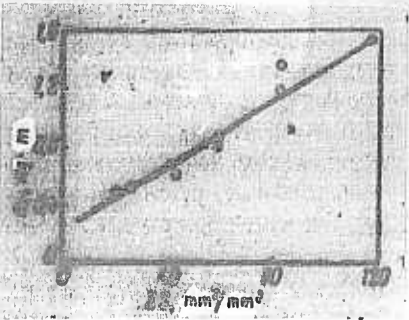


Fig.156 - Impact Strength of Eutectoid Steel Processed to a Hardness of 50 R_C, as a Function of ^{the} Value of Specific Surface of Grains. Based on test data of E.Beyn (Bibl.244), converted by author

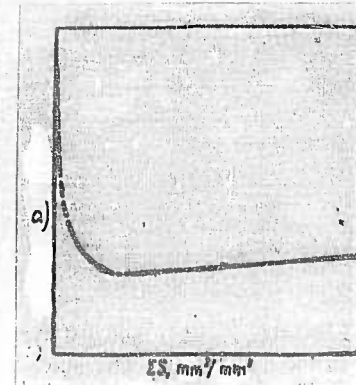


Fig.157 - ~~Narrowing of section~~ during Shearing as Function of ^{the} Value of Specific Surface of Grain (Diagram)
a) ~~Narrowing of section~~ reduction in area

(shearing strain)
proceed the displacive deformation at correspondingly higher stresses and, ^{the} in final analysis, the higher the indexes of plasticity of the metal.

It follows from what has been said that ^{the} specific surface plays a dual role.

Its increase decreases the possibility of plastic deformation in ^{the} outer layers of a sample, lowering ^{the} relative volume of zone of free deformation, and at the same time increases the chance of plastic deformation of the ~~HIGH~~ internal zone.

This also explains the type of dependence of ~~HIGH~~ viscosity upon ^{the} value of specific surface expressed by a curve with a minimum (Fig.157). The position of the point of minimum is defined by the relationship between diameter of sample and average linear size of crystallites.

In structures containing more than one phase, the effect of specific surface is complicated by a simultaneous and apparently more powerful influence of other structural factors, specifically by the structural composition of the alloy and by the "architecture" of boundary zones. For instance, N.N.Lyulicheva found that in steel, the carbon content affects the value of narrowing to a greater extent than changes in the annealing conditions, accordingly changing the value of specific surface of carbides (Bibl.84). L.S.Moroz established that a satisfactory correlation

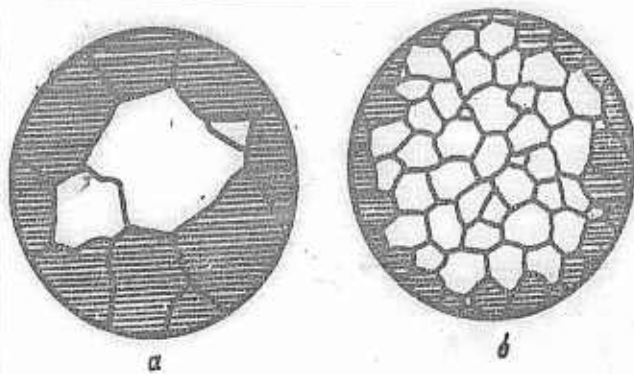


Fig.158 - Zones of Relatively Free Displacive Deformation in Coarsely Grained (a) and Finely Grained (b) Samples

exists between the concentrated contraction and ^{the} parameter P , constituting a function of total surface of carbides ΣS_k and their diameter D . With an increase of this parameter, the concentrated contraction decreases according to ~~the law of~~ ^{a rectilinear law} (Bibl.255). Since L.S.Moroz assumes that microparticles of carbides are of equal size, the parameter proposed by him can be transformed as follows:

$$P = D^{1/2} \sum S_k = D^{1/2} \pi D^3 N = \pi D^{1/2} N$$

(N equals number of carbide microparticles per unit volume). It is ~~very~~ easy to see that the last expression is practically proportional to the total volume of carbides per unit volume of steel and hence the value of concentrated contraction is basically determined by the composition of the alloy.

From the viewpoint of "architecture" of boundary surfaces, of decisive importance is the presence of ^a_A continuous spatial network of surface or of enclosed contours isolated from each other.

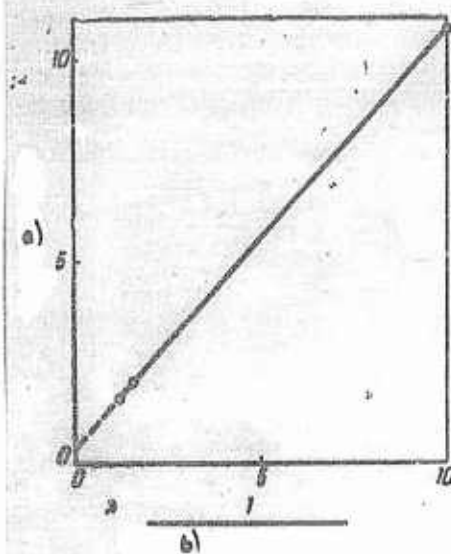


Fig.159 - Dependence of ^a_A Rate of Deformation of Lead under ^a_A Load of 0.35 kg/mm^2 upon ^a_A Value, Proportional to ^a_A Value of Specific Surface of Grains [M.Yu.Bal'shin(Bibl.256)]
a) % per day, 10^4 ; b) Diameter of grain, mm

The process of viscous flow of metal of ^{the}_A boundary zones is a diffusion process; therefore, with an increase in temperature, the intensity of deformation increases and it is accomplished at lesser forces, and the role of boundary zones and ~~XXXX~~ of value of specific surface substantially increases. As M.Yu.Bal'shin indicated, the rate of deformation during creep is linearly connected with ^{the}_A value of specific surface of crystallites. In

Fig.159, we show the dependence of ^{the} rate of deformation of lead at ^a load of 0.35 kg/mm^2

upon the value, reciprocal to the diameter of grains, which is proportional to the value of specific surface. This dependence was found by Bal'shin, who used the test data of Mak-Kiona (Bibl.256). An analysis of a series of data of other authors, relating to tests of steel at increased temperatures, indicates that the dependence established by Bal'shin is typical.

The role of the lines of juncture of three grains in the process of disruption during creep was noted by K.Ziner, who indicated that in this place, the relaxation of stresses is made more difficult, which should lead to their concentration in ~~XXX~~
an ever smaller area, and finally, ^{the} formation of a gradual crack in the junction zone of the three grains (Bibl.192). According to data of I.A.Oding, obtained ~~XXX~~
for type EYALT steel after 1000 hrs of test for creep at 625° and stress of 14 kg/mm^2 ,
the beginning of formation of microcracks is as a rule ~~XXX~~ actually localized
at the junctures of three grains (Bibl.257). Unfortunately, quantitative data on
this problem are lacking.

B. Physical and Physico-Chemical Properties

Density

It was already noted above that the formation of any boundary zones in metal is accompanied by a decrease in its density, since the actual metal of ^{the} boundary zones is less ~~XXX~~ dense than in the regular crystal lattice. This proposition is quite natural, although the fact of ^a decrease in ^{the} metal density during plastic

deformation by compression until now has sometimes caused surprise [see, e.g. (Bibl.150)].

The density of copper calculated theoretically according to ~~parameters~~
~~parameters~~
crystal lattice equals ~~is~~ 8.988 gm/cm^3 . According to data of K.Mayer, ^{the} density of actual copper samples equals (gm/cm^3):

| | |
|--------------------------|---------|
| Single crystal | 8.95235 |
| Polycrystal | 8.94153 |

According to these data it follows that a ~~single~~ crystal has around 0.40% of nominal vacancies, whereas in a polycrystal, this value equals 0.52%. If we assume the density of crystallites as equal to density of a ~~single~~ crystal of copper, it turns out that the fraction of boundary zones contains 0.12% of nominal ~~vacancies~~ vacancies, whereas the actual boundary zones in the metal occupy a relatively trivial space. Let us denote ΣV_b the relative volume of boundary zones of polycrystal by ΣV_b , and the density of metal of these zones by γ_b . Then, using the rule ~~of mixing~~ and adopting the data of K.Mayer, we can write:

$$8.95235(1 - \Sigma V_b) + \gamma_b \Sigma V_b = 8.94153 \text{ g/cm}^3,$$

whence we find the density of metal in the boundary zone

$$\gamma_b = 8.95235 - \frac{0.01092}{\Sigma V_b} \text{ g/cm}^3.$$

If the boundary zones occupy 1% of volume of polycrystal of copper, i.e. if $\Sigma V_b = 0.01$, we get a density of boundary metal equaling 7.87 gm/cm^3 , whereas the density of liquid copper at 1083° equals 8.3 gm/cm^3 . Thence it follows that the actual volume of boundary zones is evidently much greater than 1%. The adduced example shows that measurement of metal density in comparison with the parameters of its spatial structure can prove very promising for studying the extent, structure, and properties of boundary zones.

Based on data of P.Gerens, the density of technical iron containing 0.07% C, increases with an increase in annealing temperature (i.e. with decrease in specific surface) from 7.804 to 7.824 gm/cm^3 (Bibl.258). We presented earlier the data of M.G.Oknov concerning the change in density of steel during cold plastic deformation and during subsequent annealing (see Section 17). All these changes are characterized by rather large values, exceeding greatly the accuracy of determination of metal density by the method of hydrostatic suspension, which as Livshits notes, is quite suitable for research purposes in metallurgy, but, we can add, for reasons which are not understood, is scarcely used at present.

Heat Conductivity, Electric Conductivity, Magnetic Permeability

Boundary zones in metals act as barriers for heat and electrical currents, the mean free path of limiting the length of ~~free~~/electron and also obstructing the propagation of a magnetization wave. Therefore the heat transfer coefficient, electric

~~conductivity~~

The conductivity and magnetic permeability decrease with an increase M_{K} in the specific surface of crystallites.

Eucken and Dittrich determined the heat ~~conductivity~~ ^{transfer} coefficient in samples of very pure electrolytic iron, ~~with~~ distinguished by differing values M_{K} of grain. Data obtained by him (at 0°) are presented below (Bibl.259):

| Number of Grains per 1 cm | λ cal/cm. sec. deg. deg |
|------------------------------|--|
| 10 | 0.2254 |
| 130 | 0.2149 |
| 634 | 0.1967 |

These data correspond to a ^{variation} ~~change~~ in specific surface approximately from 2 to $125 \text{ mm}^2/\text{mm}^3$, which is accompanied by a decrease in heat ^{the} ~~transfer~~ coefficient by 12 - 13%.

G.Sitsco studied the maximum magnetic permeability of ~~samples~~ samples of pure iron having a varying grain size, obtained by way of annealing in vacuum. Data obtained by him are presented in Table 67, wherein the linear sizes of grains, presented by G.Sitsco, are converted by us to approximate values of specific surface.

The test data of V.S.Mes'kin and E.I.Pel'ts (Bibl.260) provide the possibility of establishing that the ~~samples~~ coercive force is linked by a linear dependence

with the value, reciprocal to the value of specific surface of crystallites of pure iron, which is shown by the curve adduced in Fig.160.

Rate of Diffusion in Metal and Other Properties

There was noted long ago the essential difference in rate of diffusion occurring in ~~the~~ volume of crystallites or of ~~single~~ crystals and along the boundaries of crystallites. The obtainment of reliable quantitative data is made difficult by the complexity of a separate determination of ~~the~~ coefficient of volumetric and boundary diffusion, especially since in ~~XXXX~~ the actual process of diffusion, progressing at increased temperatures, there occurs a change in value of ^{the} specific surface of grains of polycrystal. This leads to the condition that various researchers sometimes reach directly opposite conclusions concerning the rate of diffusion in ~~single~~ and polycrystals.

As Lengmyur, Fond and others have shown, the rate of diffusion of thorium in tungsten at 2400°K is about 100 times greater along the boundary of grains than in the grain. According to data of ~~XXXX~~ Edmunds, diffusion of copper in a ~~single~~ crystal of zinc does not ~~not~~ occur, while in polycrystalline zinc, the process transpires rapidly. During the annealing of Alclad and of bimetal, there occurs a diffusion of copper along the ^{grain} boundaries ~~boundaries~~ of pure aluminum and γ-iron respectively (Bibl.261).

Table 67

| a) | b) | c) |
|-----|-------|------|
| 11 | 0.19 | 8050 |
| 7 | 0.29 | 7680 |
| 6.3 | 0.33 | 8200 |
| 2.7 | 0.76 | 8050 |
| 1.2 | 1.71 | 7300 |
| 0.7 | 2.93 | 7550 |
| 0.6 | 3.42 | 6970 |
| 0.3 | 6.84 | 6850 |
| 0.1 | 20.50 | 4090 |

Specific
a) Grain size, mm; b) ~~specific~~ surface
(conversion) mm^2/mm^3 ; c) Magnetic
permeability, μ_{\max}

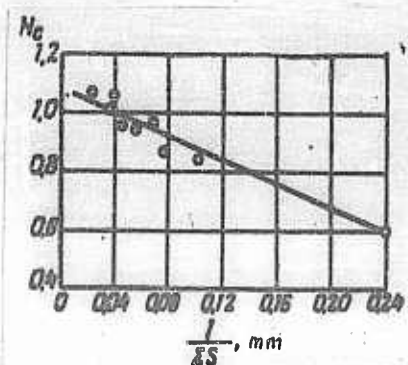


Fig. 160 - Coercive Force as a function of the value of Specific Surface of Grains. Based on test data of Mes'kin and Pelt's (Bibl. 260), converted by the author

Based on data of V. Bugakov and F. Rybalko, the coefficient of diffusion of zinc at 700° in polycrystalline brass, with an average grain size of 0.13 mm, is almost 40 times larger than in ~~the~~ a ^{single} crystal. In Fig. 161, we show the dependence of ^{the} coefficient of diffusion of zinc in copper at 700° and 800°C upon ~~the~~ value of specific surface of grains of single-phase brass (30% Zn). The curve is drawn according to test data of Bugakov, wherein the grain sizes ~~were~~ presented by him (in mm) are converted by us to values of specific surface (Bibl. 262).

P. L. Gruzin, B. M. Noskov, and V. I. Shirokov used the radioactive isotope of iron (Fe^{59}) in the study of the effect of manganese upon ~~the~~ self-diffusion of iron.

The authors note in the curve of dependence $\log D - 10^4/T$ a break at 1150°C , the existence of which provides a basis for assuming that below this temperature there occurs mainly a diffusion along the boundaries of crystallites, while at higher temperatures, this occurs within the crystallites (Bibl.263). During the self-diffusion of silver, the coefficients of boundary and volumetric diffusion at temperatures of 480 and 950° differ respectively by 10^6 and 10^3 times (Bibl.264).

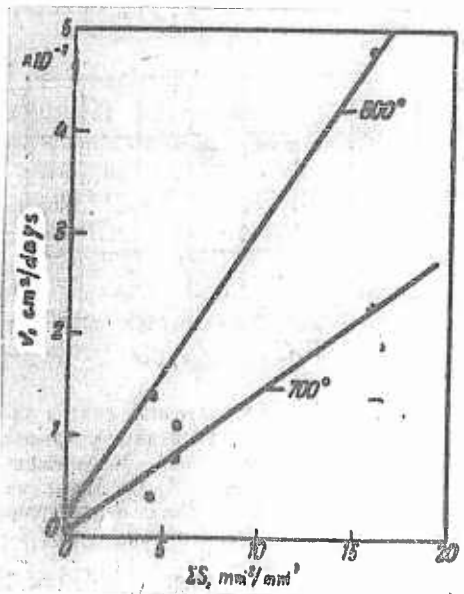


Fig.161 - Dependence of Coefficient of Diffusion of Zinc in Copper at 700 and 800° upon Value of Specific Surface of Grains of Single-Phase Brass
[V.F.Bugakov (Bibl.262)]

The data presented, as well as many other data, indicate that the coefficient of diffusion increases with an increase in specific ~~MMK~~ surface of crystallites, especially at low temperatures of diffusion or self-diffusion. Along with this, there are also those relatively scant data, according to which the effect of value of grain upon ~~the~~ rate of diffusion is not revealed. In certain cases, a reverse dependence is even established. For instance, according to data of I.Ye.Kontorovich, at diffusion

of carbon and titanium in steel, the enlargement of grain leads to an increase in the diffusion rate.

The role of boundaries of ~~grain~~ or of boundary zones in the process of diffusion is in the initial stage of study. To obtain reliable data, above all there should be developed a standardized method of determining the diffusion constants, KK reflecting the irregularity of diffusion in ~~micro volumes~~ and micro volumes of metal. As was indicated quite properly by A.S.Zav'yalov, the rate of diffusion of carbon, for instance during phase transformation, at distances of the order of hundredths of a millimeter is ~~many~~ many hundreds and even thousands of times greater than the rate of diffusion at greater distances, which occurs in such processes as cementation (Bibl.265). The estimation of erroneous rate of diffusion based on "enlarged" or "averaged" data can lead to ~~wrong conclusions~~ conclusions.

In particular, it is necessary to note the following: qualitatively, the pattern of kinetics of dissolving of carbon in iron with the formation of austenite, occurring during the heating of ferritic-graphite structures, does not leave any doubt that the rate of diffusion of carbon along the ~~grain~~ boundaries ~~of~~ ^{grain} is much higher than within ~~them~~. During the heating of malleable or gray iron, having a ferrite base, it is as if the carbon flows along the ~~grain~~ boundaries ^{grain}.

forming during subsequent cooling a unique structure of pearlitic (sorbite, troostite) network around the grains of ferrite, as if constituting a negative structure of hypoeutectoid steel. It can be noted that the principal diffusion of carbon along the ^{grain} boundaries of ~~grains~~ in ferritic malleable irons permitted one to develop a special industrial process, namely the strengthening of iron proposed by the method of normalization, ~~suggested~~ by B.A.Savatyugin (Bibl.213) and being widely used at present. Normalized malleable iron has a strong sorbite framework along the boundaries of ferritic grains and differs in comparison with usual ferritic malleable iron in the high strength combined with good viscosity.

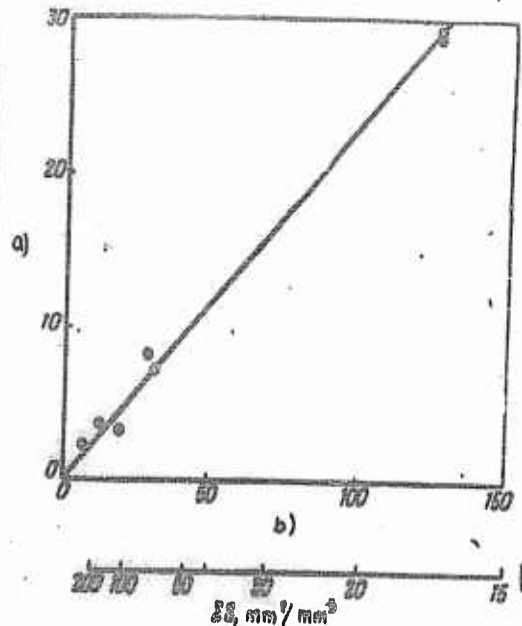
A quite similar pattern of penetration of nickel into iron was observed by V.I.Arkharov (Bibl.46).

Just as nickel, carbon is a ~~nonmetallic~~ ^{horophilic} element in relation to iron, as is indicated by the earlier presented data of ~~XXX~~ et al, indicating that of 0.026% C, occurring in soft steel, 0.015% was localized in the boundary zones, in which the ~~XX~~ concentration of carbon reached the marginal 1.7% (Bibl.211). As A.Tsou V.I.Arkharov indicates, the presence of ~~a~~ small quantities of ~~XXX~~ ^{a horophilic} admixture can have quite a substantial effect upon the ~~X~~ relationship of rates of volumetric and boundary diffusion of a third element.

Of great practical interest is the process of intercrystalline corrosion, leading to the occurrence of a seasonal cracking of brass. Measurement of the

micropotentials of grains and of the sectors adjoining their boundaries showed
that boundary zones are anodic in relation to the remaining sectors of the
alloy (in ~~aqueous~~^{agitated} solutions of ammonia). Considering that the ~~area~~ area of anode
sectors on the surface or in a section of bronze ~~XXX~~ is many times less than the
area of the cathode, it is natural to suppose that electrochemical corrosion should
lead above all to ~~the~~^{the} destruction of the metal of boundary zones, which occurs in
reality. The tensile forces, revealing the disrupted sectors, promote the
penetration of corrosion to the interior (Bibl.266).

From what has been said it follows that the increase of specific intercrystallite
surface should reflect favorably on relationship of areas of anode and cathode
sectors of brass, and finely grained brass should be less subject to
intercrystallite corrosion and cracking than coarsely grained ~~XX~~ brass. This
proposition is well confirmed by data of practice and by test data of
A.V.Bobylev (Bibl.266), through the use of which we constructed the curve in
Fig.162. The data presented relate to brass, rolled with a reduction of 10%
(circles in Fig.162) and 54% (dots). The different size of grain was achieved by
annealing at various ~~XXX~~ temperatures, therefore the residual stresses and cold
hardening should also have some effect upon the results. Nevertheless, the role
of boundary zones is exposed quite distinctly.



Cracking

Fig.162 - XX Dependence of Tendency of Brass toward XX
upon Grain Size and Specific Surface of Grains. Based on
test data of A.V.Bobylev (Bibl.266)

a) Tendency towards cracking K, min^{-1} ; b) Size of grain, microns

Section 46. Structural Composition and Mechanical Properties of Alloy

The first formulas serving for computing the strength limit ~~and~~ shear
structural
and ~~maximum~~ specific elongation based on data of quantitative ~~micrography~~ analysis,
were proposed, to the best of our knowledge, by R.Grieves and G.Righton (for
hypoeutectoid steel) (Bibl.269). In these formulas, presented below, there enter
the relative areas occupied in a cut by ferrite and pearlite, and the corresponding
coefficients taking into account the properties of the actual components:

$\sigma_b = \alpha_1 \sum F_f + \beta_1 \sum F_p \text{ kg/mm}^2$, (46.1) $\delta = \alpha_2 \sum F_f + \beta_2 \sum F_p \%$. (46.2)

4.27

The coefficients α_1 and β_1 in eqs. (46.1) and (46.2) depend upon the ~~degree of dispersion~~

~~size~~ of pearlite. The values of these coefficients given by Grieves and

Righton are presented in Table 68.

Table 68

| a) | b) | | | |
|------------------------|------------|-----------|------------|-----------|
| | α_1 | β_1 | α_2 | β_2 |
| Ferrite | 34,05 | — | 40 | — |
| Pearlite: | | | | |
| Sorbite-like | — | 110,2 | — | 10 |
| Normal | — | 86,6 | — | 15 |
| Lamellar .. | — | 55,1 | — | 5 |

a) Structural components; b) Coefficients of eqs. (46.1) and (46.2)

These formulas were checked by us for a large amount of test material and showed good agreement under condition of a certain correction of coefficients for ferrite and a more fine differentiation of coefficients of pearlite of varying degree of dispersion. Unfortunately, these ~~data~~ were lost during the years of the Patriotic War (World War II).

Basing ~~XXXX~~ on investigations of Martin and Bessemer rail steel (Bibl. 270),

A.I.Skakov proposed a series of formulas permitting one to calculate all the basic indexes of XX mechanical properties according to data of quantitative

microanalysis. By methods of statistical processing of results of mechanical tests and of quantitative microanalyses, he established that of all the parameters of plane microstructure with mechanical properties, those most closely associated are the average size of actual grain of steel and quantity of pearlite in the structure. Weakly connected with the mechanical properties are the concentration of carbon in pearlite, the nonequiaxiality of grains and the inclusions. contamination of steel by nonmetallic impurities. Below we present certain of these equations obtained by Skakov for Martin steel:

Brinell hardness

$$H_B = 2,6 F_p + 111 C_p - 0,0096F - 28,3 \pm 5,25 \text{ kg/mm}^2.$$

at
Strength limit during elongation

$$\sigma_b = 0,81 F_p + 36,2 C_p - 0,0016F - 9,2 \pm 2,3 \text{ kg/mm}^2.$$

at
The yield point during elongation

$$\sigma_t = 0,435 F_p + 0,173 C_p - 0,00081F + 5,6 \pm 1,8 \text{ kg/mm}^2.$$

The Specific elongation

$$\delta_{10} = 46,2 - 0,264 F_p - 9,62 C_p - 0,000048F \pm 0,82\%.$$

In ~~XXXXX~~ addition to those presented, equations are derived for yield point, true shear resistance, specific ~~concentration~~, fatigue limit etc. Analogous equations, distinguished by values of coefficients, are also derived for Bessemer steel.

In all cases, three parameters enter the equations: a) the quantity of pearlite

XXX

component, expressed in percent of area of microsection, - F_p , b) average area of grain, expressed ~~XXXXXX~~ in μ^2 , F and c) weight content of carbon in pearlite, expressed in %, C_p . The latter value is determined as the ratio of weight content of carbon in steel, MKK multiplied by 100, to the content of pearlite component expressed in % of area of microsection. For instance, if in the structure there is contained 40% of pearlite at MKK weight content of carbon in steel equaling 0.28%, the carbon content in pearlite will then equal

$$C_p = \frac{0.28}{40} 100 = 0.70\%.$$

In Skakov's studies of rail steels, of which the ~~material of test~~ served *data* as a basis for derivation of formulas, the contents of pearlite component varied within limits from 30 to 100% of area of microsection, the size of grain of steel varied from 400 to 16,000 μ^2 , and *the* content of carbon in pearlite ranged from 0.45 to 0.90%. It is noteworthy that the method of quantitative microanalysis which was applied was developed by A.Skakov as early as 1930, as a result of which it could not be improved.

In the equations developed by Skakov, the average size of grain of steel is roughly connected with the value of specific interface of ferrite and pearlite components and hence reflects the strengthening influence of these surfaces. The effect of dispersed state of pearlite is correspondingly reflected by the value C_p .

i.e., by concentration of carbon in quasi-pearlite.

P.O.Pashkov, proceeding from the assumption that in alloys consisting of soft and hard phases, the microparticles of hard phase do not deform (in initial stage of plastic flow), derives the following equation for the yield point of steel:

$$\sigma_t = \frac{\sigma_f}{\Sigma F_f} \text{ Kg/mm}^2, \quad (46.3)$$

where σ_f is the yield point of ~~the~~ soft component (of ferrite);

ΣF_f is the part of area of cut or section of sample occupied by soft component (Bibl.253).

An ~~experimental~~ experimental checking of ~~eq.~~ eq.(46.3) in carbon steels, type 15, 25 and 45 and in alloyed steels developed in a structure of martensite-ferrite, shows a linear dependence of yield point upon the value $1/\Sigma F_f$, if the amount of ferrite is not less than one third the area of microsection or volume of steel. At lesser content of soft phase, the microparticles of hard phase begin to deform from the very beginning of plastic flow and therefore the dependence (46.3) loses its effectiveness. This dependence does not consider the strengthening effect of boundary surfaces, i.e. of the ~~dispersion~~ ^{local dispersion of the} structure.

A correction of eq.(46.3) of P.O.Pashkov, taking into account the effect not

only of ~~the~~ amount of soft phase, but also of ~~the~~ dispersed structural state, was conducted by Lyulicheva (Bibl. 84). A formula for calculating the yield point, proposed by her, was presented above (see Section 45). Along with this formula, she also developed the formulas presented below, intended also for computing other indexes of mechanical properties:

~~Yield point~~

$$\sigma_t = \frac{26,65}{b_0} - 3,86 \text{ kg/mm}^2, \quad (46.4)$$

~~Yield point elongation~~

$$\sigma_b = \frac{22,10}{b_0} + 24,3 \text{ kg/mm}^2. \quad (46.5)$$

~~True yield elongation~~

$$\sigma'_b = \frac{23,70}{b_0} + 30,1 \text{ kg/mm}^2. \quad (46.6)$$

The equations were checked by their author in the case of carbon and alloy steels, wherein the correlation coefficients proved to equal 0.97, 0.93 and 0.94, respectively. The value b_0 , entering all three equations, is determined by the equality:

$$b_0 = 1 - \frac{\% \text{Fe}_3\text{C}}{100} - c \Sigma P. \quad (46.7)$$

()
where $\% F_3S$ ~~is the~~ area of carbide phase, being determined by the point-counting

method of A.A.Glagolev;

ΣP ~~is the~~ specific extent of boundaries, being determined by ~~the~~ method of

random secants;

c ~~is the~~ thickness of retarded layer (see Fig.155).

The data presented in Sections 43 and 46 indicate that the connection between
reliably
the mechanical properties and structure of pure metals and alloys can be expressed
as dependences, characterized by
~~XXXXXX~~/high values of correlation coefficients.

However, ~~XXX~~ all of the dependences examined are ~~XXXXXX~~ intended for individual
special types of structures and are not valid for the entire range of possible values
Structur
of parameters ~~of structure~~ and indexes of mechanical properties.

Section 47. Plastic Deformation and Stereometric Structure

The boundary interfaces of crystallites or structural components of metals
and alloys, in ~~XXXXX~~ the structure of which there are not preserved perceptible
traces of transcrystallization or of plastic deformation, are isometric. Quantitatively,
they are characterized by a fixed value of specific surface. In the process of
plastic deformation, being accomplished at low temperatures, the boundary surfaces
acquire a fixed spatial ~~XXX~~ orientation. The absolute value of specific surface
can also change. In this case, the type and degree of orientation of boundary
surfaces is entirely determined by the type and degree of deformation. Therefore, a

quantitative characteristic of structure of boundary surfaces can serve as one
of the methods of studying the mechanism of plastic flow.

Ye.Geyn (Bibl.136) first proposed the method of quantitative evaluation of
oriented structures. According to his method, the structure is estimated as
the value of ratio of links of transverse and longitudinal axes of elongated
flat grains, being observed in a lengthwise microsection.

Let us imagine two samples of the same metal, of which one is deformed by
compression (swaging), and the other by stretching (drawing). The structure of
samples in the lengthwise cuts can turn out to be quite identical, i.e. can be
appraised as the same ratio ~~XXX~~ of lengths of lengthwise and transverse axes of
flat grains. ^(At) ~~XXX~~ the same time, it is obvious that the spatial
structure of samples is considerably different: in the sample deformed by swaging,
the grains have the shape of small blades, while in the sample which has been
stretched, they have the form of fibers. Thence it follows that an evaluation
according to ~~XXX~~ Geyn is not sufficient. The most complete description of
oriented systems of boundary surfaces is given by the spatial ~~XXX~~ "rose of number
of intersection", while a numerical evaluation of the most frequently occurring
types of orientation, namely linear and plane, is given by the corresponding
coefficients of orientation, determining its degree, and by value of ~~XXX~~ specific

surface (see Sections 26 and 28).

The degree of deformation by swaging or pressing is as a rule conventionally expressed by the relationship

$$\delta_{\text{com}} = \frac{H - H_1}{H}; \quad (47.1)$$

where H is the height (thickness) of sample before deformation, while H_1 is the same after deformation. The degree of deformation being determined by eq.(47.1) can change from 0 to a maximum value less than 1 (or, correspondingly, in percents from 0 up to 100%).

The method of estimating the ~~the~~ degree of deformation during drawing should be chosen in conformity with eq.(47.1), ~~XXXXXX~~ accepted for characteristic of degree of swaging. If, for example, the degree of swaging of the sample was determined by the value $\delta_{\text{szh}} = x$, the degree of subsequent drawing of the same sample, reducing its sizes to the initial ones, should then also be expressed by the value $\delta_{\text{vvt}} = x$. The following formula meets this condition

$$\delta_{\text{str}} = \frac{F - F_1}{F} = \frac{L_1 - L}{L_1}, \quad (47.2)$$

where F and L are respectively the area of cross section and length of sample before drawing, while F_1 and L_1 are the same values afterwards.

To reveal the dependence between the degree of surface or linear orientation of boundary surfaces, being determined by eqs.(26.17) and (26.12), and by degree

of deformation by reduction or drawing, we studied samples of technical iron and of two phase brass.

The samples of technical iron, which had an original equiaxed grain, were subjected to microanalysis after cold rolling with degrees of reduction ranging from 0.05 to 0.60 (i.e. from 5 to 60%). In Fig.163 we show the derived dependence between degree of reduction and degree of plane orientation, expressed in %. The curve shows that for ~~XXXXXX~~ technical iron, both these values coincide numerically. One can hypothesize that such a dependence is typical for monophase polyhedral structures. In the upper part of Fig.163, we show the variation in absolute value of specific surface of ferrite crystallites as function of degree of deformation.

The type L59 rod brass studied by us had a structure consisting of 79% (by volume) of α phase with hardness of 128 H_B and 21% β phase with hardness of 188 H_B. Notwithstanding the preliminary annealing, there was preserved the linear orientation of interfaces of phases, characterized ~~XXXX~~ by the degree of orientation amounting to 17.6%. Round samples, the axis of which coincided with the rod axis, were subjected to swaging. The coefficient of orientation of interfaces of phases was determined in a lengthwise microsection along the axis of the sample (from one end to the other).

In Fig.164, we show the derived dependence of degree of orientation upon degree of deformation (swaging). With ~~XXXX~~ increase in swaging, the degree of

original linear orientation gradually decreases and reaches zero in case of swaging equaling 20%. With further increase in degree of swaging, there occurs numerical a progressive plane orientation. In the given case, there is no longer a ~~numerical~~ coincidence between degrees of deformation and orientation: an ~~XXXX~~ increase in upsetting (swaging) by 10% is accompanied by a change in degree of orientation by 7.5% in all. The reason for this is the differing deformability of microparticles of the α -and β -phases of brass. It is ~~XXXX~~ interesting to note that the relationship between change in degrees of deformation and orientation about coincides with relationship of microhardnesses of hard and soft components. If the difference in hardnesses of phases is more considerable, the degree of orientation depends still less upon degree of deformation. Thus, in the deformation of steel with a structure of granular pearlite, ferrite flows around the microparticles of cementite, scarcely deforming them, therefore the interface ~~XXX~~ of phases does not receive a perceptible orientation, and practically remains isometric. The "architecture" of boundary surfaces also has considerable significance. If the deformation of soft component is crowded by microparticles of hard phase, as for instance in sheet pearlite, the microparticles of both phases deform jointly and the degree of orientation depends to a large degree upon degree of deformation.

In Fig.165, we show the change in absolute value of specific interface of phases in brass as function of degree of deformation (upsetting). The dependence is

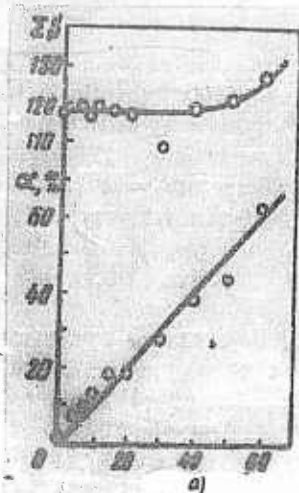


Fig.163 - Dependence of Specific Surface of Grains of Technical Iron and Degree of Orientation upon Degree of Deformation (upon value of reduction during rolling of sheet)
a) Reduction, %

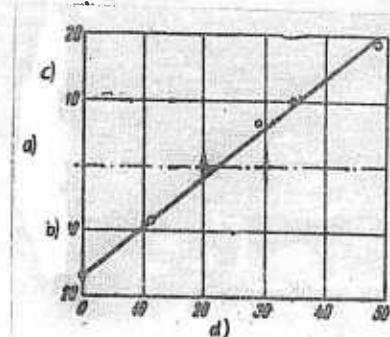


Fig.164 - Dependence of Degree of Orientation of Interfaces of Phases of Two Phase Brass (Linear and Plane) upon Degree of Deformation during Upsetting.
Original linear orientation equals 17.6.
a) Orientation, %; b) Linear; c) Plane;
d) Upsetting, %

analogous to that obtained for technical iron (see Fig.163).

A.G.Spektor ~~XXXXXX~~ obtained a somewhat different dependence of value of specific interface of ferrite and pearlite components of annealed steel upon degree of deformation. Samples of steel wire were deformed by way of drawing from a diameter of 5.5 mm to smaller diameters without ~~XXXXXX~~ annealing. The value of specific surface was measured by the ~~XXXXXX~~ method of A.G.Spektor. The degree of reduction was determined as the ratio of ~~XXXXXX~~ difference of initial and final diameters to the initial one (Bibl.61). For obtaining comparable data, we recalculated the degree of deformation in conformity with ~~XXXXXX~~ eq.(47.2), and

the data obtained ~~XXX~~ are shown in Fig.166. As we see, the value of specific surface changes here about proportional to the degree of deformation.

The study of degree of orientation and value of specific surface as a function of deformation is of great interest as a method of experimental observation of the process of plastic flow of metals and alloys. It is to be hoped that studies in this area will be continued.

In a determination of local stresses, one usually uses the application of an index grid upon the surface of sample or part, which can provide a concept of ~~XXXXXX~~ distribution of macrodeformations only on the surface. Ig.M.Pavlov with

his coworkers used the method of turning screws into the samples being deformed by compression. The axes of the screws in the cylindrical samples were located parallel to the axis of samples and direction of effective force. By change in pitch of thread during compression of sample, there was determined ~~XXXXX~~ the ~~XXXXXX~~ distribution of stresses over the height of cylinder (Bibl.271, 272).

The turning of screws into the body of the sample disrupts the solidity of the metal, which must be reflected upon the pattern of plastic flow, even if the material of sample and of screw are identical.

The boundary surfaces in metals and alloys constitute a natural spatial indexed micronetwork. Therefore, by change in orientation of boundary surfaces during plastic deformation, one can easily and exactly measure the local stresses in any point,

lying both on the surface as well as within the sample or part. For this, it is necessary ~~XX~~ to have the following data:

- a) To know the nature and degree of orientation of boundary surfaces of initial structure (if there is such an orientation);
- b) To know the dependence of degree ~~XX~~ of orientation upon degree of deformation. For pure metals and single phase alloys, it can be evidently considered that the degree of orientation and degree of deformation are numerically equal (at original isometric structure).

In Fig. 167, we show the change in degree of deformation by height of cylindrical sample of two phase brass type L59, swaged by 48.7%. Height of sample after swaging is 12 mm. Degree of local ~~XX~~ deformation changes here within wide limits, namely from zero at ends of sample to 80% at middle of its height (on the axial line). Still greater is the degree of deformation at the surface of sample at half its height, namely 87%. As we see, the maximum local deformation exceeds the average by almost 1.8 times.

Another method of measuring local deformations by change in form of grains on microsection was developed by P.O.Pashkov. In a lengthwise cut of standard Gagarin sample made of steel 45, which had a ferrite network in its structure, he measured the linear sizes of grains along and across the axis of sample. The ratio of these values in nondeformed zone of sample varied from 0.5 to 2.0. In

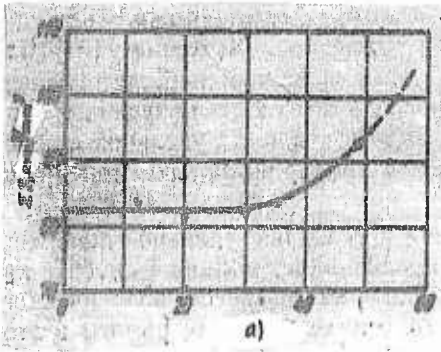


Fig.165 - Change in Value of Specific Interface of Phases of Two Phase Brass upon Degree of Deformation during Swaging
a) Swaging, %

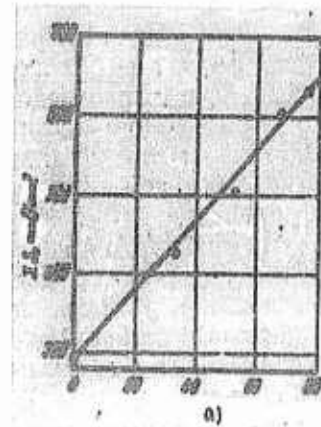


Fig.166 - Dependence of Specific Interface of Ferrite and Pearlite Components of Steel Wire upon Degree of Deformation (reduction) during Drawing. Based on test data of A.G.Spektor (Bibl.61)
a) Reduction, %

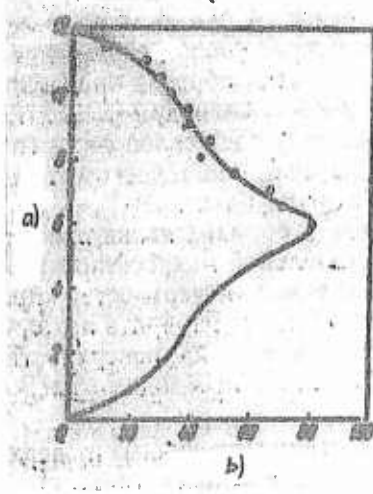


Fig.167 - Change in Degree of Deformation by Height of Round Sample of Two Phase Brass during Upsetting of Sample by 48%
a) Height, mm; b) Deformation, %

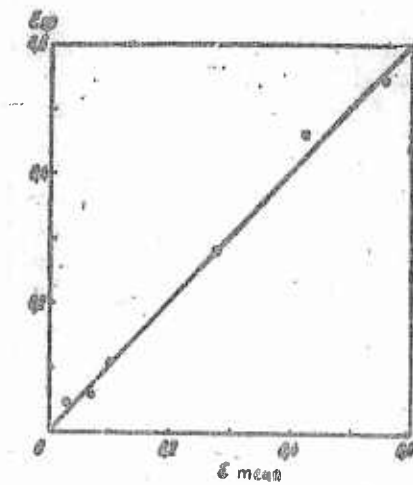


Fig.168 - True Average Deformation of Rolled Plates, Determined by Elongation during Rolling and according to Structure [after B.B.Chechulin (Bibl.175)]

the zone of uniform deformation, the ratio increased to 0.75 - 2.25, and in the zone of the neck, 1.25 to 6.0. With this method, we succeeded in establishing that the transverse (relative to the elongating force) deformations are distributed in the form of alternating bands of strong and weak deformation, exposing the periodicity of flow of metal in the deformed field (Bibl.145).

As already mentioned above (see Section 41), B.B.Chechulin used the statistically average value of ratio of diameters of flat grains, measured along and across a fixed direction, expressed in the form $\epsilon_{sr} = \ln(a/b)$, for ~~XX~~ estimating the deformation of metal. The difference of parameters ϵ_{sr} , measured after and before deformation, characterize, according to Chechulin, the true deformation (Bibl.175). In Fig.168, we show the dependence obtained by Chechulin between values of true average deformation of plates rolled under different reduction, being determined according to elongation during rolling (along x axis) and according to value of parameter ϵ_{sr} (along y axis). The correlation obtained was quite satisfactory, which permits the use of this method for estimating local deformation. For obtaining reliable data in the investigated sector, it is adequate to ~~XX~~ measure 150 - 200 grains (Bibl.175).

An estimation of degree of deformation by value of ratio of average lengths of transverse and longitudinal axes of grains in a microsection is used quite frequently in one form or another. However, the same value of this ratio can occur

at varying degrees of deformation, if the types of deformation are different.

Therefore, in Table 69, we present actual values of plane and linear orientation

(in %), corresponding to differing values of lengths of transverse and longitudinal axes of grains in a microsection (cut).

Table 69

| a) | b) | | e) | f) | |
|-----|-----|-----|-----|----|----|
| | c) | d) | | g) | h) |
| 0 | 100 | 100 | 0,6 | 25 | 34 |
| 0,1 | 89 | 88 | 0,7 | 18 | 25 |
| 0,2 | 67 | 76 | 0,8 | 11 | 16 |
| 0,3 | 54 | 65 | 0,9 | 5 | 8 |
| 0,4 | 43 | 54 | 1 | 0 | 0 |
| 0,5 | 33 | 44 | | | |

a) Average ratio of lengths of transverse and longitudinal axes of grains in cut; b) Degree of orientation, %; c) Plane; d) Linear; e) Mean ratio of lengths of transverse and longitudinal axes of grains in cut; f) Degree of orientation, %; g) Plane; h) Linear

In conclusion of the present Chapter, it is noteworthy that the material in

it does not profess to be final or complete, and the hypotheses and propositions expressed possibly require supplements, refinements and corrections. Purpose of what has been presented has been to show the role of boundary zones in the formation of structure, in the processes of transformation in alloys, and in the

determination of their properties and behavior. The author also desired to show that there exists very distinct quantitative connections (frequently quite simple) between parameters of spatial microstructure and the diverse properties of metals and alloys, and by the same token ~~HEM~~ he desired to divert attention of metallurgists to the need for the most attentive study of stereometric structure of metals and alloys, and also to point out those areas of research in which the study may prove, in the author's opinion, most effective and fruitful.

BIBLIOGRAPHY

1. - Supplement to Composition on Sword Steel of Core of Mining Engineers of Major General Anosov, containing log book of tests conducted from 1828 to 1839, with brief comments, Book Two, Zlatoust, 1841; P.O.Anosov, Collected Works, USSR Academy of Sciences Press, Moscow 1954 (1954).
2. Kurnakov,N.S. - Introduction to Physical-Chemical Analysis. USSR Academy of Sciences Press, Moscow-Leningrad, 1940.
3. - Concerning Damascus Steels, Report of core of mining engineers of Major General Anosov, St.Petersburg, 1841; P.O.Anosov, Collected Works, USSR Academy of Sciences Press (1954).
4. Chernov,D.K. ~~XXX~~ Science of Metals. Metallurgizdat, Moscow (1950).
5. Mirkin,I.L. - Problems of Theoretical Metallurgy. Collection X of Transactions of Moscow Institute of Steel ~~XXX~~ imeni Stalin. Oborongiz, Moscow-Leningrad (1938).
6. Chernyyakov,A.N. and Podvoyskiy,A.N. - Plant Laboratory, Vol.6, No.12 (1937).
7. Baboshin,A.L. - Metallography and Heat Treatment of Iron, Steel and Pig Iron. GONTI, Moscow (1935).
8. Minkevich,A.N. - Properties, Heat Treatment and Designation of Steel and Iron, Parts I - II. Gosmashmetizdat, Leningrad (1932).
9. Kuksinskaya,V.Ye., Tyulenev,V.N., and Chaykovskiy,M.D. - Plant Laboratory, Vol.8, No.10 - 11 (1939).
10. Melikhov,P.I. - Plant Laboratory, Vol.5, No.10 (1936).
11. Dvoryanov,P.A. - Plant Laboratory, Vol.17, No.6 (1951).
12. Bolkhovitinov,N.F. - Plant Laboratory, Vol.6, No.12 (1937).

13. Davidenkov, V.A. - Bulletin of USSR, Academy of Sciences, Department of Technical Sciences, No.11 - 12 (1943).
14. Minkevich, N.A. - Low Alloyed Fast Cutting Steels, Metallurgizdat, Moscow (1944).
15. Vinarov, S.M. - Bulletin of USSR Academy of Sciences, Department of Technical Sciences, No.6 (1948).
16. ~~XXXXXXXXXX~~ - Book of ASTM standards, Part I. Metals, ASTM, Philadelphia (1936).
17. Saltykov, S.A. - Introduction to Stereometric Metallography. Armenian SSR, Academy of Sciences Press, Yerevan (1950).
18. Johnson, W. - Metal Progress. Vol.49, No.1 (1946).
19. Bolkhovitinov, N.F. - Size of Grain and Properties of Steel. Metallurgizdat, Moscow (1943).
20. Shumovskiy, Ye.G. - Plant Laboratory, Vol.10, No.3 (1941).
21. Bolkhovitinov, N.F. - Metal Working and Heat Treatment. Mashgiz, Moscow (1954).
22. Baboshin, A.L. - Metallography and Heat Treatment of Steel, Iron and Pig Iron, Vol.III, Metallurgizdat, Leningrad (1940).
23. Davidenkov, V.A. - Instructions on Investigation of a Steel Ingots. PNITO of Metallurgists, Metallurgizdat, Moscow (1940).
24. Sokolova, N.K. and Vinograd, M.I. - Steel, No.7 (1950).
25. Girshovich, N.G. - Iron Casting. Metallurgizdat, Moscow (1949).
26. Bolton, D.V. - Gray Iron. ONTI NKTP USSR, Kiev (1938).
27. Troitskiy, G.N. - Properties of Iron, Metallurgizdat, Leningrad (1941).
28. Skorodzhevskiy, S.M. - Herald of Metal Industry. No.9 (1937).

29. Slavinskiy,M.P. and Kleyman,N.L. - Metallurgist, No.12 (1938).
30. Gulyayev,A.P. and Petunina,Ye.V. - Plant Laboratory, Vol.18, No.4 (1952).
31. Gulyayev,A.P. and Petunina,Ye.V. - Metallographic Investigation of Transformation of Austenite into Martensite. Mashgiz, Moscow (1952).
32. Sirota,N.N. - Bulletins of Section of Physico-Chemical Analysis of Institute of General and Inorganic Chemistry imeni N.S.Kurnakovskogo of USSR Academy of Sciences, Vol. XXIII, USSR Academy of Science Press, Moscow (1953).
33. Mirkin,I.L. - High Quality Steel, XXX No.5 (1935).
34. Sveshnikov,V.N. - Metallurgist, No.2 (1930).
35. Zamoruyev,G.M. - Metallurgist, No.7 (1936).
36. Camp,D. and Francis,K. - Production and Machining of Steel, Part III. Metallurgizdat, Moscow (1947).
37. Chervyakov,A.N. - Metallographic Determination of Impurities in Steel. Metallurgizdat, Moscow (1953).
38. Tamman,G. - Metal Working. OMTI NKTP USSR, Leningrad (1935).
39. - Imperfections in nearly perfect crystals. J.Wiley and Sons, Inc., New York (1952).
40. Reiter,S.F. - Journ. of Metals, Vol.5, No.5 (1953); Abstract Journal "Physics", No.7 (1954), Abstract 7520.
41. Khoroshev,I.I. - Plant Laboratory. Vol.19, No.3 (1953).
42. Sobolev,B.F. - Casting Production. No.6 (1953).
43. Smith,C.S. and Guttman,L. - Journ. of Metals. Vol.5, No.1 (1953).

44. Rovinskiy, B.M. and Rybakova, L.M. - Journal of Technical Physics. Vol.24,
No.6 (1954).
45. Klassen-Neklyudova, M.V. and Kontorova, T.A. - Progress in Physical Sciences.
~~XXXVII~~ Vol.22 (1939), pp.3 and 4
46. Arkharov, V.I. - Transactions of Institute of Physics of Metals. No.14, Collection
of Reports on Physical Metal Working, USSR Academy of Sciences Press,
Moscow (1954).
47. Fuks, N.A. - Progress in Physical Sciences, Vol.15, No.4 (1935).
48. Gulyayev, A.P., Lakhtin, Yu.M., and Tarusin, A.I. - Heat Treatment of Steel.
Mashgiz, Moscow (1946).
49. Oding, I.A. - Bulletin of USSR Academy of Sciences, Department of Technical
Sciences, No.8 (1954).
50. Glagolev, A.A. - Geometric Methods of Quantitative Analysis of Aggregates
under a Microscope. Gosgeolizdat, Lvov (1941).
51. Polushkin, E.P. - Trans. AIME, Vol.70 (1924); Abstract: Journal of Russian
Metallurgical Society, No.1, Part II (1926).
52. Glagolev, A.A. - Authors Certificate No.38066 for Method and Device for
Microscopic Analysis of Rocks, Priority from 19 July 1932.
53. Glagolev, A.A. - Mineral Raw Material. No.10 - 11 (1931).
54. Glagolev, A.A. - Metallurgists. No.11 (1935).
55. Belyayev, N.T. - Journal of Russian Metallurgical Society, No.1, Part II (1926);
Journ. Iron and Steel Inst., Vol.1 (1922).
56. Belyayev, N.T. - Journal of Russian Metallurgical Society, No.1, Part II (1926);
Proceedings of the Roy. Soc., A, Vol.108 (1925).

57. Rutherford,J.J., Aborn,R.H., and Bain,E. - Metals and Alloys. No.12 (1937).
58. Saltykov,S.A. - Author's Certificate No.72704 for Method of Geometric Quantitative Analysis of Metals, Alloys and Other Objects, Priority from 28 May 1945.
59. Saltykov,S.A. - Plant Laboratory, Vol.12, No.9 - 10 (1946).
60. Saltykov,S.A. - Plant Laboratory, Vol.18, No.5 (1952).
61. Spektor,A.G. - Plant Laboratory, Vol.20, No.5 (1954).
62. Scheil,E. - ~~Zeitschrift fuer Metallkunde~~ Vol.201 (1931).
63. Scheil,E. - Zeitschrift fuer Metallkunde, Vol.27, No.9 (1935).
64. Scheil,E. and Wurst,H. - Zeitschrift fuer Metallkunde, Vol.28, No.11 (1936).
65. Schwarz,H.A. - Metals and Alloys, Vol.5, No.6 (1934).
66. Saltykov,S.A. - Plant Laboratory, Vol.15, No.11 (1949).
67. Spektor,A.G. - Plant Laboratory, Vol.16, No.2 (1950).
68. Saltykov,S.A. - Plant Laboratory, Vol.18, No.9 (1947).
69. Saltykov,S.A. - Plant Laboratory, Vol.8, No.7 (1939).
70. Shteynberg,M.M., Bogachev,I.N., Zykov,G.A., Shklyar,R.SH. - Physics of Metals and Metal Working, No.1 (1955).
71. Gulyayev,B.B. - Hardening and Heterogeneity of Steel. Metallurgizdat, Moscow (1950).
72. Zarubin,N.M. - Plant Laboratory, Vol.18, No.4 (1952).
73. Gel'vikh,P.A. - Theory of Probability. Publication of Artillery Academy of RKKA, Leningrad (1933).

74. Gerens,P. - Metallography, ONTI NKTP, GNTI of Ukraine, Kiev (1935).
75. Kashenko,G.A. - Course in Metal Working. Metallurgizdat, Moscow - Leningrad (1940).
76. Chirvinskiy,P.N. - Geometric-Chemical Analysis, ONTI, Khimteoret, Moscow (1937).
77. Beck,L.H. and Smith,C.S. - Journal of Metals, Vol.4, No.10 (1952).
78. Lane,J.R. and Grant,N.J. - Trans. ASM, Vol.44 (1952); Abstract: Problems of Modern Metallurgy, No.2(8) (1953).
79. Bonaventura Cavalieri - Geometry, Presented by New Methods with Aid of ~~XX~~
Indivisibles of a Constant (Value), Vol.1, Gostekhizdat, Moscow -
Leningrad (1940).
80. Aronovich,M.S. and Lyubarshkiy,I.M. - Metallurgists. No.9 (1936).
81. Vinograd,M.I. - Nonmetallic Inclusions in Ball Bearing Steel, Metallurgizdat,
Moscow (1954).
82. - Impurities in Steel (Collection of Articles), Metallurgizdat,
Moscow (1933).
83. Buynov,N.N. and Lerinman,R.M. - Plant Laboratory, Vol.15, No.2 (1949).
84. Lyulicheva,N.N. - Use of Methods of Spatial Metallography in the Detection
of Influence of Interface of Phases upon Mechanical Characteristics of
Carbonic Steels (Author's Abstract of Dissertation), Khar'kov (1954).
85. Apayev,B.A. - Journal of Technical Physics, Vol.23, No.7 (1953).
86. Popova,N.M. - Plant Laboratory, Vol.15, No.3 (1949).
87. Gardin,A.I. - Electron ~~XX~~ Microscopy of Steel, Metallurgizdat, Moscow (1954).
88. Bokshteyn,S.Z. - Structure and Mechanical Properties of Alloyed Steel.
Metallurgizdat, Moscow (1954).

89. Spektor,A.G. - Plant Laboratory, Vol.7, No.12 (1938).
90. Kravtsov,P.Ya. - Steel, No.3 (1949).
91. Aronovich,M.S. and Yefanova,Ye.K. - Metallurgist, No.5 (1938).
92. Dontsov,P.M. - Plant Laboratory, Vol.5, No.3 (1936).
93. Danilov,A.P. and Mokhir,Ye.D. - Plant Laboratory, Vol.15, No.3 (1949).
94. Voinov,S.G. and Boyarshinov,V.A. - Steel, No.1 (1955).
95. Shpeyzman,V.M. and Yelenevskaya,Ye.V. - Plant Laboratory, Vol.14, No.7 (1948).
96. Skorodziyevskiy,S.M. - Metallurgists, No.3 (1937).
97. Warsing,A. and Heffner,J. - Methods of Processing Experimental Data. Foreign Literature
~~Engineering~~ Press, Moscow (1953).
98. Malashenko,R.B. - Plant Laboratory, Vol.13, No.1 (1947).
99. Voinov,S.G. and Boyarshinov,V.A. - Plant Laboratory, Vol.18, No.8 (1952).
100. Hurlbut,C.S. - American Journal of Science, Vol.237, No.4 (1939).
101. Gnedenko,B.V. - Course in Theory of Probability. Gostekhizdat, Moscow - Leningrad (1950).
102. Chayes,F. - The American Mineralogist, Vol.34, No.1 and 2 (1949).
103. Chayes,F. - The American Mineralogist, Vol.34 (1949), pp.600 - 601.
104. Spektor,A.G. - Plant Laboratory, Vol.16, No.9 (1950).
105. Pogodin-Alekseyev,G.I. - Theory and Practice of Metallurgy, No.12 (1936).
106. Benediks,K. and Lefkvist,Kh. - Nonmetallic Inclusions in Iron and Steel, Kiev (1935).

107. Bolkhovitinov,N.F. - Metal Working and Heat Treatment of Steel.
Metallurgizdat, Moscow (1946).
108. - Encyclopedic Handbook "Machine Construction", Vol.4, Mashgiz,
Moscow (1947).
109. - Cast Metals Handbook, AFA, Chicago (1935).
110. - Great Soviet Encyclopedia, 2nd Edition, Vol.16 (1952).
111. Yelyutin,V.P., Pavlov,Yu.A., and Levin,B.Ye. - Production of Ferro-Alloys,
Part II. Metallurgizdat, Moscow (1951).
112. Gudtsov,N.T., Baranov,F.D., and Kuz'mina,O.O. - Metallurgists, No.5, MMK
No.6 (1936).
113. Rozanov,A.N. - Collection "Metal Working and Heat Treatment", No.1.
Metallurgizdat, Moscow (1954).
114. Rozanov,A.N. - Collection "Metal Working and Modern Methods of Heat Treatment
of Pig Iron", Mashgiz, Moscow (1955).
115. Gardin,A.I. - Collection "Study of Structure of Tool Steel". Mashgiz,
Moscow (1954).
116. Oknov,M.G. - Journal of Russian Metallurgical Society, Part 1, No.1
(1928), pp.1 - 13.
117. Ishigaki,T. - Abstract: Journal of Russian Metallurgical Society, Part II,
No.2 (1928), pp.205 - 214.
118. Blanter,M.Ye. - Methods of Studying Metals and the Processing of Test Data.
Metallurgizdat, Moscow (1952).
119. Oknov,M.G. - Journal of Russian Metallurgical Society, Part II, No.2 (1911).

120. Starodubov, K.F. - Metallurgist, No.2 (1930).
121. Pelissier, G.E., Hawks, M.F., Johnson, W.A., and Mehl, R.F. - Transactions ASM, Vol.30 (1942), pp.1040 - 62.
122. Gensamer, M., Pearsall, E.B., and Smith, G. - Transactions ASM, Vol.28, No.2 (1940), p.380.
123. Gardin, A.I. and Gulyayev, A.P. - Journal of Technical Physics, Vol.23, No.11 (1953).
124. Saltykov, S.A. - Plant Laboratory, Vol.12, No.3 (1946).
125. Bokshteyn, S.Z. - Journal of Technical Physics, No.12 (1947).
126. Bokshteyn, S.Z. and Gudkova, T.I. - Transactions of VIAM, Vol.1, No.4, Physical Transformations in Alloys. Oborongiz, Moscow (1948).
127. Mirkin, I.L. - Collection "Structure and Properties of Steels and Alloys", Collection of Transactions of Moscow Institute of Steel imeni Stalin. Metallurgizdat, Vol.18, Moscow (1941).
128. Moroz, L.S. - Collection Devoted to the 70th Anniversary of Academician A.F. Hoffe, USSR Academy of Science Press, Moscow (1950).
129. Lipilin, I.P. - "Heat Treatment of Alloyed Steel", Collected Works of Moscow Institute of Steel imeni Stalin. Metallurgizdat, Moscow (1937).
130. Meijering, J.L. - Philips Res. Reports, Vol.8 (1953), pp.270 - 290.
131. Saltykov, S.A. - Plant Laboratory, Vol.12, No.3 (1946).
132. Gilenko, N.D. - Workbook on Theory of Probability. Uchpedgiz, Moscow (1943).
133. Rauzin, Ya.R., Zheleznyakova, Sh.R. - Steel, No.11 (1951).

134. Bolkhovitinov,N.F. - Metallography and Heat Treatment. Metallurgizdat, Moscow (1933).
135. Shubnikov,A.V. - Symmetry. USSR Academy of Science Press, Moscow (1940).
136. Yevangulov,M.G. and Bologdin,S.P. - Metallography, Handbook for Studying the Structure of Metals. Publication of M.G.Yevangulov, Petersburg (1905).
137. Obergoffer,P. - Technical Steel, Part II. Metallurgizdat, Leningrad (1934).
138. Saltykov,S.A. - Plant Laboratory, Vol.23, No.2 (1957).
139. - Chemical Engineers Handbook, New York - London (1934).
140. Blanter,M.Ye. and Saltykov,S.A. - Plant Laboratory, Vol.14, No.4 (1948).
141. Horikawa,E. - Journal of Iron and Steel Inst., Japan, Vol.40, No.10 (1954); Abstract Journal "Metallurgy", No.1 (1956).
142. Saltykov,S.A. - Plant Laboratory, Vol.16, No.9 (1950).
143. - Encyclopedic Handbook "Machine Construction", Vol.1, Book 1, Mashgiz, Moscow (1947).
144. - Handbook of a Machine Builder, Vol.1, Mashgiz, Moscow (1955).
145. Pashkov,P.O. - Journal of Technical Physics, Vol.19, No.3 (1949).
146. Spektor,A.G. - Plant Laboratory, Vol.21, No.8 (1955).
147. Saltykov,S.A. - Plant Laboratory, Vol.21, No.8 (1955).
148. Vasil'yev,G.Ya. - Plant Laboratory, Vol.14, No.2 (1948).
149. Osipov,K.A. and Kuz'min,A.V. - Proceedings of USSR Academy of Science, Vol.59, No.2 (1948).
150. Shvarts,G.A. - American ~~EMK~~ Malleable Iron, ONTI NKTP USSR, ~~EMK~~ Moscow (1936).

151. Saltykov,S.A. - Plant Laboratory, Vol.15, No.9 (1949).
152. Snyder,R. and Graff,H. - Metal Progress, Vol.33, No.4 (1938).
153. Gluskin,D. - Metallurgists, No.7 - 8 (1938).
154. - Studies on Metal Working and Heat Treatment of Steel, Collection III of Ural Scientific Research Institute of Ferrous Metals, Metallurgizdat, Sverdlovsk (1941).
155. Slatykov,S.A. - Plant Laboratory, Vol.6, No.7 (1937).
156. Smolenskiy,S.I. and Zamyatin,M.M. - Metallurgist, No.7 (1937).
157. Kostron,H. - Dederichs, Archiv fuer Metallkunde, No.3 (1949).
158. Dickenscheid,W. - Métaux corros.-inds., Vol.29, No.341 (1954).
159. Chmutov,K.V. - Plant Laboratory, Vol.19, No.4 (1953).
160. Kostron,H. - Wire Prod., Vol.3, No.12 (1954); Abstract Journal "Physics", No.7 (1955).
161. Spektor,A.G. - Plant Laboratory, Vol.21, No.2 (1955).
162. Saltykov,S.A. - Collection of Scientific Works of Yerevan Polytechnical Institute imeni K.Marx, No.7, Issue 1, Yerevan (1954).
163. Mirkin,I.L. and Blanter,M.Ye. - Metallurgist, No.12 (1936).
164. Roginskiy,S.Z. and Todes,O.M. - Bulletin of USSR Academy of Sciences, OKhN, No.3 (1940).
165. Roginskiy,S.Z. - Proceedings of USSR Academy of Sciences, Vol.27, No.7 (1940).
166. Blanter,M.Ye. - Plant Laboratory, Vol.14, No.4 (1948).
167. Bokshteyn,S.Z. - Journal of Technical Physics, No.3 (1950).

168. Mirkin,I.L. - High Quality Steel, No.6 (1935).
169. Schwarz,H.A. - Metals and Alloys, Vol.7, No.11 (1936).
170. Saltykov,S.A. - Metallurgists, No.8 (1939).
171. Saltykov,S.A. - Plant Laboratory, Vol.7, No.5 (1938).
172. Dvoryanov,P.A. - Ball Bearing, No.5 (1953).
173. Fullman,R.L. - Journ. of Metals, No.3 (1953).
174. Kunin,L.L. - Surface Phenomena in Metals. Metallurgizdat, Moscow (1955).
175. Chechulin,B.B. - Physics of Metals and of Metal Working, Vol.1, No.2 (1955).
176. Bunin,K.P. - Ferrous Carbonic Alloys, Mashgiz, Kiev - Moscow (1949).
177. Bunin,K.P. and Malinochka,Ya.N. - Introduction to Metallography.
Metallurgizdat, Moscow (1954).
178. Parker,E.A. and Smoluchowski,R. - Trans. of American Soc. for Met.,
Vol.35 (1945), pp.362 - 371.
179. Smith,C.S. - Metals Technol., Vol.15, No.4 (1948).
180. Smith,C.S. - Trans.Amer.Soc. for Metals, Vol.45 (1953), pp.533 - 575.
181. Harker,D. and Parker,E.A. - Trans.Amer.Soc. for Metals, Vol.34 (1945), p.156.
182. - Progress in Physics of Metals, 1, Collected Articles, Metallurgizdat,
Moscow (1956).
183. Gan,F.V. - Dispersion Analysis, Goskhimizdat, Moscow - Leningrad (1940).
184. Zeyts,F. - Physics of Metals, OGIZ - Gostekhizdat, Moscow - Leningrad (1947).
185. Kuznetsov,V.D. - Crystals and Crystallization. Gostekhizdat, Moscow (1954).

186. Umanskiy, Ya.S., Finkel'shteyn, B.N. and Blanter, M.Ye. - Physical Bases of
Metallurgy. Metallurgizdat, Moscow (1949).
187. Umanskiy, Ya.S., - Finkel'shteyn, B.N., Blanter, M.Ye., Kishkin, S.T., Fastov, N.S.,
and Gorslik, S.S. - Physical Science of Metals. Metallurgizdat, Moscow (1955).
188. Shteynberg, S.S. - Metallurgy, Vol.1. Metallurgizdat, Sverdlovsk - Moscow (1952).
189. Bogachev, I.N. - Metallography of Iron. Mashgiz, Moscow - Sverdlovsk (1952).
190. Bunin, K.P. and Chernovol, A.V. - Proceedings of USSR Academy of Science,
Vol.95, No.4 (1954).
191. Kuznetsov, V.D. - Surface Energy of Solid Bodies. Gostekhizdat, Moscow (1954).
192. - Resilience and Nonresilience of Metals, Collected Articles. Foreign
Literature Press, Moscow (1954).
193. Arkharov, V.I. and Skoryankov, N.N. - Proceedings of USSR Academy of Science,
Vol.89, No.5 (1953).
194. Clemm, P. and Fisher, J. - Acta Metallurgica, Vol.3, No.1 (1955); Abstract
Journal "Physics", IX No.3 (1956).
195. Bokshteyn, S.Z., Gudkova, T.I., Kishkin, S.T., and Moroz, L.M. - Plant Laboratory,
Vol.21, No.4 (1955).
196. Gulyayev, A.P. - Heat Treatment of Steel, Mashgiz, Moscow (1953).
197. Gertsriken, S.D. - Proc. of USSR Academy of Sciences, Vol.98, No.2 (1954).
198. Bartenev, G.M. - Journal of Experimental and Theoretical Physics, Vol.20,
No.3 (1950).
199. Kostryukov, V.N. and Strelkov, P.G. - Journal of Physical Chemistry, Vol.28,
No.10 (1954).

200. Khaykin,S.E. and Bene,N.P. - Proc. of USSR ~~USSR~~ Academy of Sciences,
Vol.23, No.1 (1939).
201. Gayev,I.S. - Metallurgists, No.11 (1936).
202. Kazachkovskiy,O.D. - Collection of Scientific Reports of Laboratory of
Metal Physics of the Ukrainian ~~USSR~~ SSR Academy of Sciences, Kiev (1948).
203. Danilov,V.I. - Collection "Problems of Metal Science and Physics of Metals".
Metallurgizdat, Moscow (1949).
204. Fridlyander,I.N. and Filippova,G. - Bulletins of Section of Physico-Chemical
Analysis, USSR Academy of Sciences, Press, Moscow, Vol.22 (1953).
205. Ivantsov,G.P. - Steel, No.10 (1952).
206. Golikov,I.N. and Kozlov,F.V. - Steel, No.7 (1952).
207. Likhtman,V.I., Rebinder,P.A., and Karpenko,G.V. - Effect of Surface-Active
Medium upon Processes of Deformation of Metals. USSR Academy of Sciences
Press, Moscow (1954).
208. Likhtman,V.I. and Maslennikov,E.M. - Proc. of USSR Academy of Sciences, Vol.67, No.1
(1949).
209. Gridnev,V.N. - Transactions of Institute of Ferrous Metallurgy of ~~USSR~~
~~USSR~~ Academy of Sciences, Vol.II, Ukrainian SSR Academy of Science
Press, Kiev (1948).
210. Tsou,A., Natting,D., and Menter,J. - Iron Steel Institute, Vol.172, No.2 (1952).
211. Tsou,A., Natting,D., and Menter,J. - Problems of Modern Metallurgy, No.4 (10)
(1953).
212. Zakladnyy,M.N. and Saltykov,S.A. - Newest Reports on Malleable Iron, Collected
Articles. Metallurgizdat, Moscow (1933).

213. Savatyugin,B.A. - Latest Reports on Malleable Iron, Collected Articles.
Metallurgizdat, Moscow (1933).
214. Bunin,K.P., Ivantsov,G.I., and Malinochka,Ya.N. - Structure of Pig Iron.
Mashgiz, Kiev - Moscow (1952).
215. Oding,A. and Lozinskiy,M.G. - Proc. of USSR Acad. of Sciences, Vol.86,
No.4 (1952).
216. Oding,I.A. and Lozinskiy,M.G. - Bulletin of USSR Acad. of Sciences, Department
of Technical Sciences, No.7 (1953).
217. Rusin,P.I. - Transactions of Rostov n/D Institute of Agricultural Machine
Construction, No.6, Rostov Book Publishers, Rostov n/D (1954).
218. Schwartz,H. and Barnett,M. - Trans. ASM, No.2 (1938).
219. Grayfer,Ye.Z. МЖХ and Salli,I.V. - Proc. of USSR Acad. of Sciences, Vol.97,
No.4 (1954).
220. Agarwala,R. and Wilman,H. - Proc.Royal Soc., Vol.223, No.1153 (1954); Abstract
Journal "Physics", No.5 (1955).
221. Agarwala,R. and Wilman,H. - J.Iron and Steel Inst., London, Vol.179, No.2 (1955);
Abstract Journal "Metallurgy", No.3 (1956).
222. Owen,E. and Jones,D. - Proc.Phys.Soc., Vol.67, No.6 (1954); Abstract Journal
"Physics", No.5 (1955).
223. Bridgman,P. - Study of Large Plastic Deformations and Shear. Foreign Literature
Publishing House, Moscow (1955).
224. Dublik,A.I. and Pines,B.Ya. - Proc. of USSR Academy of Sciences, Vol.87, No.2
(1952).

RENNY

225. Bublik,A.I., Vyazmitinova,E.I. and Pines,B.Ya. - Scientific Memoirs of Khar'kov University, Vol.49; Abstract Journal "Physics", No.3 (1955).
226. Bublik,A.I. - Proc. of USSR Academy of Sciences, Vol.95, No.3 (1954).
227. Pines,B.Ya. and Bublik,A.I. - Journal of Technical Physics, Vol.24, No.6 (1954).
228. Buynov,N.N. - Physics of Metals and Metal Science. Vol.1, No.2 (1955).
229. Buynov,N.N. and Podrezov,L.I. - Physics of Metals and Metal Science, Vol.1, No.2 (1955).
230. Afanas'yev,N.N. - Journal of Technical Physics, Vol.7, No.24,(1937).
231. Stark,B.V., Mirkin,I.L. and Romanskiy,A.N. - Collected Works of Moscow Institute of Steel imeni Stalin, No.7 (1935).
232. Kolmogorov,A.N. - ~~МОСКОВСКИЙ~~ Bulletin of USSR Academy of Sciences, Department of Mathematical and Natural Sciences, Mathematics Series, No.3 (1937).
233. Johnson,W. and Mehl,R.F. - Trans.AIMME, Vol.135 (1939), pp.416 - 458.
234. Avrami,M. (now Melvin) - Journ.Chem.Phys., Vol.7 (1939); Op cit, Vol.8 (1940); Op cit, Vol.9 (1941).
235. Girschovich,N.G. - Casting Production, No.1 (1951).
236. Spektor,A.G. - Journal of Technical Physics, Vol.20, No.9 (1950).
237. Spektor,A.G. - Plant Laboratory, Vol.15, No.7 (1949).
238. Ger,A.E. - Metal Science and Machining of Metals, No.5 (1956).
239. Spektor,A.G. - Plant Laboratory, Vol.22, No.12 (1956).
240. Saltykov,S.A. - Plant Laboratory, Vol.12, No.3 (1946).

241. Angus,H. and Summers,R. - Journ. of the Inst. of Metals, No.1 (1925);
Abstract: Journal of Russian Metallurgical Society, Part II, No.3 (1926).
242. - Size of ~~Grain~~ Grain and Property of Steel,
Metallurgizdat, Moscow (1935).
243. Ishigaki,T. - Sc.Rep.Tohoku Univer., No.3 (1927); Abstract: Journal of
Russian Metallurgical ~~Society~~ Society, Part II, No.2 (1928).
244. Beyn,E. - Effect of Alloying Elements upon Properties of Steel, Metallurgizdat,
Moscow (1945).
245. - Collection of Scientific Reports of Moscow Mechanical Institute,
No.2, Mashgiz, Moscow (1951).
246. - Collection of Scientific Transactions of Yerevan Polytechnical
Institute, No.10, Issue 2, Yerevan (1956).
247. Trubin,K.G. and Oyks,G.N. - Metallurgy of Steel, Metallurgizdat, Moscow (1951).
248. - Encyclopedic Handbook "Machine Construction", Vol.3, Mashgiz,
Moscow (1948).
249. Shteynberg,M.M. - Problems of Construction Steels, Collection of Lectures of
Conference in Leningrad, Lonitomash, Mashgiz (1949).
250. Potak,Ya.M. and Sachkov,V.V. - Journal of Technical Physics, No.3 (1949).
251. Bushanova,Ye. and Potak,Ya.M. - Journal of Technical Physics, No.1 (1951).
252. Gensamer,M., Pearsall,E., Pellini,W., and Low,I. - Trans, ASM, Vol.30 (1942),
p.983
253. Pashkov,P.O. - Journal of Technical Physics, Vol.24, No.3 (1954).
254. Konobeyovskiy,S.T. - Bulletin of USSR Acad. of Sciences, Department of
Mathematical and Natural Sciences, Chemical Series, No.5 (1957).

255. Moroz,L.S. - Journal of Technical Physics, Vol.24, No.3 (1954).
256. Bal'shin,M.Yu. - Powder Metallurgy. Metallurgizdat, Moscow (1948).
257. Oding,I.A. - Bulletin of USSR Academy of Science, Department of Technical Sciences, No.8 (1954).
258. Livshits,B.G. - Physical Properties of Alloys, Metallurgizdat, Moscow (1946).
259. Eucken, Dittrich - Archiv.f.d.Eisenhuettewesen, No.5 (1935); Abstract: Herald of Metal Industry, No.9 (1937).⁴
260. Mes'kin,V.S. - Industrial Magnetic Alloys, Leningrad (1932).
261. Meyl,R.F. - Progress in Physical Sciences, Vol.19, No.4 (1938).
262. Bugakov,B.Z. - Diffusion in Metals and Alloys. Gostekhizdat, ~~ММК~~
~~ММК~~ Leningrad - Moscow (1949).
263. Gruzin,P.L., Noskov,B.M., and Shirokov,V.I. - Proc. of USSR Acad. of Sciences, Vol.99, ~~(1954)~~ XXX No.2 (1954).
264. Umanskiy,Ya.S., Finkel'shteyn,B.N., Blanter,M.Ye., Kishkin,S.T., Fastov,N.S., and Gorelik,S.S. - Physical Metal Science. Metallurgizdat, Moscow (1955).
265. Zav'anlov,A.S. - Journal of Technical Physics, Vol.23, No.2 (1953).
266. Bobylev,A.Y. - Corrosion Fissuring of Brass. Metallurgizdat, Moscow (1956).
267. Sokolov,S.Ya. - ~~ММК~~ Proc. of USSR Acad. of Science, Vol.59, No.5 (1948).
268. Merkulov,L.G. - Journal of Technical Physics, Vol.26, No.1 (1956).
269. ~~ММК~~ Grieves,R.G. and Righton,G. - Practical Handbook on Microscopic Metallography, ONTVU, Publishing House "Steel", Khar'kov - Dnepropetrovsk (1932).
270. Skakov,A.I. - Quality of Railroad Rails. Metallurgizdat, Moscow (1955).

271. Pavlov, Ig.M., Gel'derman, L.S. and Zhukova, A.I. - Metallurgists, No.7 (1936).
- Pavlov, Ig.M.,
272. ~~Металлургист~~ Gel'derman, L.S. and Zhukova, A.I. - Metallurgists, No.12 (1936).
273. Smith, C.S. - Trans. ASM, Vol.45 (1953), pp.533 - 575.
274. Howard, R.T. and Cohen, M. - Trans. AIMME, Vol.172 (1947), pp.413 - 426.
275. Saltykov, S.A. - Plant Laboratory, Vol.8, No.5 (1939).
276. Bokshteyn, S.Z., Kishkin, S.T., and Moroz, L.M. - Metal Science and Processing of Metals, No.2 (1957).
277. Yum-Rozeri, V., Christian, G., and Pearson, V. - Diagrams of Equilibrium of Metal Systems. Metallurgizdat, Moscow (1956).

TABLE OF CONTENTS

| | |
|---|-----|
| Preface | iii |
| Chapter I. Microscopic Structure of Alloys and Methods of Their Characteristics | 1 |
| Section 1. Qualitative and Quantitative Appraisal of Microscopic Structure of Alloys | 1 |
| Section 2. Methods of Numerical Rating of Microstructure. | 5 |
| Section 3. Standard Methods of Rating the Microstructure. | 12 |
| Section 4. Spatial Structure of an Alloy and Methods of Studying it . . . | 22 |
| Section 5. Inadequacy of a Plane Evaluation of Microstructure | 25 |
| Section 6. Basic Parameters of Spatial Structure | 37 |
| Section 7. Development of Methods of Stereometric Microanalysis | 46 |
| Section 8. Technical Means and Features of Stereometric Microanalysis . . | 51 |
| Chapter II. Quantitative Phase and Structural Volumetric Composition of an Alloy | 69 |
| Section 9. Phase and Structural Composition of an Alloy | 69 |
| Section 10. Principle of Cavalieri and Its Application to Quantitative Metallographic Analysis | 73 |
| Section 11. Spatial Symmetry of Microstructure and Selection of Microsection Surface | 79 |
| Section 12. Effect of Nature of Structure | 86 |
| Section 13. Planimetric Method of Determining the Phase and Structural Volumetric Composition of Alloy | 97 |
| Section 14. Linear Method of Determining Phase and Structural Volumetric Composition of an Alloy and Its Application | 113 |

TABLE OF CONTENTS (CONT'D)

| | |
|--|-----|
| Section 15. Accuracy of Linear Method | 124 |
| Section 16. Point Method of Determining Phase and Structural Volumetric Composition of Alloy | 146 |
| Section 17. Structural and Chemical Composition of Alloy | 161 |
| Chapter III. Measurement of the Boundary Surfaces of a Section of the Grain, Phases and Structural Components | |
| Section 18. The Specific Surface and the Particular Methods of Its Measurement. | 176 |
| Section 19. Approximate Methods of Determining the Specific Surface of Polyhedral Structures. | 187 |
| Section 20. The Method of Incidental Intersecting on Planes Isometric Systems of Lines on a Plane and the Measurement of Their Length. | 193 |
| Section 21. Non-isometric Systems of Lines on a Plane and Their Characteristics. | 207 |
| Section 22. Method of Directed Intersection and Analysis of Partially Oriented Structures on a Plane | 216 |
| Section 23. Principle of Summary Projections for a Plane and the Verification of the Method of Directed Intersections. | 225 |
| Section 24. Method of Incidental Intersections for Space. | 232 |
| Section 25. Measurement of Specific Surfaces by the Method of Incidental Intersections for Space. | 239 |
| Section 26. Measurement of the Unit of Surfaces by the Method of Directed Intersections for Space. | 251 |

(TABLE OF CONTENTS - CONT'D)

| | |
|--|-----|
| Section 27. Rule of the Summary of Projections for Space and the Verification of the Method of Directed Intersections. | 264 |
| Section 28. Oriented Analysis of the Systems of Limited Surfaces | 270 |
| Section 29. Norms of Accuracy of the Method of Intersections. . . | 286 |
| Section 30. Measurement of the Linear Elements of Spatist Structure of Metals and Alloys. | 303 |
| Chapter IV. Determining the Number of Micro Particles in a Unit of Volume Metal Alloy. | 310 |
| Section 31. The Contact Between Spacial Structure and Surface Con- struction. | 310 |
| Section 32. Determination of the General Amount of Surface Grain on a Unit of the Areas of Cross-section. Planimetric Method and The Method of TS. Dzheffris. | 318 |
| Section 33. Determination of the General Amount of Surface Grain on a Unit of the Areas of Cross-section. The Method of Main Points and the Approximate Methods. | 329 |
| Section 34. Differential Estimate of the Surface Grain by Size and Amount. | 335 |
| Section 35. The System of Spheres and Its Cross-sections by Means of the Surface. The Method of Inverted Diameters of S. S. A. Saltykov. | 345 |
| Section 36. Calculation of the Distribution of Microunits by Sizes According to the Method of E. Sekeil - G. Schwartz - S. A. Saltykov. | 356 |

mch-905/1+2

— 602 —